

15th **NANOVATION**
MOVE FORWARD TO BETTER FUTURE

NANOTEC
a member of NSTDA



NANO THAILAND 2018

The 6th Thailand International Nanotechnology Conference
"From frontier research to innovation and commercialization"

NANO
THAILAND 2018

DECEMBER 12-14, 2018

Thailand Science Park Convention Center
Pathum Thani, Thailand



Program and Abstract Book







Contents

Welcome message from Chairman of the conference and Head of the organizing committee	4
Welcome message from Executive Director; National Nanotechnology Center (NANOTECH)	5
Organizing committee	6
Overview plan	8
Scientific program	12
Abstracts:	
Plenary speakers	29
Keynote speakers	33
Invited speakers	48
Oral presentation	88
Poster presentation	179
General information	264

Welcome message



On behalf of the Nanotechnology Association of Thailand and Chulalongkorn University, it is with great pleasure and privilege to extend a warm invitation to you for participating in the 6th Thailand International Nanotechnology Conference (NanoThailand 2018), which will be held between December 12th-14th, 2018, at Thailand Science Park Convention Center, Pathum Thani, Thailand. The theme of the conference is “From frontier research to innovation and Commercialization”.

The objectives are to apply nanotechnology in various fields for a better life, to create a platform for knowledge exchange to further advance technological areas, and to exhibit the latest innovations of the industries.

In order to realize the objective of the conference, outstanding keynote speakers, guest speakers and researchers are invited to present significant progress which has been made in the areas of their expertise. The conference will provide a platform for experienced researchers in nanotechnology and practitioners from both academics, as well as industry to meet and share cutting-edge development in the field.

On behalf of the organizing committee, we would like to express our strong belief the participating in the NanoThailand 2018 will be a memorable experience, and we look forward to welcoming you to Thailand.

Prof. Dr. Jumras Limtrakul
Chairman of the conference

Prof. Dr. Mongkol Sukwattanasinitt
Head of the Organizing Committee

Welcome message



On behalf of NANOTECH, we are delighted to welcome our international and national presenters and delegates to NanoThailand 2018, the 6th International Nanotechnology Conference to be held at Thailand Science Park during 12-14 December. The conference theme is “From Frontier Research to Innovation and Commercialization” which reflects the rapid advances being made in the field of nanotechnology, all for the goal of matching research with market needs. The event will bring together leading researchers, scientists, and innovators to exchange experiences and create an environment that will promote new ideas and collaborations.

NANOTECH is celebrating its 15th Anniversary on 13 August and participation at NanoThailand 2018 is one of the events of celebration activities. NANOTECH is providing awards to honour young and upcoming researchers who have demonstrated dedication to their career in nanotechnology research and help them gain broad recognition domestically and internationally.

I would like to take this opportunity to express my sincere appreciation to the organizer of this special event and also thank all the speakers and participants who have taken time out of their busy schedule to join us. We value very much your participation.

Dr. Wannee Chinsirikul
Executive Director
National Nanotechnology Center
(NANOTECH)

Organizing committee

Advisory Committee

Prof. Dr. Sirirung Songsivilai, Honorary President:

Nanotechnology Association of Thailand

Assoc. Prof. Dr. Vittaya Amornkitbamrung Honorary President:

Nanotechnology Association of Thailand

Prof. Dr. Jumras Limtrakul, President:

Nanotechnology Association of Thailand

Dr. Wannee Chinsirikul, NANOTEC & Nanotechnology Association of Thailand

Dr. Uracha Ruktanonchai, NANOTEC

Dr. Pavadee Aungkavattana, NANOTEC

Assoc. Prof. Dr. Surin Laosooksathit, Nanotechnology Association of Thailand

Mr. Por Punyaratabandhu, Nanotechnology Association of Thailand

Mr. Phoosak Hiranyatrakul, Nanotechnology Association of Thailand

Assoc. Prof. Dr. Somchai Ratanathamphan,

Nanotechnology Association of Thailand

Asst. Prof. Dr. Tanakorn Osochan, Nanotechnology Association of Thailand

Dr. Sirasak Tepakum, Nanotechnology Association of Thailand

International Advisory and Scientific Committee

Prof. Jay S. Siegel, Dean, Health Science Platform, Tianjin University, China

Prof. Dr. Oliver Reiser, Universität Regensburg, Germany

Prof. Dr. Burkhard König, Universität Regensburg, Germany

Dr. Jahangir Bin Kamaldin, Universiti Sains, Malaysia

Prof. Ruiqin Zhang, City University of Hong Kong, Hong Kong

Assoc. Prof. Horacio Cabral, The University of Tokyo, Japan

Dr. Kaito Takahashi, Institute of Atomic and Molecular Sciences,
Academia Sinica, Taiwan

Prof. Dr. Hiroshi Yamamoto, Institute for Molecular Science, Japan

Dr. Manoj B. Gawande, Palacky University, Czech Republic

Local Organizing Committee

Prof. Mongkol Sukwattanasinitt, Head of the Organizing Committee,
Chulalongkorn University

Assoc. Prof. Paitoon Rashatasakhon, Chulalongkorn University

Assoc. Prof. Sumrit Wacharasindhu, Chulalongkorn University

Assist. Prof. Yongsak Sritana-anant, Chulalongkorn University

Dr. Supawadee Namuangruk, NANOTECH

Mr. Tortrakul Poolsopha, NANOTECH

Ms. Sasinee Watcharaput, NANOTECH

Ms. Benyapa Suwan, NANOTECH

Ms. Wipaporn Ekamornthanakul, NANOTECH

Mr. Ramjitti Indaraprasirt, NANOTECH, Nanotechnology Association of Thailand

Mr. Pongsit Rattanakonvit, NANOTECH, Nanotechnology Association of Thailand

Scientific Committee

Assoc. Prof. Dr. Patchanita Thamyongkit, Chairman Scientific Committee,
Chulalongkorn University

Prof. Dr. Sanong Ekgasit, Chulalongkorn University

Prof. Dr. Orawon Chailapakul, Chulalongkorn University

Prof. Dr. Nongnuj Muangsin, Chulalongkorn University

Prof. Dr. Suttichai Assabumrungrat, Chulalongkorn University

Assoc. Prof. Rattikorn Yimnirun, VISTEC

Assist. Prof. Dr. Boosayarat Tomapatanaget, Chulalongkorn University

Assist. Prof. Dr. Worawat Meevasana, Suranaree University of Technology

Assist. Prof. Dr. Montree Sawangphruk, VISTEC

Dr. Wiyong Kungwansupamongkol, NANOTECH

Dr. Udom Assakpirom, NANOTECH

Dr. Kajonsuk Fuangnawakit, NANOTECH

Dr. Nuttaporn Pimpha, NANOTECH

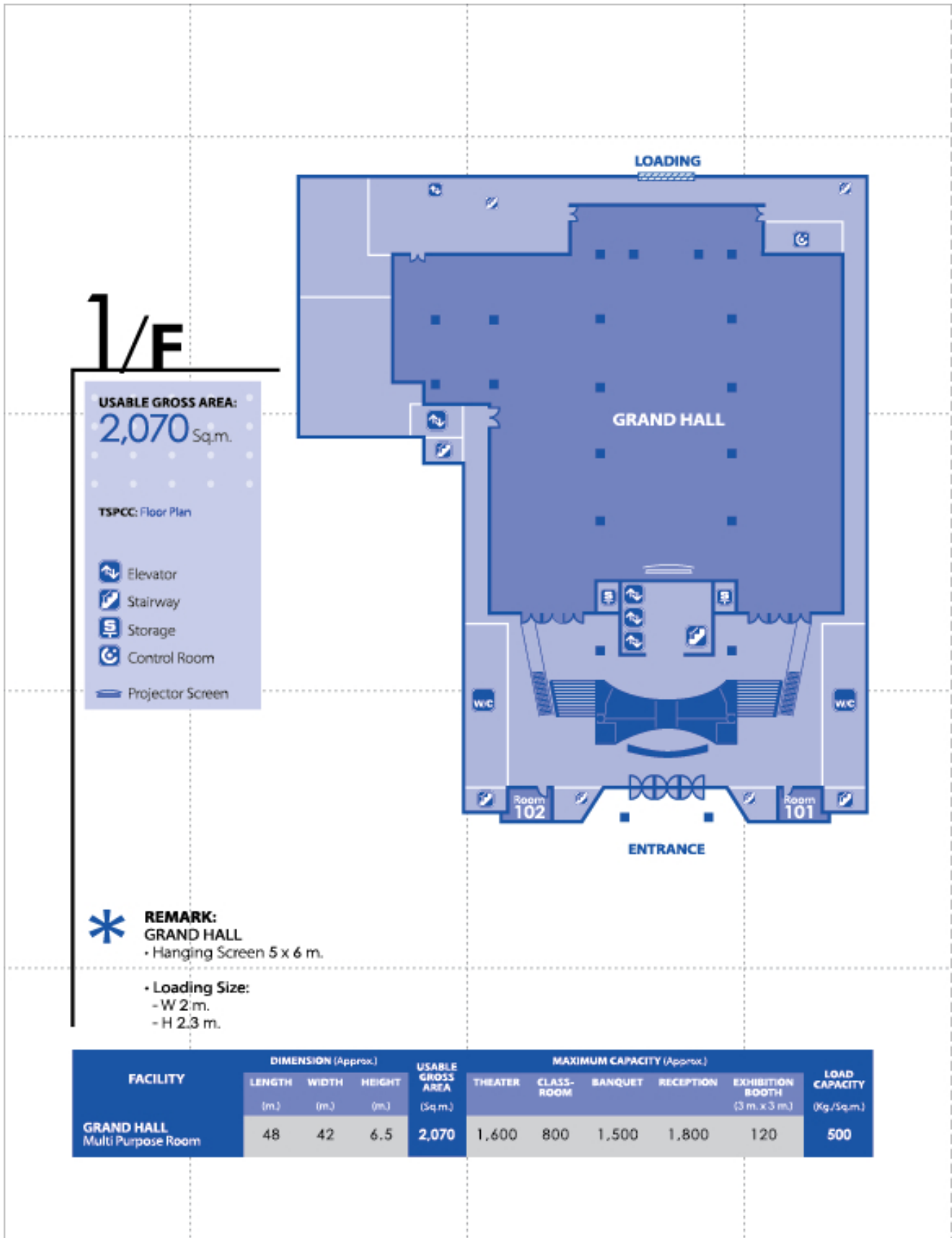
Dr. Varol Intasanta, NANOTECH

Dr. Supawadee Namuangruk, NANOTECH

Dr. Vinich Promarak, VISTEC

Mr. Ramjitti Indaraprasirt, NANOTECH

Overview Plan

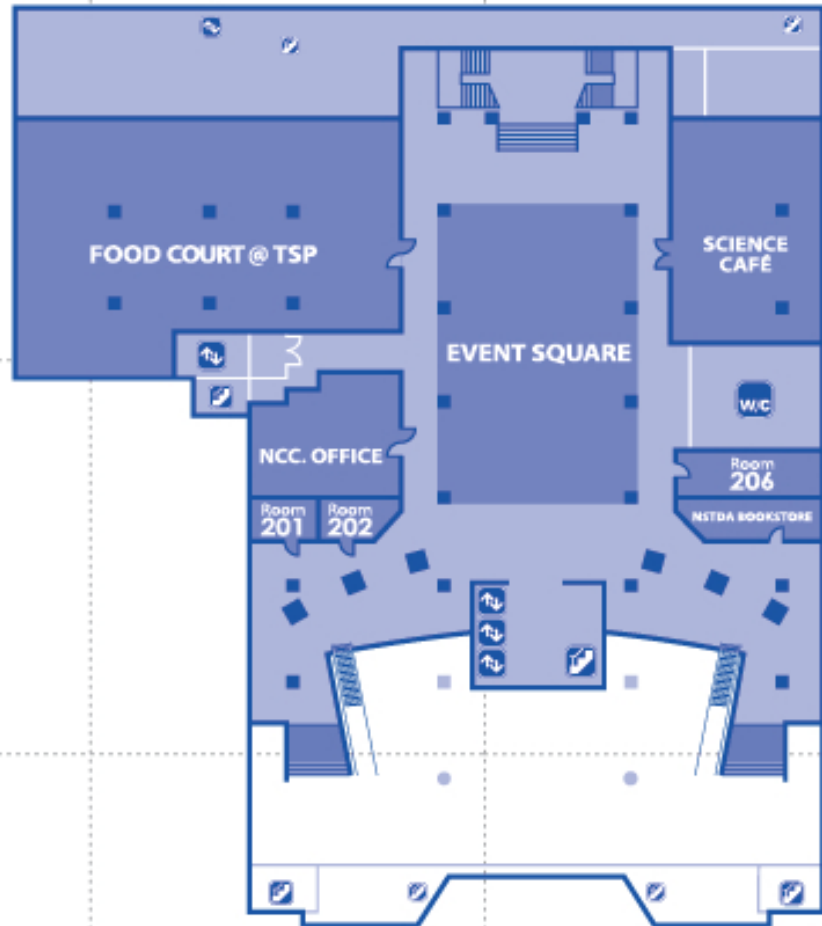


2/F

USABLE GROSS AREA:
410 Sq.m.

TSPCC: Floor Plan

- Elevator
- Stairway



FACILITY	DIMENSION (Approx.)			USABLE GROSS AREA (Sq.m.)	MAXIMUM CAPACITY (Approx.)					LOAD CAPACITY (Kg./Sq.m.)
	LENGTH (m.)	WIDTH (m.)	HEIGHT (m.)		THEATER	CLASS-ROOM	BANQUET	RECEPTION	EXHIBITION BOOTH (3 m. x 3 m.)	
EVENT SQUARE Multi Purpose Area	25	17	4	410	400	-	220	600	40	500

3/F

USABLE GROSS AREA:
1,140 Sq.m.

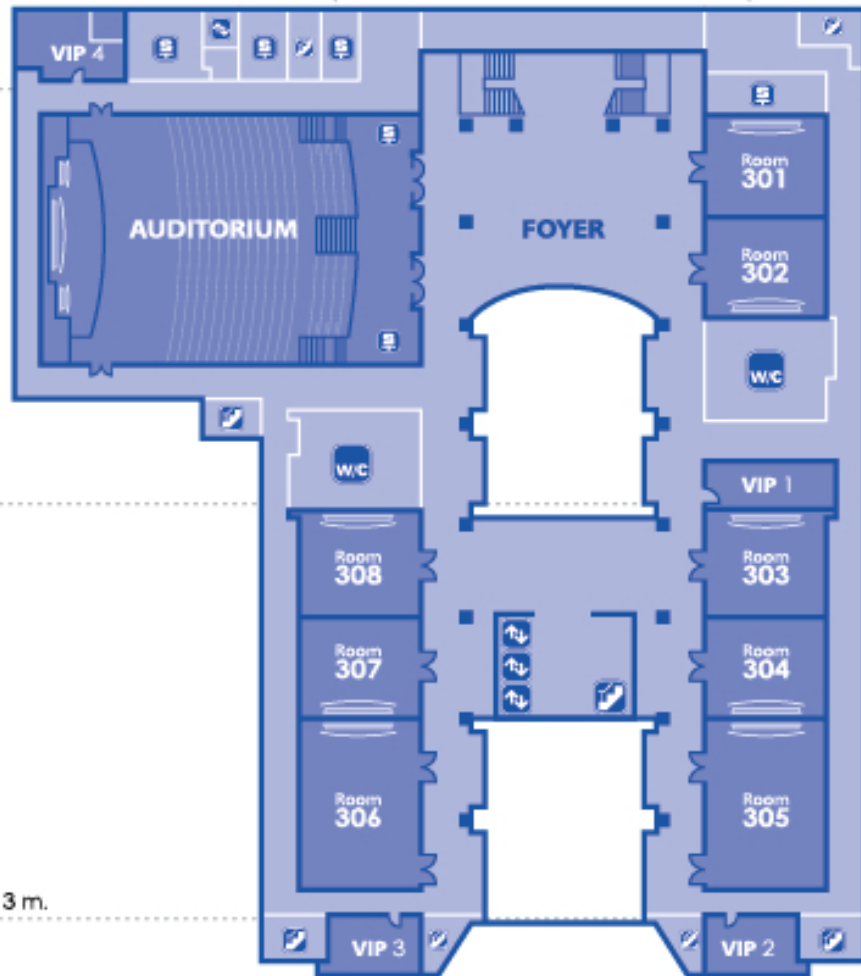
TSPCC: Floor Plan

- Elevator
- Stairway
- Storage
- Projector Screen



REMARK:
Room 301-308
- Hanging Screen 2 x 3 m.

Auditorium
- 3 Hanging Screens
L - 2.4 x 3 m.; M - 4 x 3 m.; R - 2.4 x 3 m.



FACILITY	DIMENSION (Approx.)			USABLE GROSS AREA (Sq.m.)	MAXIMUM CAPACITY (Approx.)					LOAD CAPACITY (Kg./Sq.m.)
	LENGTH (m.)	WIDTH (m.)	HEIGHT (m.)		THEATER	CLASS-ROOM	BANQUET	RECEPTION	EXHIBITION BOOTH (3 m. x 3 m.)	
Room 301 Seminar Room	7.5	9	3	68	50	32	-	-	-	500
Room 302 Seminar Room	7.5	9	3	68	50	32	-	-	-	500
Room 303 Computer Training Room	7.5	9	3	68	-	20	-	-	-	500
Room 304 Computer Training Room	7.5	9	3	68	-	20	-	-	-	500
Room 305 Seminar Room	13.5	9	3	122	90	63	-	-	-	500
Room 306 Seminar Room	13.5	9	3	122	90	63	-	-	-	500
Room 307 Seminar Room	7.5	9	3	68	50	32	-	-	-	500
Room 308 Seminar Room	7.5	9	3	68	50	32	-	-	-	500
AUDITORIUM Seminar Room	25	19.5	6	488	376	-	-	-	-	500



FACILITY	DIMENSION (Approx.)			USABLE GROSS AREA (Sq.m.)	MAXIMUM CAPACITY (Approx.)					LOAD CAPACITY (Kg./Sq.m.)
	LENGTH (m.)	WIDTH (m.)	HEIGHT (m.)		THEATER	CLASS-ROOM	BANQUET	RECEPTION	EXHIBITION BOOTH (3 m. x 3 m.)	
Room 404 Seminar Room	12.5	9	3	112	90	63	-	-	-	500
Room 405 Seminar Room	14	9	3	126	90	70	-	-	-	500
BOARDROOM Seminar Room	14	9	3	126	-	-	61	-	-	500

Scientific program

Wednesday 12/12/2018						
Time	Auditorium	305	306	307	404	405
08.00-09.00	Registration					
09.00-10.00	Opening Ceremony					
10.00-10.45	Plenary Lecture I <i>Kazunori Kataoka</i>					
10.45-11.00	Break					
		Chair: Pawitrabhorn Samutrtai	Chair: Nattika Saengkrit	Chair: Supawadee Namuangruk	Chair: Patchanita Thamyongkit	Chair: Kajornsak Fuangnawakij, Aniwat Pengsawang
11.00-12.00		SAF-K-01: <i>Jahangir Bin Kamaldin</i> SAF-I-01: <i>Masashi Gamo</i>	MED-K-01: <i>Istvan Toth</i> MED-I-01: <i>Horacio Cabral</i>	THE-K-01: <i>Ruiqin Zhang</i> THE-Oral Presentations	ELE-K-01: <i>Kevin Burgess</i> ELE-Oral Presentations	FAB-K-01: <i>Ken-ichi Shimizu</i> FAB-Oral Presentations
12.00-13.00	Lunch					
		Chair: Pawitrabhorn Samutrtai	Chair: Mattaka Khongkow	Chair: Jianwen Liu	Chair: Sanong Ekgasit	Chair: Rungthiwa Methaapanon
13.00-14.30	15th NANOTEC: Nanovation Move Forward to Better Future	SAF-I-02: <i>June-Woo Park</i> SAF-I-03: <i>Christina A. Binag</i> SAF-I-04: <i>Baeg Gyeong Hun</i>	MED-I-02: <i>Manop Pithukpakorn</i> MED-Oral Presentations	THE-I-01: <i>Kaito Takahashi</i> THE-I-02: <i>Gang Feng</i> THE-Oral Presentations	ELE-K-02: <i>Dietrich R. T. Zahn</i> ELE-Oral Presentations	FAB-I-01: <i>Teera Butburee</i> FAB-I-02: <i>Sareeya Bureekaew</i> FAB-Oral Presentations
14.30-15.30	Break & Poster session I (ELE, FAB, MED, SAF, THE)					
		Chair: Pawitrabhorn Samutrtai	Chair: Manop Pithukpakorn	Chair: Kaito Takahashi	Chair: Sanong Ekgasit	Chair: Teera Butburee
15.30-16.45	15th NANOTEC: Nanovation Move Forward to Better Future	SAF-I-05: <i>Jen-Kun Chen</i> SAF-K-02: <i>Jahangir Bin Kamaldin</i> Q&A/closing remark	MED-Oral Presentations	THE-I-03: <i>Jianwen Liu</i> THE-Oral Presentations	ELE-I-01: <i>Sanpon Vantasin</i> ELE-Oral Presentations	FAB-I-03: <i>Rungthiwa methaapanon</i> FAB-Oral Presentations

Thursday 12/13/2018					
Time	Auditorium	305	306	307	308
09.00-09.45	Plenary Lecture II <i>Vincent M. Rotello</i>				
09.45-10.00	Break				
		Chair: Weena Siangproh	Chair: Nakorn Niamnont	Chair: Vinich Promarak	Chair: Nongnuj Muangsin
		Chair: Weena Siangproh	Chair: Nakorn Niamnont	Chair: Vinich Promarak	Chair: Nongnuj Muangsin
10.00-12.00	SEN-K-01: <i>Yukako Asano</i> SEN-Oral Presentations	STE-K-01: <i>Jay S. Siegel</i> STE-I-01: <i>Eiji Yashima</i> STE-I-02: <i>Kim Baldrige</i> STE-I-03: <i>Steve Zimmerman</i>	ENE-K-01: <i>Akira Baba</i> ENE-I-01: <i>Jean Roncali</i> ENE-Oral Presentations	AGR-I-01: <i>Fang Zhang</i> AGR-I-02: <i>Supason Wanichwecharungruang</i> AGR-Oral Presentations	GRA-K-01: <i>Satoshi Horike</i> GRA-I-01: <i>Adisorn Tuantranont</i> GRA-Oral Presentations
12.00-13.00	Lunch				
		Chair: Boosayarat Tomapatanaget, Gamolwan Tumchareen	Chair: Jay S. Siegel	Chair: Vinich Promarak	Chair: Sumrit Wacharasindhu
13.00-14.30	SEN-I-01: <i>Quan Jason Cheng</i> SEN-Oral Presentations	SUP-I-01: <i>Mark A. Olson</i> SUP-I-02: <i>Ognjen S. Miljanic</i> SUP-I-03: <i>Ivan Aprahamian</i> SUP-I-04: <i>Ali Trabolsi</i>	ENE-I-02: <i>Chi-How Peng</i> ENE-I-03: <i>Hiroshi Yamamoto</i> ENE-Oral Presentations	CAT-K-01: <i>Oliver Reiser</i> CAT-Oral Presentations	GRA-I-02: <i>Pisith Singjai</i> GRA-Oral Presentations
14.30-15.30	Break & Poster session II (AGR, CAT, ENE, GRA, MOX, SEN, SUP)				
		Chair: Quan Jason Cheng	Chair: Steve Zimmerman	Chair: Vinich Promarak	Chair: Sumrit Wacharasindhu
15.30-16.45	SEN-I-02: <i>Rudolf Heer</i> SEN-Oral Presentations	SUP-I-05: <i>Ali Coskun</i> SUP-I-06: <i>Amar Flood</i>	ENE-I-04: <i>Fabrice Goubard</i> ENE-Oral Presentations	CAT-Oral Presentations	

Friday 12/14/2018			
Time	Auditorium	305	306
		Chair: Adisorn Tuantranont	Chair: Varol Intasanta
09.00-09.30	CAT-K-02: <i>Burkhard König</i>	MOX-I-01: <i>Anurat Wisitsoraat</i>	CEL-K-01: <i>Takeshi Kikutani</i>
09.30-09.50	CAT-I-01: <i>Bunjerd Jongsomjit</i>	MOX-Oral Presentations	CEL-I-01: <i>Ali Abbasi</i>
09.50-10.10	CAT-I-02: <i>Manoj B. Gawande</i>		CEL-Oral Presentations
10.10-10.40	CEL-I-02: <i>Suwabun Chirachanchai</i>		
10.40-11.00	Break		
11.00-12.00	Awards Ceremony and Closing remarks		
12.00-13.00	Lunch		

Sessions:

AGR	Nanotechnology for food, agriculture and environment
CAT	Nanotechnology for catalysis and industry
CEL	Cellulose and fibers
ELE	Nano-electronics photonics and optics
ENE	Nanotechnology for energy
FAB	Nanomaterials and nanofabrication
GRA	Graphene and carbon nanotube
MED	Nanomedicine and pharmaceuticals
MOX	Metal-oxide nanomaterials
SEN	Nanotechnology for sensing and analysis
STE	Nanomolecular stereochemistry
SUP	Supramolecular nanomaterials
THE	Theory and simulation of nanosystem
Special Session:	
SAF	Nanosafety Technical Forum 2018

Overall program

Nanotechnology for food, agriculture and environment (AGR)			
THU 13 th , Room: 307			
Time	ID	Presenter	Title
Chairperson: Prof. Dr. Nongnuj Muangsin			
10.00-10.20	AGR-I-01	Fang Zhang	Aerosol-Assisted Fabrication of Mesoporous Single-Site Organometallic Catalyst
10.20-10.40	AGR-I-02	Supason Wanichwecharungruang	Technology to Aid Applications of Some Natural Product Extracts
10.40-10.55	AGR-O-02	Chamorn Chawengkijwanich	Zero Valent Iron Nanoparticles Stimulate Exopolymer Synthesis by Pseudomonas putida
10.55-11.10	AGR-O-06	Sudkanueng Singto	Development of Hydrophilic Polyamide Thin-Film Composite (TFC) Membranes on Polyvinylidene Fluoride (PVDF) Hollow Fiber Membranes for Nanofiltration
11.10-11.25	AGR-O-07	Sathita Taksadej	Surface-Enhanced Raman Scattering Detection of Polycyclic Aromatic Hydrocarbons by Thiol-Modified Silver Nanoparticle Film Substrate
11.25-11.40	AGR-O-08	Eko Sutrisno	Study Preparation for Fabricating Cellulose Nanofibers (CNFs) from Pulp of Macaranga sp

Nanotechnology for catalysis and industry (CAT)			
THU 13 th , Room: 307			
Time	ID	Presenter	Title
Chairperson: Assoc. Prof. Sumrit Wacharasindhu			
13.00-13.30	CAT-K-01	Oliver Reiser	Mag(net)ic Nanocatalysts - Concepts and Applications
13.30-13.45	CAT-O-01	Jiaqian Qin	Rational Design and Synthesis of High Efficient Photocatalyst for Hydrogen Production
13.45-14.00	CAT-O-02	Christine Adelle Rico Yuson	Environment-friendly Alternative to Copper Cyanide-based Electroplating Bath for Nanocoating Applications
14.00-14.15	CAT-O-05	Tanasan Intana	Enhancement of Furfural Hydrogenation to Furfuryl Alcohol over Copper-based Catalysts: Effect of Catalyst Synthesis Methods
14.15-14.30	CAT-O-07	Worapak Tanwongwan	Surface Enhancement and Structure Formation of Metakaolin from Thailand Kaolin on the Various Calcination Temperature
Break & Poster Session			
Chairperson: Assoc. Prof. Sumrit Wacharasindhu			
15.30-15.45	CAT-O-08	Tripob Longprang	Influence of Acid Additive on Nanoporous Carbon Materials via HTC for Catalyst Supporter
15.45-16.00	CAT-O-09	Pongtanawat Khemthong	In situ XAFS Characterization of CuFe ₂ O ₄ Catalysts under Oxidation, Reduction and Steam Reforming Conditions
16.00-16.15	CAT-O-10	Sirapassorn Kiatphuengporn	Analysis Study of Surface Acidity of Alumina Catalysts by Ammonia IRMS-TPD and its Role in Catalytic Conversion of D-xylose to Lactic Acid

FRI 14 th , Room: Auditorium			
Time	ID	Presenter	Title
Chairperson: Assoc. Prof. Dr. Patchanita Thamyongkit			
09.00-09.30	CAT-K-02	Burkhard König	Making and Breaking of Chemical Bonds Using Visible Light and Nano Photocatalysts
09.30-09.50	CAT-I-01	Bunjerd Jongsomjit	Ethanol Dehydration Over Alumina-Based Catalysts
09.50-10.10	CAT-I-02	Manoj B. Gawande	Advanced Nanomaterials – Synthesis and Applications in Organic Transformations

Cellulose and fibers (CEL)			
FRI 14 th , Room: 306			
Time	ID	Presenter	Title
Chairperson: Dr. Varol Intasanta			
9.00-9.30	CEL-K-01	Takeshi Kikutani	Melt-Processed Polyethylene Products Containing Micro-Fibrillated Cellulose Fibers
9.30-9.50	CEL-I-01	Ali Abbasi	Opportunities on Nanofibers Technologies; from Lab to Industry
9.50-10.05	CEL-O-01	Jirapat Wattanaruangkowit	Cotton Coated with Trimethylsilylcellulose
10.05-10.20	CEL-O-02	Apiwat Promchat	Simple Paper-Based Sensor for Zn ²⁺ Ion from Aminoquinoline Derivatives
10.20-10.35	CEL-O-04	Phattananawee Nalaoh	Mechanoresponsive “Turn-On” Transparent Luminescent Cellulose Nanopaper with Mechanochromic Aiegen
10.35-10.50	CEL-O-05	Jadetapong Klahan	Development of Bacterial Cellulose as Substrates for Sensing Applications

FRI 14 th , Room: Auditorium			
Time	ID	Presenter	Title
Chairperson: Assoc. Prof. Dr. Patchanita Thamyongkit			
10.10-10.30	CEL-I-02	Suwabun Chirachanchai	Shape Memory Mechanochromic Poly (Caprolactone): A Novel Approach for a Functional Color Changable and Shape Recoverable Polyester

Nano-electronics photonics and optics (ELE)

WED 12th, Room: 404

Time	ID	Presenter	Title
Chairperson: Assoc. Prof. Dr. Patchanita Thamyongkit			
11.00-11.30	ELE-K-01	Kevin Burgess	On "Tumor -seeking" Near IR-Dyes
11.30-11.45	ELE-O-06	Praetip Khammultri	Thermally Activated Delayed Fluorescence (TADF) Polymer Based on Thioxanthone Monomer
11.45-12.00	ELE-O-02	Chanikarn Tomon	Novel Visible-Light-Driven Photocatalytic Zn-Air-Batteries with Cobalt Oxides Cathode
Lunch break			
Chairperson: Prof. Dr. Sanong Ekgasit			
13.00-13.30	ELE-K-02	Dietrich R.T. Zahn	Enhanced Spectroscopies of Semiconductor Nanostructures
13.30-13.45	ELE-O-03	Ketsuda Kongsawatvoragul	The Visible Light Driven Hybrid Energy Storage Device
13.45-14.00	ELE-O-04	Anna Pachariyangkun	Perylene Diimide Functionalized with Fused-thiophenes as N-Type Semiconductor for Solution-processable OFETs
14.00-14.15	ELE-O-01	Jon-Paul Wells	Spectroscopic Studies of Europium Doped Calcium Fluoride Nanoparticles
Break & Poster Session			
Chairperson: Prof. Dr. Sanong Ekgasit			
15.30-15.50	ELE-I-01	Sanpon Vantasin	Characterization of Graphene by Plasmon, Manipulation of Plasmon by Graphene
15.50-16.05	ELE-O-07	Patchareepond Panoy	Solution-Processable Spirobifluorene Derivatives as Deep-Blue Emitters for Electroluminescent Devices
16.05-16.20	ELE-O-08	Jirat Chatsirisupachai	Chrysene Derivatives as Solution-Processable Deep Blue Emitters for OLEDs
16.20-16.35	ELE-O-09	Jakkapan Kumsampao	Molecular Design of Triphenylamine End-capped Benzothiadiazoles as Thermally Activated Delayed Fluorescence (TADF) Materials for OLEDs

Nanotechnology for energy (ENE)

THU 13th, Room: 306

Time	ID	Presenter	Title
Chairperson: Dr. Vinich Promarak			
10.00-10.30	ENE-K-01	Akira Baba	Development of Plasmonic Organic Devices and Biosensors
10.30-10.50	ENE-I-01	Jean Roncali	Molecular Switches and Memory Devices Based on Dynamic π -Conjugated Systems
10.50-11.05	ENE-O-01	Jiaqian Qin	Research on Mass Production of High Performance Anodes for Lithium-ion Batteries
11.05-11.20	ENE-O-02	Thakorn Wichaidit	Thin Film Composite Hollow Fiber Membrane of Zeolite Y for Biogas Upgrading
11.20-11.35	ENE-O-03	Thatchai Chevapruck	Solution-Based Ni-Al ₂ O ₃ Solar Selective Coating using Convective Deposition
11.35-11.50	ENE-O-05	Supeera Nootchanat	Enhancement of Thin-Film Organic Solar Cell Efficiency by Surface Plasmon Resonance and Plasmonic-Enhanced Fluorescence
Lunch break			
Chairperson: Dr. Vinich Promarak			
13.00-13.20	ENE-I-02	Chi-How Peng	The Dual Responsive Block Copolymers for Drug Delivery System with Spatiotemporal Precision
13.20-13.40	ENE-I-03	Hiroshi Yamamoto	Organic Field-Effect-Transistor with Strongly Correlated Electrons
13.40-13.55	ENE-O-06	Thanitporn Narkkun	Poly(ether block amide)/Polyetherimide Hollow Fiber Membranes for CO ₂ /CH ₄ Separation
13.55-14.10	ENE-O-07	Sangchai Sarawutanukul	Novel Urchin-like Structure Nickel Cobalt Sulfide as an Efficient Bifunctional Catalyst toward ORR and OER for Zinc-air Batteries
14.10-14.25	ENE-O-08	Surasak Kaenket	The Effect of Nitrogen Content in 3D N-doped Graphene Oxide Aerogel as Interlayers for High-performance Lithium-sulfur Batteries
Break & Poster Session			
Chairperson: Dr. Vinich Promarak			
15.30-15.50	ENE-I-04	Fabrice Goubard	Design of New Organic Hole Transporting Materials and Effects of Doping for Perovskite Solar Cells
15.50-16.05	ENE-O-09	Suchakree Tubtimkuna	Polyaniline Modified Hydrolyzed Polyethylene and Polyethylene Dual Separators to Enhance Lithium-Sulfur Batteries
16.05-16.20	ENE-O-10	Nattapol Ma	The Effect of Intercalated Cations in Layered Manganese Oxides as Neutral Electrochemical Capacitor
16.20-16.35	ENE-O-11	Nattha Chaiyapo	Electrode Materials from Biomass Sources for Aluminum ion Battery Applications
16.35-16.50	ENE-O-12	Soracha Kosasang	Insight into the Effect of Intercalated Alkaline Cations of Layered Manganese Oxides as Bifunctional Electrocatalysts for Zn-air Batteries

Nanomaterials and nanofabrication (FAB)

WED 12th, Room: 405

Time	ID	Presenter	Title
Chairpersons: Dr.Kajornsak Fuangnawakij, Dr.Aniwat Pengsawang			
11.00-11.30	FAB-K-01	Ken-ichi Shimizu	Case Study on the Mechanism of Heterogeneous Catalysis
11.30-11.45	FAB-O-02	Kullavadee Karn-orachai	Dependence of Plasmon Coupling Enhancement on SERS Probe-Substrate Distance
11.45-12.00	FAB-O-05	Aroonsri Ngamaroonchote	Plasma-etched Nanosphere Conductivity-Inverted Lithography (PENCIL): A Facile Fabrication of Size-Tunable Gold Disc Array on Conductive Substrate
Lunch break			
Chairperson: Dr.Rungthiwa Methaapanon			
13.00-13.20	FAB-I-01	Teera Butburee	Facet-Engineered Titanium Dioxide Directly Grown on a Conductive Substrate as an Efficient Photoelectrode
13.20-13.40	FAB-I-02	Sareeya Bureekaew	Control of Polymorphism of Metal-Organic Frameworks Using Mixed-Metal Approach
13.40-13.55	FAB-O-06	Yanisa Sanguansap	3D Self-Assembled Magnetic Au-Ni NWs for SERS substrate
13.55-14.10	FAB-O-08	Tin Srimake	Synthesis of MgAl LDHs Accumulate on Magnetite and Investigations of Phosphate Adsorption
14.10-14.25	FAB-O-10	Kitti Yuwawech	Preparation and Characterizations of Iron Oxide Decorated Graphene Nanoplatelets for Use as Barrier Enhancing Fillers in Polyurethane Based Solar Cell Encapsulant
Break & Poster Session			
Chairperson: Dr.Teera Butburee			
15.30-15.50	FAB-I-03	Rungthiwa Methaapanon	Atomic Layer Deposition for Battery Applications (Review)
15.50-16.05	FAB-O-11	Malinee Niamlaem	Wireless Synthesis of Thermoresponsive Janus Nanostructured Carbon Materials using Bipolar Electrochemistry
16.05-16.20	FAB-O-13	Piboonwan Insiti	One-Step Fabrication of Urchin-Like Gold Nanoparticle Film on PDMS Substrates for SERS Applications
16.20-16.35	FAB-O-18	Porapak Suriya	Fabrication of Silver Sponge Film via Thermal Decomposition of Rod Shape Silver Acetate under PDMS-Suppressed Sintering
16.35-16.50	FAB-O-03	Muhammad Najam Khan	Photocatalytic Degradation of Dyes using Hydrothermal Synthesized Zinc Tin Oxide (ZTO) Nanoparticles at Room Temperature, Effect of Concentration of Dyes on Photocatalytic Activity

Graphene and carbon nanotube (GRA)			
THU 13 th , Room: 308			
Time	ID	Presenter	Title
Chairperson: Assist. Prof. Dr. Montree Sawangphruk			
10.00-10.30	GRA-K-01	Satoshi Horike	Glass and Liquid Metal-Organic Frameworks for Energy Application
10.30-10.50	GRA-I-01	Adisorn Tuantranont	Graphene, its Applications, and Commerlization
10.50-11.05	GRA-O-03	Sarika Pradhan	Development of Electrochemical Electrodes using Carbon Nanotube and Metal Phthalocyanine to Classify Pharmaceutical Drugs
11.05-11.20	GRA-O-04	Sathyamoorthi Sethuraman	High Rate Graphene Sponge Supercapacitor with Hybrid Dual Ionic Liquid-Aqueous Electrolyte
11.20-11.35	GRA-O-05	Chalita Aphirakaramwong	A Novel High-Performance Lithium-Ion Hybrid Capacitors Using Three-Dimensional Nanostructure of Reduced Graphene Oxide Aerogel and Carbon Nanotube Composites
Lunch break			
Chairperson: Dr. Adisorn Tuantranont			
13.00-13.20	GRA-I-02	Pisith Singjai	Mass scale production, applications and commercialization of carbon nanotubes in Thailand
13.20-13.35	GRA-O-06	Juthaporn Wutthiprom	Designing an Interlayer of Reduced Graphene Oxide Aerogel and Nitrogen-rich Graphitic Carbon Nitride by a Layer-by-layer Coating for High-energy Lithium Sulfur Batteries
13.35-13.50	GRA-O-07	Nutthaphon Phattharasupakun	High-performance Lithium-Ion Capacitors Using 3D Nitrogen-Doped Reduced Graphene Oxide Aerogel as a Negative Electrode: A Hydrodynamic Investigation

Nanomedicine and pharmaceuticals (MED)

WED 12th, Room: 306

Time	ID	Presenter	Title
Chairperson: Dr. Nattika Saengkrit			
11.00-11.30	MED-K-01	Istvan Toth	Self-Adjuvanting Lipopeptide Nanoparticulate Vaccine Candidates
11.30-12.00	MED-I-01	Horacio Cabral	Engineering Tumor Microenvironment Toward Enhanced Drug Delivery
Lunch break			
Chairperson: Dr. Mattaka Khongkow			
13.00-13.20	MED-I-02	Manop Pithukpakorn	Cancer Precision Medicine in Thailand
13.20-13.35	MED-O-01	Anyanee Kamkaew	Aza-BODIPY Based Polymeric Nanoparticles for Cancer Cell Imaging
13.35-13.50	MED-O-03	Soumyashree Dhal	Fabrication of Upconversion Nanoparticle Incorporated Oleogel for Potential Application As Skin Tissue Imaging Agent
13.50-14.05	MED-O-04	Kittipan Siwawannapong	PEGylated Pyropheophorbide-a Nanodots for Fluorescence/Photoacoustic Dual-modal Imaging-guided Photodynamic Therapy
14.05-14.20	MED-O-05	Kanyani Sangpheak	In Silico and in Vitro Studies of Chalcones as Potent Anticancer Agents with EGFR Tyrosine Kinase
Break & Poster Session			
Chairperson: Assoc.Prof. Manop Pithukpakorn			
15.30-15.45	MED-O-06	Jakarwan Yostawonkul	Alpha Mangostin-Loaded Nanostructured Lipid Carriers as Innovative Veterinary Medicine for Non-surgical Castration of Male Animals
15.45-16.00	MED-O-07	Kanlaya Prapainop	Synthesis and Cytotoxicity of Cadmium Telluride Quantum Dots in Leptospira
16.00-16.15	MED-O-09	Tawin Iempridee	Identification of Circulating Long Non-Coding RNA Reference Genes and Cancer Biomarkers from Serum of Cervical Cancer Patients
16.15-16.30	MED-O-10	Phattharachanok Khumkhong	Development of Biosensor Cells for Anti-aging Compounds Screening from Natural Products
16.30-16.45	MED-O-11	Duolikon Tuerxun	Occupational Exposure Risks of Engineered Nanomaterials in relation to Toxicology

Metal-oxide nanomaterials (MOX)			
FRI 14 th , Room: 305			
Time	ID	Presenter	Title
Chairperson: Dr. Adisorn Tuantranont			
9.00-9.20	MOX-I-01	Anurat Wisitsoraat	Development of Carbon/Metal-Oxide Nanostructured Composites for Gas-Sensing Applications
9.20-9.35	MOX-O-03	Thiha Soe	Atomic Structure of Cobalt Doped Copper Ferrite Thin Film
9.35-9.50	MOX-O-04	Tin Htet Htet Lynn	Nano-Flower Structure of Indium and Gallium doped Zinc Oxide Powder
9.50-10.05	MOX-O-05	Nontakoch Siriphongsapak	Hydrothermal Growth of ZnO Nanostructures using Sodium Hydroxide as Source of Hydroxyl Ion

NanoSafety Technical Forum 2018 (SAF)			
WED 12 th , Room: 305			
Time	ID	Presenter	Title
Chairperson: Dr. Pawitrabhorn Samutrtai			
11.00-11.30	SAF-K-01	Jahangir Bin Kamaldin	Organizing Nanosafety Studies in Adherence to OECD-GLP
11.30-12.00	SAF-I-01	Masashi Gamo	Risk Assessment of Nanomaterials (Case Studies and Methodologies) and Intratracheal Instillation Method for Testing Nanomaterials
Lunch break			
13.00-13.30	SAF-I-02	June-Woo Park	Method Development for in Vivo Nanotoxicity Assessment Using Zebrafish Embryos
13.30-14.00	SAF-I-03	Christina A. Binag	ZnO Nanoparticles Studies: Chronic Toxicity to Freshwater Calanoid Copepod <i>Arctodiaptomus dorsalis</i> and Antibacterial Activity against Uropathogens
14.00-14.30	SAF-I-04	Baeg Gyeong Hun	The Use of <i>Drosophila</i> as a Platform to Study Nanotoxicity
Break & Poster Session			
15.30-16.00	SAF-I-05	Jen-Kun Chen	Chamber System for Controllable and Quantitative Exposure of Airborne Nanoparticles for Both the in Vitro Cell Culture and in Vivo Animal Studies
16.00-16.30	SAF-K-02	Jahangir Bin Kamaldin	Safety Evaluation Across the Lifecycle of Manufactured Nanomaterials from the Regulatory Perspective
16.30-16.45	Q&A and Closing remarks		

Nanotechnology for sensing and analysis (SEN)

THU 13th, Room: Auditorium

Time	ID	Presenter	Title
Chairperson: Assoc.Prof.Weena Siangproh			
10.00-10.30	SEN-K-01	Yukako Asano	Development of a Microdevice for Reduction of Nitrate Ion Including Micro-Tubular Carriers Made of Copper
10.30-10.45	SEN-O-01	Chuleekorn Chotsuwan	Ion Transport in Composite Gel Electrolyte based on Cellulose Acetate for Electrochemical Applications
10.45-11.00	SEN-O-02	Kantapat Chansaenpak	Coumarin Probe for Selective Detection of Fluoride Ions in Water
11.00-11.15	SEN-O-03	Noppadol Aroonyadet	Top-Down and Sensitive In ₂ O ₃ Nanoribbon Field Effect Transistor Biosensor Chips Integrated with On-Chip Gate Electrodes toward Point of Care Applications
11.15-11.30	SEN-O-04	Titilope John Jayeoye	A Simplistic Approach into Colorimetric Sialic Acid Determination Based on Boronic Acid and Un-functionalized Gold Nanoparticles
11.30-11.45	SEN-O-05	Anuwut Petdum	Design and Synthesis of New Heavy Metal Ions Fluorescence Sensors and Their Applications in Commercial Products and Living Cell
11.45-12.00	SEN-O-06	Emmanuel Arella Florido	Comparison of Methane Gas Sensing of Zinc Oxide Film and Tin Oxide Film
Lunch break			
Chairperson: Assist. Prof. Dr. Boosayarat Tomapatanaget , Co-chairperson: Dr. Gamolwan Tumcharern			
13.00-13.20	SEN-I-01	Quan Jason Cheng	Calcinated Nanofilm on Gold Surface for SPR and MALDI Analysis of Proteins and Peptides
13.20-13.35	SEN-O-07	Sarawut Kingchok	Polydiacetylene/Zinc-Aluminium Layered Double Hydroxides Nanocomposites with Reversible Thermochromism
13.35-13.50	SEN-O-08	Ma Theint	Effects of Group I (Alkali) Metal Cations on Self-assemblies and Color-transition Behaviors of Polydiacetylene
13.50-14.05	SEN-O-09	Phatsawit Wuamprakhon	The Effect of Alkaline Intercalant on Birnessite Structure towards Hydrazine Oxidation Mechanism and Sensing Application
14.05-14.20	SEN-O-10	Sirin Sittiwanchai	Highly Sensitive Detection of Ractopamine Using Surface-Enhanced Raman Scattering Based Lateral Flow Immunosensor
14.20-14.35	SEN-O-11	Christopher Estandarte	Gas Response of SILAR Fabricated Zinc Oxide Thin Film to Ammonia and Methane Gas at Room Temperature
Break & Poster Session			
Chairperson: Prof. Quan Jason Cheng			
15.30-15.50	SEN-I-02	Rudolf Heer	Preparation and Integration of Specifically Functionalized Nano- and Biosensors for Biomolecular Detection in Liquid Biopsy
15.50-16.05	SEN-O-12	Suthikorn Jantra	Styryl-BODIPY as Fluorescent Probe for Gold(III) Ion in Aqueous Media
16.05-16.20	SEN-O-14	Chonticha Sahub	Two-biosensor Systems Based on Graphene Quantum Dots via Enzymatic Reaction for Photoluminescence Detection of Organophosphate Pesticide
16.20-16.35	SEN-O-15	Thanyada - Sukmanee	Chemically Modified Tip-Enhanced Raman Scattering (TERS) for Enantiomeric Discrimination
16.35-16.50	SEN-O-16	Wireeya Chawjiraphan	Fluorescence-based Aptasensor for Albumin Detection in Urine

Nanomolecular stereochemistry (STE)			
THU 13 th , Room: 305			
Time	ID	Presenter	Title
Chairperson: Assist.Prof. Dr. Nakorn Niamnont			
10.00-10.30	STE-K-01	Jay S. Siegel	Corannulene, Chirality and CIP
10.30-10.50	STE-I-01	Eiji Yashima	Helical Polymers as Unique Chiral Materials
10.50-11.10	STE-I-02	Kim Baldrige	Structure-Property Relationships of Curved Materials from First Principles
11.10-11.30	STE-I-03	Steve Zimmerman	Supramolecular Catalysis Using Single Chain Polymeric Nanoparticles as a Strategy for Performing Organic Synthesis in Living Cells
Supramolecular nanomaterials (SUP)			
THU 13 th , Room: 305			
Time	ID	Presenter	Title
Chairperson: Prof. Jay S. Siegel			
13.00-13.20	SUP-I-01	Mark A. Olson	Exploring the Optical Properties of Non-Stoichiometric Hydrates and Anhydrates of Donor-Acceptor Charge Transfer Salts
13.20-13.40	SUP-I-02	Ognjen S. Miljanic	Novel Aromatics as Precursors to Porous Molecular Crystals
13.40-14.00	SUP-I-03	Ivan Aprahamian	Hydrazone-Based Switches and Fluorophores
14.00-14.20	SUP-I-04	Ali Trabolsi	Synthesis and Applications of Metal-Organic Knots
Break & Poster Session			
Chairperson: Dr. Steve Zimmerman			
15.30-15.50	SUP-I-05	Ali Coskun	Tailoring Supramolecular Polymers for Gas Separation and Energy Storage Applications
15.50-16.10	SUP-I-06	Amar Flood	Fluorescent Materials by Hierarchical Assembly

Theory and simulation of nanosystem (THE)

WED 12th, Room: 307

Time	ID	Presenter	Title
Chairperson: Dr. Supawadee Namuangruk			
11.00-11.30	THE-K-01	Ruiqin Zhang	Carbon Nitride Films from Vacuum Free Depositions for Photoelectrochemical Applications
11.30-11.45	THE-O-01	Thodsaphon Lunnoo	In Silico Study of Gold Nanoparticle Uptake into Mammalian Cell: Interplay of Size, Shape, and Surface Charge
11.45-12.00	THE-O-02	Teeranan Nongnual	Velocity Autocorrelation Function as a Fast Estimation of Diffusion Coefficients
Lunch break			
Chairperson: Prof. Jianwen Liu			
13.00-13.20	THE-I-01	Kaito Takahashi	Issues on the Theoretical Simulation of Oxygen Reduction Reaction Catalysis
13.20-13.40	THE-I-02	Gang Feng	Exploring the Catalytic Property Of Cu-Al Spinel Towards Methanol Steam Reforming Reaction Using Density Functional Theory
13.40-13.55	THE-O-03	Salatan Duangdangchote	Effect of Electrolyte Additives on the Stability and Electrochemical Performance of Lithium-Sulfur Batteries
13.55-14.10	THE-O-04	Kunal Sharma	Surface Plasmon Resonance Sensor using Thin Film of Aluminium—a Theoretical Study
14.10-14.25	THE-O-05	Veerachart Paluka	Theoretical Study on Diels-Alder Reaction of Furan and Methyl Acrylate over Lewis Acidic Sn-BEA Zeolite
Break & Poster Session			
Chairperson: Dr. Kaito Takahashi			
15.30-15.50	THE-I-03	Jianwen Liu	Bridge the Catalysis and Electrocatalysis by First Principles
15.50-16.05	THE-O-06	Tanabat Mudchimo	Carbon-doped Boron Nitride Nanosheet as a Promising Metal-free Catalyst for NO Reduction: DFT Mechanistic Study
16.05-16.20	THE-O-07	Pongsakorn Chasing	Structure Activity Relationship on Pyridine-amine Nickel Complexes for Polyethylene Polymerization: Theoretical Study
16.20-16.35	THE-O-09	Unchittha Prasatsap	Equivalent Circuit Parameters of Hybrid Quantum-Dot Solar Cells
16.35-16.50	THE-O-10	Tinnakorn Saelee	The Reactivity and Selectivity of Ni(111) for Propane Dehydrogenation to Produce Propylene

Poster presentation session 1 (WED 14.30-15.30)

Nano-electronics photonics and optics (ELE)

ID	Presenter	Title
ELE-P-02	Chatphorn Theppitak	Color Tuning in Two Series of Lanthanide Coordination Polymers Base on Hydrazide Ligand
ELE-P-03	Jedsada Manyam	Test Cell for Electrical Double-Layer Capacitor
ELE-P-04	Ponart Aroonratsameruang	Revealing Charge Carrier Dynamics of Co ₃ O ₄ Film by Transient Absorption Spectroscopy (TAS)
ELE-P-05	Thannarasmi Khunsriya Samerpak	A Feasibility of Developing Crosslinked Poly(acrylic acid) for Use as a Solid Adhesive Electrolyte in Electrochromic Glasses

Nanomaterials and nanofabrication (FAB)

ID	Presenter	Title
FAB-P-04	Kay Khaing Oo	Effect of Substrate Temperature on GaAs Nanowires Growth Directly on Si (111) Substrates by Molecular Beam Epitaxy
FAB-P-05	Dat Quoc Dang	Preparation of Three-Dimensional PolyAspAm(EDA/EA)/TA-Graphene Aerogel Containing Silver NPs and the Antibacterial Property
FAB-P-06	Artit Ramdongbang	Biocompatibility and Bone Sensing Technology of Graphene Oxide Nanomaterial
FAB-P-07	Komthep Silpcharu	Novel Sulfonamido Spirobifluorenes as off-on Fluorescent Sensors for Mercury(II) Ion and Glutathione
FAB-P-08	Saowaluk Chaleawler-umpon	A Binder-Free and Sustainable Lignin Composite Electrode for Energy Storage Applications
FAB-P-09	Pichayada Techaniyom	Investigation of Osteopontin Protein and Gene Expression on Graphene Oxide Electrodeposited Titanium Implants
FAB-P-10	Lalida Suppaso	Electrochemical Characterization of Graphene Oxide Modified Electrodes Fabricated by Electrophoretic Deposition
FAB-P-11	Patsaya Anukunwithaya	A Simple and Eco-Friendly Method for Preparation of Tryptophan Intercalated Zinc Aluminium/Layered Double Hydroxide
FAB-P-12	Veerachart Paluka	Study of Butyl-Substituted Diquaternary Cations as Organic Structure Directing Agents in Synthesis of Pentasil Zeolites
FAB-P-13	Pawinee Siritongsuk	Long-Term Efficacy of Self-Disinfecting Coating by Nanomaterial for Decrease Incidence of Infectious Disease
FAB-P-14	Chaiyon Chaiwai	Red Organic Light Emitting Diodes Based on Benzothiadiazole-Thiophene Core fluorescent materials dope with CBP host
FAB-P-15	Siripak Jittirattanakun	Guest Exchange in Soft Porous Zinc(II) Supramolecular Compounds

Nanomedicine and pharmaceuticals (MED)		
ID	Presenter	Title
MED-P-01	Pongpat Oungeun	Materials for Sustain Release of Antibiotics in Bone Spacer
MED-P-03	Supatchaya Jaemsai	Development of Nanoparticles Containing Litsea glutinosa and Centella asiatica as a Promising Active Ingredient in Hair Care Product
MED-P-04	Waleewan Eaknai	Formulation and Characterization of Liponiosome Encapsulating Fenugreek Extract for Cosmeceutical Usages
MED-P-05	Angkana Jantimaporn	Effect of Nanoparticle Containing Butterfly pea as an Active Ingredient for Hair Treatment
MED-P-06	Thanyada Rungrotmongkol	QM/MM Study on Cleavage Mechanism Catalyzed by NS2B/NS3 Serine Protease of Zika virus
MED-P-07	Nutthanit Thumrongsiri	Lignin-Based Bioadhesive for Skin Retention of Topically Applied Compounds
MED-P-08	Narin Paiboon	Herbal Medicine-Loaded Nanostructure Lipid Carrier (NLC) for Topical Delivery System: Physicochemical and Bioactivity Properties
MED-P-11	Sathit Malawong	Antibacterial Synergistic of Ceftazidime with Silver Nanoparticles as a Possible Alternative for Treatment of Melioidosis
MED-P-12	Saengrawee Thammawithan	Anisotropic Silver Nanoparticles, an Alternative Treatment as the Effective Antimicrobial Agents

NanoSafety Technical Forum 2018 (SAF)		
ID	Presenter	Title
SAF-P-01	Chitrada Kaweeteerawat	Silver Nanoparticles Lead to Antibiotic Resistance in Bacteria

Theory and simulation of nanosystem (THE)		
ID	Presenter	Title
THE-P-10	Jittima Meeprasert	Theoretical Study of CO ₂ Hydrogenation on Cd ₄ /TiO ₂ Catalyst
THE-P-11	Panuwat Watthaisong	First-Principles Study of Electron Transport in α -V ₂ O ₅ Cathode Materials for Li-ion Batteries
THE-P-12	Nawee Kungwan	Excited State Proton Transfer (ESPT): Theoretical Study on Principal Photophysics of New Chromophores, Fluorescent Molecular Probes and Luminescent Materials
THE-P-13	Nootcharin Wasukan	In Silico Model for Prediction of Silver Nanoparticle-mediated Cytochrome P450 Enzyme Inhibition
THE-P-14	Nattida Maeboonruan	The Esterification Reaction of Propanoic Acid with Bioethanol on H-Beta zeolite: An ONIOM study
THE-P-15	Pattraporn Srirattanasakunsuk	The Glycerol Dehydration on UiO-66-SO ₃ H Catalyst : A DFT Study
THE-P-17	Rusrina Salaeh	Structural and Electronic Properties of Co ₁₃ and Ni ₁₃ clusters on α -Al ₂ O ₃ support: A Density Functional Theory Study
THE-P-18	Thantip Roongcharoen	Theoretical Insight into Methane Oxidation to Methanol on Single Fe-Embedded Nitrogen-Doped Graphene

Poster presentation session 2 (THU 14.30-15.30)

Nanotechnology for food, agriculture and environment (AGR)

ID	Presenter	Title
AGR-P-01	Thaksinan Chotchuang	Simple and Selective Colorimetric Detection for Fumonisin B1 in Corn Samples
AGR-P-02	Plernta Sukjarengaikul	Physicochemical Studies of Turmeric Nanoemulsions Using Different Sources of Turmeric Extracts
AGR-P-03	Siwapech Sillapaprayoon	Production and Characterization of Encapsulated Proteins from the Giant River Prawn
AGR-P-04	Somrudee Kaewmalun	Formulation and in vitro Evaluation of Bile Salt-Based NPs for Controlled Release of Essential Oils in Gastrointestinal Tract
AGR-P-05	Thanida Chuacharoen	Stability of Curcumin Loaded Nanoparticles Compared to Nanoemulsions under Thermal Processing and Storage Conditions
AGR-P-06	Thanawan Nitikriengkrai	Colorimetric Sensor for Shrimp Spoilage
AGR-P-07	Sirikorn Kitiyodom	Development of Mucoadhesive Nanovaccine Against Flavobacterium Columnare for Immersion Vaccination in Farmed Tilapia
AGR-P-08	Naiyaphat Nittayasut	The Cinnamon Oil Nanoparticles in pH-responsive Microsphere as an Antibiotic Alternative Against Food-borne Pathogens

Nanotechnology for catalysis and industry (CAT)

ID	Presenter	Title
CAT-P-02	Nopparat Thavornsin	Synthesis of Poly(aryleneethnylene)s Using Palladium Supported on Calcium Carbonate as Heterogeneous Catalyst
CAT-P-03	Anittha Prasertsab	The Catalyzing the Catalytic Hydrogen Transfer of Furfural to Furfuryl Alcohol over Lewis Acid Beta Zeolite
CAT-P-04	Preeyaporn Ruengrung	Synthesis of Bagasse Ash-Derived Silica-Aluminosilicate Composite for Methanol Adsorption
CAT-P-05	Orrakanya Phichairatanaphong	Synthesis of Silica-Aluminosilicate as a Support from Bagasse Ash
CAT-P-06	Marisa Ketkaew	Highly Efficient Metals-Modified Hierarchical MFI Zeolite for Selective Oxidation of Alcohols
CAT-P-07	Saros Salakhum	Bimetallic Pt-Ru over Hierarchical H-ZSM5 Nanosheets for Mild Hydrodeoxygenation (HDO) of Lignin-Derived Compounds
CAT-P-08	Siriluck Tesana	Hydrogenation of CO ₂ to Methanol Using Atomically Precise Ruthenium-Gold Containing Clusters Deposited on TiO ₂
CAT-P-09	Trin Saetan	Pd Nanoparticles Immobilized on Individual Calcium Carbonate Plate derived from Mussel Shell Waste: An Eco-Friendly Catalyst for Copper-Free Sonogashira and Suzuki Coupling Reactions

Nanotechnology for energy (ENE)

ID	Presenter	Title
ENE-P-02	Piyarach Srimara	Parametric Study on the Synthesis of Ni Nanochains for Cermet Selective Solar Absorbers by Chemical Reduction Method
ENE-P-04	Pimpisut Worakajit	Improving Charge Transport in CuSCN Hole Transport Layer by Anti-Solvent Treatment and Application in High-Efficiency Organic Solar Cells
ENE-P-05	Jidapa Chaopaknam	New Wide Band Gap Inorganic Semiconductor tin(II) Thiocyanate [Sn(NCS) ₂] as Its Application in Organic Solar Cell
ENE-P-07	Phitsamai Kamonpha	A Fast Route to Synthesis Hybrid Perovskite CH ₃ NH ₃ PbI ₃ by using Acetone as Iodine Reduction Agent during Methyl Ammonium Iodide Preparation
ENE-P-09	Thawalrat Ratanadachanakin	A Polycalixene Family as Potential Molecular Wires
ENE-P-10	Khamin Praweerawat	The Preparation and Characterization of SiO ₂ Films by Spray Coating Technique for Radiative Cooling Glass Application
ENE-P-11	Kenta Nakayama	The Effect of Ratio and Porous Structure of NiO/TiO ₂ Composite Film for Increasing Efficiency of Dye Sensitized Solar Cell
ENE-P-12	Napat Kaewtrakulchai	Activated Carbon from Palm Fiber via Microwave Assisted KOH Activation as Alternate Catalyst Supporter

Graphene and carbon nanotube (GRA)

ID	Presenter	Title
GRA-P-02	Pattraporn Tanawattanaprasert	Electrochemical Portable Mini-Potentiostat for Graphene Electrochemical Sensors
GRA-P-03	Theerapol Thurakitsee	Fingerprinting Seamless Single-Walled Carbon Nanotube Junctions and Diameter Modulation : Are SWNT Continuous with Different Diameters?
GRA-P-04	Thanakrit Thana-charoenchanaphas	A Study on the Performance of Digital Microfluidic Microchip with NrGO Electrochemical Detector fabricated by Screen Printing Method
GRA-P-05	Pacharabhorn Tanurat	The Effects on Proliferation and Differentiation of Bone-Forming Cells using Electrodeposited Graphene Oxide

Metal-oxide nanomaterials (MOX)

ID	Presenter	Title
MOX-P-01	Poonyawee Keattanong	Synthesis and Determination of Stability Constant of Meso-2,3-Dimercaptosuccinic acid for Complexation with Zinc Oxide Nanoparticles
MOX-P-02	Papada Natsathaporn	Comparison of Photocatalytic Property of Metal Oxides/Silica Nanofibers Fabricated by Different Processes

Nanotechnology for sensing and analysis (SEN)

ID	Presenter	Title
SEN-P-01	Sawinee Ngerpimai	Resonance Rayleigh Scattering Nano-Sensor for Hg ²⁺ Detection Based on Hg ²⁺ - DNA Complex Induced Gold Nanorods Aggregation
SEN-P-02	Piyaporn Matulakul	Gold Nanoparticle-Based Colorimetric Aptasensor for Rapid Detection of 8-Oxo-Dg in Urine
SEN-P-03	Pimporn Reoksrungruang	A Simple Paper-based Surface-enhanced Raman Scattering (SERS) for Cancer Cell Detection
SEN-P-04	Malinee Niamlaem	Carbon Nanofibers Prepared via C ₂ H ₂ -CO ₂ Reaction over Eggshell Waste with Gold Nanoparticles for H ₂ O ₂ Detection
SEN-P-05	Tanthip Eamsa-ard	Non-invasive measurement of Liver Disease for Monitoring Health Status by using Electronic Nose
SEN-P-06	Mon Myat Swe	Detecting Urinary Volatile Compounds by Electronic Nose for Early Diagnosis of Diabetes
SEN-P-07	Suchanat Boonkaew	A Label-Free Electrochemical Origami Paper-Based Immunoassay for C-Reactive Protein Detection in Human Serum
SEN-P-08	Shongpun Lokavee	Development of Low-cost Sleep Monitoring Systems
SEN-P-09	Kiattipoom Rodpun	Innovative Colorimetric Sensor for Detection of Chloramine by Using Nano Sodium Iodide in Amylose Helix
SEN-P-10	Ibrar Alam	Electrochemical Investigation on The Interaction of L-Cysteine with Lysozyme-Functionalized rGO/MnO ₂ /PPy Composite.
SEN-P-11	Suwadee Jiajaroen	Novel Lanthanide Coordination Polymers as Luminescent Probes for Small Organic Sensing
SEN-P-12	Chanika Pinyorosphatum	Anti-Aggregation of 2-Mercaptoethanesulfate Modified Silver Nanoplates for Detection of Phosphate on Paper-Based Device
SEN-P-13	Jirapa Rueangsuwan	Preparation of Reversible Thermochromic Polydiacetylene/Zn ²⁺ Nanocomposites in Aqueous Suspension and their Colorimetric Responses to Chemical Stimuli

Supramolecular nanomaterials (SUP)

ID	Presenter	Title
SUP-P-01	Auraya Manaprasertsak	Selectivity Encapsulation of Zingiber Cassumunar Roxb. Oil by Beta-Cyclodextrin Derivatives
SUP-P-02	Piyanan Pranee	Effective Fluorescence Probes Based on Nanomicelles for Specific Determination of Long-Chain Aldehydes

Abstract

Plenary Speakers

Plenary Lecture I

Self-Assembled Supramolecular Nanosystems for Smart Diagnosis and Targeted Therapy of Intractable Diseases

Kazunori Kataoka

*Innovation Center of NanoMedicine, Kawasaki Institute of Industrial Promotion,
Kawasaki 210-0821, Japan; Policy Alternatives Research Institute, The University of Tokyo,
Tokyo 113-0033
kataoka@pari.u-tokyo.ac.jp*

Nanotechnology-based medicine (Nanomedicine) has received progressive interest for the treatment of intractable diseases, such as cancer, as well as for the non-invasive diagnosis through various imaging modalities. Engineered polymeric nanosystems with smart functions play a key role in nanomedicine as drug carriers, gene vectors, and imaging probes. This presentation focuses present status and future trends of supramolecular nanosystems self-assembled from designed block copolymers for therapy and non-invasive diagnosis of intractable diseases. Nanosystems with 10 to 100 nm in size can be prepared by programmed self-assembly of block copolymers in aqueous entity. Most typical example is polymeric micelle (PM) with distinctive core-shell architecture. PMs have several properties relevant for nanosystems, including controlled drug release, tissue penetrating ability, and reduced toxicity^{1,2}. Furthermore, smart functionalities, such as pH- and/or redox potential responding properties, can be integrated into the PM structure³. These smart PMs loaded with various chemotherapy reagents were evidenced to have a significant utility in the treatment of intractable and metastatic cancers, including pancreatic cancer⁴, glioblastoma⁵, and tumors harboring recalcitrant cancer stem cells (CSCs)⁶. Eventually, five different formulations of the PMs developed in our group have already been in clinical trials world-wide, including Japan, Asia, USA and European countries⁷.

Versatility in drug incorporation is another relevant feature of PMs for drug delivery. Nucleic acid-based medicine can be assembled into PM through the electrostatic interaction with oppositely-charged polycationic block copolymers⁸. In this way, siRNA- or antisense oligo (ASO)-loaded PMs were prepared, and their utility in molecular therapy of cancer has been revealed^{9,10}. Recently, PM-based imaging reagents were developed, opening a new avenue for the novel type of theranostic nanomedicines¹¹. PM-based nanosystems hold promise for the treatment of intractable diseases other than cancer. Very recently, we developed PMs decorated with glucose to crossing blood-brain barrier by recognizing glucose-transporter overexpressing on brain endothelial cells, indicating a novel route to deliver versatile drugs into brain for the treatment of neurodegenerative diseases, including Alzheimer's disease¹².

- (1) H. Cabral and K. Kataoka, *J. Control. Rel.* 190 (2014) 465-476.
- (2) Y. Matsumoto, et al, *Nature Nanotech.* 11 (2016) 533-538.
- (3) H. Cabral, K. Miyata, K. Osada, and K. Kataoka, *Chem. Rev.* 118 (2018) 6844-6892.
- (4) H. Cabral, et al, *Nature Nanotech.* 6 (2011) 815-823.
- (5) Y. Miura, et al, *ACS Nano* 7 (2013) 8583-8592.
- (6) H. Kinoh, et al, *ACS Nano* 10 (2016) 5643-5655.
- (7) N. Nishiyama, et al, *Cancer Sci.* 107 (2016) 867-874.
- (8) K. Miyata, et al, *Chem. Soc. Rev.* 41 (2012) 2562-2574.



- (9) H. Nishida, et al, J. Control. Rel. 231 (2016) 29-37.
- (10) K. Katsushima, et al, Nature Commun. 7 (2016) 13616.
- (11) P. Mi, et al, Nature Nanotech. 11 (2016) 724-730.
- (12) Y. Anraku et al, Nature Commun. 8 (2017) 1001.



Plenary Lecture II

Interfacing nanomaterials with biology: from CRISPR to antimicrobials

Vincent Rotello

Department of Chemistry University of Massachusetts-Amherst rotello@chem.umass.edu,

<http://www.umass.edu/rotellogroup/>

A key issue in the use of nanomaterials is controlling how they interact with themselves and with the outer world. Our research program focuses on the tailoring of nanoparticles of surfaces for a variety of applications, coupling the atomic-level control provided by organic synthesis with the fundamental principles of supramolecular chemistry. Using these nanoparticles, we are developing new strategies for biological applications. This talk will focus on the interfacing of nanoparticles with biosystems, and will discuss the application of self-assembled nanoparticles as delivery vehicles. We will demonstrate the delivery of proteins and nucleic acids into the cytosol, including in vitro and in vivo delivery of functional CRISPR genome editing systems. Finally, this presentation will also feature the use of nanoparticles as therapeutics against multi-drug resistant bacteria, providing a potential strategy for combatting this emerging threat.

Abstract

Keynote Speakers

Mag(net)ic Nanaocatalysts – Concepts and Applications

Benjamin Kastl, Lisa Stadler, Andreas Hartl, Maryam Homafar, O. Reiser*

Department of Organic Chemistry, University of Regensburg, 93053 Regensburg, Germany

e-mail: oliver.reiser@chemie.uni-regensburg.de

Sustainability is the edifice for the development of efficient chemical processes. Catalytic transformations are especially attractive owing to the generally mild and selective reaction conditions and the reduction of waste byproducts. Nevertheless, even catalysts need to be efficiently removed from a reaction mixture, often down to the ppm levels due to the toxicity of some transition metals that are being used. Magnetic nanoparticles are attractive platforms for catalysts and reagents, which can be rapidly and quantitatively removed with the aid of an external magnet. Choosing examples from our research group, strategies for covalent and non-covalent immobilization of catalysts, emphasizing the incorporation of catalytically active nanoparticles into magnetically supported, microporous polymers will be discussed. The resulting catalysts are applied to industrially relevant applications such as the hydrogenation of alkenes and arenes, derived from renewable resources, in organic or aqueous solvent systems.

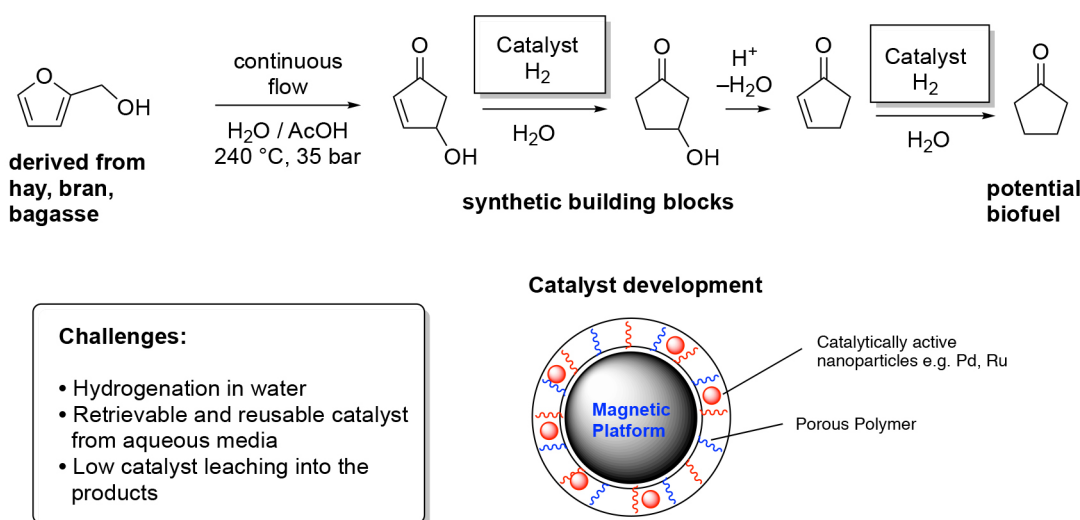


Figure 1. A green road to cyclopentenone and cyclopentanone

Leading Reference

O. Reiser, *Acc. Chem. Res.* **2016**, *49*, 1990-1996.

Making and Breaking of Chemical Bonds Using Visible Light and Nano Photocatalysts

Burkhard König

Faculty of Chemistry and Pharmacy, University of Regensburg, Regensburg, Germany

Burkhard.koenig@ur.de

The use of visible light in organic synthesis has received a lot of attention over the last decade,¹ although the idea was promoted already more than 100 years ago.² Visible light is easily generated, safe, leaves no trace as a reagent in the reaction mixture and can provide energy to initiate kinetically hindered or even endothermic reactions.

We have developed homogeneous photocatalysts that allow utilizing more than one photon for bond activation. Stable aryl chloride bonds can be activated for synthesis by visible light using this technology.^{3,4}

Quantum dots are extremely photostable and therefore ideal photocatalysts. We discuss the use of visible light absorbing quantum dots as photocatalysts in synthesis.⁵ Mesoporous carbon nitrides are photocatalytically active and combine several advantages if used in synthetic photocatalysis: The material is very stable against aggressive chemical reagents or intense irradiation; it can be easily recycled and due to its two-dimensional surface new reaction pathways can be opened.⁶

References

- ¹ L. Marzo, S. K. Pagire, O. Reiser, B. König, *Angew. Chem. Int. Ed.* **2018**; DOI:10.1002/anie.201709766.
- ² G. Ciamician, *Science* **1912** September 27.
- ³ I. Ghosh, T. Ghosh, J. I. Bardagi, B. König, *Science* **2014**, *346*, 725.
- ⁴ I. Ghosh, B. König, *Angew. Chem. Int. Ed.* **2016** *55*, 7676.
- ⁵ A. Pal, I. Ghosh, S. Sapra, B. König, *Chemistry of Materials* **2017**, *29*, 5225.
- ⁶ A. Savateev, I. Ghosh, B. König, M. Antonietti, *Angew. Chem. Int. Ed.* **2018**; <http://dx.doi.org/10.1002/anie.201802472>

Acknowledgements

We thank the German Science Foundation (GRK 1626) for financial support. This project has received funding from the European Research Council (ERC) under the European Union's Horizon 2020 research and innovation programme (grant agreement No 741623).



Melt-Processed Polyethylene Products Containing Micro-Fibrillated Cellulose Fibers

Yuta Sekiguchi, Wataru Takarada, Takeshi Kikutani

Department of Materials Science and Engineering, Tokyo Institute of Technology

INTRODUCTION

Cellulose nanofiber (CeNF) is considered to be a good candidate as a filler for the composite materials, especially for the composites of commodity plastics. However, mass production of CeFRP still remain a great challenge because of its time consuming process and high cost. Thus, developing a new CeFRP processing strategy to overcome these problems has been set as the next challenge. Reactive micro-Fibrillation Extrusion Process (RFE process) is one of the new processes proposed recently. In this work, we focused on the CeFRP prepared by the RFE process, and investigated the effect of melt processing conditions on the structure and mechanical properties of final products.

EXPERIMENTAL

Melt spinning of CeFRP was carried out with the extrusion temperature and the mass-throughput rate of 200 °C and 5 g/min, respectively. To maintain reasonable spinnability, only 1 wt% of wood pulp was blended into commercial high density polyethylene (HDPE, MFR=5.0). Take-up velocity was changed from 0.5 km/min to the attainable maximum speed. Injection molding of various types of CeFRP with the wood pulp content of 10 or 20 wt% was also carried out at the injection and mold temperatures of 160 and 30 °C, respectively, and the injection speed of 20 mm/s. Structure and its distribution in the cross-section of the melt-processed products were characterized mainly utilizing the wide-angle X-ray diffraction and laser-Raman spectroscopy measurements. Mechanical properties of the products were also examined.

RESULTS AND DISCUSSION

In the melt-spun CeFRP fibers, bimodal crystalline orientation distribution with ordinary c-axis oriented PE crystals and a small amount of the c-axis oriented crystals of extremely high degree of orientation. Azimuthal intensity distributions of (200) reflection for the neat PE and CeFRP fibers prepared at various take-up velocities are compared in Fig.1. It was considered that the mechanical properties of the melt-spun CeFRP fibers was improved in comparison with the neat PE fibers at the same spinning condition not only by the incorporation of oriented CeNF but also by the enhancement of the orientation of PE molecules.

In the injection molded products of CeFRP, orientation of PE crystal was suppressed at the skin and enhanced in the core in comparison with the neat PE products as shown in Fig.2. On the other hand, degree of orientation of CeNF in the injection molded products was rather uniform with the orientation factor of around 0.4 throughout the thickness direction. It was speculated that the increase in the orientation of PE crystals in the core was due to the development of trans-crystals from the surface of the oriented CeNF. Tensile modulus and tensile strength of the injection molded products were improved through the incorporation of CeNF, addition of maleic anhydride HDPE, and the use of the wood pulp of higher L/D. Tensile modulus was exclusively improved with the increase in the composition of the wood pulp of higher L/D.

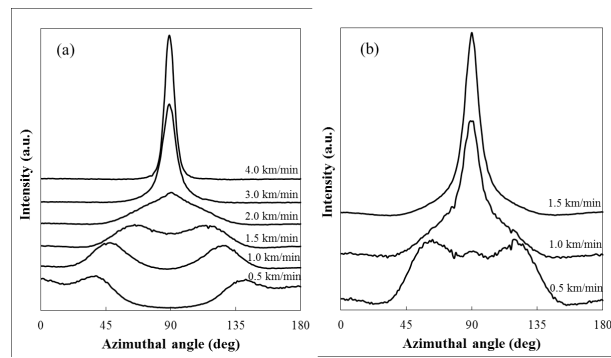


Figure 1. Azimuthal intensity distribution of (200) reflections of HDPE crystals for (a) Neat PE and (b) CeFRP fibers prepared at various take-up velocity.

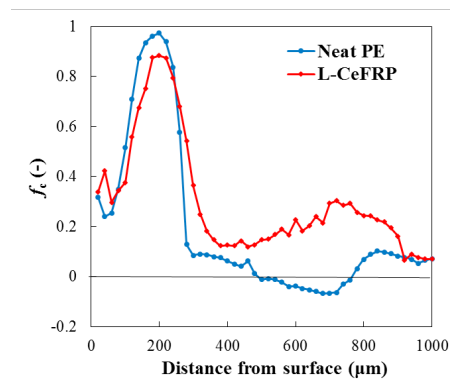


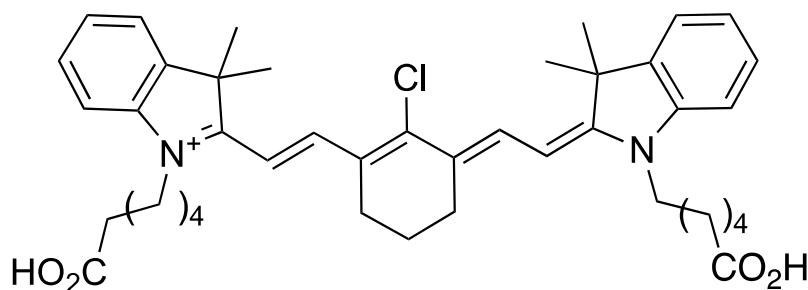
Figure 2. Orientation distribution of PE crystals along thickness direction in injection molded products of neat PE and CeFRP.

On “Tumor-seeking” Near IR-Dyes

Kevin Burgess

*Texas A & M University, Department of Chemistry
PO Box 30012, College Station, TX 77842-3012, USA
burgess@tamu.edu*

Cyanine **A** is typical of an elite group of “tumor-seeking” dyes known to accumulate in tumors *in vivo*. Fluor **A** in mice is easily visualized in animal studies because light used to excite at its absorption maxima, near 780 nm, penetrates tissue well, and because its quantum yield is acceptable for detection. Dyes like this are precious tools for *in vivo* optical imaging because they conspicuously reveal tumor tissue.



A

$\lambda_{\text{max abs}} \sim 780 \text{ nm}$, $\lambda_{\text{max emis}} \sim 800 \text{ nm}$

This talk will discuss what was known about **A** is imported into tumor cells, and data from our lab that furthers this understanding of how it accumulates in cancer tissues. A novel derivative of **A** will also be described; this dye, we call it **QCy**, has complementary solubility characteristics and similar photophysical properties. Both **A** and **QCy** have been modified to become near-IR sensitizers for singlet oxygen production with potential applications in photodynamic therapy. Modifications and applications of fluors like **A** and **QCy** in theranostics for treatment and optical imaging of cancer will also be covered.

Enhanced Spectroscopies of Semiconductor Nanostructures

Dietrich RT Zahn

Semiconductor Physics, Chemnitz University of Technology

Email: zahn@physik.tu-chemnitz.de

The ever decreasing dimensions of components in (opto-)electronic devices towards the nanometer scale clearly reveals the need for optical spectroscopies to be sensitive to ultra-small amounts of matter as well as break the diffraction limit of light in order to achieve ultra-high lateral resolution. Raman spectroscopy is a widely used optical spectroscopy as it provides a vast amount of information including *e.g.* composition, strain, crystal structure, and crystallinity.

Here I will first review techniques to enhance the Raman signals of very small amounts of material. One important ingredient of enhancing Raman signals is employing resonance excitation, *i.e.* choosing the exciting laser photon energy so that it coincides with a maximum in optical absorption. Often resonance enhancement alone is not sufficient when the amount of matter is very small, for instance for detecting the Raman spectrum of a few or even a single nanostructure. Then further enhancement strategies need to be engaged such as interference-enhanced Raman spectroscopy (IERS) and in particular surface-enhanced Raman spectroscopy (SERS). In the case of SERS manifold realisations using ordered nanostructured surfaces with various metals have been applied. The metallic nanostructures can be prepared by expensive techniques such as electron beam lithography or less expensive ones such as nanosphere lithography or films on nanospheres. Signals can be even further enhanced by combining metal nanostructures with photonic crystals.

The last part of the lecture will be devoted to achieving lateral resolution on the nanoscale using tip-enhanced Raman spectroscopy (TERS). The technique requires the combination of a Raman spectrometer and an atomic force microscope using a conductive tip for the plasmonic enhancement so that the lateral resolution is determined by the tip radius. Giant enhancement is observed when detecting the Raman spectra of materials in the plasmonic gap between the metallic tip and metallic nanostructures. Finally the detection of the Raman spectrum of a single semiconductor quantum dot is demonstrated.

Development of Plasmonic Organic Devices and Biosensors

Akira Baba*, Supeera Nootchanat, Chutiparn Lertvachirapaiboon, Kazunari Shinbo, Keizo Kato

Graduate School of Science and Technology, Niigata University,

8050 Ikarashi 2-Nocho, Nishi-ku, Niigata 950-2181, Japan

*ababa@eng.niigata-u.ac.jp

Surface plasmon resonance (SPR) phenomena have attracted considerable attention since many years because of the extremely strong enhancement and confinement of electric fields near metal surfaces. Recently, we have studied grating-coupled surface plasmon-based multiple plasmonic structures for electric-field enhanced organic device applications such as biosensors and photo-electric conversion devices as shown in Figure 1¹⁻⁷. We have focused on utilization of plasmonic properties of different kind of nano-objects (i.e., metallic grating and metal nanostructures) to improve the efficiency of thin-film OSCs and transmission type surface plasmon sensor applications. Furthermore, we studied simultaneous propagating surface plasmon and localized surface plasmon excitations for the improvement of the devices. In this talk, we will introduce our recent progress on surface plasmon enhanced devices.

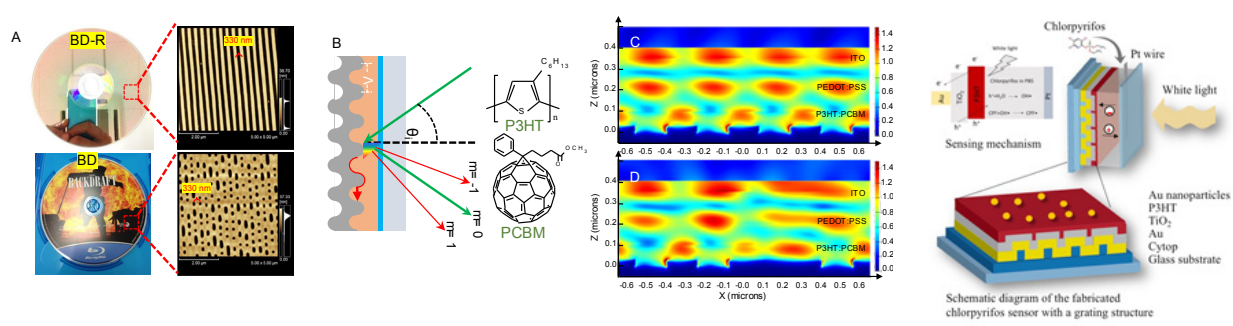


Figure 1. (A) Photographs and AFM images of BD-R and BD. (B) schematic of an OSC device with grating structures. FDTD simulations of the electric field in the OSCs with (C) BD-R and (D) BD grating structures. (E) plasmonic photoelectrochemical sensor

References

- Baba, A.; Tada, K.; Janmanee, R.; Sriwichai, S.; Shinbo, K.; Kato, K.; Kaneko, F.; Phanichphant, S. *Adv. Funct. Mater.* **2012**, *22*, 4383-4388.
- Lertvachirapaiboon, C.; Baba, A.; Ekgasit, S.; Shinbo, K.; Kato, K.; Kaneko, F. *Biosens. Bioelectron.* **2018**, *99*, 99-415.
- Nootchanat, S.; Pangdam, A.; Ishikawa, R.; Wongravee, K.; Shinbo, K.; Kato, K.; Kaneko, F.; Ekgasit, S.; Baba, A. *Nanoscale*, **2017**, *9*, 4963.
- Hara, K.; Lertvachirapaiboon, C.; Ishikawa, R.; Ohdaira, Y.; Shinbo, K.; Kato, K.; Kaneko, F.; Baba, A. *Phys. Chem. Chem. Phys.*, **2017**, *19*, 2791-2796.
- Pangdam, A.; Nootchanat, S.; Ishikawa, R.; Shinbo, K.; Kato, K.; Kaneko, F.; Thammacharoen, C.; Ekgasit, S.; Baba, A. *Phys. Chem. Chem. Phys.*, **2016**, *18*, 18500-18506.
- Pangdam, A.; Nootchanat, S.; Lertvachirapaiboon, C.; Ishikawa, R.; Shinbo, K.; Kato, K.; Kaneko, F.; Ekgasit, S.; Baba, A. *Part. Part. Syst. Character.*, **2017**, *34*, 1700133.
- Thepudom, T.; Lertvachirapaiboon, C.; Shinbo, K.; Kato, K.; Kaneko, F.; Kerdcharoen, T.; Baba, A. *MRS Comm.* **2018**, *8*, 107.

Case Study on the Mechanism of Heterogeneous Catalysis

Ken-ichi Shimizu

Institute for Catalysis, Hokkaido University, N-21, W-10, Sapporo, 001-0021, Japan

1. W-V oxides for selective oxidation

Ammonoxidation and oxidation of toluene by V-based catalysts are typical examples of redox/acid cooperative catalysis. V-loaded catalysts in the previous reports show low yields and have limited information on atomic level surface structure. Considering that WO_x is acidic co-catalyst for V-catalysts, W-V oxides with “M1 phase”-like structure can act as effective catalysts for selective oxidation, through such materials have not reported in the literature. In this presentation, we show the first example of the W-V oxide with M1 phase-like local structure, which is highly effective for ammonoxidation of toluene, Eqn. (1), and oxidation of toluene to benzoic acid, Eqn. (2).

W-V complex metal oxide with W/V ratio of 83/17 (W83V17) was prepared by hydrothermal synthesis method. Characterization of W83V17 showed three structural features: (i) layered-type structure characterized by diffraction peaks at $2\theta = 23^\circ$ and 46° due to the (0 0 1) and (0 0 2) planes of the layered structure along c-axis direction, (ii) long rod-shaped crystal morphology due to stacking of the layers along the c-axis by sharing the apex oxygen, (iii) the presence of micropore. Atomic resolution HAADF-STEM observation and its intensity analysis shows the ordered *a-b* plane structure which is composed of W_6O_{21} pentagonal units which are linked with MO_6 (M=V or W) octahedra forming hexagonal and heptagonal channel. The outermost layer of the heptagonal channel consists of VO_6 adjacent to WO_6 . Crystallites of orthorhombic phase (“M1 phase”) are also observed (Fig. 1). W83V17 shows higher yields than the previously reported catalysts for ammonoxidation of toluene to benzonitrile, and the selective oxidation of toluene to benzoic acid. Combined with the mechanistic results of in situ IR, we propose a catalyst design concept based on cooperation between redox sites (VO_6) and adjacent WO_x -based acid site at the heptagonal channel on the *a-b* plane.

I will show other two mechanistic studies of heterogeneous catalysis: (1) Cu-zeolites for NH_3 -SCR, and (2) Pt nanoparticle catalysts for organic synthesis and biomass transformation.

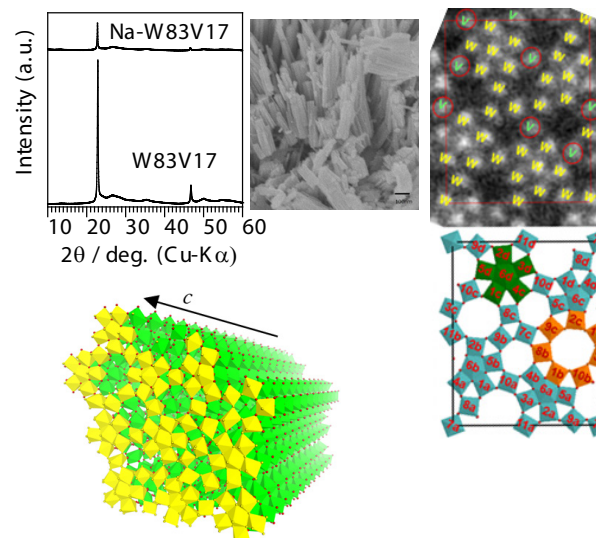
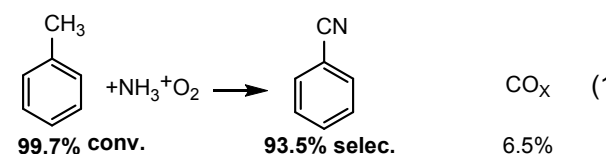
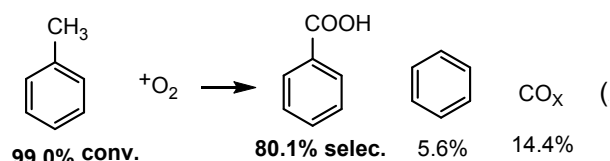


Figure 1. XRD patterns, SEM and HAADF-STEM images, and polyhedral models of microporous and layered W-V oxide (W83V17). The top layer of the model is highlighted in yellow.



toluene/ $NH_3/O_2/He = 1/10/4/34$, 400°C , $W/F=2.45 \text{ g s mL}^{-1}$.



toluene/ $O_2/He = 1/10/4/34$, 400°C , $W/F=2.45 \text{ g s mL}^{-1}$.

Glass and Liquid Metal-Organic Frameworks for Energy Application

SATOSHI HORIKE

Kyoto University, Institute for Integrated Cell-Material Sciences, Institute for Advanced Study

Metal-organic frameworks, MOFs or coordination polymers (CPs) constructed from metal ions and bridging molecular ligands are promising materials for energy-related application. They work as electrolyte for fuel cell/battery, electrocatalyst, functional carbon precursor for example.

Recently we have focused on the glassy and liquid states of MOF/CP crystals (Figure 1).^[1] Some of them show stable liquid state upon heating, and we fabricate glassy state of MOF/CPs by quenching. The glasses show unique physical and chemical properties. We found permanent microporosity, or high proton conductivity in glassy state. X-ray total scattering/adsorption, solid-state NMR measurements suggest the glassy state retain identical coordination geometry to those in the crystalline states, and even network structures. Some MOF/CP crystals directly transform to glassy state by mechanical milling.^[2] They also have an ability to capture reactive molecules by a simple co-milling technique.^[3] Potential of MOF/CPs in liquid/glass states as a functional materials will be discussed.

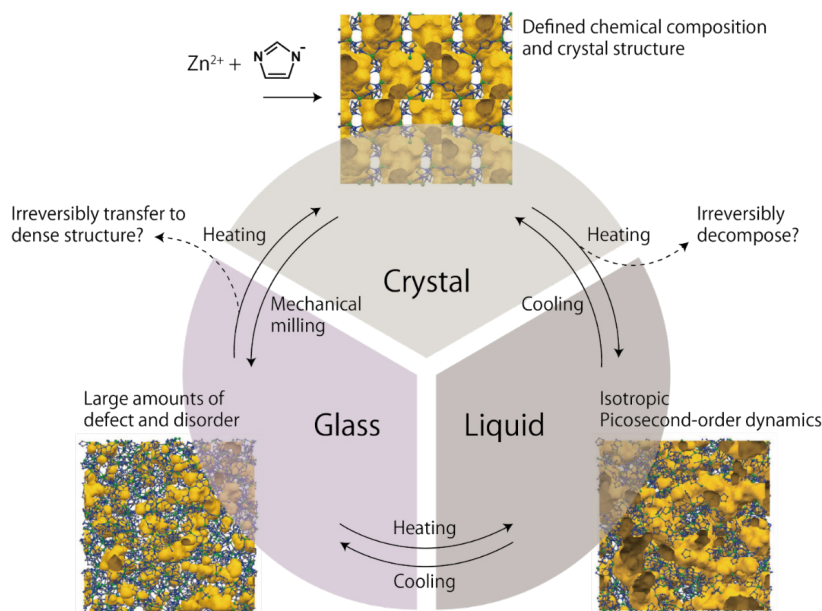


Figure 1. Scheme of phase diversity of metal-organic frameworks or coordination polymers.

References

1. *Nat. Rev. Mater.* 2018, in press. <https://doi.org/10.1038/s41578-018-0054-3>
2. *Angew. Chem. Int. Ed.* 2016, 55, 5195.
3. *Chem. Commun.* 2018, 54, 6859.

Self-Adjuvanting Lipopeptide Nanoparticulate Vaccine Candidates

Istvan Toth^{1,2,3}, Rachel J Stephenson¹ and Mariusz Skwarczynski¹

¹ School of Chemistry and Molecular Biosciences, The University of Queensland, Brisbane, QLD, Australia

² School of Pharmacy, The University of Queensland, Brisbane, QLD, Australia

³ Institut for Molecular Bioscience, The University of Queensland, Brisbane, QLD, Australia

The development of an effective vaccine for group A streptococci (GAS) has been challenged by the induced autoimmunity of epitopes derived from the C-repeat regions, unsuitable B-cell epitopes that have been shown to react with human heart tissue, and the minimal B-cell epitopes, which believed to be safe, shows little or no immunogenicity unless bound to a delivery platform including the conjugation to an inbuilt adjuvant. The relationship between a vaccine's physicochemical properties and the type of immune response acquired is critical for the advancement of vaccine adjuvants. This underpins our goal to study the structure-activity relationship between self-adjuvanting lipid-based vaccine candidates containing a model ovalbumin (OVA) CD4 and CD8 peptide epitopes (Fig 1) to determine the optimal architecture for stimulation of potent cell-mediated immune responses. Constructs that formed small nanoparticles showed higher cytolytic activity and enhanced tumour growth inhibition. Based on these findings, self-adjuvanting lipid core peptide (LCP) liposome systems where the antigen(s), carrier and adjuvant were within the same molecular entity has been developed.

Vaccine candidates with longer lipids at the N-terminus of the OVA CD4 epitope formed long β -sheet fibrils, and induced higher CD8⁺ T cell proliferation and IFN- γ secretion compared with constructs containing an internal placement of lipids. Constructs that formed small nanoparticles showed higher cytolytic activity and enhanced tumour growth inhibition.

The LCP amphiphilic construct was incorporated into liposomes to produce particles with the desired size. The construct alone elicited high-levels of antibody titers comparable to that of the positive control (J14 + Complete Freund's Adjuvant). Large proportion of systemic antibodies elicited by J14-D immunized mice recognised also native GAS M protein derived sequence p145. The developed strategy to produce nanoparticles, consisting of a peripheral antigenic epitope layer conjugated to a dendrimer core, which is both self-adjuvanting and produces a strong immune response to the GAS M-protein, offers an attractive alternative to conventional vaccine approaches (even after oral administration).



Figure 1. The model OVA vaccine

References

Marasini N, et al. *Biochemical Compounds*. **2017**;5(1). <http://dx.doi.org/10.7243/2052-9341-5-1>
 Sharareh Eskandari et al. *Chemistry A Eu. J.* Accepted 1 May 2018; 0.1002/chem.201801378

Keywords: vaccine delivery, immunoadjuvant, nano-vaccine

Development of a Microdevice for Reduction of Nitrate Ion Including Micro-Tubular Carriers Made of Copper

Yukako Asano^{a,*}, Shigenori Togashi^a, Yuzuru Ito^b, Yoshishige Endo^c, and Ryo Miyake^c

^aResearch & Development Group, Hitachi, Ltd., Japan

^bIndustrial Products Business Unit, Hitachi, Ltd., Japan

^cDepartment of Bioengineering, School of Engineering, The University of Tokyo, Japan

*e-mail: yukako.asano.dp@hitachi.com

Introduction

Nitrite-nitrogen is one of the required analysis items in water quality management. Quantitative analyses for nitrite-nitrogen require the reduction of nitrate ion to nitrite ion with a cadmium-copper (Cd/Cu) column and a large amount of waste solution including heavy metal ions is a challenge. In this study, we developed a simple microdevice for reduction of nitrate ion including micro-tubular carriers made of copper to obtain quantitative performance of reduction.

Experimental Methods

Seven pieces of micro-tubular carriers made of copper were layered in the straight portions of the channel of a square 2 mm in a microdevice for reduction. Here, the micro-tubular carriers were used whose outer diameter and inner diameter of 0.5 mm and 0.2 mm, respectively (Figure 1).

The performance of the microdevice for reduction was evaluated by reduction of nitrate ion in nitric acid aqueous solutions of 2.5×10^{-3} , 5×10^{-3} , 10^{-2} , and 2×10^{-2} mmol/L as samples and a solution of 10^{-2} mmol/L was defined as a reference. Nitric acid aqueous solution was introduced into the microdevice for reduction in a chemical analysis unit. Nitrate ion was reduced on the surfaces of the micro-tubular carriers made of copper and the reduced solution was obtained.

The nitrite ion was analyzed using naphthylethylenediamine absorptiometry. A chromogenic reaction between nitrite ion and a reagent proceeded in the micro-reaction channel after mixing. The obtained solution was introduced into an optical flow cell and analyzed at a wavelength of 525 nm.

Experimental Results and Discussion

Nitrate ion was reduced to nitrite ion using a microdevice for reduction. As shown in Figure 2, the reduction efficiency reached 100% for quarter concentration of the reference solution at longer than 22.7 min. The ratios among the reduction efficiencies for the concentrations of nitric acid aqueous solution were approximately inversely proportional to the ratios among the concentrations of nitric acid aqueous solution at 22.7 min and 30.4 min just after the reduction efficiency reached 100% for quarter concentration of the reference solution. Therefore, quantitative performance of reduction of nitrate ion was obtained using the microdevice for reduction including micro-tubular carriers made of copper.

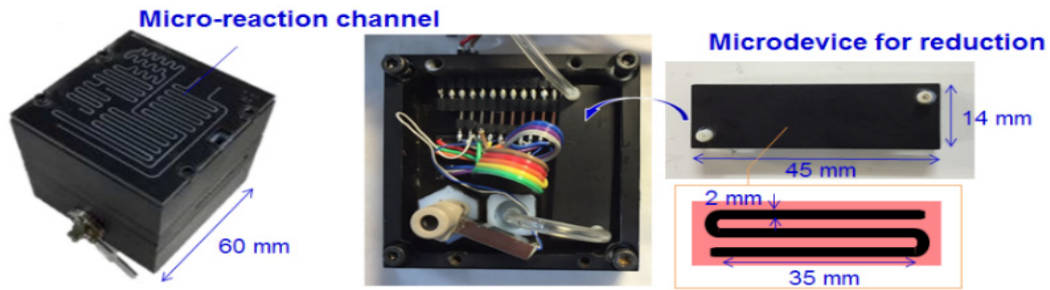


Figure 1. Chemical analysis unit including the microdevice for reduction

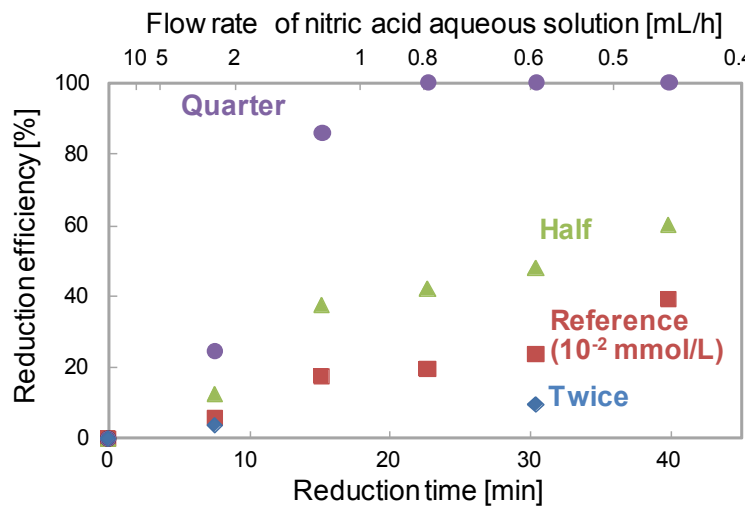


Figure 2. Dependence of the reduction efficiency on the reaction time

Acknowledgments

This work was supported by CREST, Japan Science and Technology Agency (JST).

Keywords: Microdevice, Reduction, Nitrate Ion, Nitrite Ion, Water Quality



Corannulene, Chirality and CIP

Jay S. Siegel

Tianjin University

Corannulene, a bowl-shaped polynuclear aromatic hydrocarbon, has C_{5v} symmetry in its static bowl form, and is distinctly not chiral. In contrast, all of the hydrogens of corannulene are chirotopic; therefore, simple substitution of H by X yields a chiral product. The study of chiral bowls opens up avenues of research in molecular dynamics, chiral recognition, stereo-selectivity and chiroptical properties. Extended chiral bowls exemplify new isomeric structures, which challenge the element of CIP as well as the concept of quantification of chirality.

References

1. Seiders, T.J.; Baldrige, K.K.; Grube, G.H.; Siegel, J.S. Structure/Energy Correlation of Bowl Depth and Inversion Barrier in Corannulene Derivatives: Combined Experimental and Quantum Mechanical Analysis. *J. Am. Chem. Soc.* 2001, 123, 517
2. Bandera, D.; Baldrige, K. K.; Linden, A.; Dorta, O.; Siegel, J.S. Stereoselective Coordination of C₅-Symmetric Corannulene Derivatives with an Enantiomerically Pure [Rh I(nbd*)] Metal Complex. *Angew. Chem. Int. Ed* 2011, 50, 865
3. Wang, Y.; Allemann, O.; Balaban, T.S.; Vanthuyne, N. Linden, A.; Baldrige, K. K.; Siegel, J.S. Chiral Atropisomeric Indenocorannulene Bowls: Critique of the Cahn–Ingold–Prelog Conception of Molecular Chirality *Angew. Chem. Int. Ed* 2018, 57, online [DOI: 10.1002/anie.201801325]

Carbon Nitride Films from Vacuum Free Depositions for Photoelectrochemical Applications

Rui-Qin Zhang

Department of Physics, City University Hong Kong, Hong Kong SAR

Beijing Computational Science Research Center, Beijing

E-mail: aprqz@cityu.edu.hk

Graphitic carbon nitride (g-CN) are promising materials for applications as photocatalysts for fuel conversion, degradation of organic pollutants, bioimaging and sensing, owing to their moderate band gaps, low cost and nontoxicity. In this presentation, I will first describe their electronic and optical properties derived from both computations [1] and experimental studies [2]. I will then introduce our work on synthesising g-CN films using a thermal vapor condensation method which is vacuum free and g-CN applications in photoelectrochemical (PEC) H₂ generation. The g-CN film shows photocurrent density as high as 0.12 mA cm⁻², the highest to date for g-CN based photoanode, at the bias of 1.35 V vs reversible hydrogen electrode with Na₂S as the sacrificial reagent [3]. Further, by copolymerizing 2, 6-Diaminopyridine molecules with melamine, C domains are incorporated into g-CN to adjust the electronic properties of g-CN, leading to significantly improved optical, electronic and PEC properties of the modified CN films. The optimal modified CN film exhibits a photocurrent density four times higher than the photocurrent density exhibited by the pristine g-CN film [4]. We are actively working on doping of g-CN material using efficient approaches [5,6] for practical PEC applications.

References

1. X. Ma, Y. Lv, J. Xu, Y. Liu, R.Q. Zhang, and Y. Zhu, *Journal of Physical Chemistry C*, **116**, pp 23485–23493 (2012)
2. J. Bian, J. Li, S. Kalytchuk, Y. Wang, Q. Li, T. C. Lau, T. A. Niehaus, A. L. Rogach and R.Q. Zhang, *ChemPhysChem*, **16**, 954 –959 (2015)
3. J. Bian, Q. Li, C. Huang, J. Li, Y. Guo, M. Zaw, R.Q. Zhang, *Nano Energy*, **15**, Pages 353–361 (2015)
4. J. Bian, L. Xi, J. Xu, C. Huang, A.L. Kathrin, M. Antonietti, R.Q. Zhang, M. Shalom, *Advanced Energy Materials*, **1600263** (2016)
5. Y.G. Yu, R.Q. Zhang et al. *Angew. Chem. Int. Ed.* **57**, xxx (2018); doi.org/10.1002/anie.201803928
6. M.Y. Huang, R.Q. Zhang et al. *Catalysis B: Environmental* (revised, 2018)



Abstract

Invited Speakers

Aerosol-Assisted Fabrication of Mesoporous Single-Site Organometallic Catalyst

Fang Zhang*

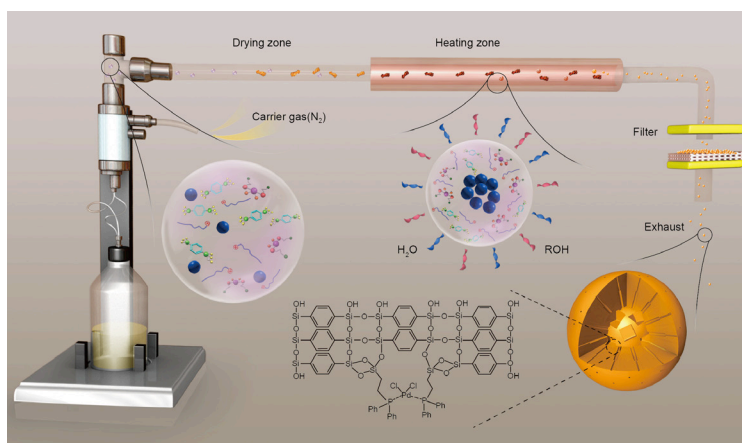
Department of Chemistry, Shanghai Normal University, Shanghai, 200234

*Corresponding author: zhangfang@shnu.edu.cn

Introduction

Homogeneous organometallic catalysts are widely used for the production of high-value fine chemicals.¹ Despite their high activity and selectivity, these catalysts are relatively expensive and cannot be recycled and reused.² Accordingly, heterogeneous organometallic catalysts (HOCs) are believed as an effective way to address these problems. However, the synthetic protocols of the reported HOCs were typically conducted in the tedious and time-consuming solution-based technique.³ Therefore, the development of a low-cost, facile and scalable approach for the fabrication of highly active HOCs is urgently needed.

Methodology



Scheme 1 Scheme for the preparation of mesoporous organometallic catalysts by an aerosol-assisted assembly method.

In this contribution, we reported an aerosol-assisted assembly technique that can be used as a low cost, rapid and scalable approach for the preparation of single-site heterogeneous organometallic catalysts with hierarchical porous structure. It was achieved by using organometallic silane ($M[PPH_2(CH_2)_2Si(EtO)_3]_2Cl_2$) as single-site active specie, organosilane 1,4-bis(triethoxysilyl)benzene ($Ph[Si(EtO)_3]_2$) as the silicate scaffold with surfactant cetyltrimethylammonium bromide (CTAB) and inorganic salt NaCl as the dual templates on a home-built aerosol spraying instrument (Scheme 1).

AGR-I-01

Results and Discussion

TEM image showed that the representative Pd-PPh₂-HOCs catalyst was comprised of uniform spheres with average size around 400 nm. It displayed the cubic cavities with diameter around 60 nm in the sphere chamber. Furthermore, the catalytic results revealed that these M-PPh₂-HOCs catalysts exhibited comparable activities and selectivities with the corresponding homogeneous catalysts in water-medium terminal alkynes acylation reaction, Suzuki reaction, isomerization reaction and Miyaura-Michael reaction, respectively. Meanwhile, they could be reused at least 10 times without significant decrease in catalytic activity, showing the good potential in the future industrial application.

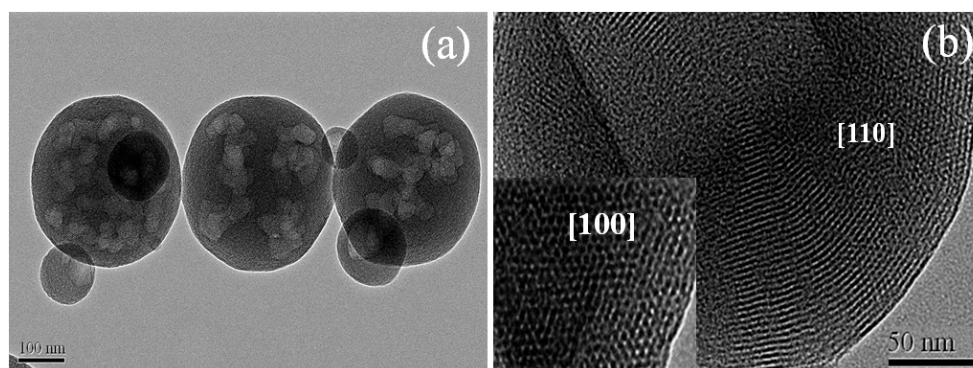


Figure 1 TEM image of Pd-PPh₂-HOC catalyst.

Conclusion

In summary, we have developed an aerosol-spraying approach for rapidly synthesizing mesoporous single-site organometallic catalysts with enhanced catalytic performances in the water-medium cross-coupling reactions.

References

- D.E. De Vos, M. Dams, B.F. Sels, P.A. Jacobs, *Chem. Rev.* 102 (2002) 3615–3640.
 S.E. Pratsinis, *AIChE J.* 56 (2010) 3028–3035.
 J.M. Thomas, R. Raja, D.W. Lewis, *Angew. Chem. Int. Ed.* 44 (2005) 6456–6482.

Keywords: Aerosol synthesis; Mesoporous catalyst; Organometallic



AGR-I-02



Technology to Aid Applications of Some Natural Product Extracts

Supason Wanichwecharungruang

Natural remedies have long been integrated with Thai people, and various traditional medicinal recipes have been practiced. With aids of modern science and technology, many bioactive molecules have been identified from edible plant extracts. Their biochemical activities and mechanisms of action have also been elucidated. Natural product industries have emerged into many modern consumable products. To strengthen this industry, technology that can tackle problems are required. Here the talk will focus on the use of cellulose encapsulation technology to both stabilize bioactive molecules and make them compatible in water medium.

Keywords: natural product extract; cellulose nanoparticles; encapsulation

Ethanol Dehydration Over Alumina-Based Catalysts

Jakrapan Janlamoon and Bunjerd Jongsomjit

Center of Excellence on Catalysis and Catalytic Reaction Engineering

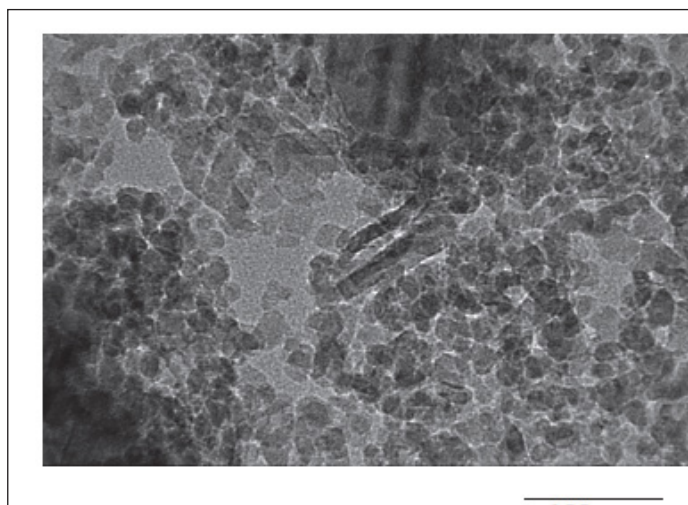
Department of Chemical Engineering, Faculty of Engineering

Chulalongkorn University

Bangkok 10330, Thailand

Corresponding author; e-mail: bunjerd.j@chula.ac.th

The study aims to investigate the catalytic dehydration of ethanol with the alumina-based catalysts. For instance, the nanocrystalline γ - and χ - aluminas that display the attractive chemical and physical properties. The correlation between the acid density and ethanol conversion was observed. The high acid density apparently results in high catalytic activity, especially for the equally mixed γ - and χ - phase alumina (G50C50). In order to obtain a better understanding on how different catalysts would affect the ethylene yield, one of the most powerful techniques such as X-ray photoelectron spectroscopy (XPS) was performed. Hence, the different O 1s surface atoms can be identified and divided into three types including lattice oxygen (O, 530.7 eV), surface hydroxyl (OH, 532.1 eV) and lattice water (H_2O , 532.9 eV). It was remarkably found that the large amount of O 1s surface atoms in lattice water can result in increased ethylene yield. In summary, the appearance of metastable χ -alumina structure exhibited better catalytic activity and ethylene yield than γ -alumina. As the result, it was found that the G50C50 catalyst exhibits the ethylene yield (80%) at the lowest reaction temperature ca. 250°C among other catalysts.



TEM image of γ - (wrinkled sheet) and χ - (spherical) aluminas

Keywords: ethanol dehydration, XPS analysis, solvothermal method, mixed phase alumina



CAT-I-02



Advanced Nanomaterials – Synthesis and Applications in Organic Transformations

Manoj B. Gawande

Regional Centre of Advanced Technologies and Materials, Faculty of Science, Department of Physical Chemistry, Palacky University, Olomouc, Šlechtitelů 11, 783 71, Olomouc, Czech Republic.

Email: manoj.gawande@upol.cz

(Prof. Manoj B. Gawande, PhD. FRSC)

Advanced nanomaterials have grown considerable admiration among the researchers as they are widely explored in important catalytic developments and benign organic transformations. The nanocomposites described would include magnetic-supported nanocatalysts, core-shell (Pd@Pt) catalysts and N-doped nanocatalysts. Advanced nanotechnology advances over the years have allowed important and exceptional series of advances in the evolution of benign heterogeneous nanocatalysts. Notably, nanomaterials for catalysis can now be designed and prepared with need for targeted catalytic applications. Core-shell nanocatalysts, iron-based nanocatalyst and NSO doped catalysts can be prepared via more ecological pathways with unique structure, morphology and composition. Our recent research activity on the use of advanced nanomaterials/nanocatalyst and its catalytic applications will be highlighted.

Recent Publications: Gawande *et al.* *Account of Chemical Research* 2014, 47, 1338–1348; *Chemical Society Reviews* 2013, 42, 3371-3393; *Green Chemistry* 2013, 15, 1895-1899, *ChemCatChem* 2014, 2014, 6, 12, 3312–3313; *ACS Catalysis* 2017, 7, 7038–7042.



CEL-I-01

Opportunities on Nanofibers Technologies; from Lab to Industry

Reza Faridi-Majidi

*Department of Medical Nanotechnology, School of Advanced Technologies in Medicine,
Tehran University of Medical Sciences, Tehran, Iran
Chairman of the Board of FNM Ltd, Tehran, Iran*

Nanofibers are an exciting new class of materials providing some fascinating properties (high surface area, ease of mass-production, flexibility in procedures and low-cost production) and usable for several value added applications such as medicine (including tissue engineering, wound dressings, drug releasing systems), biotechnology, air and liquid filtration, textiles, barrier, wipes, personal care, composite, garments, insulation, energy storage, sensors and biosensors. Nanofibers with a diameter range of a few nanometers to a micron can be achieved by choosing suitable electrospinning parameters. Nanofibers also have unique characteristics such as high surface area per unit mass, high porosity, excellent structural mechanical properties and high axial strength combined with extreme flexibility. An additional advantage of nanofibers technology is that they have been up-scaled for nanofiber production on an industrial scale. Meanwhile, science and technology related to nanofibers have been utilized in a variety of different areas that resulted in the annual publications of about 10,000 articles worldwide. Fortunately, some of nanofibrous products are now available on the market such as nano-enhanced air filters for cars and industry, respiratory mask, wound dressing, cell scaffolds. Now many companies in the world are developing the technologies related to nanofibers and their applications. This presentation will review our activities including academic research and industrial efforts in the field of nanofibers.



CEL-I-02

Shape Memory Mechanochromic Poly (Caprolactone): A Novel Approach for a Functional Color Changable and Shape Recoverable Polyester

Nattawat Yenpech ^a, Varol Intasanta^b and Suwabun Chirachanchai* ^{a,c}

^{a)} *The Petroleum and Petrochemical College, Chulalongkorn University, Bangkok, 10330, Thailand*

^{b)} *Nano Functional Textile Laboratory, National Nanotechnology Center (NANOTEC), National Science and Technology Development, Pathumthani, 12120, Thailand*

^{c)} *Center for Petroleum, Petrochemical, and Advance Materials, Chulalongkorn University, Bangkok 10330, Thailand*

Corresponding author e-mail : csuwabun@chula.ac.th

Up to the present, mechanochromic fibers have been known for the coating of microspheres consisting photonic crystals onto polymer fibers and the color changing is derived from the stretching. The different colors are realized by varying the diameter of microsphere to induce the changes of refractive index. Generally, polyester is widely used for fibers or clothes, however, the shape memory mechanochromic polyester fiber based on the polymer structure itself has never been reported. On this viewpoint, our group focuses on polycaprolactone (PCL) which is known as a biodegradable polymer and combine the concept of molecular design of hard and soft segments along with the mechanochromic molecule, i.e. spiropyran (SP) to achieve the shape memory mechanochromic PCL. The presentation will demonstrate the steps of preparation and the properties including the reversible and repeatable functions of color changing and shape recovery.

Characterization of Graphene by Plasmon, Manipulation of Plasmon by Graphene

Sanpon Vantasin^{*a}, Yukihiro Ozaki^b, Yoshito Tanaka^a, Tsutomu Shimura^a

^a*Institute of Industrial Science, The University of Tokyo*

^b*School of Science and Technology, Kwansei Gakuin University*

^{*}*e-mail: sanpon.vantasin@gmail.com*

This study consists of two parts. For the first part, nanostructures on graphene is explored by plasmon-assisted spectroscopy. Graphene nanostructures are important for true understanding of graphene because real graphene samples are not perfectly flat as usually portrayed. Electrical and mechanical properties of graphene can be significantly affected by nanoscale ridges, cracks, bumps, etc. One of the best techniques to characterize graphene is Raman spectroscopy which can reveal number of layers, doping, and strain of graphene. However, the spatial resolution of Raman spectroscopy is limited by diffraction limit ($\lambda/2NA$) and not enough to probe the nanostructures. This was overcome by tip-enhanced Raman spectroscopy (TERS), a technique utilizing enhanced electromagnetic field from confined surface plasmon at the apex of metallic tip. The improved resolution allowed the measurement of nanoscale strain on the nanoridge structures, which, for the first time, provided the evidence for the long-suspecting mechanism of nanoridge formation.

In the second part, we found that the nanoridge itself can produce surface plasmon when illuminated by mid-infrared (mid-IR) light. Surface plasmon in the mid-IR frequencies exists because graphene is a metal in these frequencies range. Previous researches have shown that with gold/silver nano-antenna, not only surface plasmon can be launched onto graphene sheet, but its wavefront and direction can be controlled as well. Nevertheless, these techniques require foreign object to be placed on graphene (introduce defect) and mid-IR illumination with precise angled (difficult). Both of these greatly limit the practicability. By using nanoridge as a plasmon launcher, these limitations are avoided because nanoridge itself is a natural part of graphene sheet. With a single nanoridge, we demonstrated that graphene plasmon can be launched onto flat part of graphene or confined on the ridge, depending on the relationship between plasmon wavelength and ridge curve length. Using double nanoridge with proper arrangements, graphene plasmon can be controlled to propagated to both direction or only one direction. Mixed-frequency illumination can also be separated into left and right propagating plasmon with different frequency.

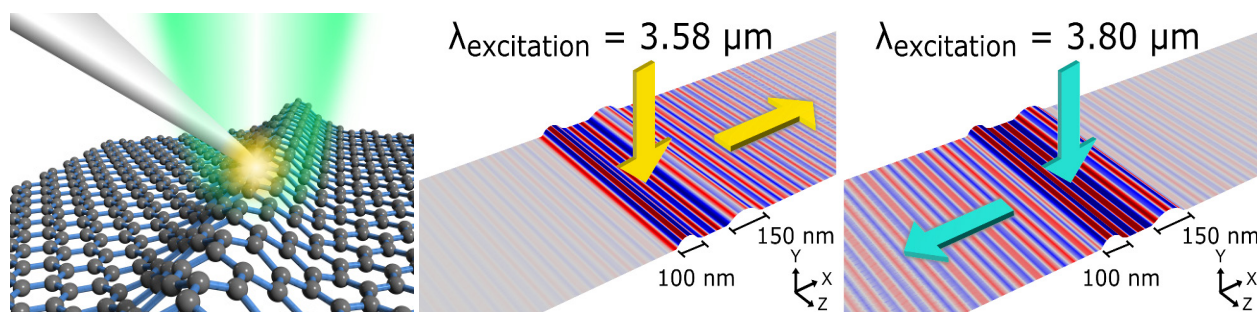


Figure 1. (left) Characterization of a graphene nanoridge by (plasmon-enhanced) TERS. (right) Graphene plasmon controlled by graphene nanoridges.

Keywords: surface plasmon, nanostructures, graphene, Raman spectroscopy

References

1. Vantasin, S. et al. *J. Phys. Chem. C* **2014**, *118*, 25809–25815.
2. Vantasin, S. et al. *Phys Chem Chem Phys* **2015**, *17*, 28993–28999.
3. Vantasin, S. et al. *ACS Photonics* **2018**, *5*, 1050–1057.



ENE-I-01



Molecular Switches and Memory Devices Based on Dynamic π -Conjugated Systems

Jean Roncali*

Group Linear Conjugated Systems, CNRS, Moltech-Anjou, University of Angers

2Bd Lavoisier, 49045 Angers, France

e-mail : jeanroncali@gmail.com

The switch of the electrical conductance of molecules or molecular architectures is a basic phenomenon which plays a key role for the design and study of nanoscale molecular switches and memories. Some years ago, we have shown that the geometry and hence effective conjugation of pi-conjugated oligothiophenes could be reversibly modified by means of a driving group introduced in a loop attached at two fixed points of the pi-conjugated system and sensitive to external chemical or physical stimulations.^{1,2}

In this presentation various examples of application of this principle to the control of the conductance of single photoswitchable molecular architectures will be presented and discussed on the basis of devices derived from Self-Assembled Monolayers (SAMs) and gold nanoparticles (GNPs) decorated with peripheral thiophene-based electropolymerizable or photoisomerizable conjugated systems.³⁻⁷

Keywords: Oligothiophenes, Molecular switches, Photoisomerization, Self-assembled monolayers, Gold Nanoparticles.

References

1. B. Jousselme, P. Blanchard, E. Levillain, J. Delaunay, M. Allain, P. Richomme, D. Rondeau, N. Gallego-Planas, J. Roncali, *J. Am. Chem. Soc.* **2003**, *125*, 1364.
2. B. Jousselme, P. Blanchard, N. Gallego-Planas, J. Delaunay, M. Allain, P. Richomme, E. Levillain, J. Roncali, *J. Am. Chem. Soc.* **2003**, *125*, 2888.
3. K. Smaali, S. Lenfant, S. Karpe, M. Oçafraïn, P. Blanchard, D. Deresmes, S. Godey, A. Rochefort, J. Roncali, D. Vuillaume. *ACS Nano*, **2010**, *4*, 2411.
4. T.K. Tran, K. Smaali, M. Hardouin, Q. Bricaud, M. Oçafraïn, P. Blanchard, S. Lenfant, S. Godey, J. Roncali, D. Vuillaume, *Adv. Mater.* **2013**, *25*, 427.
5. S. Lenfant, Y. Viero, C. Krzeminski, D. Vuillaume, D.
6. Demeter, I. Dobra, M. Oçafraïn, P. Blanchard, J. Roncali, C. Van Dyck, J. Cornil, *J. Phys. Chem. C.* **2017**, *121*, 12414. A. Yassin, M. Oçafraïn, P. Blanchard, R. Mallet, J. Roncali. *ChemElectroChem.* **2014**, *1*, 1312.
7. T. Zhang, D. Guérin, Alibart, D. Vuillaume, K. Lmimouni, S. Lenfant, A. Yassin. Oçafraïn, P. Blanchard, J. Roncali, *J. Phys. Chem. C.* **2017**, *121*, 10131.

The Dual Responsive Block Copolymers for Drug Delivery System with Spatiotemporal Precision

Hung-Hsun Lu^a, Cheng-Hung Huang^a, Ting-Yun Shiue^b, Fu-Sheng Wang^a, Ko-Kai Chang^a,
Yunching Chen^b, Chi-How Peng^{*a}

^a Department of Chemistry and Frontier Research Center on Fundamental and Applied Sciences of Matters, National Tsing Hua University, 101, Sec 2, Kuang-Fu Rd., Hsinchu 30013, Taiwan

^b Institute of Biomedical Engineering and Frontier Research Center on Fundamental and Applied Sciences of Matters, National Tsing Hua University, 101, Sec 2, Kuang-Fu Rd., Hsinchu 30013, Taiwan

*e-mail: chpeng@mx.nthu.edu.tw

The nanoparticle-based gene delivery systems for cancer therapy are always hampered by biological barriers to deliver effective gene therapeutics in cytoplasm. One of the major obstacles to gene carriers is a lack of driving forces to unpack encapsulated gene payloads beyond endosomal escape. Herein, we developed a core-corona micelles formed from the triblock copolymer of poly(ethylene glycol)-*b*-poly(N,N-dimethylamino-2-ethylmethacrylate)-*b*-poly(pyrenylmethyl methacrylate) (PEG-*b*-PDMAEMA-*b*-PPy) that undergo trinity-phase transition in response to light- and pH-stimuli. These triblock copolymer micelles can carry the siRNA with high stability in physiological condition and efficiently release the siRNA after the light irradiation. The nanostructural transformation was investigated to rationalize the high contrast between the stability and release efficiency before and after the photo irradiation (Figure 1). The photo-responsive micelleplexes formed by siRNA and PEG-*b*-PDMAEMA-*b*-PPy can protect siRNA from leakage and release siRNA in spatiotemporal precision and thus could be the next-generation gene delivery system.

Keywords: micelleplexes, siRNA delivery, photoresponsive block copolymer

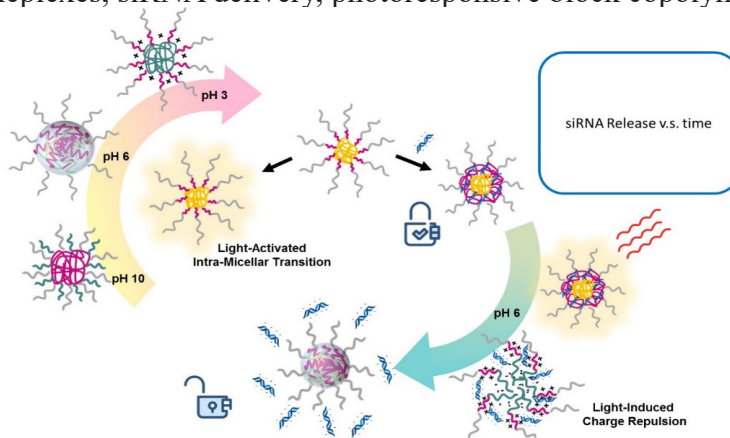


Figure 1. Illustration of mechanism for trinity-phase transition of nanoparticle, which is formed from siRNA and PEG-*b*-PDMAEMA-*b*-PPy, triggered by light- and pH-stimuli.

References

1. R. Kanasty, J. R. Dorkin, A. Vegas, D. Anderson, *Nat. Mater.* **2013**, *12*, 967–977.
2. M. Elsabahy, G. Heo, S.-M. Lim, G. Sun, K. L. Wooley, *Chem. Rev.* **2015**, *115*, 10967–11011.



ENE-I-03



Organic Field-Effect-Transistor with Strongly Correlated Electrons

Hiroshi M. Yamamoto¹

¹ Center of Integrative Molecular Systems, Institute for Molecular Science,
Myodaiji, Okazaki, Aichi 444-8585, Japan
E-mail: yhiroshi@ims.ac.jp

Molecular conductors are a class of materials that show high electrical conductivity. Some of them exhibit metallic conductivity and even superconductivity at low temperature, often associated with various phase transitions. Our interest is to utilize these electronic phase transitions in developing new and highly efficient electric devices. For this purpose, we have employed thin-layer crystal growth in electrochemical process to develop organic field-effect-transistors (FETs) with strongly correlated electron systems such as Mott-insulators. Mott-insulator is quite interesting material because it shows variety of phase transitions mentioned above. In our study, we employed κ -type BEDT-TTF, κ -(BEDT-TTF)₂Cu[N(CN)₂]X (X = Br: κ -Br, X = Cl: κ -Cl), as an organic Mott-insulator and expected ON/OFF switching of insulator-to-metal or insulator-to- superconductor transitions in the FET channel as well as photo excitation [1-8]. Indeed, by preparing high-quality thin-film single crystal of κ -Cl/Br laminated onto various kinds of substrates, we have succeeded in demonstrating gate-electric-field-induced and/or photo-induced Mott-transition and superconductivity at organic Mott-device. At the same time, the device mobility of the FET exceeded 200 cm²/Vs for some of the devices. Other kinds of stimuli such as mechanical strain have been also employed to induce the superconductivity in our recent studies.

References

1. Y. Kawasaki, et al, *Phys. Rev. Lett*, **103**, (2009), 116801.
2. H. M. Yamamoto, et al, *Nature Commun.* **4**, (2013), 2379.
3. M. Suda, et al, *Adv. Mater.*, **26**, (2014), 3490.
4. M. Suda, et al, *Science*, **347**, (2015), 743.
5. Y. Kawasaki, et al, *Nature Commun.* **7**, (2016), 1 2356.
6. Y. Sato, et al, *Nano Lett.* **17**, (2017), 708.
7. H. Yamakawa, et al, *Nature Mater.* **16**, 1100 (2017).
8. Y. Kawakami, et al, *Nature Photonics*, *in press*.

Design of New Organic Hole Transporting Materials and Effects of Doping for Perovskite Solar Cells

Maria Ulfa,^a Thierry Pauporté,^a Thanh-Tuân Bui,^b Fabrice Goubard,^b

^a *Chimie-ParisTech, PSL Research University, CNRS, Institut de Recherche de Chimie Paris (IRCP), 11 rue P. et M. Curie, F-75005 Paris, France. *Email: thierry.pauporte@chimie-paristech.fr*

^b *Laboratoire de Physicochimie des Polymères et des Interfaces, Université de Cergy-Pontoise, 5 mail Gay Lussac, 95000 Neuville-sur-Oise, France.*

The hole transporting material (HTM) is a key component of many highly efficient optoelectronic devices, especially of perovskite solar cells (PSCs). The study and optimization of the HTM remain a great challenge. The hole extraction/transport and the device stability are strongly dependent on the molecular structure and doping of the HTM. The use of organic HTM has allowed the PSC power conversion efficiency to steeply increase from 3.8% to 23.3% within only nine years. In a first step, we were interested in the comparison of molecular and polymeric HTMs (Ref 1). The electrical response of PSCs prepared with the benchmark molecular Spiro-OMeTAD HTM (Figure 1a) and the conducting polymer poly(3-hexylthiophene-2,5-diyl) (P3HT) (Figure 1b), selected as a low-cost and efficient polymer HTM, was compared. The device performance was improved in a much less extent by doping in the case of the polymeric HTM. The additives were shown to limit the charge recombination at the interface, to reduce the interfacial defects and to favor the hole transfer from the perovskite to the HTM layer. The conductivity increase was significant only in the case of the molecular HTM.

Developing new and cheap molecular HTMs is also an important topic. We have synthesized a new molecular dendritic core carbazole HTM, called B186, designed for PSC application (Figure 1c) (Ref 2). Besides the photovoltaic efficiency and device stability, the role of doping agents in B186 PSCs was also investigated. We showed that B186 is a promising HTM characterized by good performance and better device stability compared to Spiro-OMeTAD. By deeply studying the electrical impedance response of the HTMs/perovskite interface, we could conclude that the doping agents improve dramatically the quality of the HTMs/perovskite interface and then the charge transfer leading to high efficiency PSCs (Ref 3).

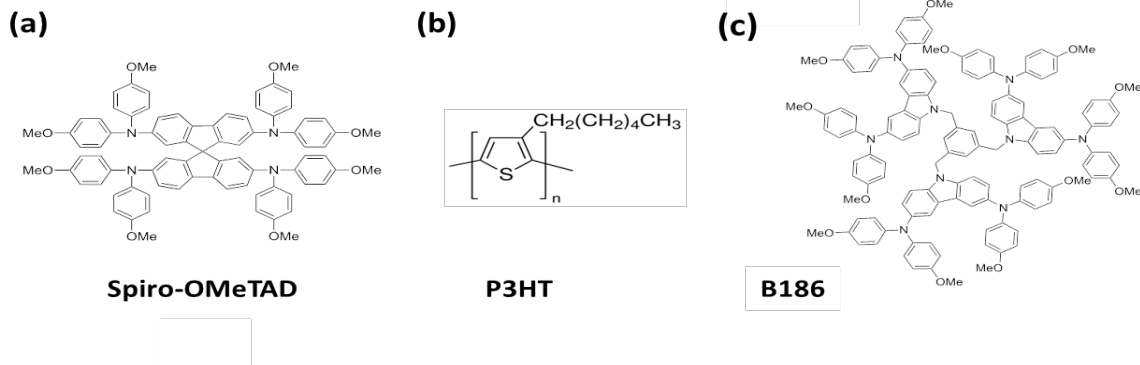


Figure 1. Molecular structure of (a) Spiro-OMeTAD, (b) P3HT and (c) B186

References:

1. M. Ulfa, T. Zhu, F. Goubard , Th. Pauporté, *J. Mater. Chem. A.*, **2018**, 6, 13350 - 13358
2. T.-T. Bui, M. Ulfa, F. Maschietto, A. Ottochian, M.-P. Nghiem, I. Ciofini, F. Goubard, T. Pauporté. *Organic Electronics*, **2018**, 60, 22-30. DOI: 10.1016/j.orgel.2018.05.024
3. M. Ulfa, T. Pauporté, T.-T. Bui, F. Goubard. *J. Phys. Chem. C*, **2018**, 122, 11651-11658. DOI: 10.1021/acs.jpcc.8b02141.

FAB-I-01

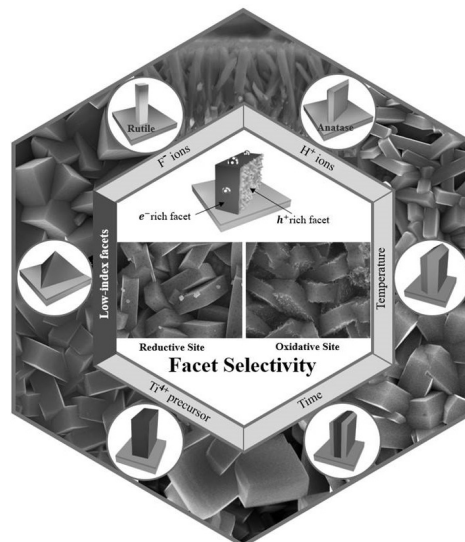
Facet-Engineered Titanium Dioxide Directly Grown on a Conductive Substrate as an Efficient Photoelectrode

Teera Butburee¹, Papasara Kotchasarn², Pussana Hirunsit¹, Pongthanawat Khemthong¹,
Weeradech Thongsuwan², Pisist Kumnorkaew¹, and Kajornsak Faungnawakij¹

¹ National Nanotechnology Center, National Science and Technology Development Agency

² Department of Physics and Materials Science, Faculty of Science, Chiangmai University

Engineering crystals of titanium dioxide (TiO_2) to expose with the most reactive facet has been intensively studied in the past decade, and proved that can significantly improve photocatalytic performance. While most of TiO_2 with facets reported in the past were in a particle form, herein we directly grow TiO_2 with arbitrarily tunable facets onto the transparent conductive substrate. This could reduce interparticle boundaries, and thus facilitate more efficient charge transport compared to particle-assembled films. Experimental and theoretical (Density Function Theory, DFT) studies about the factors controlling the facets reveal that protons (H^+) promote the growth of the high energy $\{001\}$ facet rather than fluoride ions (F^-), which is contrary to the conventional understanding. However, F^- is necessary to keep the crystal phase to anatase that exposes with low-index facets. Moreover, the reductive and oxidative facets are clearly elucidated by selective deposition of a noble metals and a metal oxide. Different photocatalytic tests manifested that $\{001\}$ facet, which is conventionally believed as the highest reactive facet, does not always show highest performance. On the other hand, the suitable facets appeared to depend on the types of reactions (reduction or oxidation) and the synergy of co-existence of facets. These findings may clarify the ambiguous



Control of Polymorphism of Metal-Organic Frameworks Using Mixed-Metal Approach

**Thanadporn Tanasaro, Kanyaporn Adpakpang, Ladawan Pakdeejorhor,
Kajornsak Faungnawakij, Teera Butburee, Suttipong Wannapaiboon,
Makoto Ogawa and Sareeya Bureekaew**

*School of Energy Science and Engineering, Vidyasirimedhi Institute of Science and Technology,
555 Moo 1 Payupnai, Wangchan, Rayong 21210, Thailand.*

e-mail: sareeya.b@vistec.ac.th

Several hundred metal-organic frameworks (MOFs) have been synthesized so far. Some are isomers which have similar chemical components but different properties. The difference originates from the distinct connectivity of the components to construct the frameworks. Those MOFs are so-called polymorphs or topological isomers. Even though such polymorphs are constructed from the same chemical moieties, but they provide different properties such as thermal/chemical stability, pore shape/size, surface area and the respond to external stimuli. This research aims at understanding the effect of the second metal or ligand on the formation of the polymorphs. The presence of iron(III) as second metal on the formation of chromium(III) and terephthalic based MOFs have been studied.

References

1. Tanasaro, Thanadporn; Adpakpang, Kanyaporn; Ittisanronnachai, Somlak; Faungnawakij, Kajornsak; Butburee, Teera; Wannapaiboon, Suttipong; Ogawa, Makoto; Bureekaew, Sareeya Crystal Growth

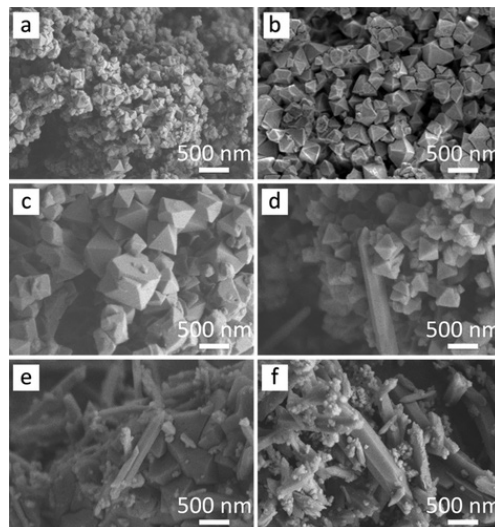


Figure 1. SEM images of synthesized materials with various Fe/Ce ratio.



FAB-I-03

Atomic Layer Deposition for Battery Applications (Review)

Rungthiwa Methaapanon *

Center of Excellent in Particle Technology, Chemical Engineering Department, Chulalongkorn University, Thailand
*Rungthiwa.m@chula.ac.th**

Atomic Layer Deposition (ALD) has a unique ability to provide the most controllability over the thickness, uniformity, and conformality down to the atomic scale. Due to its self-limited nature, ALD offers impeccable step coverage in the nano-size high aspect ratio structures. As the size of devices becomes significantly smaller and their efficiency have been pushed closer to the theoretical limit, ALD plays an important role in achieving the expected functionalities and improving the capability of the devices.

ALD has also increased its significance in energy applications recently, being incorporated into solar cells, fuel cells, and batteries. Particularly for batteries, modification layers have been used to alter anodes, cathodes, and electrolytes properties. While these layers help to enhance the performance of the batteries, excessive thickness of these layers can retard the ion transportation rate and in turn increase battery resistance. The technique that allows controllable ultra-thin deposition of materials like ALD is therefore necessary, especially when the electrode assemblies have shifted toward hierarchical hollow nanostructures to achieve high surface area and short ion transportation length. The deposition inside these structures is feasible by ALD while rather challenging by other techniques. Additionally, ALD can be utilized as a tool to fabricate advanced composite material scaffold to be used as electrodes or electrolytes in batteries.



GRA-I-01



2D and 3D graphene Technology for Energy Storage Applications

Adisorn Tuantranont*, Chakrit Sriprachuabwong, Chatwarin Poochai, Yaowamarn Chumminjak, Anurat Witsitsoraat

Thailand Organic and Printed Electronics Innovation Center, National Electronics and Computer Technology Center, National Science and Technology Development Agency

**e-mail: adisorn.tuantranont@nectec.or.th*

There are growing research interests in developing high-performance energy storage systems to meet the demands for large-scale and sustainable energy storage. Graphene-based materials in two-dimensional (2D) and three-dimensional (3D) configurations are promising as electrode materials for supercapacitors and Lithium-Sulfur (Li-S) battery due to their large surface area, excellent electrical conductivity, high electrochemical activity and high stability. Several methods are used for the preparation of graphene for energy storage devices such as chemical reduction of graphene oxide, chemical vapor deposition (CVD), the arc discharge method, the ball milling approach, solvent-assisted exfoliation and the chemical synthesis approach [1]. In case of supercapacitors, traditional electrode materials made from highly porous conductive material, such as activated carbon, but the pores increase the resistance of devices. Therefore, highly surface area and conductive material such as graphene could be used instead of activated carbon. Previously works, it has been demonstrated that the specific capacitance of pristine 2D graphene is considerably larger than those of single-walled and multi-walled carbon nanotube (CNTs) [2]. In addition, there have been reported incorporation of conductive polymer, metal oxides as well as three-dimensional porous carbon nano-architectures can be significantly increased specific capacitance of graphene [3, 4]. Furthermore, 3D structure of graphene nanohybrids that combine with CNTs, metal oxide and polymer as foam and aerogels have also been explored to enhance the specific capacitance and power density of graphene-based supercapacitor [5]. Lithium-sulfur batteries are a recently potential energy storage device due to their exceptionally high energy density compared with other batteries. However, the Li-S batteries are hindered by the low utilization and the rapid capacity decay of the pure sulfur. Graphene is one of the promising materials to solve these problems [6,7]. In our research work, graphene-based materials have been used as the sulfur hosts to be used as a cathode in Li-S batteries, such as graphene oxide-sulfur, graphene-sulfur, graphene-sulfur-carbon, graphene-sulfur-polymer, graphene-sulfur-metal oxide and graphene-Li₂S. In addition, 3D graphene demonstrated excellent electrical conductivity and interconnected structure is emerging as one of the most promising conducting templates for both supercapacitor and battery. Graphene as foam and sponge structures have shown synergistic effects of conductivity and network facilitating rapid electron and ion transport in Li-S batteries. Therefore, 2D and 3D graphene-based materials have provided suitable functions to improve their practical devices in energy storage applications.

GRA-I-01

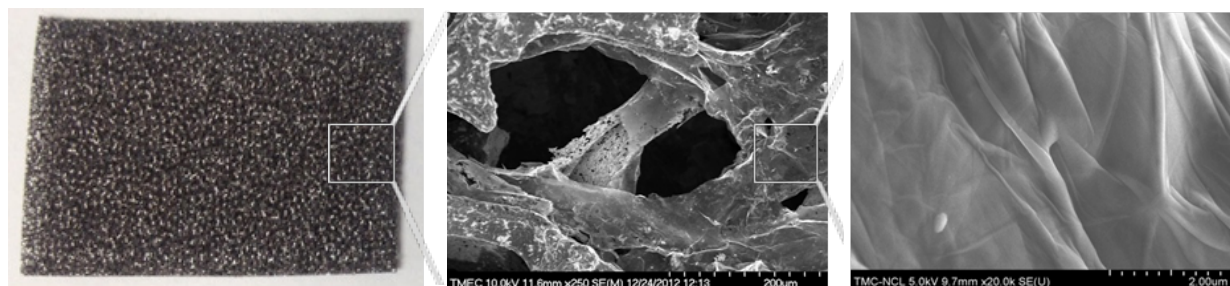


Figure 1. 3D graphene foam used as electrode in energy storage devices.

Keywords: 2D Graphene, 3D Graphene, Energy Storage Devices, Supercapacitor, Battery

References

1. X. Gu, S. Zhang and Y. Hou, *Chin. J. Chem.* **2016**, 34, 13.
2. S.R.C. Vivekchand et al., *J. Chem. Sci.*, **2008**, 120, 9.
3. R.B. Rakhi et al., *J. Mat. Chem.*, **2011**, 21, 16197.
4. J. Liang et al., *ACS Nano*, **2012**, 6, 4508.
5. X. Fan and X. Chen, *Current Opinion in Colloid & Interface Science*, **2015**, 20, 429.
6. Q. Zhang et al., *J. Materiomics*, **2015**, 1, 333.
7. G. Zhou et al., *Nano Energy*, **2015**, 11, 356.



GRA-I-02



Mass Scale Production, Applications and Commercialization of Carbon Nanotubes in Thailand

Pisith Singjai

*Department of Physics and Materials Science, Faculty of Science, Chiang Mai University,
Thailand 50200*

E-mail: pisith.s@cmu.ac.th

Latest science and technology towards achieving mass productions and commercialization of carbon nanotubes (CNTs) will be addressed in this talk. In many choices, chemical vapor deposition is one of the most likely suitable and scalable methods for the average quality and large quantity of CNTs. Many areas of applications have been firmly investigated due to their extraordinary properties. However, many published works pointed out that the significant challenges still exist in exploiting these CNT properties in some particular applications such as composites, electrodes, and sensors. This talk also includes a summary of future chances of CNTs as the materials used in some innovative products.

Engineering Tumor Microenvironment Toward Enhanced Drug Delivery

**John Martin¹, Thahomina Khan¹, Myrofora Panagi², Triantafyllos Stylianopoulos²,
Kazunori Kataoka^{3,4}, Horacio Cabral¹**

¹ *Department of Bioengineering, Graduate School of Engineering, The University of Tokyo, Bunkyo, Tokyo, Japan.*

² *Cancer Biophysics Laboratory, Department of Mechanical and Manufacturing Engineering, University of Cyprus, Nicosia, Cyprus.*

³ *Innovation Center of NanoMedicine, Kawasaki Institute of Industrial Promotion, Kawasaki, Kanagawa, Japan.*

⁴ *Policy Alternatives Research Institute, The University of Tokyo, Bunkyo, Tokyo, Japan.*

Progress in cancer nanomedicine have led to the development of various systemically administered nanocarriers to treat various tumor types, including breast and pancreatic cancers. Nevertheless, despite the enhanced permeability and retention (EPR) effect has served as a key rationale for using nanocarriers to target cancer cells or improve their pharmacokinetic properties for treating solid tumors, it does not enable uniform delivery to all regions of the tumors in sufficient quantities due to barriers posed by the abnormal tumor microenvironment (TME). Thus, clinically approved nanomedicines might have succeeded in reducing adverse effects due to their preferential accumulation to tumors, but survival benefits are modest in most cases, owing primarily to inefficient delivery.

The effective delivery of nanomedicines to solid tumors is hindered by abnormalities in the tumor vasculature, which can drastically reduce tumor perfusion and the delivery of blood-borne drugs. Moreover, the dense tumor extracellular matrix and the rapid proliferation of cancer cells in the confined space surrounding the tumor result in the development of intratumoral mechanical forces that can strain components of the TME, including blood vessels, thus causing vessel compression. Thus, both the vessel hyper-permeability and the compression can reduce the tumor blood flow, leading to hypo-perfusion of tumors and hypoxia. Such impaired blood supply and hypoxic conditions not only limit nanomedicine delivery, but also facilitate the escape of cancer cells to the immune system, while increasing their invasive and metastatic potential.

Herein, we focused on strategies capable of normalizing the tumor interstitial space and the vasculature for improving tumor perfusion and efficacy of nanocarriers. While an agent that simultaneously repairs vessel leakiness and compression has been elusive, we found that dexamethasone, which is a glucocorticoid steroid that is given to cancer patients to manage chemotherapy-induced toxicities, repairs vessel leakiness and compression, which normalizes the mechanical TME towards increasing vessel permeability and potentiating DDS-based chemotherapy. Our findings suggest that normalization of not only the primary, but also the metastatic TME promotes the delivery and efficacy of nanomedicine.



Cancer Precision Medicine in Thailand

Manop Pithukpakorn

Precision medicine is an emerging paradigm for disease diagnosis, treatment and prevention that takes individual genetic and molecular variability, environmental and lifestyle difference of each person into account. Contrary to “one-size-fits-all” approach, precision medicine will allow doctors and researchers to predict more accurately which treatment and prevention strategies for a particular disease will work in which patients.

Cancer is the best example to demonstrate the benefit of precision medicine. It has been universally accepted that cancer is a genetic disorder that results in abnormal cell growth and the invasiveness and spreading potential to other parts of the body. Better understanding in cancer genetics leads to new types of cancer diagnostic tests and several novel drugs which are designed to target specific genetic abnormalities in cancer.

The unprecedented throughput, speed and cost of next generation sequencing (NGS) enables researchers to investigate genetic contribution of cancer and implement this technology to the real world medical practice. We currently see widespread use of NGS to discover genetic alterations in each patient, to identify potential treatment target, and to predict response of medical treatment. In clinical practice, oncologists could select the best and most appropriate treatment for each patient, based on the patient’s genetic data. Precision medicine widely becomes a standard approach in cancer diagnosis and treatment. Patients with lung or breast cancers with specific genetic alterations could get significant benefit from novel targeted therapies that specifically act on certain molecular pathway. Precision medicine also predict what medication would not work and that treatment could be avoided. This novel approach would improve cancer treatment efficacy, patient outcome, quality of life, reduce healthcare cost and overall social and economic burden.

Many studies have shown that genetic diversity plays role in phenotypic differences among various ethnic groups with the same diseases. Some cancer types are significantly more prevalent in Asian than in Western population. Some cancers display difference in subtypes among countries. Many similar cancers from various ethnic groups also have different treatment outcome and prognosis. To be able to determine the role of genetic diversity in Thai cancer patients, as well as development and implementation of cancer precision medicine in Thailand, a multi-institute research collaboration was established under the ‘Research University Network’ (RUN). The research network aims to study genetic alterations in Thai cancer patients, develop a study platform for cancer biology and cancer treatment, apply clinical genetic testing for Thai cancer patients and develop precision medicine guidelines for cancer diagnosis and treatment. Since the inception, the network has established a collection of clinical data and bio-specimens from more than 1,500 cancer patients as well as several hundreds of cancer genome data. The research team has also developed the three-dimensional model of cancer cell culture and collection of primary cancer ‘organoids’ for high-throughput cancer drug testing platform.

In conclusion, cancer precision medicine research network has established databases of Thai cancers and generated vast amount of the clinical and genomic data, which could propel cancer researches in various aspects. The research has also led to several Thailand’s first successes including integrated genetic diagnostic laboratory for cancer diagnosis, patient-derived three-dimensional cancer cell cultures (cancer avatar), cancer drug testing system, cancer cell culture in zebrafish. The research can be translated to a comprehensive cancer diagnosis and treatment of cancer. In addition, Thai cancer patients could also benefit from widespread use of genetic testing and precision medicine approach for cancer care, which could result in an increased treatment effectiveness and improved quality of life.

Development of Carbon/Metal-oxide Nanostructured Composites for Gas-Sensing Applications

A. Wisitsoraat¹, A. Tuantranont¹, D. Phokharatkul¹, M. Horpartum¹, K. Jaruwongrangsee¹,
T. M. Daneil¹, C. Sriprachuabwong¹, S. Phanichphant², C. Liewhiran³

¹ National Electronic and Computer Technology Center, Pathumthani, Thailand

² Materials Science Research Center, Chiang Mai University, Chiang Mai, Thailand

³ Dept. of Physics and Materials Science, Chiang Mai University, Chiang Mai, Thailand

Metal oxide/carbon nanostructures and their composites are promising for various gas-sensing applications due to their huge specific surface area, excellent electronic/chemical characteristics and high environmental stability. Over the past several years, we have developed highly sensitive gas sensors based on carbon-incorporated metal-oxides prepared by different methods. Firstly, carbon-nanotubes (CNTs)-metal oxide (SnO_2 , WO_3 and MoO_3) nanocomposites are developed by means of powder mixing and electron beam evaporation. Appropriate compositions of the nanocomposites lead to enhance responses towards gases such as NO_2 , ethanol, acetone and H_2 . Secondly, carbon-doped metal oxide nanostructures such as WO_3 nanorods are produced by sputtering with glancing angle deposition (GLAD) and demonstrated to offer a significantly higher gas-sensing response compared with conventional undoped dense thin film prepared by conventional sputtering method. Thirdly, carbon-coated 3D ZnO nanotetrapods fabricated by two-step vapor phase transport shows considerably enhanced response towards NO_2 compared with uncoated ZnO nanotetrapods. Lastly, graphene-metal oxides (SnO_2 and WO_3) composite thick film gas sensors are fabricated based on one-step flame spray pyrolysis (FSP), electrolytic exfoliation and spin coating. The gas-sensing characteristics towards ethanol, acetone and NO_2 gases of the composite are found to be significantly improved with optimal graphene loading concentrations in the range of 0.5–5 wt%.

Keywords: Carbon-Metal oxide nanostructures, Nanocomposite, Gas sensor.



SAF-I-01



Intratracheal Instillation Method for Testing Nanomaterials

Masashi Gamo

National Institute of Advanced Industrial Science and Technology (AIST)

Considering that many different nanomaterials are increasingly in the market or under development, there is an immediate need for a less expensive and less time consuming test method to examine the inhalation toxicity of nanomaterials. Intratracheal instillation (IT) method has been expected to be useful for such purpose as categorization or read-across. The test nanomaterial is administered as suspension to respiratory tract of animals in IT study, while the aerosol of nanomaterial is introduced to exposure chambers to be inhaled by animals in inhalation exposure study. In the presentation, I will briefly show the results of Japanese national projects regarding comparison between inhalation study and IT study, inter-laboratory study of IT method, and comparative studies of nanomaterials using IT method.



SEN-I-01

Calcinated Nanofilm on Gold Surface for SPR and MALDI Analysis of Proteins and Peptides

Quan “Jason” Cheng

Department of Chemistry, University of California, Riverside, CA 92521, USA

Fluorescent, radioactive, and other labels have been long employed for detections in immunoassays and molecular binding events but they have limitations. There has been considerable interest and unprecedented growth in developing label free techniques over the last two decades. As one of the most advanced label free methods, surface plasmon resonance (SPR) continues to be at the forefront of evolving sensing technology that offers high sensitivity and convenience for quantitation of molecular interactions [1]. This talk will present the latest advances in SPR and the strategies employed in our lab to improve the detection performance, especially use of SPR biochips that enable excitation of SPPs in patterns for background-free imaging analysis and the fabrication of calcinated nanofilms to facilitate the establishment of biomimetic lipid membrane interface. Applications of the calcinated nanofilms in membrane stability assessment, *in situ* construction of polymer coating, and host-guest chemistry with artificial receptors, will be discussed. In addition, application of calcinated nanofilms in surface-based MALDI method for protein and peptide analysis will be discussed.

References

1. S.S. Hinman, K.S. McKeating and Quan Cheng. “Surface Plasmon Resonance: Material and Interface Design for Universal Accessibility”, *Analytical Chemistry*, **2018**, 90 (1), 19–39.



SEN-I-02



Preparation and Integration of Specifically Functionalized Nano- and Biosensors for Biomolecular Detection in Liquid Biopsy

Rudolf Heer, Eva Melnik, Paul Müllner, Jörg Schotter, Giorgio Mutinati, Rainer Hainberger

Austrian Institute of Technology

The decentralization of the health care system, driven by the demographic change, creates a strong demand for biosensors that enable molecular diagnostics outside of laboratories at the point-of-care. Today, a variety of detection concepts, suitable for measuring physiological relevant biomarker concentrations in liquid biopsy, exists.

I will present photonic, magnetic and electrochemical biosensors and will put focus on their target specific functionalization making full use of printing technologies.

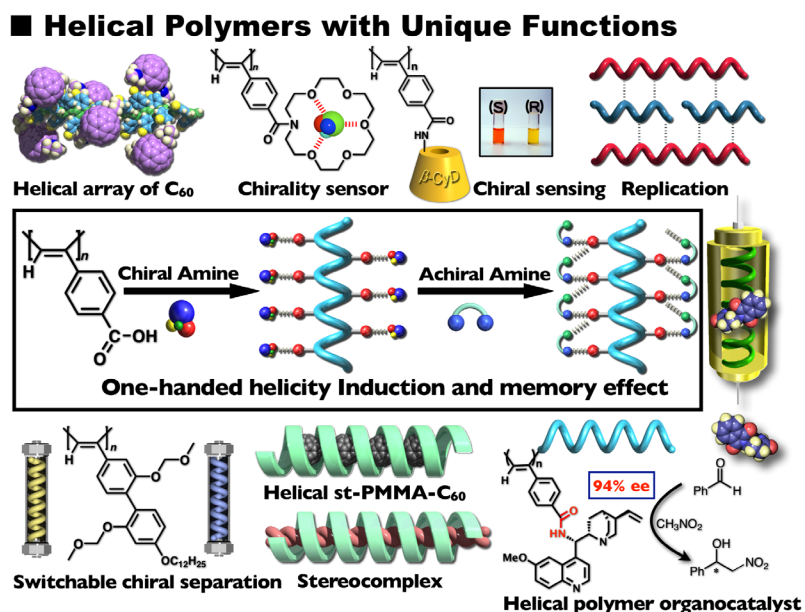
In particular, the progress in printing technologies is opening new possibilities for the fabrication of electronic components in combination with functional materials, which are key components in biosensors.

Helical Polymers as Unique Chiral Materials

Eiji Yashima

*Department of Molecular and Macromolecular Chemistry, Graduate School of Engineering,
Nagoya University, Chikusa-ku, Nagoya 464-8603, Japan
yashima@chembio.nagoya-u.ac.jp*

The helix is ubiquitous in nature, and one of the most popular structural motifs for biological polymers, which play key roles in their sophisticated functions. In polymer and supramolecular chemistry, the control of helicity is an attractive challenge because of possible applications in materials science.^[1] Here we show unique macromolecules that fold into a one-handed helical conformation induced by chiral residues covalently bonded to the main-chain or external chiral stimuli followed by memory of the helicity, which can provide useful chiral materials for separating enantiomers as well as asymmetric catalysis.^[2,3] The helicity induction and memory strategy has a remarkable advantage from a practical viewpoint such that a preferred-handed helicity can be induced in commodity plastics, such as syndiotactic poly(methyl methacrylate) (st-PMMA).^[4] The direct observations of helical structures of synthetic helical polymers by atomic force microscopy (AFM) are now possible.



References

1. E. Yashima, N. Ousaka, D. Taura, K. Shimomura, T. Ikai, and K. Maeda, *Chem. Rev.* 116, 13752-13990 (2016). "Supramolecular Helical Systems: Helical 2. Assemblies of Small Molecules, Foldamers, and Polymers with Chiral Amplification and Their Functions".
2. K. Shimomura, T. Ikai, S. Kanoh, E. Yashima, and K. Maeda, *Nature Chem.* 6, 429-434 (2014). "Switchable Enantioseparation Based on Macromolecular Memory of a Helical Polyacetylene in the Solid State".
3. K. Maeda, D. Hirose, N. Okoshi, K. Shimomura, Y. Wada, T. Ikai, S. Kanoh, and E. Yashima, *J. Am. Chem. Soc.* 140, 3270-3276 (2018). "Direct Detection of Minute- and Crypto-chirality of Tertiary and Quaternary Hydrocarbons and Isotopically Chiral Compounds by a Helical Polyacetylene through Chiral Amplification and Memory".
4. N. Ousaka, F. Mamiya, Y. Iwata, K. Nishimura, and E. Yashima, *Angew. Chem., Int. Ed.* 56, 791-795 (2017). "Helix-in-Helix" Superstructure Formation through Encapsulation of Fullerene-Bound Helical Peptides within a Helical Poly(methyl methacrylate) Cavity".



STE-I-02



Structure-Property Relationships of Curved Materials from First Principles

Kim K Baldrige

Tianjin University

Of growing interest are *ab initio* predictive theories for solids that can provide atomic scale insights into properties of bulk materials, interfaces, and nanostructures. Adaption of the quantum chemical framework is challenging in that no single theory exists that provides prediction of all observables for every material type. However, through a combination of interdisciplinary efforts, a portfolio of methods is developing that hold promise for quantitative predictions of materials and device properties. Particularly relevant for device applications are organic semiconductors (OSC), such as aromatic hydrocarbons, with high polarizabilities, small band-gaps, and delocalized pi electrons that support mobile charge carriers. The special nature of optical excitations in the form of bound excitons holds promise for use in devices, such as organic light emitting diodes (OLEDs), organic photovoltaics (OPVs), organic field-effect transistors (OFETs), and molecular nanojunctions. Added morphological features, such as curvature, lead to additional physical phenomena and offer exploration of a wealth of phenomenology as a function of environment and functionalization. This talk will highlight our efforts in the use of curved aromatics for key materials technologies.



STE-I-03

Supramolecular Catalysis Using Single Chain Polymeric Nanoparticles as a Strategy for Performing Organic Synthesis in Living Cells

Steve Zimmerman

Department of Chemistry

University of Illinois

A significant portion of the enormous catalyst power of enzymes is derived from their ability to bind substrates. Binding can provide proximity between two substrates for coupling or between the substrate and key functional groups in the enzyme active site. Driven by our interest in building bioactive compounds within cells, we have developed polymeric catalysts that in a very broad sense mimic metalloenzymes. Some of these are single-chain polymeric nanoparticles (SCNP) wherein an amphiphilic polymer is cross-linked to give a water-soluble folded structure that loosely resembles a folded protein. This lecture will focus on how supramolecular chemistry, including substrate binding, is central to the functioning of these catalysts and discuss the prospects of ultimately embedding nanoscale manufacturing centers within cells to produce therapeutic agents and other bioactive species.

Exploring the Optical Properties of Non-Stoichiometric Hydrates and Anhydrates of Donor-Acceptor Charge Transfer Salts

Mark A. Olson

*School of Pharmaceutical Science and Technology, Health Science Platform
Tianjin University*

92 Weijin Road, Nankai District, Tianjin 300072, P. R. China

Web: www.olsonlaboratory.com, Twitter: @MARK_A_OLSON

**E-mail: molson@tju.edu.cn*

Stimuli-responsive materials, such as hydrochromics, have found mass usage and profitability in manufacturing and process control. By incorporating competing n-to- π^* and π -to- π^* charge transfer interactions into charge transfer-based functional supramolecular materials, we have developed materials which exhibit tunable solid state hydrochromism. This optical behavior is triggered upon the reversible formation of non-stoichiometric hydrates which can be exploited for the production of thermochromes. This methodology has proven to be an ideal strategy to construct processable optically responsive multifunctional assemblies. These assemblies are composed of bis-bipyridinium-derived acceptors and a series of synthetic and commercially available donors – including the neurotransmitter melatonin and its analogue bioisosteres. By tailoring the chemical structure of the donors and/or the acceptors, the strength of the charge transfer interactions can be tuned with concomitant changes in their hydrochromic/thermochromic properties. Hydrochromic/thermochromic aerogels and inks of these materials can be prepared, with a large selection of colors, in environment-friendly solvents and demonstrate tunable thermochromic transition temperatures ranging from 45 to 105 °C. Favorable compatibility of these materials with commercial inks and inkjet printers afford excellent pattern quality with extended color options. Mechanistic studies reveal that two types of water molecules were bound to the supramolecular complexes with differing strengths, and that the more weakly bound water is responsible for the hydrochromic/thermochromic transitions for these hydrates.

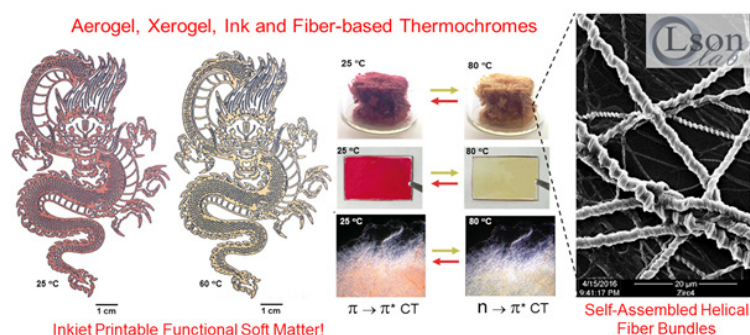


Figure 1. Ink-jet prints, aerogels, xerogel films, and helical fibers comprised of hygroscopic donor-acceptor charge transfer complexes at both above and below their thermochromic transition temperature.

Keywords: Soft Matter, Template-Directed Self-Assembly, Charge Transfer Interactions, Hydrochromism, Thermochromism

SUP-I-01

References

1. Xu, Y.; Yuan, T.; Nour, H. F.; Fang, L.; Olson, M. A., *Chem. Eur. J.* **2018**, DOI:10.1002/chem.201803496.
2. Yuan, T.; Xu, Y.; Zhu, C.; Jiang, Z.; Sue, H.-J.; Fang, L.; Olson, M. A. *Chem. Mater.* **2017**, *29*, 9937-9945.
3. Yuan, T.; Vazquez, M.; Goldner, A. N.; Xu, Y.; Contrucci, R.; Firestone, M. A.; Olson, M. A.; Fang, L. *Adv. Funct. Mater.* **2016**, *47*, 8604-8612.



SUP-I-02



Novel Aromatics as Precursors to Porous Molecular Crystals

Ognjen Š. Miljanić

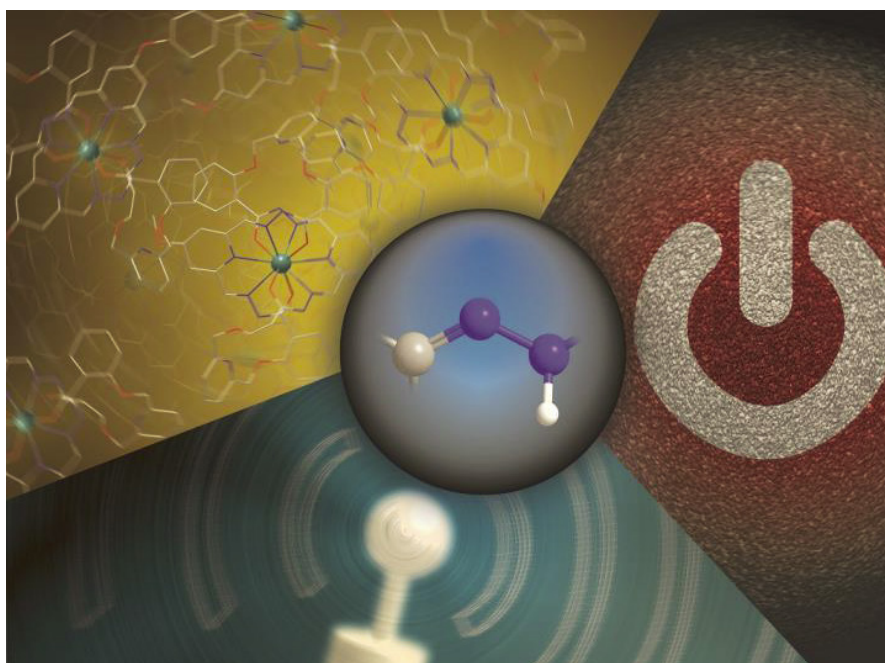
Department of Chemistry, University of Houston, email: miljanic@uh.edu

Porous molecular crystals are a class of solid state porous materials which are composed of discrete molecules rather than extended polymeric structures. Their molecular nature makes them fundamentally interesting, as small molecules typically closely pack in the solid state, without leaving large voids. In addition, porous molecular crystals have higher solution and vapor phase processability than their polymeric counterparts, which allows their easier incorporation into thin films and devices. Our recent work has identified two new classes of porous molecular crystals. The first is based on rigid fluorinated aromatic compounds which are terminated with pyrazole or tetrazole end groups. These termini are capable of hydrogen bonding and aromatic stacking and their solid-state assembly results in extrinsically porous structures with modular hexagonal pores. These pores have been shown useful in adsorption of Freons, hydrocarbons, and fluorinated anesthetics. The second class of molecular precursors to porous structures are cyclobenzoin: shape-persistent macrocycles produced by the benzoin condensation of rigid aromatic dialdehydes. Cyclobenzoin offer rich derivatization chemistry through esterification or condensation with 1,2-phenylenediamines, and a number of these derivatives are found to be porous and capable of guest binding in solution and solid state.

Hydrazone-Based Switches and Fluorophores

Ivan Aprahamian,
Dartmouth College

For the past few years we have been developing structurally simple, easy to make, modular, and tunable hydrazone-based functional materials (*e.g.*, switches, sensors and fluorophores).^{1,2} This presentation will deal with our recent advances with these systems, with an emphasis on feedback loops,³ fluorescent molecular rotors (viscometers),⁴ and light activated photochromic compounds.⁵



Representative references:

1. X. Su, I. Aprahamian *Chem. Soc. Rev.* **2014**, 43, 1963–1981
2. L. Tatum, X. Su, I. Aprahamian *Acc. Chem. Res.* **2014**, 47, 2141–2149
3. S. Pramanik, I. Aprahamian *J. Am. Chem. Soc.* **2016**, 138, 15142–15145
4. H. Qian, M. E. Cousins, E. H. Horak, A. Wakefield, M. D. Liptak, I. Aprahamian *Nature Chem.* **2017**, 9, 83–87
5. a) Y. Yang, R. P. Hughes, I. Aprahamian, *J. Am. Chem. Soc.* **2014**, 136, 13190–13193; b) H. Qian, Y.-Y. Wang, D.-S. Guo, I. Aprahamian, *J. Am. Chem. Soc.* **2017**, 139, 1037–1040; b) Qian, H.; Pramanik, S.; Aprahamian, I. *J. Am. Chem. Soc.* **2017**, 139, 9140–9143

Synthesis and Applications of Metal-Organic Knots

Ali Trabolsi,^{*a} Thirumurugan Prakasam,^a Farah Benyettou,^a Partha Sarathi Mukherjee,^b
and Gennaro Esposito^a

^a *New York University Abu Dhabi, Abu Dhabi, UAE.* ^b *Department of Inorganic and Physical
Chemistry, Indian*

Institute of Science, Bangalore, India.

Trefoil knots are the most frequently observed knotted topology in proteins. It is speculated that knotted topologies play important roles in protein function by enhancing their catalytic activity, ligand-binding affinity, and increasing their macromolecular thermodynamic, kinetic, and mechanical stability. Co-ordination driven self-assembly has been established as a nice protocol towards the synthesis of complex architectures including molecular knots. However, reports on the practical application and utility of such molecular knots remain very limited. In my talk, I will discuss the preparation of different metal-based trefoil knots and their use in three new applications: (i) catalysis,¹ (ii) protein-protein interactions inhibition,² and (iii) cancer therapy.³

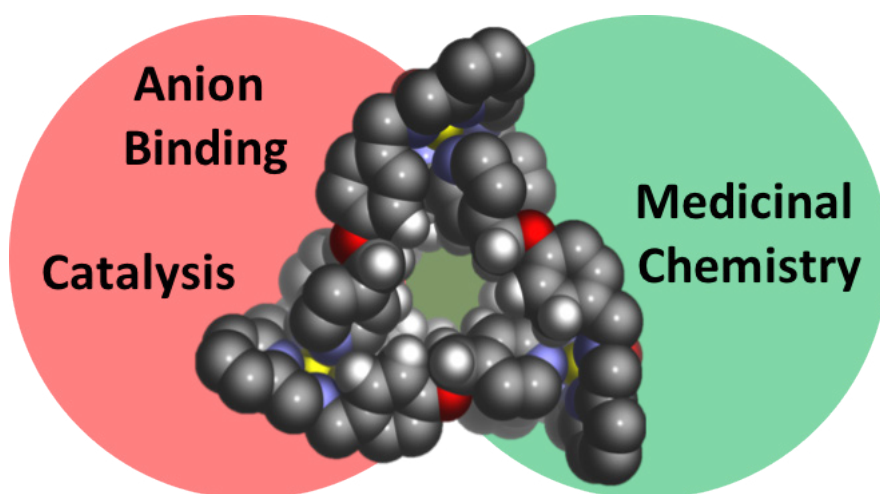


Figure 1. Single crystal structure of a metal-organic knot and its potential applications.

References

1. Prakasam, T.; Devaraj, A.; Saha, R.; Matteo Lusi, M.; Olson, M. A.; Brandel, J.; Esteban-Gómez, D.; Ptas-Iglesias, C.; Mukherjee, P. S.; Trabolsi, A. under review.
2. Prakasam, T.; Cantarutti, C.; Sharma, S. K.; Jaganna than, R.; Palmisano, G.; Giorgetti, S.; Corazza, A.; Bellotti, V.; Fogolari, F.; Olsen, J.-C.; Trabolsi, A.; Esposito, G.; under review.
3. Benyettou, F.; Prakasam, T.; Nair, A. R.; Gunn, I.-I.; Skorjanc, T.; Alhashimi, M.; Edelpi, K. S.; Trabolsi, A. under review.

Tailoring Supramolecular Polymers for Gas Separation and Energy Storage Applications

Ali Coskun

Department of Chemistry, University of Fribourg

Chemin du Musée 9, 1700 Fribourg, Switzerland

Web: www.coskunlab.com, Twitter: @Coskunlab

**E-mail: ali.coskun@unifr.ch*

Nanotechnology can be regarded as controlling matter on an atomic or a molecular level at nanoscale dimensions. Our main approach in this field is the so-called “bottom-up” approach where the concepts of molecular recognition and self-assembly are being used along with covalent synthesis to arrange molecules to form multifunctional integrated systems for addressing energy and environmental challenges. In this direction; we have developed [1-3] porous organic polymers incorporating molecular cages/macrocycles as monomeric units and showed that their intrinsic properties such as their ability to bind guest molecules in solution can be transferred into the solid-state for affinity-based separation of gas mixtures. In an effort to tackle restacking problem of graphene and to take full advantage of its high π -surface area, we proposed [4,5] to introduce a permanent ‘spacer’ such as porosity between graphene nanoribbons and graphene layers within the microporous polymers. We utilized both noncovalent and covalent approaches to form microporous graphene frameworks (MGFs). In our studies of lithium ion batteries (LIBs), we have recognized the potential of supramolecular chemistry as a general strategy to solve capacity fading problem associated with silicon anodes, which offers extremely high-capacity compared to conventional graphite based anode materials. We have demonstrated [6] that by incorporating small amount of polyrotaxanes into the conventional binders, it is possible to form binder networks with unparalleled elasticity, which enabled stable cycle life for silicon microparticle anodes at commercial-level areal capacities.

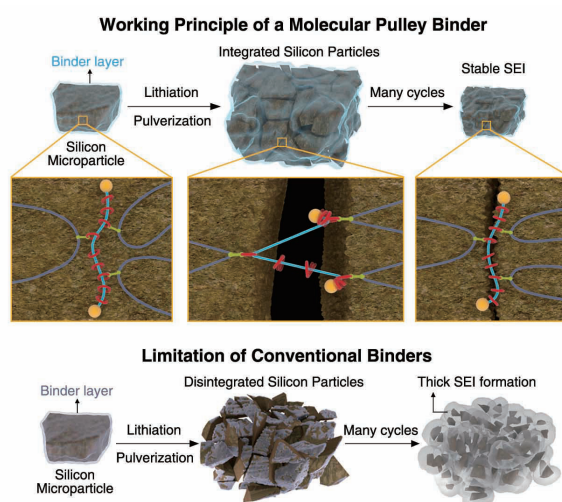


Figure 1. Schematic representation of battery operation for polyrotaxane binder.

Keywords: Porous organic polymers, CO₂ capture, Li-ion batteries, molecular recognition

SUP-I-05

References

1. H. A. Patel, S. H. Je, J. Park, D. P. Chen, Y. Jung, C. T. Yavuz, A. Coskun, *Nature Commun.*, **2013**, *4*, 1357.
2. O. Buyukcakil, Y. Seo, A. Coskun, *Chem. Mater.*, **2015**, *27*, 4149–4155.
3. S. N. Talapaneni, D. Kim, G. Barin, O. Buyukcakil, S. H. Je, A. Coskun, *Chem. Mater.*, **2016**, *28*, 4460–4466.
4. S. Srinivasan, S. H. Je, S. Back, G. Barin, O. Buyukcakil, R. Guliyev, Y. Jung, A. Coskun, *Adv. Mater.*, **2014**, *26*, 2725–2729.
5. S. N. Talapaneni, T. H. Hwang, S. H. Je, O. Buyukcakil, J. W. Choi, A. Coskun, *Angew. Chem. Int. Ed.*, **2016**, *55*, 3106–3111.
6. S. Choi, T. -w. Kwon, A. Coskun, J. W. Choi, *Science*, **2017**, *357*, 279-283.



SUP-I-06



Fluorescent Materials by Hierarchical Assembly

Christopher R. Benson^a, Wei Zhao^a, Maren Pink^a, Josh Chen^a, Bo W. Laursen^b and Amar H. Flood^a

^a*Indiana University*

^b*University of Copenhagen*

**e-mail: aflood@indiana.edu*

Methods to simply and predictably form optical materials that retain the optical properties of the organic dyes they are made from has been a challenge ever since Perkins made the first synthetic dye over 150 years ago. Aggregation produces color changes and quenches emission. As a solution to this persistent problem, we present the discovery of a new optical material based on small molecule dyes. Bright and surprisingly predictable absorption and emission properties are obtained in a solid-state material composed of dyes that are organized hierarchically into small-molecule isolation lattices (SMILES). The optical properties we observe reproduce dilute solutions but emerge with the high-density packing in the solid state that spatially and electronically isolates fluorophores from each other. The characteristics and properties of these new supramolecular materials will be presented.

Keywords: Hierarchical Assembly, Optical Materials, Supramolecular

Issues on the Theoretical Simulation of Oxygen Reduction Reaction Catalysis

Kaito Takahashi*^a, Do Ngoc Son^a

^a*Institute of Atomic and Molecular Sciences, Academia Sinica Taiwan*

*e-mail: kt@gate.sinica.edu.tw

Presently the efficiency of the proton exchange membrane fuel cell is limited due to the slow kinetics of the oxygen reduction reaction (ORR), $O_2 + 4(H^+ + e^-) \rightarrow 2H_2O$, in the cathode. Theoretical calculation using the periodic density functional theory (DFT) methods, as well as the model of Norskov et al.¹ has been utilized to predict the ORR activity on metal catalyst surfaces theoretically. In this presentation, we will use PdCo alloy surface as an example to illustrate the issues that one should consider when evaluating the catalytic activity of alloy metal surfaces for ORR. We performed a systematic evaluation to understand the effect of Co arrangement as well as alloying percentage toward the catalytic activity of the PdCo alloy. We found that maximizing the number of Co atoms in the second atomic layer underneath the Pd skin provides the highest activity. Furthermore, we found that the activity will saturate after alloying with 30% Co. see figure below. In the usual simulations, we determine the surface content with the lowest barrier for reaction, since theoretically, it should show the highest activity. However, there are many cases where the most reactive surface may not necessarily be stable for continuous ORR use. We examined how surface segregation of the Co atom from the second atomic layer can greatly alter the stability of the PdCo alloy surface in the presence of reaction intermediates of ORR.^{2,3}

Keywords: Oxygen reduction reaction, PdCo alloy surface, density functional theory

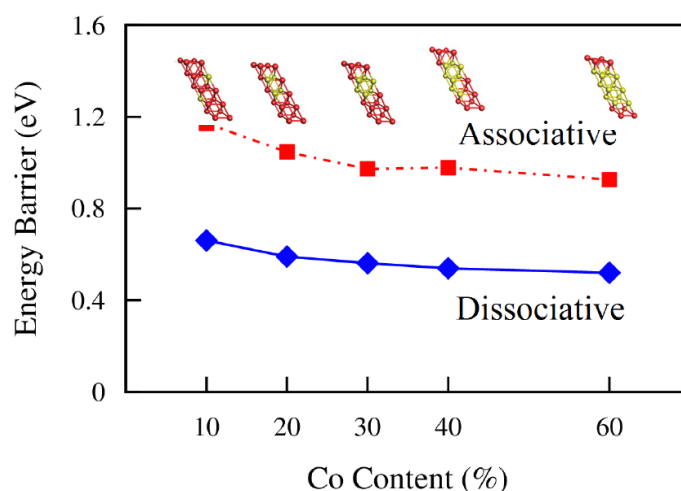


Figure 1. Co content versus the energy barrier for the rate determining step for the ORR reaction for the PdCo alloy surface.

References

1. J. K. Norskov, J. Rossmeisl, A. Logadottir, L. Lindqvist, J. R. Kitchin, T. Bligaard, H. Jonsson, *J. Phys. Chem. B*, **2004**, *108*, 17886-17892.
2. D. N. Son, K. Takahashi, *J. Phys. Chem. C* **2012**, *116*, 6200-6207.
3. D. N. Son, O. K. Le, V. Chihaiia, K. Takahashi *J. Phys. Chem. C* **2015**, *119*, 24364-24372.

Exploring the Catalytic Property of Cu-Al Spinel Towards Methanol Steam Reforming Reaction Using Density Functional Theory

Gang Feng^{1,*}, Shaojun Qing², Rongbin Zhang¹, Zhixian Gao^{2,*}

1. College of Chemistry, Nanchang University, Nanchang, 330031, PR China

2. Institute of Coal Chemistry, Chinese Academy of Sciences, Taiyuan, 030001, PR China

Gang Feng: fenggang@ncu.edu.cn, Zhixian Gao gaozx@sxicc.ac.cn

Methanol steam reforming (MSR) is an efficient way for hydrogen production. The Cu/alumina catalysts show excellent activity for MSR. However, the stability of Cu/alumina catalysts is limited due to the aggregation of Cu during the reaction. The spinel aluminates, CuAl_2O_4 of cubic structure, show excellent stability for MSR, since the active Cu atoms could be gradually released during the reaction. Investigation into the surface structure and catalytic properties of Cu-Al spinel towards MSR, *e.g.* the adsorption of methanol, water, hydrogen, carbon monoxide and carbon dioxide, as well as the reduction process of the surface is of the most fundamental for catalysts designing. These interesting points are investigated using the PBE functional with periodic model.

Hydrogen molecule could form dissociative adsorption on the spinel surface with two H atoms bond to surface O sites, with the adsorption energy of -2.26 eV. Water molecule prefers to adsorb on surface Cu atoms (-1.05 eV) than Al atoms (-0.76 eV). The C atom of CO could bond to surface Cu atoms, with the adsorption energy of (-1.44 eV). However, CO_2 could only form physical adsorption on spinel surface. The molecular adsorption of methanol on the surface with its O atom bonds to surface Cu or Al, which are exothermic by -1.21 and -0.89 eV, respectively. The dissociation of C-H bond of the methanol over surface Cu atom are more energetically favored. Simulation on the reduction process of the surface reveal that the oxygen atom could be abstracted by hydrogen and migration of surface Al and Cu atoms are involved.



THE-I-03



Bridge the Catalysis and Electrocatalysis by First Principles

Jianwen Liu, Xian-zhu Fu, Jingli Luo

Shenzhen University, China.

Energy conversion and storage technologies are important strategies for addressing the global challenge of energy crisis and environmental pollution. Based on first principles calculations, some promising metal oxides (such as vanadium oxide etc) and zeolites (such as ZSM-5, SSZ-13 etc) were studied for the catalytic/electrocatalytic activities. The detailed catalytic mechanisms for the conversion of light alkanes (methane and propane) were proposed to understand the energy conversion and storage process. These studies are helpful for understanding the mechanisms of these catalytic /electrocatalytic reactions and developing accurate catalytic descriptors, which can be employed to screen high-activity catalysts in future high-throughput calculations and provide valuable clues for experiments.



Oral Presentation

Zero Valent Iron Nanoparticles Stimulate Exopolymer Synthesis by *Pseudomonas putida*

Chonlada Pokhum, Warayuth Sajomsang, Chamorn Chawengkijwanich*

*National Nanotechnology Center, National Science and Technology Development,
Thailand Science Park, Pathumthani, 12120 Thailand*

*e-mail: chamorn@nanotec.or.th

The effect of coated zero valent iron nanoparticles (nZVIs, 25 nm, Sigma-Aldrich) on biofilm development was investigated in batch assay using *Pseudomonas putida*, a representative of soil bacteria, in aerobic condition of 30°C. The impact of these iron nanoparticles on biofilm formation was daily tracked for 7 days. The synthesis of exopolymer was estimated by measuring the decrease in color intensity of alcian blue (Fig. 1a). The study showed that the greater amount of exopolymer was obtained in media with iron nanoparticles, and increased with increasing iron nanoparticles concentrations. The result demonstrated that iron nanoparticles not only promoted biofilm development, but also changed biofilm structure as revealed by scanning electron microscopy (SEM) images. Fourier transform infrared spectroscopy (FTIR-spectroscopy) technique was used to examine the biofilm composition. The result from transmission electron microscopy (TEM) indicated that the iron nanoparticles formed small aggregates in growth media and did not diffuse through the bacterial cell (Fig. 1b). The results of this study revealed a response of *P. putida* biofilm to zero valent iron nanoparticles.

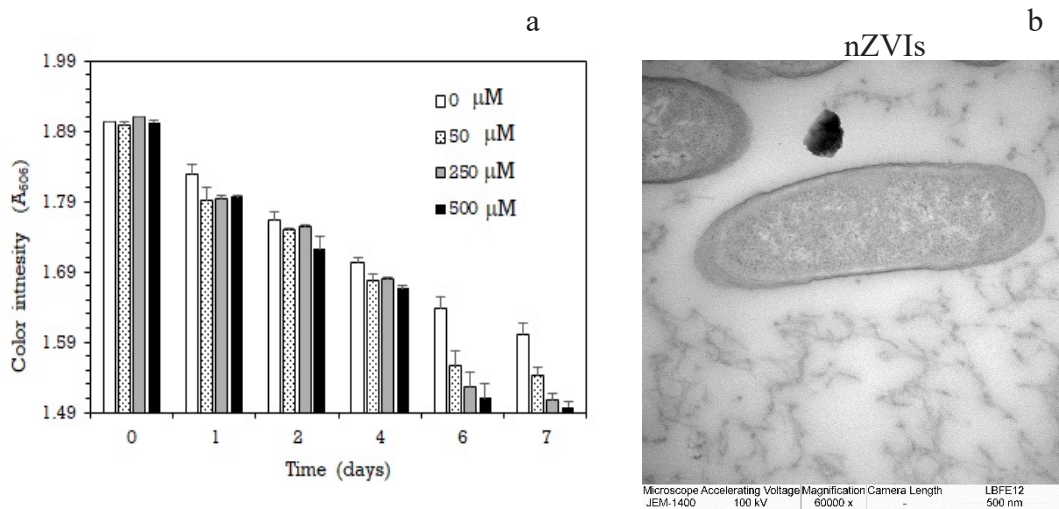


Figure 1. (a) Experiment data of exopolymer synthesis in media with iron nanoparticles at different concentrations (0 - 500 μM), (b) TEM image of *P. putida* in media with iron nanoparticles at 50 μM .

Keywords: Iron, Biofilm, Nanoparticles, *Pseudomonas*.

References

1. P. Vandevivere, D.L. Kirchman, *Appl. Environ. Microbiol.* **1993**, 59, 3280-3286.

Development of Hydrophilic Polyamide Thin-Film Composite (TFC) Membranes on Polyvinylidene Fluoride (PVDF) Hollow Fiber Membranes for Nanofiltration

Sudkaneung Singto^{}, Warayuth Sajomsang^{**}, Chalita Ratanatawanate^a,
Sineenat Thaiboonrod^a, Pattarapond Gonil^a**

^aNational Nanotechnology Center, National Science and Technology Development Agency (NSTDA),
Thailand Science Park, Phahonyothin Road, Khlong Luang, Pathum Thani 12120, Thailand

*e-mail: Sudkanueng.Sin@nanotec.or.th, Warayuth@nanotec.or.th

The polyamide thin-film composite (TFC) membranes synthesized via interfacial polymerization (IP) are commonly used in membrane technologies such as nanofiltration (NF) and reverse osmosis (RO) membrane. The polyamide selective layer is the key factor to success of the nanofiltration because of their high selectivity and permeability. Even though polyamides are effective, a lot of effort is being made in developing new blend monomers to achieve a better membrane performance such as high water flux, high salts and organic dyes rejection and reduce of fouling on membrane surface.

This work presents the development of newly hydrophilic polyamide (PA) thin film are synthesized from interfacial polymerization (IP) using two diamines on the surface functionalized (i.e. polyphenol/aminosilane coupling) PVDF hollow fiber membranes as shown in Figure 1. The blended diamine solutions were performed using the conventional aromatic diamine monomer, m-phenylenediamine (MPD) and various concentration of aliphatic diamine monomers (i.e. Diamine1, Diamine2, Diamine3, Diamine4 and Diamine5) at 1, 2, 3 and 4 wt.%, which are the equivalent molar mass. The result showed that incorporating aliphatic diamine units into the polyamide network substantially increased hydrophilic (water contact angle 19-50°) comparing to conventional MPD (water contact angle 79°). High resolution SEM images show the surface morphologies of hydrophilic polyamide film significantly change with introduce aliphatic diamines from large ridge and valley structure to enlarge nodular and porosity structure as shown in Figure 2. By comparing the roughness within the group of hydrophilic polyamides, at 2 wt.% of longer chain aliphatic polyamides (i.e. Diamine2, Diamine3, Diamine4, and Diamine5) showed a slightly lower roughness than that of 1 wt.% except Diamine1 shorter chain counterpart, which are confirmed with AFM surface analysis. The effect of various concentrations of aliphatic diamine monomer on the nanomechanical properties was investigated by a nanoindentation test method. At 1-2 wt.% hydrophilic polyamides the nanohardness decreased from 0.023-0.025 GPa for shorter chain aliphatic polyamides (i.e. Diamine1 and Diamine2) to 0.012-0.016 GPa for longer chain aliphatic polyamides (i.e. Diamine3, Diamine4 and Diamine5) while elastic modulus of longer chain aliphatic polyamides increased by 39 %. This was probably due to the influence of an internal molecular packing of polyamides and the flexibility of the polymer chains. The hydrophilic polyamide (i.e. Diamine1) also showed a high water flux ($4.5 \pm 0.1 \text{ L m}^{-2} \text{ h}^{-1} \text{ bar}^{-1}$ under 2 bar), which is 3 times higher than that of hydrophobic polyamide and rejection to methylene blue (> 70%) because the thin and defect free hydrophilic polyamide selective layer is formed on the polyphenol/aminosilane coupling interlayer. Based on these results, the hydrophilic polyamides can be considered to be promising membrane for nanofiltration.

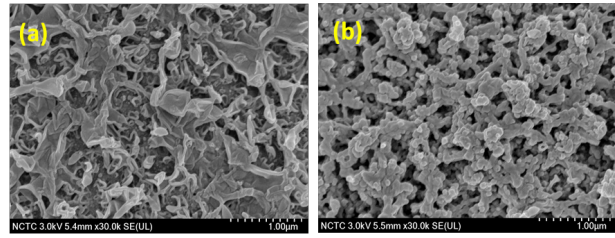
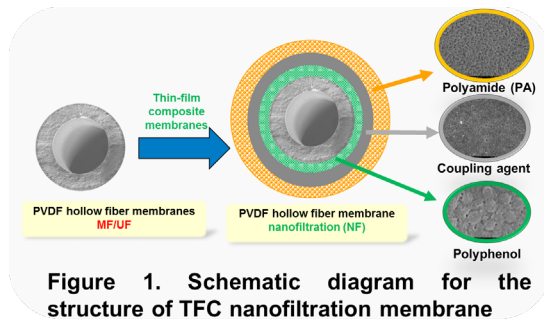


Figure 2. SEM images of surface of (a) polyamide without aliphatic diamine (b) polyamide with aliphatic diamine

Keywords: Nanofiltration, Interfacial Polymerization, Hydrophilic Polyamide

Surface-Enhanced Raman Scattering Detection of Polycyclic Aromatic Hydrocarbons by Thiol-Modified Silver Nanoparticle Film Substrate

Sathita Taksadej^{a,b,c}, Kanet Wongravee^{b,c}, Sanong Ekgsait^{b,c},
Prompong Pienpinijtham^{b,c*}

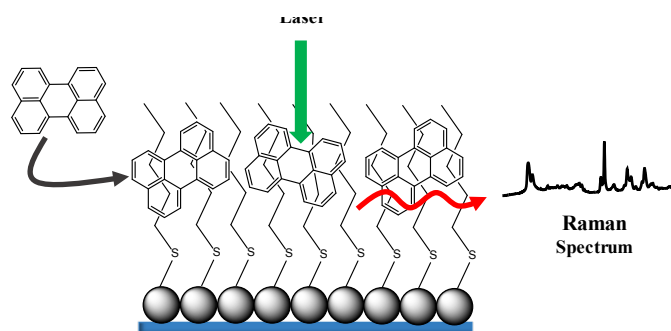
^aProgram in Petrochemistry and Polymer Science, Faculty of Science, Chulalongkorn University,
254 Phyathai Road, Patumwan, Bangkok 10330, Thailand

^bSensor Research Unit (SRU), Department of Chemistry, Faculty of Science, Chulalongkorn University,
254 Phyathai Road, Patumwan, Bangkok 10330, Thailand

^cNational Nanotechnology Center of Advanced Structural and Functional Nanomaterials,
Department of Chemistry, Faculty of Science, Chulalongkorn University, Thailand

*e-mail: prompong.p@chula.ac.th

Polycyclic aromatic hydrocarbons (PAHs) are known as hazardous substances and considered to be carcinogen, mutagen, and teratogen. Surface-enhanced Raman scattering (SERS) for PAHs trace analysis can be performed by using metal nanoparticles as substrates where PAHs are attached and affected by the enhanced electromagnetic field. One common obstacle is to modify the metal nanoparticles surface to create the suitable environment for PAHs, which have very low affinity with metal nanoparticle surface, to deposit on. In this research, different kinds of thiol substances are used to modify the surface of silver nanoparticles to create hydrophobic environments for PAHs to be adsorbed on substrate. By fabricating modified silver nanoparticles into films, the obtained substrate is more stable and more convenient for using and storing comparing to silver nanoparticles in a colloidal form. The results show that PAHs can attach on the substrate surface and show their characteristic peaks in SERS spectra. Because the difference in characteristic peaks of PAHs and substrates is difficult to determine, chemometric techniques, *i.e.*, principal component analysis (PCA) and partial least square (PLS) regression, are employed to help for data analysis both qualitatively and quantitatively. Nine kinds of PAHs can be detected both individually and in the mixture of PAHs, with the maximum obtained R^2 of 0.9992. This substrate can be used for *in situ* detection of PAHs both in laboratory and on-site.





AGR-O-07



Figure 1. PAH on thiol-modified silver nanoparticle film for SERS measurement.

Keywords: surface-enhanced Raman scattering (SERS), polycyclic aromatic hydrocarbons (PAHs), silver nanoparticles (AgNPs), trace analysis

References

1. Y. Xie, X. Wang, X. Han, W. Song, W. Ruan, J. Liu, B. Zhao, Y. Ozaki, *J. Raman Spectrosc.* **2011**, *42*, 945–950.
2. P. Pienpinijtham, X. X. Han, S. Ekgasit, Y. Ozaki, *Phys. Chem. Chem. Phys.*, **2012**, *14*, 10132-10139
3. J. Kubackova, G. Fabriciova, P. Miskovsky, D. Jancura, S. Sanchez-Cortes, *Anal. Chem.* **2015**, *87*, 663–669.

Preparation of Cellulose Nanofibers (CNFs) from Pulp of *Macaranga sp.*

E. Sutrisno^a, S. Chuangchote^{b*}, S. Tanpichai^c and M. Phiriyawirut^b

- a. *Nanoscience and Nanotechnology Graduate Program, King Mongkut's University of Technology Thonburi (KMUTT), 126 Pracha Uthit Rd., Bangmod, Thungkhru, Bangkok 10140, Thailand.*
- b. *Department of Tool and Materials Engineering, Faculty of Engineering, King Mongkut's University of Technology Thonburi (KMUTT), 126 Pracha Uthit Rd., Bangmod, Thungkhru, Bangkok 10140, Thailand.*
- c. *Learning Institute King Mongkut's University of Technology Thonburi (KMUTT), 126 Pracha Uthit Rd., Bangmod, Thungkhru, Bangkok 10140, Thailand.*

* e-mail: surawut.chu@kmutt.ac.th

Macaranga sp. is one of source alternatives for wood fibers in pulp and paper industries. The International Association of Wood Anatomists (IAWA) classified macaranga tree as the long wood fiber. It can produce pulp with high strength. Based on these characters, cellulose derived from macaranga tree is very potential as a raw material for cellulose nanofibers (CNFs). The principles of fabrication of CNFs are separation and purification. In this work, CNFs from pulp of macaranga tree were prepared by following the fabrication steps, i.e. pretreatment, alkali treatment, and acid hydrolysis. These simple methods can produce CNFs from macaranga pulp in diameter 300nm. Each fabrication step has effect on the characters of the fibers produced. Scanning electron microscopy (SEM) was used to determine the changes of fiber dimensions and Fourier-transform infrared spectroscopy (FT-IR) was used to investigate the changes from cellulose type I to cellulose type II. Furthermore, the integrated treatments were also studied to produce uniform and separated CNFs.

Keywords: Cellulose Nanofibers (CNFs), Fabrications, Fibers, Macaranga, Pulp.

Rational Design and Synthesis of High Efficient Photocatalyst for Hydrogen Production

Jiaqian Qin^{a,b,*}, Chengwu Yang^b, Xinyu Zhang^{b,*}, and Riping Liu^b

^a*Metallurgy and Materials Science Research Institute, Chulalongkorn University, Bangkok 10330, Thailand.*

^b*State Key Laboratory of Metastable Materials Science and Technology, Yanshan University, Qinhuangdao 066004, P. R. China.*

*e-mail: jiaqian.q@chula.ac.th, xyzhang@ysu.edu.cn.

Photocatalytic technology, as a green and efficient technology, can convert solar energy into chemical energy and degrade organic pollutants^{1,2}. To obtain high photocatalytic performance, we designed and prepared a variety of photocatalyst materials. C-TiO₂/g-C₃N₄ composite was prepared by heat treatment³. C-TiO₂ and g-C₃N₄ form a binary heterojunction structure, effectively separating photogenerated electron-hole pairs and optimizing the band gap and optical absorption properties (Figure 1a, 1b). Alternatively, Bi₂O₂CO₃ modified g-C₃N₄ material was also prepared (Figure 1c). It is found that this material is a direct Z-scheme heterojunction system, which can further separate charge carriers and improve photocatalytic activity (Figure 1d). In addition, a ternary composite photocatalyst, WS₂/g-C₃N₄/C-TiO₂, was prepared by impregnation method (Figure 1e). The significantly enhanced photocatalytic performance for splitting seawater was achieved (Figure 1f). These photocatalysts with high photocatalytic activity and stability provide a promising candidate to make clean energy in rational use of water resources.

Keywords: photocatalyst, C-TiO₂/g-C₃N₄, Bi₂O₂CO₃/g-C₃N₄, WS₂/g-C₃N₄/C-TiO₂

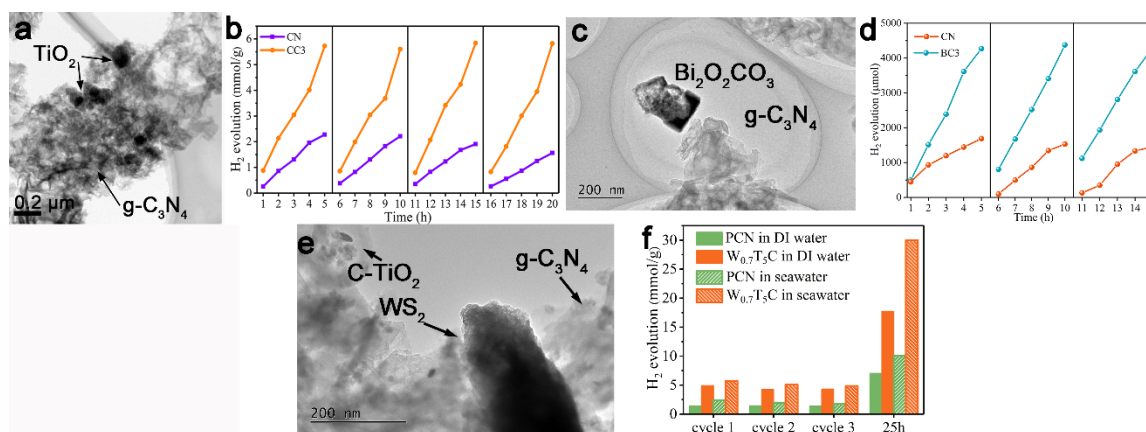


Figure 1. a) TEM image and b) photocatalytic activity of C-TiO₂/g-C₃N₄. c) TEM image and d) photocatalytic activity of Bi₂O₂CO₃/g-C₃N₄. e) TEM image and f) photocatalytic activity of WS₂/g-C₃N₄/C-TiO₂.

References

1. D. W. Wakerley, M. F. Kuehnel, K. L. Orchard, K. H. Ly, T. E. Rosser and E. Reisner, *Nature Energy*, **2017**, *2*, 17021.
2. L. Qian, J. F. Chen, Y. H. Li, L. Wu, H. F. Wang, A. P. Chen, P. Hu, L. R. Zheng and H. G. Yang, *Angew Chem Int Ed Engl*, **2015**, *54*, 11467-11471.
3. C. Yang, J. Qin, Z. Xue, M. Ma, X. Zhang and R. Liu, *Nano Energy*, **2017**, *41*, 1-9.

Environment-friendly Alternative to Copper Cyanide-based Electroplating Bath for Nanocoating Applications

Christine Adelle Rico Yuson^{a,b}, Tanujjal Bora^{a,c*} and G. Louis Hornyak^{a,c}

^a*Nanotechnology, Industrial Systems Engineering, School of Engineering and Technology, Asian Institute of Technology, PO Box 4, Klong Luang, Pathumthani – 12120, Thailand*

^b*Department of Physics, College of Arts and Sciences, Central Mindanao University, Musuan, Maramag, Bukidnon – 8710, Philippines*

^c*Center of Excellence in Nanotechnology, Asian Institute of Technology, PO Box 4, Klong Luang, Pathumthani – 12120, Thailand*

**e-mail: tboraa@ait.ac.th*

Copper-cyanide is widely used as an electrolyte in electroplating baths providing good adhesion of copper onto a metallic or alloyed surface, which is a common practice in almost all electroplating industries across the world. However, there has been a current awareness of the impact generated onto the environment and the enterprises' workers by the wastes and toxic debris from copper-cyanide. Various regulating commissions worldwide including Thailand's Pollution Control Department have urged electroplating industries to urgently phase-out the use of cyanide which is considered as "highly toxic chemicals used in the plating baths lethal to a human". Thus, there is a need to change copper-cyanide into a more environment-friendly alternative.

In this study, a cyanide-free electroplating bath containing glutamate as a complexing agent is investigated as an environment-friendly alternative for copper plating. A naturally occurring non-essential amino acid, glutamate reacts with copper in an aqueous solution which exhibits similar properties to copper-cyanide by forming complexes¹. The pH of the electroplating bath is chosen from equilibrium diagrams to avoid the formation of insoluble complexes and oxides at varying copper: glutamate molar ratio. Cyclic voltammetry enabled the characterization of the electrochemical response of the plating system in copper deposition. The results suggest the occurrence of one cathodic peak indicating a single-step reduction of copper complexes to copper metal, taking place in a two-electron electrochemical mechanism. The electrochemical response of the plating bath at a scan rate of 100 mVs⁻¹ on a stationary electrode confirms 1:3 molar ratio and pH =8 to exhibit successful copper deposition onto the substrate. The preliminary results from our study suggests that copper-glutamate electroplating bath is a potential alternative to copper-cyanide bath without the need of additives allowing a one-step electroplating process. By carefully controlling the current flowing through the circuit, the process can deposit nanometer-thin layers of materials onto the substrate suitable for nanocoating applications.

Keywords: Copper-glutamate, Copper-cyanide, Cyanide toxicity, Cyclic voltammetry, Electroplating

References

1. Ibrahim, M. A. M. & Bakdash, R. S. New non-cyanide acidic copper electroplating bath based on glutamate complexing agent. *Surf. Coatings Technol.* **282**, 139–148 (2015).



CAT-O-05



Enhancement of Furfural Hydrogenation to Furfuryl Alcohol over Copper-based Catalysts: Effect of Catalyst Synthesis Methods

Tanasan Intana^a, Anita Leong Su Juan^b, Sirapassorn Kiatphueangporn^a,
Sutarat Thongratkaew^a and Kajornsak Faungnawakij^{a,*}

*a Nanomaterials for Energy and Catalysis Laboratory,
National Nanotechnology Center (NANOTEC),*

National Science and Technology Development Agency (NSTDA),

111 Thailand Science Park, Paholyothin Rd., Klong Laung, Pathumthani 12120, Thailand

b Chemical Engineering Department, Universiti Teknologi PETRONAS,

Bandar Seri Iskandar, 32610 Perak, Malaysia

** e-mail: kajornsak@nanotec.or.th*

Furfuryl alcohol is one of the valuable platform chemicals in the manufactures of vitamin C, lysine, plasticizer, dispersing agent and resins. The series of copper-based catalysts with different metals (Fe, Mn, Zn, Al, Zr) used in this work were prepared by co-precipitation and sol-gel combustion methods. Physiochemical properties of all Cu-based catalysts were characterized by X-ray diffraction (XRD), N₂ physisorption, X-ray photoelectron spectroscopy (XPS), H₂ temperature-programmed reduction (H₂-TPR) and N₂O chemisorption. The catalytic performance was evaluated by studying the effects of catalyst synthesis methods and calcination temperatures in the co-precipitation method. Among all the catalysts tested in the reaction, Cu/ZnO calcined at 700°C (CZ700) and CuMn₂O₄ demonstrated high activity with high furfural conversion and furfuryl alcohol selectivity in respective synthesis methods, however, the CuMn₂O₄ gave the highest turnover frequency (TOF) of 94.5%. In addition, the effects of H₂ pressures (20–40 bar) and reaction temperatures (130°C–190°C) were investigated on the CZ700 and CuMn₂O₄ catalysts. The optimal temperature and H₂ pressure of CZ700 and CuMn₂O₄ catalysts were 170°C at 20 bar, and 150°C at 20 bar, respectively.

Keywords: Furfural, Furfuryl alcohol, Copper-based catalysts, Co-precipitation, Sol-gel combustion

References

1. R.V. Sharma, U. Das, R. Sammynaiken, A.K. Dalai, *Appl. Catal. A : Gen.* **2013**, *454*, 127–136.
2. W. Gong, C. Chen, Y. Zhang, H. Zhou, H. Wang, H. Zhang, Y. Zhang, G. Wang, H. Zhao, *ACS Sustainable Chem. Eng.* **2017**, *5*, 2172–2180.
3. F. Wang, Z. Zhang, *ACS Sustainable Chem. Eng.* **2017**, *5*, 942–947.
4. J. Zhang, K. Dong, W. Luo, H. Guan, *ACS Omega* **2018**, *3*, 6206–6216.

CAT-O-07

Surface Enhancement and Structure Formation of Metakaolin from Thailand Kaolin on the Various Calcination Temperature

**Worapak Tanwongwan^a, Thanapat Wongkitikun^a, Kobchai Onpecht^a, Suphada Srilai^a,
Suttichai Assabumrungrat^b, Nuwong Chollacoop^c, and Apiluck Eiad-ua^a**

^a*College of Nanotechnology, King Mongkut's Institute of Technology Ladkrabang (KMITL),
Chalongkrung Rd., Ladkrabang, Bangkok 10520, Thailand*

^b*Department of Chemical Engineering, Faculty of Engineering, Chulalongkorn University,
Phayathai Rd., Phatumwan, Bangkok, 10330, Thailand*

^c*National Metal and Materials Technology Center (MTEC), National Science and Technology
Development Agency (NSTDA), Phahonyothin Rd. Khlong Luang,
Pathum Thani 12120, Thailand*

**e-mail: apiluck.ei@kmitl.ac.th*

Kaolin from Thailand selected from 3 different sources including Ratchaburi, Narathiwat, and Uttaradit was used as starting materials for synthesis of metakaolin. The calcination temperature of this study was chosen in the range of 500 to 1000°C for 2 h. The results which were obtained by X-ray diffraction, Fourier transform infrared spectroscopy, and scanning electron microscopy techniques show that the most appropriate temperature for metakaolin synthesis is about 800°C. The calcination temperature significantly affected the function group, surface morphology and configuration of metakaolin. The metakaolin was chosen as a starting material for the synthesis of the zeolite because it exhibited high crystallinity, reactivity and purity to be used as raw material.

Keywords: Kaolin, Metakaolin, Calcination temperature

Influence of Acid Additive on Nanoporous Carbon Materials via HTC for Catalyst Support

Tripob Longprang^a, Dolrudee Jaruwat^b, Buachum Udomsap^c, Nuwong Chollacoop^c and Apiluck Eiad-ua^{a*}

^aCollege of Nanotechnology, King Mongkut's Institute of Technology Ladkrabang, Thailand

^bDepartment of Chemical Engineering, Faculty of Engineering, Chulalongkorn University, Phayathai Rd., Phatumwan, Bangkok, 10330, Thailand

^cNational Metal and Materials Technology Center, National Science and Technology Development Agency, Pathumthani 12120, Thailand

*e-mail: apiluck.ei@kmitl.ac.th

Nanoporous carbon materials were successfully synthesized via hydrothermal carbonization with acid additives. In this study the effect of hydrothermal temperature (160-200 °C), hydrothermal time (4-24 h) and influence of acid additive (HCl, HNO₃, H₂SO₄ and H₃PO₄) have been chosen in order to improve the surface structure. The samples have been characterized by scanning electron microscopy, nitrogen sorption, Fourier transform infrared spectroscopy and X-ray diffraction. The experimental results revealed that hydrothermal carbonization process and acid addition have effect on the properties of catalyst support. The results indicated that hydrothermal process at 200°C for 12 hr and activation with H₃PO₄ at 900°C for 2 hr, exhibited the highest surface area, porosity and pore volume leading to increased distribution of metal on the carbon support.

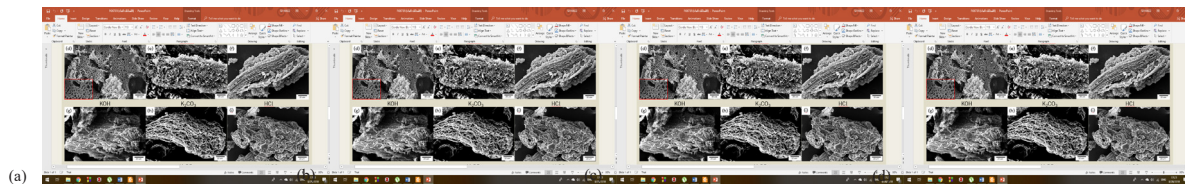


Figure 1. SEM image of carbon supports activated with (a) HCL, (b) HNO₃, (c) H₂SO₄ and (d) H₃PO₄ after HCT process

Keyword: Biomass, Nanoporous Carbon, Catalyst support, Hydrothermal carbonization

Enhancement of Furfural Hydrogenation to Furfuryl Alcohol over Copper-based Catalysts: Effect of Catalyst Synthesis Methods

Tanasan Intana^a, Anita Leong Su Juan^b, Sirapassorn Kiatphueangporn^a, Sutarat Thongratkaew^a and Kajornsak Faungnawakij^{a,*}

^a*Nanomaterials for Energy and Catalysis Laboratory, National Nanotechnology Center (NANOTECH), National Science and Technology Development Agency (NSTDA), 111 Thailand Science Park, Paholyothin Rd., Klong Laung, Pathumthani 12120, Thailand*

^b*Chemical Engineering Department, Universiti Teknologi PETRONAS, Bander Seri Iskandar, 32610 Perak, Malaysia*

**e-mail: kajornsak@nanotec.or.th*

Furfuryl alcohol is one of the valuable platform chemicals in the manufactures of vitamin C, lysine, plasticizer, dispersing agent and resins. The series of copper-based catalysts with different metals (Fe, Mn, Zn, Al, Zr) used in this work were prepared by co-precipitation and sol-gel combustion methods. Physiochemical properties of all Cu-based catalysts were characterized by X-ray diffraction (XRD), N₂ physisorption, X-ray photoelectron spectroscopy (XPS), H₂ temperature-programmed reduction (H₂-TPR) and N₂O chemisorption. The catalytic performance was evaluated by studying the effects of catalyst synthesis methods and calcination temperatures in the co-precipitation method. Among all the catalysts tested in the reaction, Cu/ZnO calcined at 700°C (CZ700) and CuMn₂O₄ demonstrated high activity with high furfural conversion and furfuryl alcohol selectivity in respective synthesis methods, however, the CuMn₂O₄ gave the highest turnover frequency (TOF) of 94.5%. In addition, the effects of H₂ pressures (20–40 bar) and reaction temperatures (130°C–190°C) were investigated on the CZ700 and CuMn₂O₄ catalysts. The optimal temperature and H₂ pressure of CZ700 and CuMn₂O₄ catalysts were 170°C at 20 bar, and 150°C at 20 bar, respectively.

Keywords: Furfural, Furfuryl alcohol, Copper-based catalysts, Co-precipitation, Sol-gel combustion

References

1. R.V. Sharma, U. Das, R. Sammynaiken, A.K. Dalai, *Appl. Catal. A : Gen.* **2013**, *454*, 127–136.
2. W. Gong, C. Chen, Y. Zhang, H. Zhou, H. Wang, H. Zhang, Y. Zhang, G. Wang, H. Zhao, *ACS Sustainable Chem. Eng.* **2017**, *5*, 2172–2180.
3. F. Wang, Z. Zhang, *ACS Sustainable Chem. Eng.* **2017**, *5*, 942–947.
4. J. Zhang, K. Dong, W. Luo, H. Guan, *ACS Omega* **2018**, *3*, 6206–6216.



CAT-O-10



Surface Enhancement and Structure Formation of Metakaolin from Thailand Kaolin on the Various Calcination Temperature

Worapak Tanwongwan^a, Thanapat Wongkitikun^a, Kobchai Onpecht^a, Suphada Srilai^a, Suttichai Assabumrungrat^b, Nuwong Chollacoop^c, and Apiluck Eiad-ua^a

^a*College of Nanotechnology, King Mongkut's Institute of Technology Ladkrabang (KMITL), Chalongkrung Rd., Ladkrabang, Bangkok 10520, Thailand*

^b*Department of Chemical Engineering, Faculty of Engineering, Chulalongkorn University, Phayathai Rd., Phatumwan, Bangkok, 10330, Thailand*

^c*National Metal and Materials Technology Center (MTEC), National Science and Technology Development Agency (NSTDA), Phahonyothin Rd. Khlong Luang, Pathum Thani 12120, Thailand*

**e-mail: apiluck.ei@kmitl.ac.th*

Kaolin from Thailand selected from 3 different sources including Ratchaburi, Narathiwat, and Uttaradit was used as starting materials for synthesis of metakaolin. The calcination temperature of this study was chosen in the range of 500 to 1000°C for 2 h. The results which were obtained by X-ray diffraction, Fourier transform infrared spectroscopy, and scanning electron microscopy techniques show that the most appropriate temperature for metakaolin synthesis is about 800°C. The calcination temperature significantly affected the function group, surface morphology and configuration of metakaolin. The metakaolin was chosen as a starting material for the synthesis of the zeolite because it exhibited high crystallinity, reactivity and purity to be used as raw material.

Keywords: Kaolin, Metakaolin, Calcination temperature

CEL-O-01

Influence of Acid Additive on Nanoporous Carbon Materials via HTC for Catalyst Support

Tripob Longprang^a, Dolrudee Jaruwat^b, Buachum Udomsap^c, Nuwong Chollacoop^c
and Apiluck Eiad-ua^{a*}

^aCollege of Nanotechnology, King Mongkut's Institute of Technology Ladkrabang, Thailand

^bDepartment of Chemical Engineering, Faculty of Engineering, Chulalongkorn University,
Phayathai Rd., Phatumwan, Bangkok, 10330, Thailand

^cNational Metal and Materials Technology Center, National Science and
Technology Development Agency, Pathumthani 12120, Thailand

*e-mail: apiluck.ei@kmitl.ac.th

Nanoporous carbon materials were successfully synthesized via hydrothermal carbonization with acid additives. In this study the effect of hydrothermal temperature (160-200 °C), hydrothermal time (4-24 h) and influence of acid additive (HCl, HNO₃, H₂SO₄ and H₃PO₄) have been chosen in order to improve the surface structure. The samples have been characterized by scanning electron microscopy, nitrogen sorption, Fourier transform infrared spectroscopy and X-ray diffraction. The experimental results revealed that hydrothermal carbonization process and acid addition have effect on the properties of catalyst support. The results indicated that hydrothermal process at 200°C for 12 hr and activation with H₃PO₄ at 900°C for 2 hr, exhibited the highest surface area, porosity and pore volume leading to increased distribution of metal on the carbon support.

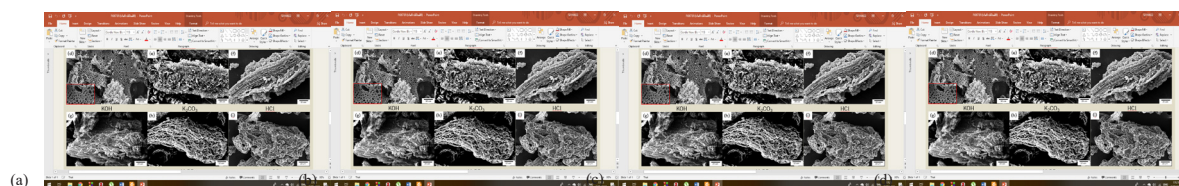


Figure 1. SEM image of carbon supports activated with (a) HCL, (b) HNO₃, (c) H₂SO₄ and (d) H₃PO₄ after HCT process

Keyword: Biomass, Nanoporous Carbon, Catalyst support, Hydrothermal carbonization

***In situ* XAFS Characterization of CuFe_2O_4 Catalysts under Oxidation, Reduction and Stream Reforming Conditions**

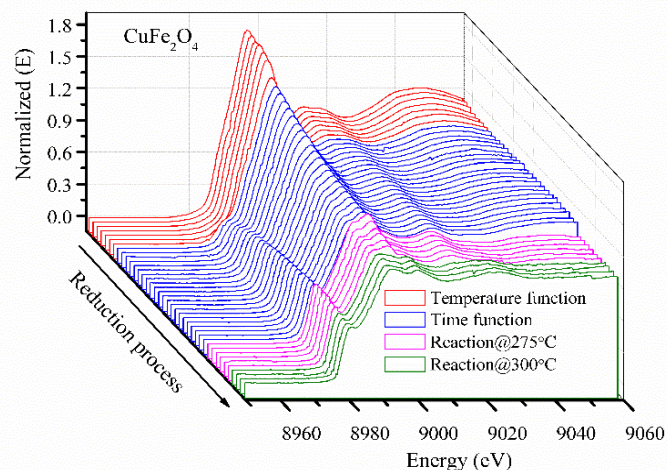
Pongtanawat Khemthong^{1*}, Kajornsak Faungnawakij¹, Chanapa Kongmark²

¹*National Nanotechnology Center, National Science and Technology Development Agency, Thailand*

²*Department of Materials Science, Faculty of Science, Kasetsart University, Bangkok, Thailand*

*e-mail: pongtanawat@nanotec.or.th

Copper ferrite (CuFe_2O_4) spinel can provide excellent performance for generating hydrogen feeds through methanol steam reforming reaction. The activity of CuFe_2O_4 spinel is strongly dependent on method to synthesis because it can influence on the Cu particle size and its dispersion which could lead to better catalytic performance. Thus, in this work, a series of CuFe_2O_4 catalysts prepared from different methods, including sol-gel combustion, space confined-synthesis and hard template removal, have been studied and compared for their oxidation, reduction and catalytic behaviors. Throughout this investigation, the advanced *in situ* X-ray absorption fine structure (*in situ* XAFS) technique, including the extended X-ray absorption fine structure (EXAFS) and X-ray absorption near edge structure (XANES) are performed to elucidate the relationship between synthesis methods and catalytic performance on hydrogen production from methanol steam reforming under various conditions. We have expected that the understanding of structural behaviors of the three different Cu-Fe spinel catalysts prepared in this work could rationally explain their catalytic performance for production of H_2 from methanol. In addition, the calcined samples were confirmed phase as a spinel-type structure by X-ray diffraction (XRD). The morphology was observed by transmission electron microscope (TEM). The porosity of these samples was also investigated by N_2 sorption isotherm and being calculated by BET method.



CEL-O-04

Analysis Study of Surface Acidity of Alumina Catalysts by Ammonia IRMS-TPD and its Role in Catalytic Conversion of D-xylose to Lactic Acid

Sirapassorn Kiatphuengporn^a, Chuleporn Luadthong, Kajornsak Faungnawakij^{a,*}

^a *Nanomaterials for Energy and Catalysis Laboratory, National Nanotechnology Center (NANOTEC),*

National Science and Technology Development Agency (NSTDA),

Klong Laung, Pathumthani 12120, Thailand

**e-mail: kajornsak@nanotec.or.th*

Lactic acid, a valuable platform chemical, has increasing attention in wide applications of food, pharmaceutical and chemical industries. For the lactic acid production, the total acid sites and type of surface acidity are essential factors effecting the catalytic performance. Accordingly, in this research, the acidic properties of calcined Al₂O₃ catalysts at different temperatures (RT, 500, 700, 1100°C) were analyzed by using an infrared-mass spectroscopy combined with temperature-programmed desorption of adsorbed ammonia (IRMS-TPD). Moreover, the role of acidic properties on the activity in lactic acid production from D-xylose was investigated in a batch reactor. It was found that the total acid sites decreased with increasing the calcination temperature. Al₂O₃ catalyst (Al-RT) exhibited the highest D-xylose conversion (> 99%) and lactic acid yield (85%). This outstanding performance was attributed to the total acid sites and surface acidity, especially Lewis acid site, leading to the increase of catalytic and selective conversion to lactic acid.

Keywords: Lactic acid production, Acidity, Alumina catalyst, IRMS-TPD

References

1. A.A. Marianou, C.M. Michailof, A. Pineda, E.F. Iliopoulou, K.S. Triantafyllidis, A.A. Lappas, *Applied Catalysis A: General* **2018**, 555, 75-87.
2. S. Sukanuma, K. Nakamura, A. Okudaira, N. Katada, *Molecular Catalysis* **2017**, 435, 110-117.

Cotton Coated with Trimethylsilylcellulose

Jirapat Wattanaruangkwit^a, Radchada Bunttem^{b*}, Duangkhae Srikun^a

^a*Department of Chemistry, Mahidol Wittayanusorn School, Nakhon Pathom 73170, Thailand.*

^b*Department of Chemistry, Faculty of Science, Silpakorn University, Nakhon Pathom 73000, Thailand.*

**e-mail: radchadab@yahoo.com*

The modification of cotton surface to increase its hydrophobicity has been attempted by various substances. This surface modification helps increase the anti-fungal and stain-resistance capabilities. Trimethylsilyl cellulose (TMSC) is a very interesting candidate due to its compatibility and environmental-friendly properties. It was prepared by reacting cotton linters with hexamethyldisilaxae (HMDS). Cotton linter (10 g) was soaked with 1 M ethylenediamine. Then it was dissolved in dimethylacetamide/LiCl and HMDS is added to produce TMSC. It was then characterized by FT-IR, NMR spectroscopy and Scanning Electron Microscopy-Energy Dispersive X-ray (SEM-EDX). The IR spectrum show the absorption bands indicating the presence of $-\text{Si}(\text{CH}_3)_3$ groups: $\nu_{\text{Si-O}}$ at 1081 cm^{-1} , $\nu_{\text{C-Si}}$ at $1252, 842$ and 750 cm^{-1} . The $^1\text{H-NMR}$ result confirms the presence of $-\text{Si}(\text{CH}_3)_3$ groups at $\gg 0$ ppm and pyranose ring protons in the range of 2.8-4.5 ppm. SEM image of TMSC shows the fibrous characteristics of cellulose while the EDX shows the presence of Si. The degree of substitution (DS) values calculated from FT-IR and EDX data are 2.32 and 2.51 respectively. 0.25% w/v TMSC solutions were prepared using two different solvents: acetone and THF. A Small piece of cotton fabric was dipped into the TMSC solution. The contact angle measurement, FT-IR spectroscopy and SEM-EDX were performed on the coated cottons. The cotton coated by TMSC/acetone has an average contact angle of 129° . While the cotton coated by TMSC/THF has an average contact angle of 124° . FT-IR spectrum of coated cotton gives the absorption band of $\nu_{\text{Si-O}}$ and $\nu_{\text{C-Si}}$. The SEM-EDX of coated cotton shows the thick film of TMSC with the presence of Si on the cotton surface. The cotton coated by TMSC/acetone yields a higher percentage of Si evidencing the higher amount of TMSC on the cotton surface.

Keywords: Hydrophobic cotton, Trimethylsilyl cellulose, Cellulose Modification

References

1. Y. Yao, A. Gellerich, M. Zauner, X. Wang, *Cellulose* **2018**, *25*, 1329-1338.
2. A. He, D. Liu, H. Tian, Y. Jin, Q. Cheng and J. Song, *Cell. Chem. Technol.* **2014**, *48*, 19-23.
3. H. Kono, T. Erata and M. Takai, *Macromolecules* **2003**, *36*, 3589-3592.

Simple Paper-Based Sensor for Zn²⁺ Ion from Aminoquinoline Derivatives

Apiwat Promchat^{a,b}, Mongkol Sukwattanasinitt^{a,b} and Thanit Praneenarat^{a,c*}

^aDepartment of Chemistry, Faculty of Science, Chulalongkorn University, Phayathai Rd., Pathumwan, Bangkok, 10330, Thailand

^bNanotec-CU Center of Excellence on Food and Agriculture, Chulalongkorn University, Bangkok 10330, Thailand

^cThe Chemical Approaches for Food Applications Research Group, Faculty of Science, Chulalongkorn University, Phayathai Rd., Pathumwan, Bangkok, 10330, Thailand.

*e-mail: thanit.p@chula.ac.th

A highly sensitive fluorescence turn-on probe for Zn²⁺ ion was developed based on amide derivatives of aminoquinolines. A selected set of three amide derivatives of aminoquinolines were synthesized from the condensation of three aminoquinolines and glycine. Only derivatives from 8-aminoquinoline and glycine (**Gly.8AQ**) showed strong fluorescence response selectively to Zn²⁺, which can be clearly observed in the micromolar range by naked eyes. The probe **Gly.8AQ** was then further developed into a paper-based sensing kit that can selectively detect Zn²⁺ ion in the submicromolar range by converting the image into numerical data via an imaging processing software.

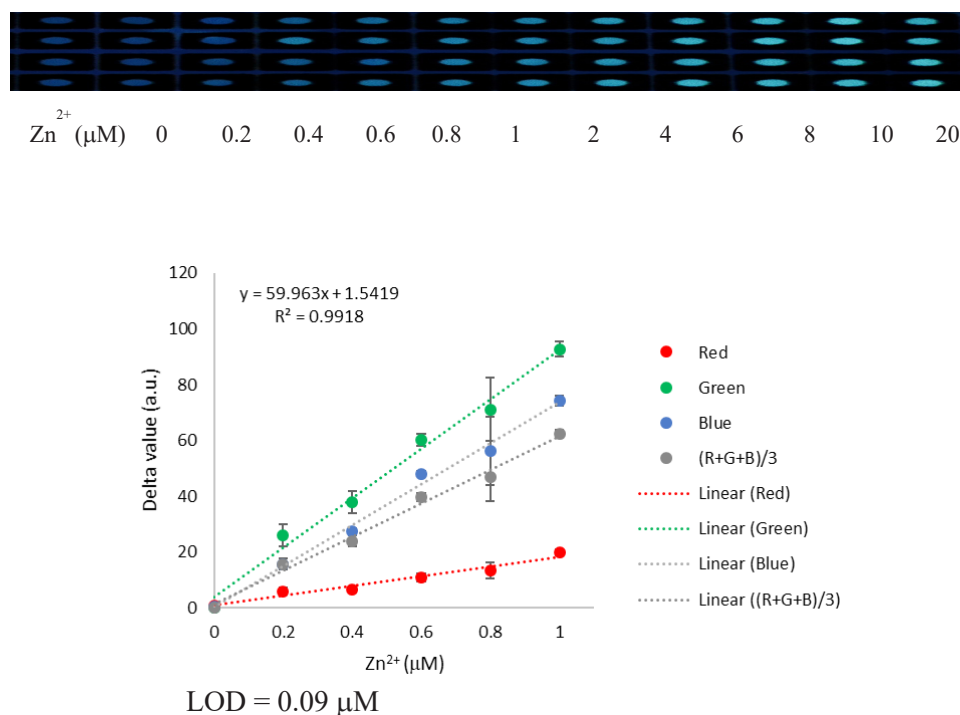


Figure 1. Picture of paper-based sensor after test with Zn²⁺ ions (0-20 μM) and linear calibration line for quantitative determination of Zn²⁺ concentration.

Keywords: Paper-based Sensor, Zn²⁺ ion Sensor, Aminoquinoline, Fluorescent Sensor

References

- ¹⁰⁶ K. Boonkitpatarakul, A. Smata, K. Kongnukool, S. Srisurichan, K. Chainok, M. Sukwattanasinitt, *J. Luminescence* **2018**, *198*, 59-67.

Mechanoresponsive “Turn-On” Transparent Luminescent Cellulose Nanopaper with Mechanochromic Aiegen

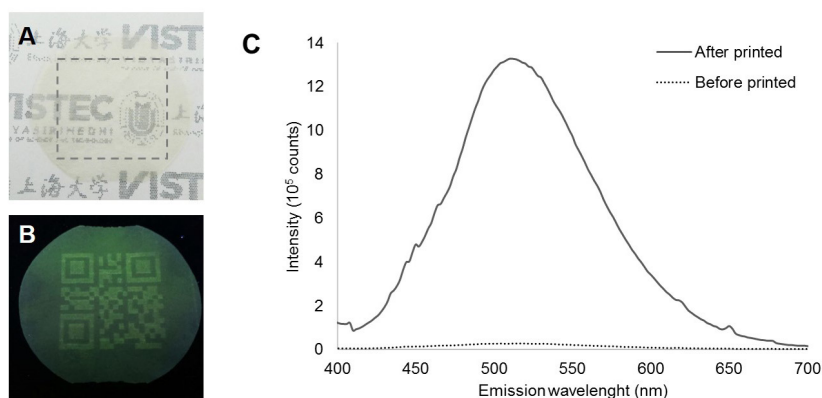
Phattananawee Nalaoh^{a,b}, Miao Miao^a, Vinich Promarak^{*b}, and Feng Xin^{*a}

^aResearch Center of Nano Science and Technology, Shanghai University, Shanghai, 200444, P.R. China.

^bSchool of Molecular Science and Engineering, Vidyasirimedhi Institute of Science and Technology (VISTEC), Wangchan, Rayong, 21210, THAILAND.

*e-mail: fengxin@shu.edu.cn, Vinich.p@vistec.ac.th

Transparent luminescent cellulose nanopaper with mechanochromic responsive properties offers the new application of transparent paper with luminescent properties which can be induced by giving mechanical force on the paper with mechanochromic compound. Tetrakis(4-nitrophen-1-yl)ethene (NTPE) has been known as good mechanochromic response which showed green emission after crystal deformation with mechanical force. Herein, we reported the synthesis and characterization properties of flexible and freestanding mechanoresponsive nanopaper preparing from crystalline cellulose nanofiber (CNF) as fibrous skeletons and NTPE microcrystalline as a mechanochromic aggregation-induced emission (AIE) compound. The suspension of CNF and NTPE in water was assembling on polycarbonate membrane using nitrogen compression, followed by drying under vacuum oven to give NTPE-CNF paper. The paper showed good transparency with low photoluminescent under UV irradiation. However, after the force was given with dot matrix printer, the designed area showed the high fluorescence than the outer area (Figure 1). The cause



of emission colour and intensity changing by crystal deformation was investigated and proven by scanning electron microscope (SEM) imaging and X-ray diffraction (XRD) spectroscopy.

Figure 1. (A) NTPE-CNF paper with printed area (in dashed square) showed good transparency in daylight ambient. (B) Quick response (QR) code using dot matrix printer was appeared under UV irradiation. (C) The emission intensity was increased after the mechanical force was given to the NTPE-CNF paper.

Keywords: Cellulose Nanofiber Paper, Aggregation-induced Emission, Mechanochromism

References

1. M. Miao, J. Zhao, X. Feng, Y. Cao, S. Cao, Y. Zhao, X. Ge, L. Sun, L. Shi and J. Fang, *J. Mater. Chem. C*, 2015, **3**, 2511-2517.
2. T. Yu, D. Ou, Z. Yang, Q. Huang, Z. Mao, J. Chen, Y. Zhang, S. Liu, J. Xu, M. R. Bryce and Z. Chi, *Chem. Sci.*, 2017, **8**, 1163-1168.

Development of Bacterial Cellulose as Substrates for Sensing Applications

Jadetapong Klahan^a, Chindanai Pongpreda^b, Kanokthorn Boonkitpatarakul^c and Mongkol Sukwattanasinitt^{d*}

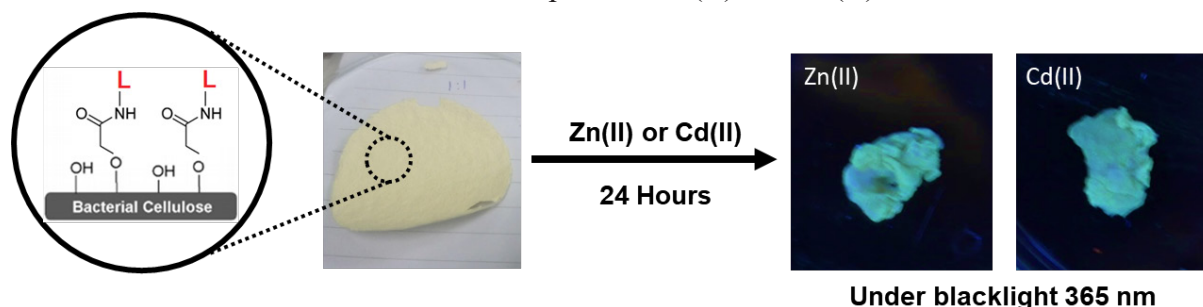
^{a,c}Program of Petrochemistry, Faculty of Science, Chulalongkorn University, Bangkok 10330, Thailand

^bDepartment of Chemistry, Faculty of Science, Chulalongkorn University, Bangkok 10330, Thailand

^dNanotec-CU Center of Excellence on Food and Agriculture, Chulalongkorn University, Bangkok 10330, Thailand

*e-mail: smongkol@chula.ac.th

Bacterial cellulose (BC), a biomaterial produced by certain types of bacteria, constitutes of a three-dimensional network of ribbon-shaped microfibrils of cellulose with <130 nm width. Its advantageous properties such as high purity, high surface area, high porosity and high water-holding capacity make BC appealing for many applications. Herein, we present a utilization of BC as a substrate for immobilization of an 8-aminoquinoline derivative. The immobilization was characterized by FT-IR UV-vis and CHN analysis. The functionalized BC was prepared as a paper thin sheet and tested for detection and adsorption of Zn(II) and Cd(II) in water. The functionalized



BC sheet exhibited highly selective fluorescence turn-on with strong green emission toward Zn(II) and Cd(II) ions. After immersing the film in metal ion solution for 24 hours, the ICP-OES analysis showed high adsorption capacities of Zn(II) and Cd(II) of functionalized BC. The functionalized BC sheet is thus potentially useful for analysis and separation of Zn(II) and Cd(II) in water.

Figure 1. Functionalized BC sheet used in detection of Zn(II) and Cd(II) ions in water.

Keywords: Bacterial cellulose, 8-Aminoquinoline, Metal ion detection, Fluorescent sensor, Water treatment

References

1. S. Rastogi, P. Pal, D. Aston, T. Bitterwolf, L. Branen, *ACS Appl. Interfaces*. 2011, 3, 1731-1739.
2. Y. Zhang, X. Guo, W. Si, L. Jia, X. Qian, *Org. Lett.* 2008, 3, 473-476.



ELE-O-01

Spectroscopic Studies of Europium Doped Calcium Fluoride Nanoparticles

Jon-Paul R. Wells^{a,b*}, Jamin Martin^a, Adam J. Pamplin^a, Michael F. Reid^{a,b} and Vladimir Golovko^{a,b}

^a *School of Physical and Chemical Sciences, University of Canterbury, PB4800, Christchurch, New Zealand*

^b *Dodd-Walls Centre for Photonic and Quantum Technologies, New Zealand.*

**e-mail: jon-paul.wells@canterbury.ac.nz*

Lanthanide-doped luminescent nanoparticles are important candidates for low-toxicity imaging agents and intracellular nano-thermometers for biomedical applications [1]. Lanthanide ions doped into bulk CaF_2 crystals are known to form a variety of sites, and to form clusters at concentrations as low as 0.01 mol%, becoming the dominant centre by 0.1 mol% [2, 3]. This clustering gives enhanced energy transfer, promising significant improvements in applications requiring up-conversion or down-conversion via energy transfer.

Previous work on lanthanide-doped CaF_2 nanoparticles has made use of low-resolution spectroscopy at high temperatures, and was therefore unable to discriminate between the different sites. Indeed, work on sodium-stabilized Eu^{3+} -doped CaF_2 nanoparticles [4] makes the assumption that the sites are predominately $C_{4v}(F^-)$, though sodium is known to suppress $C_{4v}(F^-)$ sites in bulk crystals.

In this work we present high resolution laser spectroscopy of core-only sodium-stabilized $\text{CaF}_2:\text{Eu}^{3+}$ nano-particles at cryogenic temperatures (10 K). Selective excitation and emission, and lifetime measurements are presented. $C_{4v}(F^-)$ sites appear to be suppressed in these materials. An enhancement of O_h and $C_{2v}(\text{Na}^+)$ sites, and evidence of cluster and surface sites is observed. We are currently investigating nano-particles with inert shells to confirm the presence of surface states and co-doped samples to isolate potential cluster centres.

Keywords: Europium, Laser Spectroscopy, Core-Shell Nanoparticles

References

1. W. Zheng, S. Zhou, Z. Chen, P. Hu, Y. Liu, D. Tu, H. Zhu, R. Li, M. Huang, and X. Chen, *Angew. Chem. Int. Ed.* 2014, 52, 6671.
2. K.M. Cirillo-Penn and J.C. Wright, *J. Lumin.* 1991, 48-49, 505.
3. J.-P. R. Wells, G. D. Jones and R. J. Reeves, *J. Lumin.* 1997, 72-74, 977.
4. L. Song, J. Gao, R. Song, *J. Lumin.* 2010, 130, 1179.

Novel Visible-Light-Driven Photocatalytic Zn-Air-Batteries with Cobalt Oxides Cathode

**Chanikarn Tomon^a, Sangchai Sarawutanukul^b, Saran Kalasin^c, Salatan Duangdangchote^d,
Atiweena Krittayavathananonand^e and Montree Sawangphruk^{*}**

^aDepartment of Chemical and Biomolecular Engineering, School of Energy Science and Engineering,
Vidyasirimedhi Institute of Science and Technology (VISTEC), Rayong 21210, Thailand.

*e-mail: montree.s@vistec.ac.th

Even the rechargeable Zn-air batteries (ZABs), as a result of their high energy densities, have been one of the most promising energy storage devices¹, the practical application is still far from theoretical value due to the sluggish oxygen evolution reaction (OER) and oxygen oxidation reaction (ORR) on cathodes during charge/discharge processes². To achieve high-performance electronics, the engineering design of a ZAB cell with a cobalt oxide cathode operated under the light illumination was first introduced. Under the exposure of light, the photoactive-cobalt oxides coated on indium tin oxide electrode ($\text{Co}_3\text{O}_4/\text{ITO}$) exhibits ca. 30% higher current density than the dark condition with the lower overpotential of OER and ORR around 10% - 20%. By assembling the artificial ZAB cell, the higher catalytic activity obtained from the $\text{Co}_3\text{O}_4/\text{ITO}$ under the visible light ensures the exceptionally high performance for the ZAB. This new idea can open up opportunities in many applications requiring the conversion and storage of energy within a single cell.

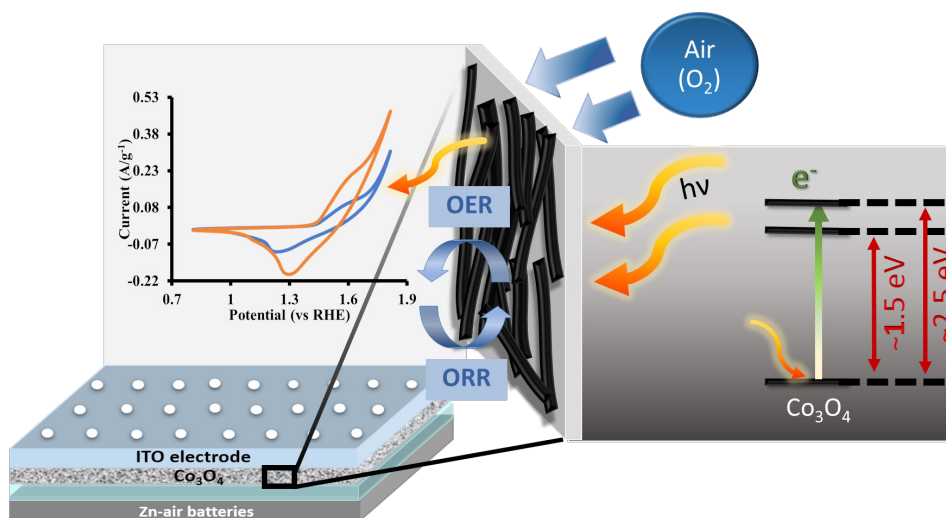


Figure 1. The schematic of visible-light-driven Photocatalytic Zn-Air-Batteries with cobalt oxides cathode

Keywords: Zn-air batteries, Oxygen reduction reaction, Oxygen evolution reaction, Cobalt oxide

References

1. E. Davari, D. G. Ivey, *RSC Adv.* 2018, 2, 39-67.
2. N. Suen, S. F. Hung, Q. Quan, N. Zhang, Y. Xu, H. M. Chen, *Chem. Soc. Rev.* 2017, 46, 377

The Visible Light Driven Hybrid Energy Storage Device

Ketsuda Kongsawatvoragul^a, Saran Kalasina^a, Montakan Suksomboon^a, Nuthaphon Phattharasupakun^a, Juthaporn Wuttiptom^a, and Montree Sawangphruk^{a,*}

^aDepartment of Chemical and Biomolecular Engineering, School of Energy Science and Engineering, Vidyasirimedhi Institute of Science and Technology (VISTEC), Rayong, 21210, Thailand.

*e-mail: montree.s@vistec.ac.th

The Hybrid Energy Conversion and Storage Cell (HECS) is recently discussed as one of the new concepts which combine the conversion and storage system together. The photoactive material, such as semiconductor, can generally generate the photoelectrons via the photovoltaic effect under the light illumination. Each material can absorb the light differently depending on their band structure. Interestingly, the Cobalt hydroxide ($\text{Co}(\text{OH})_2$), appearing as the green colour, is considering as the photoactive materials and can absorb in the visible light region. It can undergo a photovoltaic effect whilst also store charges. The optical band gap of the $\text{Co}(\text{OH})_2$ is *ca.* 2.85 eV. Herein, the $\text{Co}(\text{OH})_2$ and the reduced graphene oxide aerogel (rGO) were used as cathode and anode electrodes, respectively for the asymmetric cell configuration. The $\text{Co}(\text{OH})_2$ was prepared via the electrodeposition method on the Fluorine-doped tin oxide (FTO) current collector. The electrochemical performance was investigated via the cyclic voltammogram (CV) and the galvanostatic charge-discharge (GCD) in the dark and white light illumination.

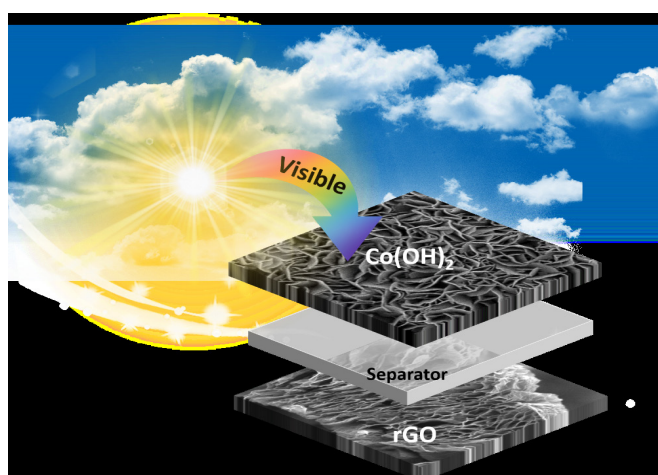


Figure 1. Schematic diagram of HECS cell of $\text{Co}(\text{OH})_2$ //rGO under light illumination

Keywords: Hybrid energy conversion and storage, Photoactive cobalt hydroxide, Reduced-Graphene oxide

References

1. S. Kalasina, P. Pattanasattayavong, M. Suksomboon, N. Phattharasupakun, J. Wuttiptom, M. Sawangphruk, *Chem Comm.* **2017**, 53(4), 709-712
2. S. Kalasina, N. Phattharasupakun, N. Maihom, V. Promarak, T. Sudyoasuk, J. Limtrakul, M. Sawangphruk, *Scientific Reports.* **2018**, 8(1)
3. S. Kalasina, N. Phattharasupakun, M. Sawangphruk, *J. Mater. Chem. A*, **2018**, 6, 36-40

Perylene Diimide Functionalized with Fused-thiophenes as N-Type Semiconductor for Solution-processable OFETs

**Anna Pachariyangkun, Taweesak Sudyoadsuk, Pichaya Pattanasattayavong,
Vinich Promarak***

*Department of Materials Science and Engineering, School of Molecular Science and Engineering,
Vidyasirimedhi Institute of Science and Technology, Wang Chan, Rayong 21210, Thailand*

**e-mail: vinich.p@vistec.ac.th, s15_anna.p@vistec.ac.th*

Development of organic semiconducting materials for organic field effect transistors (OFETs) has been researched intensively due to their great potential in the field of “plastic electronics” in terms of production cost, light-weight substrates, and large area production. The key to high performance OFETs is to design and synthesize molecules with high planarity, good stability, high charge carrier mobility, large on/off ratio, and low threshold voltage. Both p-type and n-type organic semiconductors are needed in the industrial applications, however, the development of n-type organic semiconductor material falls far behind p-type organic semiconductor. Perylene diimides (PDI)s have been extensively used in organic electronics as n-type organic semiconductor due to their excellent chemical and physical properties such as its high electron affinity, charge mobility, as well as absorptivity. Herein, we report the synthesis, characterizations, and OFET characteristics of new n-type organic semiconductors based on PDI derivatives having thieno-thiophene (**PDI-T**) and dithieno-thiophene (**PDI-DT**) functionalized at bay positions. Both **PDI-T** and **PDI-DT** showed high crystalline properties with deep LUMO level of -5.7 eV and -5.6 eV respectively, which is promising for air stable electron transport. OFET devices were fabricated in bottom-gate top-contact configuration with octadecyltrichlorosilane (OTS) treatment as shown in Fig 1. The spin-coated films of **PDI-T** and **PDI-DT** were annealed at 120 °C for 1 h and the devices exhibited electron mobility of 1.55×10^{-4} and $2.5 \times 10^{-4} \text{ cm}^2 \text{ V}^{-1} \text{ s}^{-1}$ respectively.

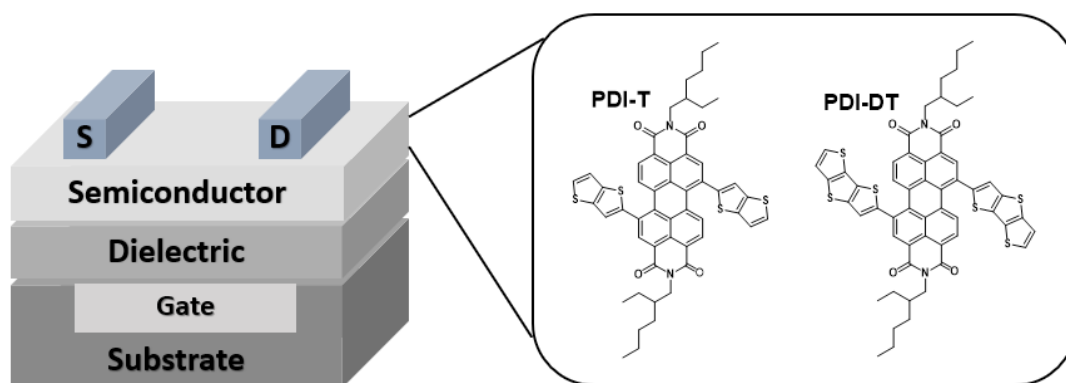


Figure 1. OFET device configuration of PDI-T and PDI-DT.

Keywords: OFETs; n-type semiconductor; Fused-thiophenes; Charge mobility

References

1. W. Wu, Y. Liu, D. Zhu, *Chem. Soc. Rev.* **2010**, 39 (5), 1489-1502.
2. S. R. Forrest, *Nature.* **2014**, 428 (6986), 911-918.
3. M. Wang, M. Ford, H. Phan, J. Coughlin, T. Nguyen, G. Bazan, *Chem Commun.* **2016**, 52 (15), 3207-3210.
4. H. Cheng, J. Huai, L. Cao, Z. Li, *Appl. Surf. Sci.* **2016**, 378, 545-551.
5. Y. Zhao, Y. Guo, Y. Liu, *Adv. Mat.* **2013**, 25 (38), 5372-5391.

Thermally Activated Delayed Fluorescence (TADF) Polymer Based on Thioxanthone Monomer

Praetip Khammultri^a, Taweesak Sudyoadsuk^a, Supawadee Namuangruk^b,
Vinich Promarak^{*a}

^aDepartment of Materials Science and Engineering, School of Molecular Science and Engineering,
Vidyasirimedhi Institute of Science and Technology, Wang Chan, Rayong 21210, Thailand

^bNational Nanotechnology Center (NANOTEC), Thailand Science Park, Patumthani 12120, Thailand

*e-mail: vinich.p@vistec.ac.th, s15_namthip.k@vistec.ac.th

In the last decade, OLEDs have become famous technology due to their potential application in flexible display, large-area, low-cost and solid-state lighting. Thermally activated delayed fluorescence (TADF) recently has been developed as emissive materials for organic light-emitting diodes (OLEDs), owing to outstanding of internal quantum efficiency up to 100%. This property effect to enhance external quantum efficiency of OLEDs devices. TADF polymers are attractive because of they can be solution process fabrication, which can be reducing cost in up-scale processing. In this work, novel TADF polymers were investigated based on 2-(4-(diphenylamino)phenyl)-9H-thioxanthen-9-one 10,10-dioxide (TXTPA) as TADF core monomer. The TXTPA monomer was polymerized with carbazole and fluorene monomers by using Suzuki cross-coupling reaction. The TADF polymers have molecular weight in the range of 9,000-20,000 Dalton. They were studied the photophysical and the TADF properties by UV-VIS spectrophotometer, steady state, fluorescence lifetime and phosphorescence lifetime spectrometer (FLS). All polymers demonstrate outstanding TADF properties, assuring a promising high OLEDs performance.

Keywords : OLEDs, TADF polymer, Thioxanthone, Carbazole, Fluorene

References

1. H. Wang, L. Xie, Q. Peng, L. Meng, Y. Wang, Y. Yi, P. Wang, *Adv. Mater.* **2014**, *26*, 5198-5204.
2. R. S. Nobuyasu, Z. Ren, G. C. Griffiths, A. S. Batsanov, P. Data, S. Yan, A. P. Monkman, M. R. Bryce, F. B. Dias, *Adv. Opt. Mater.* **2016**, *4*, 597-607.
3. Y. Xie, Z. Li, *J. Polym. Sci., Part A: Polym. Chem.* **2017**, *55*, 575-584.

Solution-Processable Spirobifluorene Derivatives as Deep-Blue Emitters for Electroluminescent Devices

Patchareepond Panoy^{a†}, Taweesak Sudyoadsuk^a, Supawadee Namuangruk^b, Pichaya Pattanasattayavong^a, and Vinich Promarak^{a*}

^a*Department of Materials Science and Engineering, School of Molecular Science and Engineering, Vidyasirimedhi Institute of Science and Technology, Wangchan, Rayong 21210, Thailand*

^b*National Nanotechnology Center (NANOTECH), 130 Thailand Science Park, Klong Luang, Pathumthani 12120, Thailand*

*e-mail: *vinich.p@vistec.ac.th, †1530310@vistec.ac.th*

New deep blue light-emitting materials based on 2,2',7,7'-substituted spirobifluorene derivatives with 7,9,9-tris(4-diphenylaminophenyl)fluorene as substituent, namely **SBTT** was synthesized, characterized, and used as an emissive material in the fabrication of solution-processable organic light-emitting diodes (OLEDs). The emission spectra of **SBTT** showed in the deep blue region cover around 400-450 nm in solution. This material exhibited high fluorescence quantum yield over 70% in solution and 20% in thin film. After doping 10wt% and 20wt% of **SBTT** in CBP, fluorescence quantum yields of the thin films increased up to 50% and 40%, respectively. This compound showed high thermal stability with decomposition temperature over 450 °C at 5% weight loss. The structure of fabricated OLEDs were evaluated as follows; ITO/PEDOT:PSS/EML/TPBi/LiF:Al. Non-doped OLEDs of **SBTT** showed an emission peak at 436 nm, with a maximum luminance of 2931 cd/m², EQE of 1.00%, and CIE coordinates of (0.159, 0.139). Moreover, further studies demonstrated that doping 20wt% of SBTT in CBP had a better efficiency than non-doped one with a maximum luminance of 2144 cd/m², EQE of 3.33%, and CIE coordinates of (0.148, 0.082).

Keywords: Organic light-emitting diodes (OLEDs); Spirobifluorene; Triphenylamine (TPA) substituted fluorene

References

1. L. Hayoon, J. Hyocheol, K. Seokwoo, H. H. Jin, I. H. Sang, P. Jongwook, *J. Org. Chem.* **2018**, 83 (5), 2640.
2. A. Thangthong, N. Prachumrak, S. Namuangruk, S. Jungsuttiwong, T. Kaewin, T. Sudyoadsuk, V. Promarak, *Eur. J. Org. Chem.* **2012**, 5263.
3. W. Fang-ly, R. D. Sahadeva, S. Ching-Fong, L. Michelle S., J. Alex K.-Y., *Chem. Mater.* **2003**, 15, 269.

Chrysene Derivatives as Solution-Processable Deep Blue Emitters for OLEDs

**Jirat Chatsirisupachai^{a†}, Taweesak Sudyoadsuk^a, Supawadee Namuangruk^b,
Vinich Promarak^{a*}**

^a*Department of Materials Science and Engineering, School of Molecular Science and Engineering,
Vidyasirimedhi Institute of Science and Technology, Wangchan, Rayong, 21210, Thailand*

^b*National Nanotechnology Center (NANOTEC), 130 Thailand Science Park, Klong Luang,
Pathumthani 12120, Thailand*

*e-mail : *vinich.p@vistec.ac.th, †1530306@vistec.ac.th*

A series of carbazole dendrons end capped-chrysene namely **G1PhChrPhG1 (1)** and **G2PhChrPhG2 (2)** was designed, synthesized and characterized. Both synthesized compounds are soluble in most common organic solvents and possessed excellent thermal stability with 5% weight loss temperature over 500 °C. Photophysical properties of the compounds were investigated both in toluene solution and in thin film. Absorption profiles showed similar pattern with two major absorption peaks at around 300 nm and 350 nm. Both compounds show emission spectra in the deep blue region, with emission peak at 428 nm. Absolute fluorescence quantum yields of the solid films were measured to be as high as 0.52. HOMO energy levels of solid films were measured, using the electron photoemission in air technique, and found to be in range of -5.77 to -5.84 eV. LUMO energy levels were calculated from HOMO energy levels and absorption edge wavelengths to be -2.70 and -2.71 eV. Organic light-emitting diodes (OLEDs) were fabricated by spin-coating of the emissive layer (EML) with simple device structure of ITO/PEDOT:PSS/EML/TmPyPB/LiF/Al. Highest EQE of 1.6% and max luminance up to 1500 cd m^{-2} were obtained. The coordinates of the emitted light specified by the Commission Internationale De L'Eclairage (CIE) are (0.16, 0.07) which is slightly shifted from the standard deep blue colour (0.14, 0.08), standardized by the National Television System Committee.

Keywords: Chrysens, Carbazole, Deep-blue, Organic Light-Emitting Diodes

References

1. S. Hwangyu, J. Hyocheol, K. Beomjin, L. Jaehyun, M. Jiwon, K. Joonghan, and P. Jongwook, *J. Mater. Chem. C*, **2016**, *4*, 3833–3842.
2. P. Moonsin, N. Prachumrak, R. Rattanawan, T. Keawin, S. Jungsuttiwong, T. Sudyoadsuk, and V. Promarak, *Chem. Commun.* **2012**, *48*, 3382–3384.

Molecular Design of Triphenylamine End-capped Benzothiadiazoles as Thermally Activated Delayed Fluorescence (TADF) Materials for OLEDs

**Jakkapan Kumsampao^{b,†}, Taweesak Sudyoadsuk^b, Supawadee Namuangruk^a,
Vinich Promarak^{*}**

^aNational Nanotechnology Center (NANOTECH), 130 Thailand Science Park, Klong Luang, Pathumthani 12120, Thailand

^bDepartment of Materials Science and Engineering, School of Molecular Science and Engineering, Vidyasirimedhi Institute of Science and Technology, Wangchan, Rayong 21210, Thailand

*e-mail: vinich.p@vistec.ac.th, †jakkapan.k_s15@vistec.ac.th

An ideal perspective for the development of highly efficient fluorescent OLEDs would be achieved by thermally activated delayed fluorescence (TADF) materials owing to 100% internal quantum efficiency and needless expensive metallic elements. Here in, three novel TADF molecules, TPA-BTZ-2H, TPA-BTZ-2F and TPA-BTZ-2CN based on D-A-D structures of benzothiadiazole (BTZ-2H), difluoro-benzothiadiazole (BTZ-2F), and dicyano-benzothiadiazole (BTZ-2CN) as acceptors and triphenylamine (TPA) as donor, were successfully synthesized by using Suzuki coupling reaction. The HOMO energy levels of the synthesized compounds were estimated from AC-2 and ranged from 5.31 to 5.60 eV. UV-Vis, and steady state fluorescence phosphorescence lifetime spectrometer (FLS) were used to study their photophysical properties and TADF characteristics. The TADF feature was studied by the air-saturated and degassed solutions of three target molecules in toluene, and it is interesting to note that they can evidently lead to increase the fluorescence intensity especially in case of TPA-BTZ-2CN. The results showed that TPA-BTZ-2CN achieved stronger TADF property than the others. Additionally, the delayed fluorescence lifetime of TPA-BTZ-2CN tends to obviously move upward as well with the increasing temperature. Moreover, using different electron withdrawing groups can control the fluorescence color of these TADF molecules. Not only does this method represents fine-tune the band gap that cover the range from yellow to red color emission but also benefit and practicability for fabrication of the OLEDs.

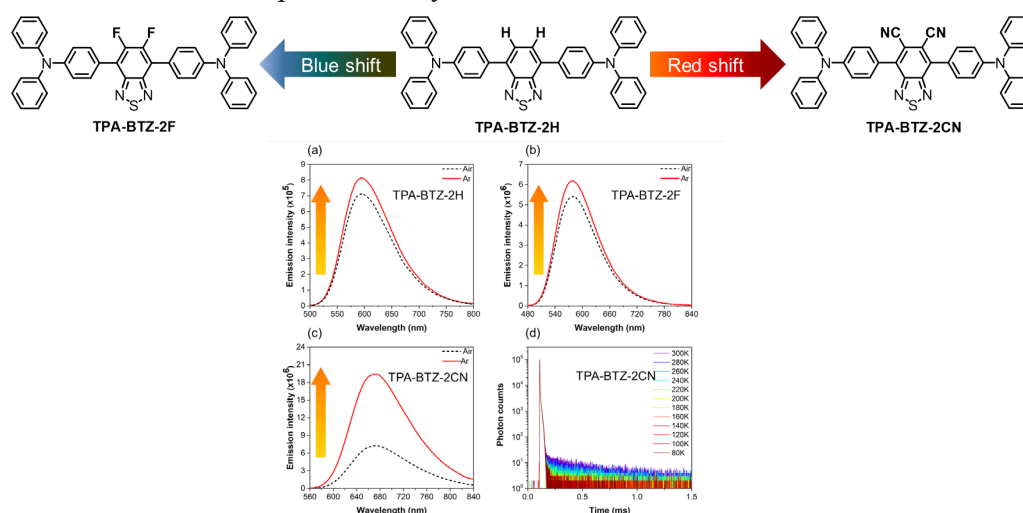


Figure 1. PL spectra of TPA-BTZ-2H (a), TPA-BTZ-2F (b) and TPA-BTZ-2CN (c) in toluene under air and argon. (d) Temperature dependence of the transient PL decay of TPA-BTZ-2CN in doped CBP film (1 wt%) from 80 to 300 K.

Keywords: TADF, OLEDs, Benzothiadiazole, Triphenylamine

Research on Mass Production of High Performance Anodes

**Jiaqian Qin^{a,b,*}, Songjie Cao, Chenyang Li, Chengwu Yang^b, Xinyu Zhang^{b,*},
and Riping Liu^b**

^a*Metallurgy and Materials Science Research Institute, Chulalongkorn University,
Bangkok 10330, Thailand.*

^b*State Key Laboratory of Metastable Materials Science and Technology, Yanshan University,
Qinhuangdao 066004, P. R. China.*

*e-mail: jiaqian.q@chula.ac.th., xyzhang@ysu.edu.cn.

With the significant advantages of the long cycle life, high energy density and high safety, lithium-ion batteries (LIBs) is becoming increasingly important in portable electronic devices. Graphite as the commercial LIBs anode material has a low theoretical specific capacity of 372 mAh/g, which unable to satisfy the increasingly needs. Many researchers focus on Si-based and Sn-based materials for their attractive theoretical capacities, while their cycle performance still unsatisfactory. Our group is devoted to study new anode materials to improve these problems.

First, our group successfully prepare a new core-shell structure of titanium carbon @ carbon-doped titanium dioxide composite (TiC@C-TiO₂) using oxidative growth of C-TiO₂ onto TiC nanoparticles, which exhibits high reversible capacity of 352.8, 253.6 and 158.1 mAh/g at 0.1, 1 and 10 A/g and outstanding cycle stability (~150 mAh/g at 10A/g after 400 cycles).¹

Second, we try to anodize 51Zr in 98 vol% glycol and 2 vol% aqueous containing 0.2 mol/L NH₄F and get the final anode at voltage 30V for 4h, label as 51Zr-30-4, which displays 174, 103, 75, 56 and 33 μAh/cm² at 20, 50, 100, 200, 500 μAh/cm².

Besides, our we pay attention to Ti₃SiC₂ a group of MAX phases, owing its excellent electrical conductivity (about 10-1 S/cm²).² We synthesize a novel SiC/TiC material by ball mill Ti₃SiC₂, showing wonderful performance that its capacity increases with cycling. Next, we oxidize SiC/TiC in air and fabricate a peculiar core-shell of SiC/TiC@SiO_x/TiO₂.³ It delivers preminent long-term cycle performance, which a reversible capacity of 217 mAh/g at 1 A/g is retained without any capacity decay even after 1000 cycles.

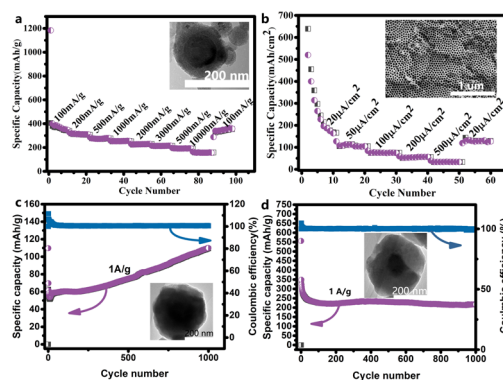


Figure 1. a) Rate performance of TiC@C-TiO₂ at different current rates from 100 to 10000 mA/g. b) Rate performance of 51Zr-30-4 at different current rates from 20 to 500 μA/cm². c) Long-term cycling performance of SiC/TiC at 1A/g. d) Long-term cycling performance of SiC/TiC@SiO_x/TiO₂.

Keywords: Lithium-ion battery, Oxidation, Anodize, Ball-milling.

References

1. S. Cao, Z. Xue, C. Yang, J. Qin, L. Zhang, P. Yu, S. Wang, Y. Zhao, X. Zhang, R. Liu, *Nano Energy*, **2018**, *50*, 25-34.
2. W. Barsoum Michel, T. El-Raghy, *Journal of the American Ceramic Society*, **1996**, *79*, 1953-1956.
3. C. Yang, X. Zhang, J. Qin, X. Shen, R. Yu, M. Ma, R. Liu, *Journal of Catalysis*, **2017**, *347*, 36-44.

Thin Film Composite Hollow Fiber Membrane of Zeolite Y for Biogas Upgrading

Thakorn Wichidit^a, Kajornsak Faungnawakij^b, and Chalida Klaysom^{a*}

^a Department of Chemical Engineering, Chulalongkorn University

^b National Nanotechnology Center (NANOTECH), National Science and Technology Development Agency

*e-mail: Chalida.kl@chula.ac.th

Biogas production has been globally promoted due to the need of renewable energy. Membrane gas separation is the most appropriate technology for biogas upgrading. Polymeric membrane with high selectivity and high permeability are most desirable in membrane gas separation. In this study aims to develop the hollow fiber membrane for CO₂ separation from biogas. The synthesized composite membrane were composed of support layer of Polysulfone (PSf) and thin film selective layer of poly block amide (PEBAX 1657). 3-aminopropyl trimethoxysilane (APMS) in isopropyl alcohol was proposed to modify zeolite Y before adding into selective layer. The concentration of filler unmodified and modified zeolite Y were investigated. The morphology of membrane was characterized by scanning electron microscopy (SEM) for evaluated dispersion of filler. Thermogravimetric analysis (TGA), BET surface area and pore volume were performed to characterized the grafted zeolite.

Keywords: Zeolite Y, Biogas upgrading, Thin film composite membrane, Aminosilane, PEBAX 1657

References

1. OG Nik, XY Chen, S Kaliaguine. *Journal of Membrane Science*. **2011**, 379, 468-478
2. OG Nik, M Sadrzadeh, S Kaliaguine. *Chemical Engineering Research and Design*. **2012**, 90, 1313-1321.
3. AB Amooghini, M. Omidkhah, A. Kargari. *Journal of Membrane Science*. **2015**, 490, 364-379
4. L. Zhao, Y. Chen, B. Wang, C. Sun, S. Chakraborty. *Journal of Membrane Science*. **2016**, 498, 1-13
5. M. Asghari, M. Mosadegh, HR. Harami, *Chemical Engineering Science*. **2018**, 187, 67-78

Solution-Based Ni-Al₂O₃ Solar Selective Coating using Convective Deposition

**Thatchai Chevaprak^a, Narin Chomcharoen^a, Tanyakorn Muangnapoh^{b,*},
Pisist Kumnorkaew^b, Ratchatee Techapiesancharoenkij^a, Krissada Surawathanawises^{a,*}**

^a*Department of Materials Engineering, Faculty of Engineering, Kasetsart University, Bangkok, 10900, Thailand*

^b*Nanofunctional Coating Laboratory, National Nanotechnology Center (NANOTEC), National Science and Technology Development Agency, 111 Thailand Science Park, Phahonyothin Rd., Khlong Nueng, Khlong Luang, Pathumthani 12120, Thailand*

*e-mail: krissada.s@ku.th / tanyakorn.mua@nanotec.or.th

In the past century, an interest in solar power grows rapidly due to its renewable source and pollution-free. One technology to accumulate solar energy is using a concentrating solar power (CSP)¹ system which contains a solar absorber as a key part. A role of solar absorber is to convert solar energy into heat. In this study, a technique called rapid convective deposition² is used to produce a thin film of ceramic-metal (cermet) solar absorber. A cermet Ni-Al₂O₃ solution is prepared in water and mixed with chelating agent and wetting agent³. The rapid convective deposition is used for a coating of cermet thin film onto a 304 stainless steel substrate. This technique has capability to control the thickness of coating and produce maximum productivity with small amount of substances. Finally, the coated solution is treated at high temperature in nitrogen atmosphere. During the heat-treatment, the aluminum ions are converted into a matrix of Al₂O₃, and nickel ions are converted into nickel nanoparticles embedded in this matrix. The solar absorptance and thermal emittance of cermet thin film is strongly dependent on a total metal ion concentration and molar ratio of nickel and alumina⁴. As metal ion concentration increases, the range of absorptance is shifted toward longer wavelength. On the other hand, the absorptance is increased when the molar ratio of Ni:Al₂O₃ is higher. The optimum results are the solar absorptance of 0.71 and the thermal emittance of 0.09 which are based on the total metal concentration of 2 M and the molar ratio of Ni:Al₂O₃ of 9:1, respectively.

Keywords: Concentrating Solar Power, Solar Absorber, Cermet, Nickel-Alumina, Rapid Convective Deposition

References

1. S. Janjai, J. Laksanaboonsong, T. Seesaard, *Applied Energy*. **2011**, 88, 4960-4967
2. P. Kumnorkaew, Y. Ee, N. Tansu, J. F. Gilchrit, *Langmuir*. **2008**, 24, 12150-12157.
3. Z. Li, J. Zhao, *Applied Surface Science*. **2013**, 268, 231-236
4. Z. Li, J. Zhao, L. Ren, *Solar Energy Materials & Solar Cells*. **2012**, 105, 90-95.

Enhancement of Thin-Film Organic Solar Cell Efficiency by Surface Plasmon Resonance and Fluorescence.

Supeera Nootchanat^a, Apichat Phengdaam^b, Sopit Phetsang^a
 Ryousuke Ishikawa^a, Chutiparn Lertvachirapaiboon^a, Kazunari Shinbo^a
 Keizo Kato^a, Akira Baba^{a*}

^a Graduate School of Science and Technology, Niigata University, 8050 Ikarashi 2-Nocho, Nishi-ku, Niigata 950-2181, Japan.

^b Department of Chemistry, Faculty of Science, Prince of Songkla University, Hat Yai, Songkhla 90110, Thailand.
 *e-mail: ababa@eng.niigata-u.ac.jp

A thin-film organic solar cell (OSC) is a device of the future that delivers clean electricity by harvesting the sunlight. The OSC is normally constructed from laminated films including transparent electrode, electron transport layer (ETL), photoactive layer, hole transport layer (HTL) and back electrode. Due to the short diffusion length of charge carriers inside the photoactive layer of OSCs, the standard OSC generally has a very thin photoactive layer thickness (~100 – 300 nm) [1]. The thin photoactive layer is the origin of insufficient light absorption which is the issue of standard OSCs. Recently, plasmonic nanoobjects have been utilized in photovoltaic devices aiming to improve photon harvesting [2]. The increase of light absorption leads to the improvement of photon-to-electron conversion efficiency [2]. In this work, we would like to demonstrate the utilization of plasmonic grating [3, 4], and gold quantum dots (AuQDs) [5] to improve light harvesting in OSC devices which result in enhancement of photocurrent (J_{sc}) and efficiency (η). The grating-coupled surface plasmon (GCSPR) enables improvement of J_{sc} and η for ~11% and ~19%, respectively (Figure 1A). Meanwhile, the utilization of AuQDs as an internal-visible-light emitter in HTL provide the enhancement of η for ~10% (Figure 1B). Nevertheless, the incorporation of fluorescence of AuQDs and GCSPR in OSC devices could be also multiple enhancement effects providing the improvement of J_{sc} and η for ~14% and ~19%, respectively (Figure 1C).

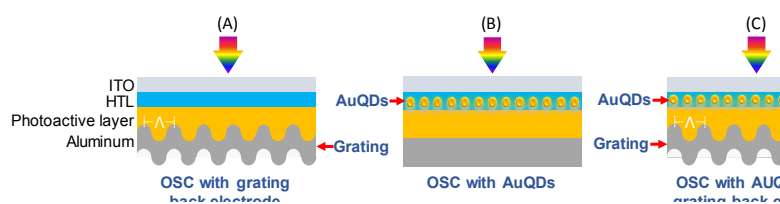


Figure 1. Schematic illustrates the designs of OSC device : (A) the OSC with plasmonic grating, (B) the OSC with AuQDs and (C) the OSC with AuQDs and plasmonic grating. The photoactive layer of OSC blended of Poly(3-hexylthiophene-2,5-diyl) (P3HT) and [6,6]-phenyl-C61-butyric acid methyl ester (PC61BM).

Keywords: Plasmonic Solar Cells, Plasmonic-enhanced Fluorescence, Organic Solar Cells, Grating-coupled Surface Plasmon.

References

- Somani, P. R.; Somani, S. P.; Umeno, M. *Appl. Phys. Lett.*, **2007**, 91, 173503.
- Jang, Y. H.; Jang, Y. J.; Kim, S.; Quan, L. N.; Chung, K.; Kim, D. H. *Chem. Rev.*, **2016**, 116, 14982-15034.
- Nootchanat, S.; Pangdam, A.; Ishikawa, R.; Wongravee, K.; Shinbo, K.; Kato, K.; Kaneko, F.; Ekgasit, S.; Baba, A. *Nanoscale*, **2017**, 9, 4963.
- Hara, K.; Lertvachirapaiboon, C.; Ishikawa, R.; Ohdaira, Y.; Shinbo, K.; Kato, K.; Kaneko, F.; Baba, A. *Phys. Chem. Chem. Phys.*, **2017**, 19, 2791-2796.
- Pangdam, A.; Nootchanat, S.; Lertvachirapaiboon, C.; Ishikawa, R.; Shinbo, K.; Kato, K.; Kaneko, F.; Ekgasit, S.; Baba, A. *Part. Part. Syst. Charact.*, **2017**, 34, 1700133.

ENE-O-06

Poly(ether block amide)/Polyetherimide Hollow Fiber Membranes for CO₂/CH₄ Separation

**Thanitporn Narkkun^a, Panupong Chuntanalerg^a, Manit Angchotiphan^a, Parinya Phongsupa^a
and Kajornsak Faungnawakij^{a,*}**

^aNanomaterials for Energy and Catalysis Laboratory (NEC), National Nanotechnology Center

(NANOTEC) National Science and Technology Development Agency (NSTDA),

Pathumthani, 12120, Thailand

**e-mail: kajornsak@nanotec.or.th*

Poly(ether block amide) (Pebax)/Polyetherimide (PEI) hollow fiber membranes were prepared for CO₂/CH₄ separation. Porous PEI hollow fiber support was prepared by dry-jet wet spinning process. The Pebax selective layer was prepared by dip-coating technique under varying of concentrations. The SEM images revealed that PEI hollow fiber membranes were highly porous with an inside diameter of 300 μm and outside diameter of 600 μm with Pebax coating layer thickness about 3 μm. The separation performance of Pebax/PEI hollow fiber membranes were performed with 50:50 CO₂/CH₄ mixed gas at different feed pressure and temperature.

Keywords: Hollow fiber membranes; Polyetherimide; Poly(ether block amide); CO₂/CH₄ separation

Novel Urchin-like Structure Nickel Cobalt Sulfide as an Efficient Bifunctional Catalyst toward ORR and OER for Zinc-air Batteries

Sangchai Sarawutanukul,^a Nutthaphon Phattharasupakun,^a Juthaporn Wutthiprom,^a and Montree Sawangphruk^{*a}

^aDepartment of Chemical and Biomolecular Engineering, School of Energy Science and Engineering, Vidyasirimedhi Institute of Science, and Technology, Rayong 21210, Thailand

*e-mail: montree.s@vistec.ac.th

Rechargeable zinc-air batteries (ZABs) are one of the most promising energy storage system due to their high theoretical energy density (1370 Wh kg^{-1}), high power density (100 W kg^{-1}), cost effectiveness, and high safety. However, the use of ZABs in large-scale applications is still unpractical because of their low durability and huge overpotential due to the intrinsic sluggish kinetic of oxygen reduction reaction (ORR) and oxygen evolution reaction (OER) occurred at the cathode side. Therefore, the high efficiency bifunctional catalyst for both ORR/OER is highly required to enhance the ZAB performance. Herein, the unique urchin-like 3D structure of nickel cobalt sulfide microspheres (NiCo_2S_4) is properly designed and synthesized by tuning the structure and catalytic active sites via the heat treatment temperature of the sulfurization process (300°C , 400°C , and 500°C). The result shows that the as-prepared NiCo_2S_4 at a temperature of 300°C exhibits the richest sulfur-vacancy providing the best catalytic performance with an ORR onset potentials 0.87 V (vs. RHE) and Tafel slope of 115 mV dec^{-1} which is comparable to the Pt/C catalyst. In addition, the as-fabricated ZABs using the as-synthesized catalyst reveal a high-power density, small charge/discharge voltage gap, and excellent cycle stability. The excellent performance of the as-synthesized NiCo_2S_4 bifunctional catalyst is mainly due to the vacancy-rich of sulfur as well as the urchin-like structure which increase the electroactive sites and improve the electron and ion transportation pathways. Moreover, the calculation of electrocatalytic activity of NiCo_2O_4 and NiCo_2S_4 was evaluated by the density functional theory (DFT) calculation for both ORR and OER. The results suggest the understanding about the key factor of NiCo_2S_4 bifunctional catalyst characteristics towards high-performance rechargeable ZABs.

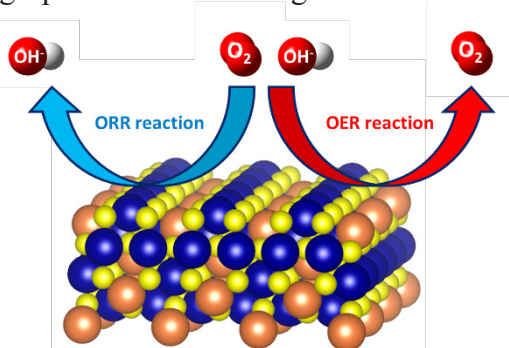


Figure 1. Schematic diagram of NiCo_2S_4 as bifunctional catalyst for OER and ORR

Keywords: Nickel Cobalt Sulfide, Bifunctional catalyst, Zn-air batteries.

References

1. M. Quan, J. Wang, H. Wo, G. Wei Ho, *Small* **2018**, 1703323.
2. W. Liu, J. Zhang, Z. Bai, G. Jiang, M. Li, K. Feng, L. Yang, Y. Dang, T. Yu, Z. Chen, A. Yu, *Adv. Funct. Mater* **2018**, 28, 1706675.

The Effect of Nitrogen Content in 3D N-doped Graphene Oxide Aerogel as Interlayers for High-performance Lithium-sulfur Batteries

Surasak Kaenket, Poramane Chiochan, Nutthaphon Phattharasupakun, Juthaporn Wutthiprom, and Montree Sawangphruk*

Department of Chemical and Biomolecular Engineering, School of Energy Science and Engineering, Vidyasirimedhi Institute of Science and Technology (VISTEC), Rayong 21210, Thailand

**e-mail: montree.s@vistec.ac.th*

Lithium-sulfur batteries have recently attracted great attention as the promising candidates for next-generation energy storage devices because of their high theoretical specific capacity and energy density. However, the practical application of LSBs is still hindered by the shuttle of soluble lithium polysulfides (LPSs) causing the poor electrochemical performance and poor cycling stability. To overcome these problems, in previous study, we introduced graphene-based interlayers with different morphologies and structures to trap LPSs and reduce the shuttle effect. The LSB using 3D N-doped reduced graphene oxide aerogel (3D NG_{ac}) interlayer exhibited the highest specific capacities which was higher than other graphene-related interlayers. In this work, we further investigate the effect of nitrogen content in 3D NG_{ac} on the Li-S batteries performance. The XPS measurement illustrates the content of nitrogen which can be deconvoluted into graphitic, pyrrolic, and pyridinic nitrogen. The interaction between nitrogen atom and LPSs results in LPSs absorption ability. The pyridinic nitrogen provides lone pair electrons at the edge of graphitic carbon. Furthermore, the DFT calculation shows the strong interaction between pyridinic nitrogen and the positive charge of Li in the intermediate. The interlayer containing 3D NG_{ac} with high content of pyridinic nitrogen can improve the performance of Li-S batteries. This material and cell configuration may be practically used in Li-S batteries for high energy applications.

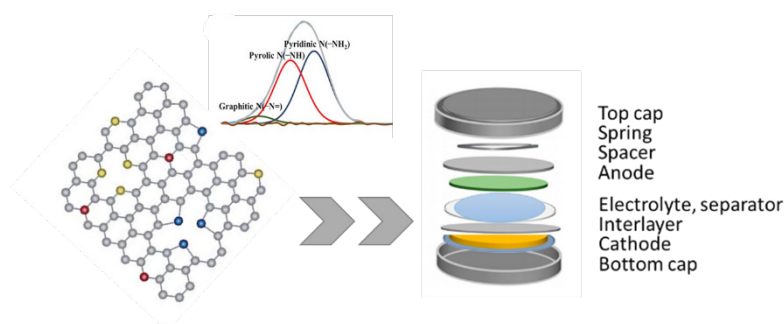


Figure 1. Schematic of N-doped graphene oxide aerogel as interlayer in Li-S batteries

Keywords: Li-S battery, Interlayer, Graphene aerogel

References

1. M. Liu, F. Ye, W. Li, H. Li and Y. Zhang, *Nano Res.* **2016**, 9, 94.
2. Y.-S. Su and A. Manthiram, *Nat. Commun.* **2012**, 3, 1166.
3. Y.-S. Su and A. Manthiram, *Chem. Commun.* **2012**, 48, 8817.
4. C. Zu, Y.-S. Su, Y. Fu and A. Manthiram, *Phys.Chem. Chem.Phys.* **2013**, 15, 2291.
5. P. Iamprasertkun, A. Krittayavathananon and M. Sawangphruk, *Carbon.* **2016**, 102, 455.

Polyaniline Modified-Hydrolyzed Polyethylene and Polyethylene Dual Separators for High-performance Lithium-Sulfur Batteries

**Suchakree Tubtimkuna, Juthaporn Wuttiptom, Poramane Chiochan, Atiweena
Krittayavathananon, and Montree Sawangphruk***

*Department of Chemical and Biomolecular Engineering, School of Energy Science and Engineering,
Vidyasirimedhi Institute of Science and Technology, Rayong 21210, Thailand*

*e-mail: montree.s@vistec.ac.th

The practical application of lithium-sulfur battery (LSB) has been limited with its poor cycling stability due to the ‘shuttle effect’ resulting from the migration of soluble lithium polysulfide intermediates. Recently, numerous strategies have been proposed to solve this issue, i.e., designing host material to control polysulfides within the cathode, developing electrolytes to be able to reduce polysulfide solubility, and adding interlayers to block polysulfide migration to anode.¹ However, these concepts are far from practical operation in the case of the high-sulfur-loading, causing the high dissolution rate of the polysulfide. Herein, we introduce the modified separator with an objective for blocking the polysulfide migration toward the anode. The hydrolyzed polyethylene (HyPE) separator is firstly functionalized with carboxylic acid (-COOH) groups before grafting polyaniline (PANI) molecules via an amide coupling process between the (-COOH) on the HyPE surface and imine groups (-N=) on the PANI structure. To trap the polysulfide which is generally generated from the cathode, the as-modified separator, PANI/HyPE, was sandwiched between a sulfur cathode and a conventional PE separator to fabricate a lithium-sulfur battery. Owing to the chemical interaction between the imine group of the quinoid ring in the structure of PANI and the lithium polysulfide molecules, the polysulfide species are retained on the PANI/HyPE surface until Li_2S is fully transformed.² This idea can improve the sulfur utilization and enhance the stability of the lithium-sulfur batteries.

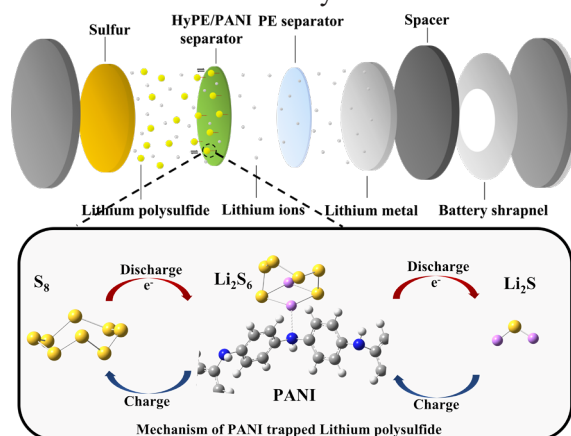


Figure 1. Schematic of the mechanism of lithium polysulfides trapped on polyaniline

Keywords : Lithium sulfur batteries, Polyaniline, Separator, Shuttle Effect

References

1. Yin, L.; Dou, H.; Wang, A.; Xu, G.; Nie, P.; Chang, Z.; Zhang, X., A functional interlayer as a polysulfides blocking layer for high-performance lithium–sulfur batteries. *New Journal of Chemistry* **2018**, *42* (2), 1431-1436.
2. Zhong, M.-e.; Guan, J.; Feng, Q.; Wu, X.; Xiao, Z.; Zhang, W.; Tong, S.; Zhou, N.; Gong, D., Accelerated polysulfide redox kinetics revealed by ternary sandwich-type S@Co/N-doped carbon nanosheet for high-performance lithium-sulfur batteries. *Carbon* **2018**, *128*, 86-96.

The Effect of Intercalated Cations in Layered Manganese Oxides as Neutral Electrochemical Capacitor

Nattapol Ma, Soracha Kosasang, Atiweena Krittayavathananon, Nutthaphon Phattharasupakun, and Montree Sawangphruk*

Department of Chemical and Biomolecular Engineering, School of Energy Science and Engineering, Vidyasirimedhi Institute of Science and Technology, Rayong 21210, Thailand.

**e-mail: montree.s@vistec.ac.th*

Electrochemical capacitors or supercapacitors are extensively studied to replace or to use as auxiliary devices together with rechargeable batteries. Their applications cover the electric vehicle, unmanned aerial vehicle, uninterruptible power supplies, renewable energy, etc. Numerous studies have been interested in manganese oxide materials due to their electrochemical properties, low cost, and natural benign. Here in, a new insight based on the influence of the structural Li^+ , Na^+ , and K^+ cations within the layers of birnessite-type δ -manganese oxide on the intercalated/deintercalated charge storage mechanism as neutral electrochemical capacitors (1 M Na_2SO_4) is demonstrated. From electrochemical evaluations (CV, GCD, and EIS), Li-MnO_x exhibits a superior performance followed by Na-MnO_x and K-MnO_x . Moreover, with the advantage of *in situ* XAS technique, the utilization of Mn active sites is 51%, 40% and 31% for Li-MnO_x , Na-MnO_x , and K-MnO_x respectively. Furthermore, rotating disk electrode (RDE) and electronic quartz crystal microbalance (EQCM) techniques were also performed to examine the influence in both the kinetics of redox reaction and the diffusion/accessibility of the compensating electrolyte ion. This could pave a new perspective and further understanding of birnessite layered manganese oxide material as energy storage materials.

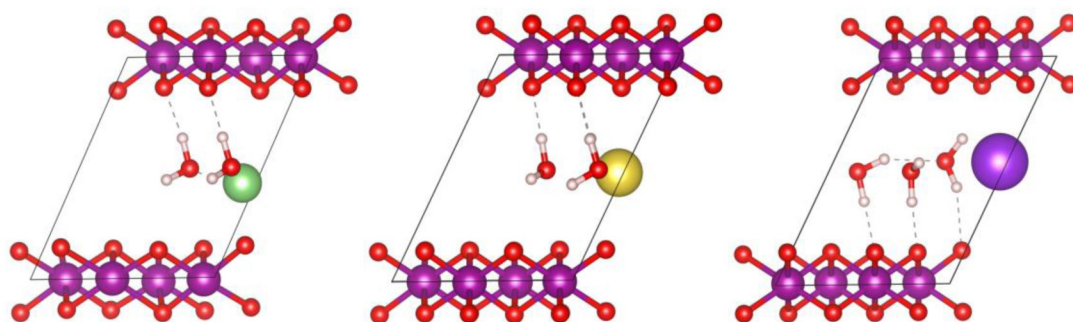


Figure 1. Schematic representation of birnessite manganese oxide with Li^+ , Na^+ , and K^+ as structural cation from left to right, respectively.

Keywords: Supercapacitor, Birnessite, Manganese Oxide, *In situ* X-ray Absorption Spectroscopy, and Energy storage.

References

1. S. Kosasang, N. Ma, P. Wuamprakhon, N. Phattharasupakun, T. Maihom, J. Limtrakul, M. Sawangphruk, *ChemComm.* **2018**, 54 (62),8575-8578.
2. O. Ghodbane, J. L. Pascal, and F. Favier, *ACS Appl. Mater. Interfaces.* 2009, 1 (5), 1130-1139.

Electrode Materials from Biomass Sources for Aluminum ion Battery Applications

Natta Chaiyapo^a, Pornjira Phuenhinlad^a, Panya Thanwisai^b, Yutthanakon Kanaphan^a, Sutham Srilomsak^{a,b,c}, Wirat Jaroenboon^{a,b,c}, Vittaya Amornkitbamrung^{a,b,c}, Chuleekorn Chotsuwan^d, Annop Klamchuen^d, and Nonglak Meethong^{a,b,c*}

^aMaterials Science and Nanotechnology Program, Department of Physics, Faculty of Science, Khon Khan University, Khon Kaen, 40002, Thailand.

^bDepartment of Physics, Faculty of Science, KhonKaen University, KhonKaen, 40002, Thailand

^cInstitute of Nanomaterials Research and Innovation for Energy (IN-RIE), Research Network of NANOTECH- KKU (RNN), Khon Kaen University, Khon Kaen, 40002, Thailand

^dNational Nanotechnology Center (NANOTECH), National Science and Technology Development Agency, Pathumthani, 12120, Thailand

*e-mail: nonmee@kku.ac.th

Aluminum ion battery is a new type of rechargeable batteries, which possesses many advantages over current commercial rechargeable batteries such as its abundance, low cost, high power, and high theoretical energy density (1060 Wh/kg vs. Li-ion batteries of around 400 Wh/kg). Nanomaterials derived from biomass sources have recently received much attention as renewable, abundant, eco-friendly, and low cost electrode materials in energy storage devices. In this work, we have compared electrochemical properties of various biomass wastes received from industries in Thailand for use as electrode materials for Aluminum ion batteries. These wastes were characterized for their functional groups, crystal structures, micro-structural morphology by infrared spectroscopy, X-ray diffraction, and electron microscopy techniques, respectively. The electrochemical properties including specific capacity, rate capacity, and cycling stability of the materials were evaluated by a galvanostatic cycling method. The results suggest that many biomass wastes from Thai industries are electrochemically active, and can potentially be used as electrode materials providing low cost Aluminum ion batteries as a next generation rechargeable battery for the future.

Keywords: Aluminum ion battery, Biomass, cathode materials, sugarcane

Insight into the Effect of Intercalated Alkaline Cations of Layered Manganese Oxides as Bifunctional Electrocatalysts for Zn-air Batteries

Soracha Kosasang,^a Nattapol Ma,^a Phatsawit Wuamprakhon,^a Nutthaphon

Phattharasupakun,^a Thana Maihom,^{abc} Jumras Limtrakul^{ac} and Montree Sawangphruk^{*a}

^aDepartment of Chemical and Biomolecular Engineering, School of Energy Science and Engineering, Vidyasirimedhi Institute of Science and Technology, Rayong 21210, Thailand.

^bDepartment of Chemistry, Faculty of Liberal Arts and Science, Kasetsart University, Kamphaeng Saen Campus, Nakhon Pathom 73140, Thailand.

^cLaboratory for Computational and Applied Chemistry, Department of Chemistry, Faculty of Science and Center for Advanced Studies in Nanotechnology and Its Applications in Chemical, Food and Agricultural Industries, Kasetsart University, Bangkok 10900, Thailand

*e-mail: montree.s@vistec.ac.th

In the past decades, there has been a strong intensive development of electrical vehicles (EVs) to replace combustion engines. Lithium-ion batteries (LIBs) have been widely used in the EVs because of their high capacity and energy efficiency. However, their energy densities remain uncompetitive as compared to the gasoline. Fortunately, the next generation of energy conversion/storage devices including metal-air batteries and fuel cells has been introduced with their superior theoretical energy densities. The metal-air batteries are driven by the oxygen reduction reaction (ORR) and oxygen evolution reaction (OER) which these reactions are sluggish. The kinetics of both reactions is a big problem for the metal-air batteries in practical applications. Here, we have introduced layered manganese oxides (birnessite structure) as bifunctional electrocatalysts to facilitate the ORR and OER. Furthermore, we have demonstrated the effect of the intercalated alkaline cations within the manganese oxide layers (Li, Na, K, Rb, and Cs-birnessite) on the ORR and OER activities. The electrochemical measurements show that the Li-birnessite exhibits the highest ORR and OER catalytic activities in agreement with the density functional theory (DFT) calculations. Moreover, we have improved a performance of our catalysts by compositing with a reduced graphene oxide (rGO) and used as air electrodes for the rechargeable Zn-air batteries. More interestingly, a cyclability of our Zn-air batteries is superior as compared to state-of-the-art Pt/C or Pt/C + RuO₂.

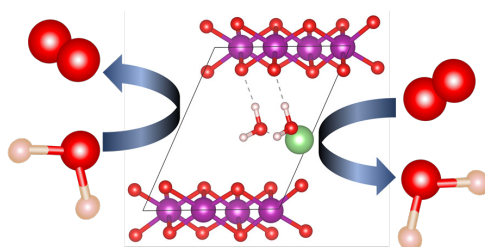


Figure 1. Schematic of the Li-birnessite as a bifunctional electrocataly for the ORR and OER.

Keywords : Oxygen reduction reaction, Oxygen evolution reaction, Bifunctional electrocatalyst, Birnessite, and Zn-air battery

References

1. S. Kosasang, N. Ma, P. Wuamprakhon, N. Phattharasupakun, T. Maihom, J. Limtrakul, M. Sawangphruk, ChemComm. **2018**, 54 (62),8575-8578.

Dependence of the Plasmon Coupling Enhancement on SERS Probe-Substrate Distance

Kullavadee Karn-orachai^{a*}

^a National Nanotechnology Center (NANOTEC), National Science and Technology Development Agency (NSTDA), Pathumthani 12120, Thailand

*e-mail: kullavadee.kar@nanotec.or.th

This study aimed to determine the distance decay of plasmon coupling between SERS-active substrate and probe as a function of the separation distance. The 2D arrays of Au@Ag core-shell nanoparticles (NPs) were served as the SERS-active substrates and the MBA-labeled AuNPs were used as the SERS probes. The separation distance between probe and substrate was created by the formation of layer-by-layer (LBL) of the positively charged polyallylamine hydrochloride (PAH) and negatively charged polyacrylic acid (PAA) on the SERS-active substrates. The outermost layer of LBL treated SERS-active substrate was the positively charged PAH layer. The negative charge of SERS probe could immobilize on the PAH outermost layer via electrostatic interaction by immersing substrates in SERS probe colloidal solution. The plot between the signal of MBA at 1089 and 1587 cm^{-1} and the number of PAA/PAH bilayers was utilized to determine the plasmon decay length of the combination between LBL treated SERS-active substrate and probe. The SERS intensity of MBA gradually decayed when the thickness of PAA/PAH bilayer increased. The decay was saturated at 33 PAA/PAH bilayers (40 nm), which defines the limits of plasmon decay length from this cooperation of SERS substrate and probe. This finding is useful for utilizing the combination of SERS probe and substrate in the SERS immunosensor application especially for the selection of biomolecular size.

Keywords: Surface-enhanced Raman scattering, SERS substrate, SERS probe, Layer-by-layer method

Photocatalytic Degradation of Dyes using Hydrothermal Synthesized Zinc Tin Oxide (ZTO) Nanoparticles at Room Temperature, Effect of Concentration of Dyes on Photocatalytic Activity

Muhammad Najam Khan^{a*}, Joydeep Dutta^b

^a*BUIITEMS University, Airport Road, Baleli, Quetta, Baluchistan, Pakistan*

^b*KTH Royal Institute of Technology, Stockholm, Sweden*

*e-mail: najammalghani@gmail.com

Zinc Stannate Nanoparticles are diverse class of metal oxides with increased stability and decent photocatalytic properties [1]. In an effort to further enhance photodegradation activity of Zinc Stannate nanoparticles, these were synthesized by hydrothermal technique at lower temperature. Size of the photocatalyst and concentration of dyes are two important parameters for photocatalytic degradation of organic matters and dyes [2-3]. Size of the photocatalyst plays an important role during photocatalysis process and is mainly dependent upon higher surface to volume ratio. Zinc Stannate nanoparticles with average size of particles around 50nm were obtained and smaller size of particles is attributed to lower concentration of the precursors. Photocatalytic studies were carried out using Methylene Blue (MB) as test contaminant. Concentration of MB was varied during the degradation process after the short intervals of time. It was observed that if MB concentration increased during the degradation process rate of the photocatalysis increases substantially indicating the role of surface atoms and higher adsorption on the active sites of photocatalyst. This observation will be helpful for obtaining optimize concentration of dyes during the photocatalysis process.

Keywords: Zinc Stannate, Hydrothermal Synthesis, Photocatalysis, dye concentration

Plasma-etched Nanosphere Conductivity-Inverted Lithography (PENCIL): A Facile Fabrication of Size-Tunable Gold Disc Array on Conductive Substrate

Aroonsri Ngamaroonchote^a, Tanyakorn Muangnapoh^a, Noppadol Aroonyadet^a, Pisist Kumnorkaew^b and Rawiwan Laocharoensuk^{a*}

^aNational Nanotechnology Center (NANO TEC), National Science and Technology Development Agency (NSTDA), Pathum Thani 12120, Thailand

*e-mail: rawiwan.lao@gmail.com

Nanosphere lithographic mask is generally employed to simply fabricate metallic hexagonal nanohole array based on metal deposition within interstices of the nanospheres. In this work, a facile method named “plasma-etched nanosphere conductivity inverted lithography (PENCIL)” was developed to fabricate metal disc array, which is an inverted pattern of nanohole array. The technique is based on integrated processing steps of nanosphere lithography, oxygen-plasma etching and electrodeposition as shown in figure 1. In the process, hexagonal close-packed polystyrene (PS) spheres assembled on the indium tin oxide (ITO)-coated glass were served as mask for blocking plasma interaction on ITO surface. Topographic images and current mappings from atomic force microscopy (AFM) revealed different thicknesses and conductivities of plasma-etched ITO surface, particularly in gap area between PS spheres and area underneath PS spheres. The area protected by PS spheres exhibits significantly higher conductivity compare with the exposed area. As a result, site-selective electrodeposition of gold is produced on patterned ITO-coated glass. The disc size, particles size and density can be tuned via size of PS spheres template, plasma etching and electrodeposition conditions. This suggests a simple and low-cost fabrication technique for design and development of metal disc array to obtain specific structure with controlled periodicity, which holds great opportunity in the further electrochemical and optical sensing applications.

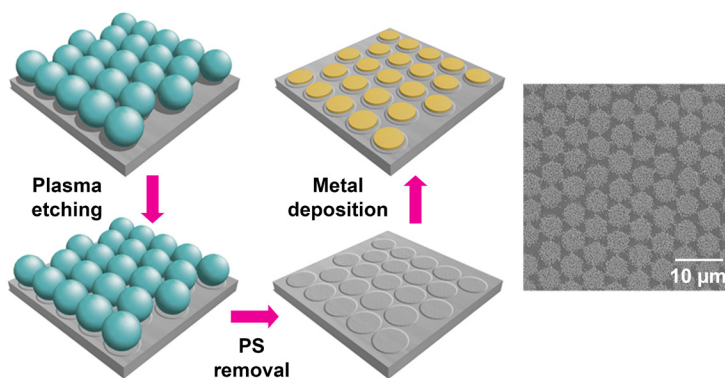


Figure 1. Fabrication procedures and FE-SEM image of gold disc arrays fabricated by this process.

Keywords: Electrodeposition, Micro/Nanodisc arrays, Nanosphere Lithography, Patterned ITO, Surface Patterning

3D Self-Assembled Magnetic Au-Ni NWs for SERS substrate

Yanisa Sanguansap^a, Kullavadee Karn-orachai^a, Karuna Pankleaub^a, Opnithi Noppa^b, Rawiwan Laocharoensuk^{a*}

^aNational Nanotechnology Center (NANOTEC), National Science and Technology Development Agency (NSTDA), Pathum Thani 12120, Thailand

^bTrace Analysis and Biosensor Research Center, Department of Chemistry, Faculty of Science, Prince of Songkla University, Songkhla, Thailand

*e-mail: lraviwan@gmail.com

Bi-segmented Gold-Nickel nanowires (Au-Ni NWs) have been synthesized by template-based electrochemical deposition using 20-nm pore-diameter of anodic aluminum oxide (AAO) membrane as a nanotemplate. Bi-segmented nanostructure consisting Au moiety serves as a signal amplifying subunit and magneto-responsive segment is Ni end acting as a self-constructing subunit. This novel design for three dimensions (3D) self-assembly of Au-Ni NWs were carried out excluding chemical and biological molecules linker to generate strong surface-enhanced Raman scattering (SERS) performance. The physical association between the multiple nanotips through Ni ferromagnetic section created nanoscale gaps which located hot spots. Tuning the aspect ratio (length to diameter) of Ni and Au affected different NWs rearrangement via both freely assemble configuration and guided alignment with external magnetic field. For self-assembly of artificial magnetic NWs, length of Au portion was fixed at 2.00 μm . Aspect ratio of Ni at 0.56, 1.00 and 1.71 explored tip-to-tip conformation (star-like structure) while tip-to-side (firecracker structure) and side-to-side configuration appeared at Ni aspect ratio of 4.06 and 5.59, respectively. By varying Au length with constant length of Ni segment of 0.28 μm , Au aspect ratio of 12.18, 16.71 and 22.00 showed tip-to-tip structure whereas the lowest Au aspect ratio of 5.94 resulted in tip-to-side arrangement. Both high aspect ratio of Au and low aspect ratio of Ni tended to control arrangement of Au-Ni NWs into tip-to-tip form; on the other hand, either tip-to-side or side-to-side structure was exhibited from low and high aspect ratio of Au and Ni, respectively. Being used 3D self-assembled Au-Ni NWs as SERS substrates, 4-mercaptobenzoic acid (4-MBA) was selected to be utilized as a Raman probe, which possesses two dominant characteristic peaks at 1080 and 1587 cm^{-1} . The SERS intensities for tip-to-tip configuration were higher than those of tip-to-side and side-to-side configurations, which correlates with the SERS performance of Au-Ni NWs assembly in the order of tip-to-tip > tip-to-side > side-to-side. These SERS performances correspond to decreasing of Ni aspect ratio or increasing of Au aspect ratio also.

Keywords: bi-segmented Au-Ni NWs, self-assembled Au-Ni NWs, aspect ratio, surface-enhanced Raman scattering (SERS) substrate

Synthesis of Mg-Al LDHs Accumulate on Magnetite and Investigations of Phosphate Adsorption

Tin Srimake^a, Khemarath Osathaphan^a and Kritapas Laohhasurayotin^{b,*}

^aDepartment of Environmental Engineering, Faculty of Engineering, Chulalongkorn University, Phayathai Road, Pathumwan, Bangkok 10330, Thailand

^bNational Nanotechnology Center (NANOTEC), National Science and Technology Development Agency (NSTDA), Pathumthani, 12120, Thailand

*e-mail: kritapas@nanotec.or.th

Layered Double Hydroxides (LDHs) are inorganic solid structure formed from stacks of brucite-like sheet containing divalent and trivalent cations. This establishes positive charge on LDH surface which is compensated by interlayer anion occupation. The nano-size of LDH particles is problematic for extending their usefulness into several application since separation and recollection requiring gravity force as well as sedimentation are not practical, materials tend to be lost although high operation cost is applied. MgAl-LDH associated with magnetite (Fe_3O_4) was prepared in this work to enhance recovering efficiency using external magnetic force. The magnetite was firstly prepared from FeCl_3 by hydrothermal process at 473 K. Subsequently, the formation of MgAl-LDH was induced by mixing the Mg^{2+} and Al^{3+} solution with NaOH in the presence of magnetite to form, after washing and drying, a magnetically separable LDH. The obtained composite was investigated using XRD and SEM to revealing that the obtained composite was not at complete homogeneity. The random distribution of LDH and magnetite in the solid powder was then concluded to an aggregated product. Adsorption experiment carried on phosphate solution was also done and it was found that with only 30 mg of MgAl-LDH/Magnetite composite with 5 h contact time, a 90% removal of phosphate (10 mg/L) was reached. However, this removal was estimated to be only 50% efficiency of that for the original MgAl-LDH, apparently due to the reduced adsorbent mass in the composite volume.

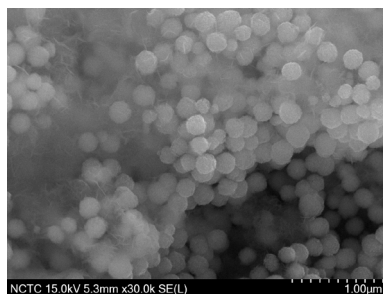


Figure 1. SEM images of MgAl-LDH/Magnetite

Keywords: Layered double hydroxides, Magnetite, Phosphate

References

1. H. Hatami, A. Fotovat, A. Halajnia, *Appl. Clay Sci.* **2018**, *152*, 333-341.
2. C. V. Luengo, M. A. Volpe, M. J. Avena, *J. Environ. Chem. Eng.* **2017**, *5*, 4656-4662.
3. J. Zheng, Z. Q. Liu, X. S. Zhao, M. Liu, X. Liu, W. Chu, *Nanotechnology.* **2012**, *23*, 1-8.

Preparation and Characterizations of Iron Oxide Decorated Graphene Nanoplatelets for Use as Barrier Enhancing Fillers in Polyurethane Based Solar Cell Encapsulant

Kitti Yuwawech^{a,b}, Jatuphorn Wootthikanokkhan^{*a,b}, Supachok Tanpichai^{a,c}

¹Nanotech KMUTT Center of Excellence on Hybrid Nanomaterials for Alternative Energy, King Mongkut's University of Technology (KMUTT), Thonburi, Bangkok 10140, Thailand

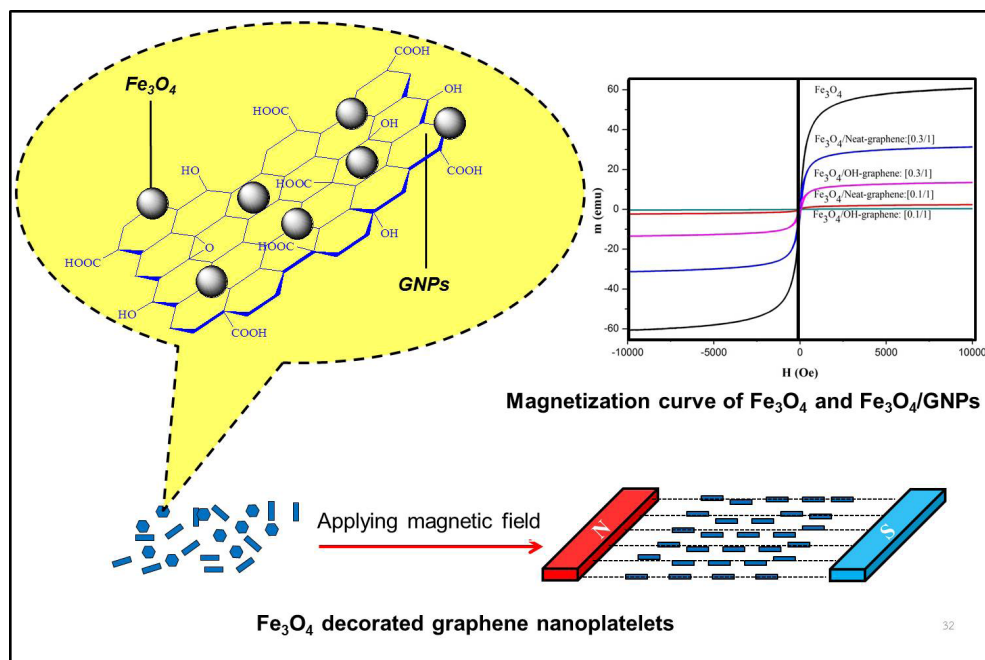
²Division of Materials Technology, School of Energy, Environment and Materials, King Mongkut's University of Technology Thonburi (KMUTT), Bangkok 10140, Thailand

³Learning Institute, King Mongkut's University of Technology Thonburi (KMUTT), Bangkok 10140, Thailand

*e-mail: jatuphorn.woo@kmutt.ac.th

This work has concerned the development of iron oxide (Fe_3O_4)/graphene nanoplatelets (GNPs) for use as barrier enhancing filler in polyurethane based encapsulating materials. The aim of this work is to investigate effects types of GNPs and concentration of Fe_3O_4 on orientation the functionalized GNPs in the PU composites under magnetic field. It was hypothesized that, by properly controlling the orientation of GNPs in the polymer matrix greater barrier properties of the composite encapsulant can be expected. Firstly, Fe_3O_4 nanoparticles were prepared by ferric chloride hexahydrate ($\text{FeCl}_3 \cdot 6\text{H}_2\text{O}$) and hydrazine (N_2H_4). After that, they were introduced onto GNPs. The ratio of Fe_3O_4 nanoparticles to GNPs was varied between 0.1 and 1. Morphology of the synthesized Fe_3O_4 on GNPs was monitored by using scanning electron microscope (SEM). The chemical composition of the materials was examined by energy dispersive x-ray spectroscopy (EDX). Furthermore, the magnetic properties of Fe_3O_4 -GNPs were evaluated by the vibrating sample magnetometer. Superparamagnetic behavior of composite was observed when the weight ratio of Fe_3O_4 to GNPs used greater than 0.3/1. Consequently, this ratio was used for preparation of polyurethane/GNPs nanocomposite. Finally, a feasibility of applying the PU/ Fe_3O_4 decorated GNPs nanocomposite as an encapsulation material for a flexible organic photovoltaic cell was explored. Performance and durability of the various devices were measured and compared.

Keyword: Graphene nanoplatelets (GNPs), Fe_3O_4 -GNPs, Magnetic properties, Super paramagnetic



Wireless Synthesis of Thermoresponsive Janus Nanostructured Carbon Materials using Bipolar Electrochemistry

Malinee Niamlaem^{a,b}, Chompunuch Warakulwit^{a,b*}, Oranit Phuakkong^c, Patrick Garrigue^d, Bertrand Goudeau^d, Alexander Kuhn^d, Valérie Ravaine^d, and Dodzi Zigah^{d*}

^aDepartment of Chemistry, Faculty of Science, Kasetsart University, Bangkok 10900, Thailand

^bNANOTECH Center of Excellence for Nanoscale Materials Design for Green Nanotechnology and Center for Advanced Studies in Nanotechnology for Chemical, Food and Agricultural Industries, Kasetsart University, Bangkok 10900, Thailand

^cDivision of Chemistry, Faculty of Science and Technology, Suratthani Rajabhat University, Suratthani 84100 Thailand

^dUniversity of Bordeaux, ISM, CNRS UMR 5255, Bordeaux, F-33400 Talence, France

*e-mail: dodzi.zigah@u-bordeaux.fr (D. Zigah), fscicpn@ku.ac.th (C. Warakulwit)

In this work, bipolar electrochemistry (BPE) is used to perform the electrodeposition of polymer on both sides of carbon fibers without physical contact between the carbon objects and the electrodes as a proof-of-principle experiment for the encapsulation of carbon nanoobjects, opening up their applications in the fields of drug delivery and storage. In BPE, a conducting bipolar electrode object is in an electrolytic solution between two feeder electrodes. When the electric field is applied, oxidation and reduction reaction will occur simultaneously at the opposite sides of the bipolar electrodes. Carbon fibers were successfully modified with a thermoresponsive poly(N-isopropylacrylamide) (pNIPAM) hydrogel layer on one side and electrophoretic paint (EP) on another side. We found that the length and thickness of pNIPAM-EP can be controlled by varying the electric field and the deposition time of the experiment. This concept can be generalized to carbon nanotubes (CNTs) and other conductive nanoobjects.

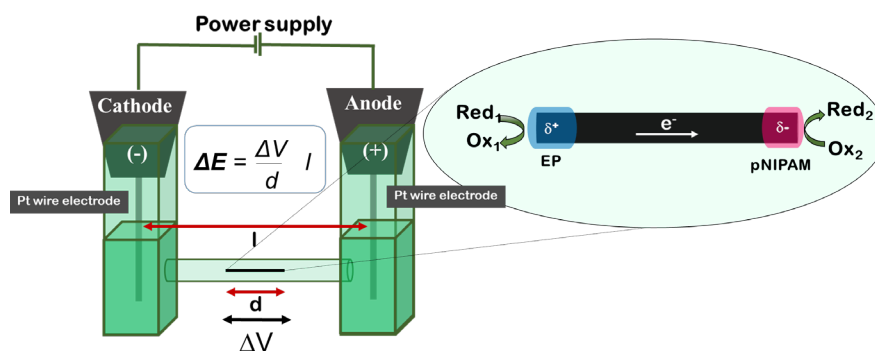


Figure 1. Schematic illustration of in situ modification of cathodic pNIPAM and anodic EP over a carbon fiber using bipolar electrochemistry

Keywords: Bipolar Electrochemistry, Poly (N-isopropylacrylamide), Carbon Fibers, Carbon Nanomaterials

References

1. G. Loget, D. Zigah, L. Bouffier, N. Sojic, and A. Kuhn, *Accounts of Chemical Research* **2013**, *46* (11), 2513-2523.
2. O. Phuakkong, M. Sentic, Ha. Li, C. Warakulwit, J. Limtrakul, N. Sojic, A. Kuhn, V. Ravaine, and D. Zigah, *Langmuir* **2016**, *32* (49), 12995–13002.

One-Step Fabrication of Urchin-Like Gold Nanoparticle Film on PDMS Substrates for SERS Applications

Piboonwan Insiti^a, Attasith Parnsubsakul^{a,b}, Umphan Ngoensawat^a and Sanong Ekgasit^{a,b*}

^aSensor Research Unit, Department of Chemistry, Faculty of Science, Chulalongkorn University, Thailand

^bNational Nanotechnology Centre of Advanced Structural and Functional Nanomaterials, Department of Chemistry, Faculty of Science, Chulalongkorn University, Thailand

*e-mail: sanong.e@chula.ac.th

Branched gold nanostructures such as urchin-like gold nanoparticles (UL-AuNPs) have shown potential applications in many areas, including chemical sensors. For instance, utilization of surface-enhanced Raman scattering (SERS) technique with UL-AuNPs on substrates is capable of sensing molecules in trace level. However, typical fabrication methods for these materials involve multi-step preparation and purification. In this present study, we develop a one-step approach for making ready-to-use SERS substrates by fabricating UL-AuNP film on a small polydimethylsiloxane (PDMS) pillar. A mixture of tetrachloroauric acid, hydrogen peroxide and silver nitrate were used as a growth solution to prepare UL-AuNP films on the PDMS at room temperature (Figure 1). A thin film of UL-AuNP developed on top of the PDMS surface within 10 min as after deposition of 50 μ L growth solution. The structure of UL-AuNP consists of solid core with 389 ± 78 nm in diameter and thorn length of 214 ± 74 nm. The core size and the thorn length could be tuned through adjusting the concentrations of silver ion. The obtained films of densely packed UL-AuNPs create hot-spots which suitable for sensitive SERS applications. Our proposed method is simple and cost-effective as well as the film surface can easily be further functionalized due to free of surfactant or stabilizer.

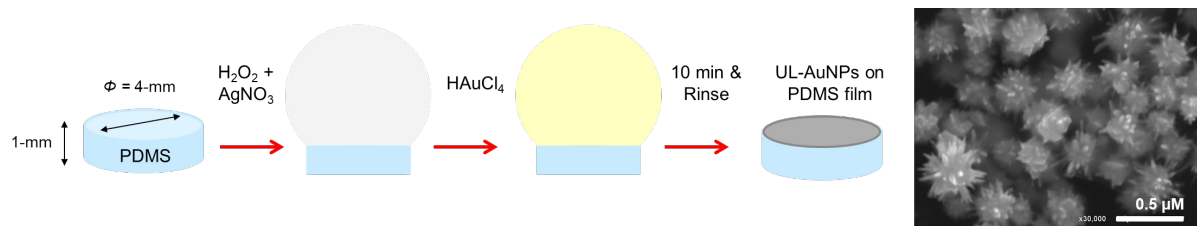


Figure 1. Fabrication process of UL-AuNP film and SEM image of the obtained film on PDMS pillar.

Keywords: Urchin-like gold nanoparticles (UL-AuNPs), Surface-enhanced Raman scattering (SERS), Polydimethylsiloxane (PDMS), Fabrication

References

1. Pangdam, A.; Wongravee, K.; Nootchanat, S.; Ekgasit, S., *Materials & Design* **2017**, *130*, 140-148.
2. Tran, N. T.; Li, A.; Chen, P.; Wang, Y.; Li, S.; Liedberg, B., *Journal of Materials Chemistry C* **2017**, *5* (20), 4884-4891.
3. Fortuni, B.; Inose, T.; Uezono, S.; Toyouchi, S.; Umemoto, K.; Sekine, S.; Fujita, Y.; Ricci, M.; Lu, G.; Masuhara, A.; Hutchison, J. A.; Latterini, L.; Uji-i, H., *Chemical Communications* **2017**, *53* (82), 11298-11301.

Fabrication of Silver Sponge Film via Thermal Decomposition of Rod Shape Silver Acetate under PDMS-suppressed Sintering

Porapak Suriya^a, Wisansaya Jaikeandee^a, Manisorn Suksawas^b, Parinton Jangtawee^b, Supeera Nootchanat^d, Sanong Ekgasit^{b,c,*}

^a Program in Petrochemistry and Polymer Science, Faculty of Science, Chulalongkorn University, Thailand

^b Sensor Research Unit, Department of Chemistry, Faculty of Science, Chulalongkorn University, Thailand

^c National Nanotechnology Center of Advanced Structural and Functional Nanomaterials, Department of Chemistry, Faculty of Science, Chulalongkorn University, Thailand

^d Graduate School of Science and Technology, Niigata University, Japan

* e-mail: sanong.e@chula.ac.th

In this research, a simple and low-cost synthetic protocol for fabricating silver sponge film was developed. The film was fabricated by a thermal decomposition of a solvent-cast film of rod-shape silver acetate (RSAcOAg) at 280°C for 15 minute. The thermal treatment induced the formation of silver nanoparticles (AgNPs) on the surface of RSAcOAg with the expense of RSAcOAg rod. AgNPs sintered into bigger particles and turned RSAcOAg film (Fig. 1A) into silver sponge film (Fig. 1B) consisting of interconnected quasi-sphere silver microparticles. The sintering decreased surface area of the film while limiting its potential applications. To suppress the sintering of the newly developed AgNPs, liquid polydimethylsiloxane (IPDMS) was coated on the surface of RSAcOAg rod before the thermal treatment (Fig. 1C). The thermally stable IPDMS inhibited mobility of AgNPs and suppressed the thermal sintering (Fig. 1D). The silver sponge film with IPDMS-suppressed sintering consisted of interconnected AgNPs ~130 nm compared with the interconnected quasi-sphere silver microparticles ~325 nm in that without IPDMS. The silver sponge film with IPDMS-suppressed sintering has potential applications as catalyst, surface enhanced Raman scattering (SERS) substrate, and conductive flexible circuit

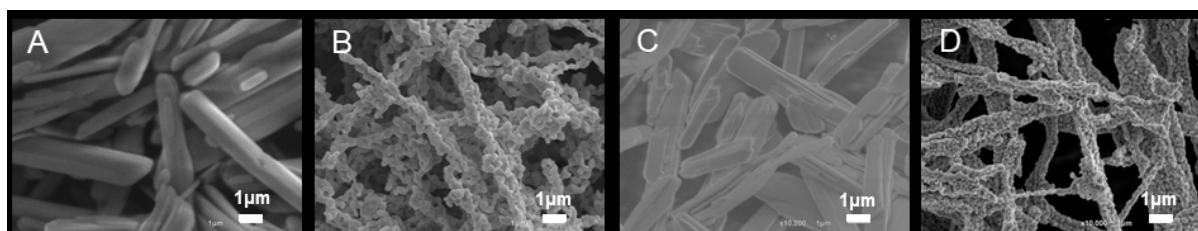


Figure 1. SEM micrographs of (A) RSAcOAg film, (B) silver sponge from thermal decomposition of A, (C) RSAcOAg film with IPDMS coating, and (D) silver sponge from thermal decomposition of C.

Keywords: silver acetate, silver sponge, silver film, porous silver film, sintering of silver nanoparticles

References

1. Larmagnac, A.; Eggenberger, S.; Janossy, H.; Voros, J., Stretchable electronics based on Ag-PDMS composites. *Scientific reports* **2014**, *4*, 7254.
2. Hu, Y.; Zhao, T.; Zhu, P.; Zhu, Y.; Shuai, X.; Liang, X.; Sun, R.; Lu, D. D.; Wong, C.-P., Low cost and highly conductive elastic composites for flexible and printable electronics. *Journal of materials chemistry* **2016**, *4* (24), 5839-5848.

Development of Electrochemical Electrodes using Carbon Nanotube and Metal Phthalocyanine to Classify Pharmaceutical Drugs

Sarika Pradhan^{a,*}, Arthit Jityen^a, Theerasak Juagwon^a, Asawin Sinsarp^b, Tanakorn Osotchan^{a,b}

^a School of Material Science and Innovation, Faculty of Science, Mahidol University, Rama VI Road, Bangkok, Thailand.

^b Department of Physics, Faculty of Science, Mahidol University, Rama VI Road, Bangkok, Thailand.

*e-mail : sarikapradhan300@gmail.com

Electronic tongues are analytical electrochemical technique which mimic human tongue. The taste sensing system like an electronic tongue has been successfully used to distinguish five basic tastes and as quality analyzing tool in food and beverages industries. In this study, the chemical electrodes with multiwall carbon nanotube were developed to classify active pharmaceutical ingredients and analyze the capability of sweetener in masking bitterness of these formulation since multiwall carbon nanotube exhibits high electrical conductivity and electrocatalytic behavior. The electronic tongue system comprises Ag/AgCl as reference electrode, platinum wire as counter electrode and working electrode was modified using four different metal phthalocyanines with multiwall carbon nanotube. The used active metal phthalocyanine powder includes cobalt, iron, zinc and magnesium phthalocyanine. The cyclic voltammogram of various pharmaceutical sample solutions of quinine, amoxicillin, ranitidine and paracetamol were examined between optimized potential range with set constant scan rate. The mapping evaluated from principal component analysis indicated that the metal phthalocyanines mixed with carbon nanotube sensors have potential to classify pharmaceutical drugs. When the pharmaceutical drugs were mixed with sweetener at different concentration, the obtained results indicated that the fabricated working electrode can be used to analyze the suppression of bitterness by sweeteners.

Keywords: Electronic Tongue, Pharmaceutical Ingredients, Phthalocyanines, Carbon Nanotube.

References

1. K. Woertz, C. Tissen, P. Kleninebudde, J. Breitreutz, *Int. J. Pharm.* **2011**, *417*, pp. 256-271.
2. Y. Zheng, P. Keeney, *Int. J. Pharm.* **2006**, *301*, pp.118-124.
3. S.E. Baghbamidi, H. Beitollahi, H.K. Maleh, S.S. Nejad, V.S. Nejad, *J. Anal Methods Chem.* **2012**, *2012*, pp.1-8.
4. A.J. Jeevagan, S.A. John, *J. Electrochimica Acta.* **2012**, *77*, pp.137-142.

High Rate Graphene Sponge Supercapacitor with Hybrid Dual Ionic Liquid-Aqueous Electrolyte

Sethuraman Sathyamoorthi, Poramane Chiochan and Montree Sawangphruk*

Department of Chemical and Biomolecular Engineering, School of Energy Science and Engineering, Vidyasirimedhi Institute of Science and Technology, Rayong 21210, Thailand

*e-mail : montree.s@vistec.ac.th

Aqueous electrolytes are an attractive choice for energy storage application due to their high conductivity, low viscosity, non-flammable, easy handling, low cost and abundant nature. Yet, the low cell voltage (1.23 V) is a major limitation for their wide usage. Neutral pH electrolytes offer the cell voltage up to 1.8 V¹. Concentrated or water-in-salt electrolytes increase the cell voltage up to 2.4 V, which is very close to the conventional acetonitrile based electrolytes². However, the high cost and low rate capability are disadvantages of these electrolytes. Also, novel ionic liquid (IL)/water based electrolytes with the ion-exchange membrane (IEM) operates up to 2.4 V, yet low rate capability and IEM make it as less attractive³. Recently, the novel idea of acetonitrile/water in the salt of dual electrolytes (5.0 M) offers a high rate capability with the cell voltage of 2.2 V⁴. Still, the concentration of salt is high. In this work, high voltage and high rate supercapacitor was demonstrated with the combination of the 3D structure of graphene sponge and hybrid dual IL/water electrolytes. Unlike, the previous reports, the newly proposed supercapacitor uses no IEM and very low volume of IL (~20 μL). The maximum cell voltage of 2.2 V was achieved with the impressive the specific rate of 50 $\text{A}\cdot\text{g}^{-1}$. Also, the excellent capacitance retention of ~90% was estimated after 10,000 cycles at 10.0 $\text{A}\cdot\text{g}^{-1}$.

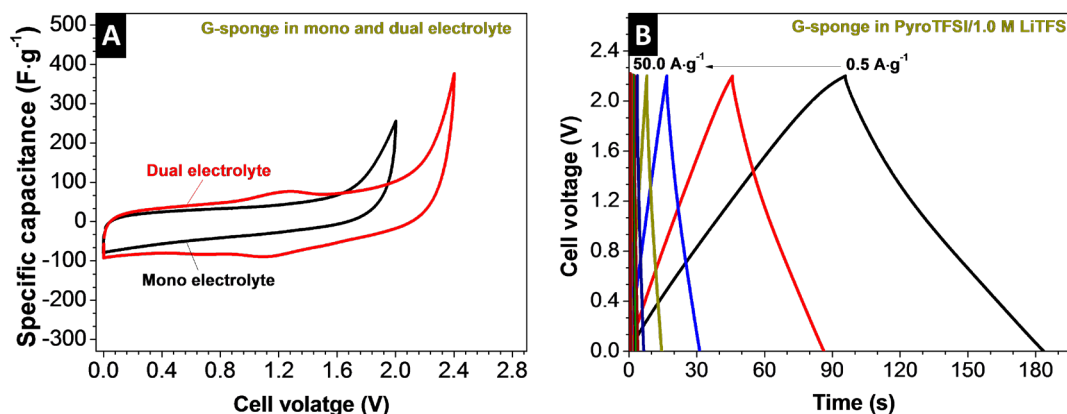


Figure 1. (A) CVs of supercapacitors with mono and dual electrolytes at $5.0 \text{ mV}\cdot\text{s}^{-1}$ and (B) galvanostatic charge-discharge profile for supercapacitor with hybrid dual IL-aqueous electrolyte.

Keywords: Graphene sponge, Hybrid dual electrolytes, High rate supercapacitors, Ionic liquid, 3D structure

References

1. Gao, Q.; Demarconnay, L.; Raymundo-Piñero, E.; Béguin, F., *Energy & Environmental Science* **2012**, 5 (11).
2. Hasegawa, G.; Kanamori, K.; Kiyomura, T.; Kurata, H.; Abe, T.; Nakanishi, K., *Chemistry of Materials* **2016**, 28 (11), 3944- 3950.
3. Ortega, P. F. R.; Gonzalez, Z.; Blanco, C.; Silva, G. G.; Lavall, R. L.; Santamaria, R., *Electrochimica Acta* **2017**, 254, 384-392.
4. Dou, Q.; Lei, S.; Wang, D.-W.; Zhang, Q.; Xiao, D.; Guo, H.; Wang, A.; Yang, H.; Li, Y.; Shi, S.; Yan, X., *Energy & Environmental Science* **2018** DOI: 10.1039/C8EE01040D

A Novel High-Performance Lithium-Ion Hybrid Capacitors Using Three-Dimensional Nanostructure of Reduced Graphene Oxide Aerogel and Carbon Nanotube Composites

Chalita Aphirakaramwong, Nutthaphon Phattharasupakun, Phansiri Suktha, Atiweena Krittayavathananon and Montree Sawangphruk*

Department of Chemical and Biomolecular Engineering, School of Energy Science and Engineering, Vidyasirimedhi Institute of Science and Technology (VISTEC), Rayong 21210, Thailand.

**e-mail: montree.s@vistec.ac.th*

A recent energy storage technology development has been proliferating due to the higher demand in applying for many applications such as various electric vehicles and portable electronic devices. Therefore, the hybrid energy storage devices called lithium-ion capacitors (LICs) are developed by employing the battery-type electrode coupling with the supercapacitors-type electrode to obtain the advantages of both high energy and power densities with excellent long-life cycles. The carbonaceous materials are one of the best choices for electrochemical applications due to high corrosive and low cost. Herein, treated multi-walled carbon nanotubes (tCNT) with negatively charges have been loaded into the three-dimensional reduced-graphene oxide (rGO) structure to improve the electrical conductivity, and lithiation/delithiation process. Using three redox probe mediators with different charges (i.e., neutral (FcOH), cationic ($\text{Ru}(\text{NH}_3)_6^{3+}$), and anionic $\text{Fe}(\text{CN})_6^{4-}$), the rGO/tCNT composite have the good permselectivity allowing the permeation of cationic ions throughout the film layers compared with other ions. As good cation adsorbed properties, the as-prepared composite was fabricated as a negative electrode in an asymmetric lithium capacitor. The positive electrode is a conventional activated carbon (AC). The combining advantages of the LICs with rGO/tCNT composites as the electrode exhibit an excellent maximum energy density and power density under 2.0-4.0 V and provide good longevity and coulombic efficiency.

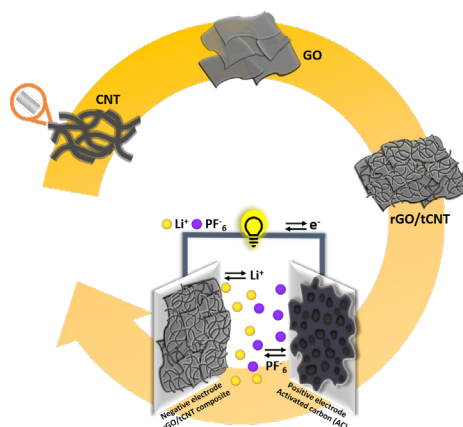


Figure 1. Schematic of rGO/tCNT synthesis as well as LICs configuration using rGO/tCNT composite as negative electrode and AC as positive electrode.

Keywords: Lithium-ion capacitor, Reduced graphene oxide, Carbon nanotubes, Adsorption isotherm

References

1. M. Kim, F. Xu, J.H. Lee, S.M. Hong, Q.M. Zhang, C.M. Koo, *J. Mater. Chem. A*. **2014**, 2(26), 10029-10033.
2. Y. Sanguansak, P. Srimuk, A. Krittayavathananon, S. Luanwuthi, N. Chinvipas, P. Chiochan, J. Khuntilo, P. Klunbud, T. Mungcharoen, M. Sawangphruk, *Carbon*. **2014**, 68, 662-669.

Designing an Interlayer of Reduced Graphene Oxide Aerogel and Nitrogen-rich Graphitic Carbon Nitride by a Layer-by-layer Coating for High-energy Lithium Sulfur Batteries

Juthaporn Wutthiprom^a, Nutthaphon Phattharasupakun^a, and Montree Sawangphruk^{a,*}

^aDepartment of Chemical and Biomolecular Engineering, School of Energy Science and Engineering, Vidyasirimedhi Institute of Science and Technology, Rayong 21210, Thailand

*e-mail: montree.s@vistec.ac.th

Lithium sulfur batteries (LSBs) become attractive energy storage devices due to their high theoretical specific capacity (1675 mAh g⁻¹) and energy density (2500 Wh kg⁻¹). However, the major drawbacks of the LSBs including the poor conductivity of both sulfur and Li₂S (the final product), the effect of shuttle mechanism producing the soluble intermediates (lithium polysulfides or LPSs) during battery operation, and the volume expansion due to the different densities of S₈ precursor and Li₂S up to ~80% leading to the poor stability and short cycle life have restricted their practical and commercial applications. Herein, reduced graphene oxide aerogel (GA) with 3D interconnected conductive and porous structure was employed as a host for sulfur encapsulation (S@GA cathode) and used together with nitrogen-rich graphitic carbon nitride (GCN) as the interlayer accommodating the soluble LPSs. The interlayer was fabricated by a layer-by-layer coating technique on the flexible and processible carbon fibre paper (CFP) substrate. The interlayer inserted between the cathode and the separator provides a strong lithium polysulfide adsorptivity. In addition, the adsorptive LPS species on the interlayer were also investigated by an ex-situ X-ray photoelectron spectroscopy. After finely tuned, the as-fabricated LSB using the S@GA cathode with the GA/GCN interlayer exhibits 75% higher specific capacity than the cell without interlayer. It has a low capacity fading of 0.056% per cycle after tested for 800 cycles. Our new design and configuration of LSB may practically be used in high-energy applications since it can effectively address many issues of the current LSBs.

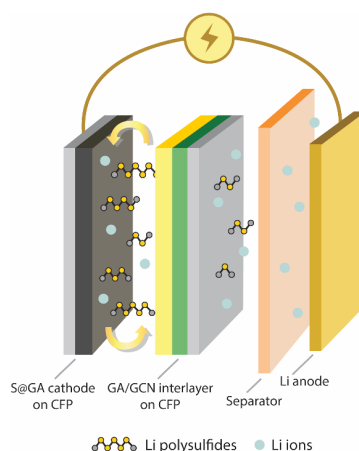


Figure 1. A schematic of a lithium sulfur battery with the S@GA cathode and the GA/GCN interlayer produced by a layer-by-layer coating method on the CFP substrate.

Keywords Lithium sulfur batteries, Reduced graphene oxide aerogel, Graphitic carbon nitride, Interlayer

References

1. J. Wutthiprom, N. Phattharasupakun, M. Sawangphruk, *Carbon* **2018**, *139*, 945-953.

High-performance Lithium-Ion Capacitors Using 3D Nitrogen-Doped Reduced Graphene Oxide Aerogel as a Negative Electrode: A Hydrodynamic Investigation

Nutthaphon Phattharasupakun, Juthaporn Wutthiprom, Phansiri Suktha, Nattapol Ma, and Montree Sawangphruk^{*,a}

^aDepartment of Chemical and Biomolecular Engineering, School of Energy Science and Engineering, Vidyasirimedhi Institute of Science and Technology, Rayong 21210, Thailand

*e-mail: montree.s@vistec.ac.th

Lithium-ion capacitors (LICs) are of interest as a novel hybrid energy storage device integrating faradaic-based lithium-ion battery negative electrodes with non-faradaic-based supercapacitor positive electrodes in lithium salt containing electrolytes. The charge storage mechanism of LICs is based on the adsorption/desorption of anions at the positive electrode (Activated carbon) and the lithiation/delithiation of cations at the negative electrode ($\text{Li}_4\text{Ti}_5\text{O}_{12}$ or graphite). However, due to the poor theoretical capacity of LTO (175 mAh g^{-1}) and graphite (372 mAh g^{-1}), the energy density of LICs is hindered due to the sluggish kinetic diffusion of lithium ions at the negative electrode. Thus, the performance of LICs will be determined by the negative electrode materials. Herein, the pre-lithiated 3D nitrogen-doped reduced graphene oxide aerogel (N-rGO aerogel) is introduced as the negative electrode and the AC is used as the positive electrode of LICs. The doping of N-containing groups is expected to generate active sites for the adsorption of lithium ions. The as-fabricated LIC of pre-lithiated N-rGO aerogel//AC exhibits a maximum specific energy of $170.28 \text{ Wh kg}^{-1}$ (144.79 Wh L^{-1}) and a maximum specific power of 25.75 kW kg^{-1} (21.89 kW L^{-1}) with a cell voltage window of 2.0–4.0 V, $\sim 100\%$ capacity retention, and 100% coulombic efficiency after 2000 cycles.

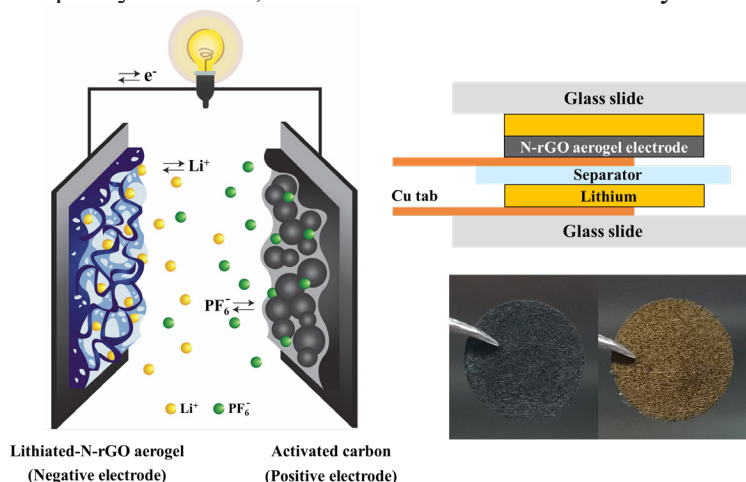


Figure 1. Schematic diagram of lithium-ion capacitor using pre-lithiated N-rGO aerogel as negative electrode and activated carbon as positive electrode (left) and lithiation process (right).

Keywords: Lithium-ion hybrid capacitors, N-doped graphene aerogel, Rotating disk electrode

References

1. Phattharasupakun, N.; Wutthiprom, J.; Suktha, P.; Ma, N.; Sawangphruk, M. *J. Electrochem. Soc.* **2018**, 165, (3), A609-A617.
2. Phattharasupakun, N.; Wutthiprom, J.; Chiochan, P.; Suktha, P.; Suksomboon, M.; Kalasina, S.; Sawangphruk, M. *Chem. Commun.* **2016**, 52, (12), 2585-2588.

Aza-BODIPY Based Polymeric Nanoparticles for Cancer Cell Imaging

Anyanee Kamkaew,^{a*} Kantapat Chansaenpak,^b Similan Tanjindaprateep^a and Nipha Chaicharoenaudomrung^c

^a*School of Chemistry, Institute of Science, Suranaree University of Technology, Nakhon Ratchasima, Thailand 30000*

^b*Functional Nanomaterials and Interfaces (FNI) Laboratory, NANOTECH, Thailand Science Park, Pathumthani, Thailand 12120*

^c*School of Biotechnology, Institute of Agricultural Technology, Suranaree University of Technology, Nakhon Ratchasima, Thailand 30000*

*e-mail: anyanee@sut.ac.th

Tissue penetration depth is a major challenge in optical imaging. Near infrared (NIR) fluorescent dyes that are widely used for cancer imaging usually suffered from their hydrophobicity. To overcome this problem, we report a biodegradable and highly effective NIR-light-activating aza-BODIPY molecule as a class of deep-tissue imaging agent. Aza-BODIPY-TM2 possesses an intense, broad NIR absorption band (600–800 nm) with a remarkably high fluorescent quantum yield. After being encapsulated with biodegradable PCL polymers and Kolliphor P188 surfactants by nanoprecipitation method, aza-BODIPY-TM2 nanoparticles (NPs) can form a spherical shape with monodisperse average size 213 nm (PDI = 0.2). Cancer cell imaging was investigated using glioblastoma cell line (U251) as a model. After the cells were exposed to the NPs, the materials appeared to be localized inside U-251 cells within 3 h and the fluorescence signal enhanced along with the increased incubation times. Moreover, 3D cell culture was used in this study to mimic tumor environment. NPs exhibited bright fluorescence from U-251 cells inside 3D Ca-alginate scaffolds after 24 h incubation (Figure 1). Our study successfully demonstrated the encapsulation of hydrophobic dyes could help enhance hydrophilicity, biocompatibility and bio applications.

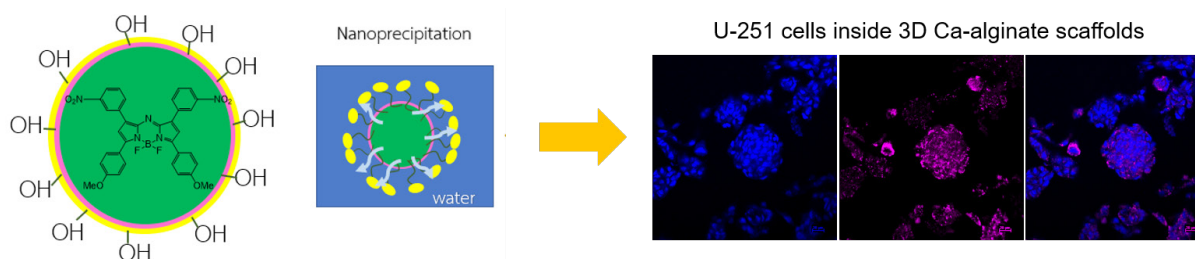


Figure 1. Schematic represents aza-BODIPY-TM2 NPs formed by nanoprecipitation method stained U-251 cells inside 3D Ca-alginate scaffolds that mimic tumor environment.

Keywords: Polymeric nanoparticles, Nanoprecipitation, Aza-BODIPY, Cancer cell imaging, 3D cell

Fabrication of Upconversion Nanoparticle Incorporated Oleogel for Potential Application as Skin Tissue Imaging Agent

Soumyashree Dhal^a, Kunal Pal^b, Indranil Banerjee^b, and Supratim Giri^{a*}

^aDepartment of Chemistry, National Institute of Technology, Rourkela, Odisha-769008, India

^bDepartment of Biotechnology and Biomedical Engineering, National Institute of Technology, Rourkela, Odisha-769008, India

*e-mail : girisupr@nitrkl.ac.in

Gels have emerged as a promising colloidal medium to deliver transdermal therapeutics over the years [1]. In order to track the gel permeation through skin by microscopic method, gels incorporated with fluorescent dyes have been developed [2]. Certain inorganic nanocrystals known as upconversion nanoparticles (UCNP) are able to convert lower energy near infra-red (NIR) laser to visible PL and such nanomaterials have been well characterized for applications in NIR induced bioimaging and subsequent photodynamic therapy [3]. Herein, an attempt was made to establish upconversion nanoparticle loaded oleogel's (UCNP-oleogel) ability to be used as a skin tissue penetration agent for bioimaging application. We have fabricated a series of oleylamine coated UCNP (OA-UCNP) incorporated oleogel through a simple two-step heat-cool procedure. The weight % of OA-UCNP was varied but the weight ratio of soybean oil:stearic acid was kept constant. The UCNP oleogels were characterized by XRD and FTIR to understand the changes occurring in the microstructures of the oleogels with varying OA-UCNP concentration. The photoluminescence (PL) spectroscopy studies showed that UG4 having highest concentration of upconversion nanoparticles showed a very bright luminescence. *In vitro* experiments were performed to validate the tissue penetration ability of UCNP oleogels. It was found that UG4 can penetrate upto 8% agarose gel mimicking skin tissue. Further, UG4 was applied on chicken skin and monitored for 24 hrs. It was found that UG4 can penetrate through chicken skin which was confirmed through fluorescence studies.

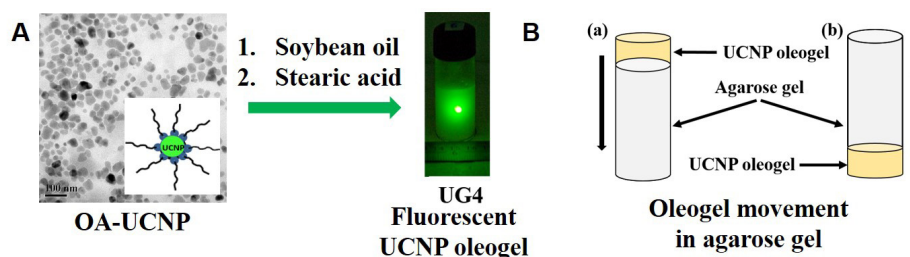


Figure 1. (A) Synthesis of UCNP-oleogel. (B) In vitro studies of oleogel movement in agarose gel.

Keywords: Upconversion Nanoparticles, Oleogels, Skin Tissue Imaging

References

1. S. Indulekha, P. Arunkumar, D. Bahadur, R. Srivastava, *Materials Science and Engineering C* **2016**, 62, 113–122.
2. A.-S. Boisgard, M. Lamrayah, M. Dzikowski, D. Salmon, P. Kirilov, C. Primard, F. Pirot, B. Fromy, B. Verrie, *European Journal of Pharmaceutics and Biopharmaceutics* **2017**, 116, 51–60.
3. Feng Wang, Debapriya Banerjee, Yongsheng Liu, Xueyuan Chen, Xiaogang Liu, *Analyst* **2010**, 135, 1839–1854.

PEGylated Pyropheophorbide-a Nanodots for Fluorescence/Photoacoustic Dual-modal Imaging-guided Photodynamic Therapy

Kittipan Siwawannapong^a, Rui Zhang^b, Anyanee Kamkeaw^{a,*}
and Liang Cheng^{b,*}

^a School of Chemistry, Institute of Science, Suranaree University of Technology, Nakhon Ratchasima 30000, Thailand

^b Institute of Functional Nano & Soft Materials (FUNSOM), Collaborative Innovation Center of Suzhou Nano Science and Technology, Soochow University, Suzhou, Jiangsu 215123, China

* e-mail: lcheng2@suda.edu.cn, anyanee@sut.ac.th

Nanoparticles (NPs) with rapidly eliminated from the body show great potential in clinical translation.^{1,2} However, preparation of an ultra-small nanotheranostic agents with renal clearance behaviors is still challenging. In this work, we report a facile method to prepare ultra-small nanoparticles as an imaging-guided photodynamic therapy (PDT) agent with renal clearable property. Pyropheophorbide-a (Pa), a near infrared (NIR) photosensitizer, was functionalized with polyethylene glycol (PEG) to obtain ultra-small nanodots (Pa-PEG) with the size of, ~2 nm. The synthesized Pa-PEG nanodots showed high singlet oxygen generation upon the 660 nm lamp irradiation. *In vitro* studies revealed good PDT effect of the Pa-PEG nanodots. When the 4T1 cells incubated with the Pa-PEG nanodots at low concentration (0.25 μ M), most of cells were destroyed after being exposed to the irradiation for 30 min. Utilizing the good optical properties of the Pa-PEG nanodots, *in vivo* photoacoustic (PA) and fluorescence (FL) imaging techniques were used to assess the suitable time for PDT treatment after intravenous injection. According to the PA/FL imaging, the nanodots could accumulate in the tumor site and reached up to maximum concentration after 8 h post injection. The tumor bearing balb/c mice were devastated by PDT in which the tumor sizes were obviously smaller than the control groups. Moreover, based on the PA/FL dual-modal imaging, Pa-PEG nanodots showed the high signal in the kidney indicating that the ultra-small nanodots could be physically excreted out of the body via renal clearance. We demonstrated excellent properties of Pa-PEG that can be an *in vivo* imaging-guide PDT agent with renal clearable function, which highlighted the Pa-based porphyrin nanoagents for cancer therapy in the future.

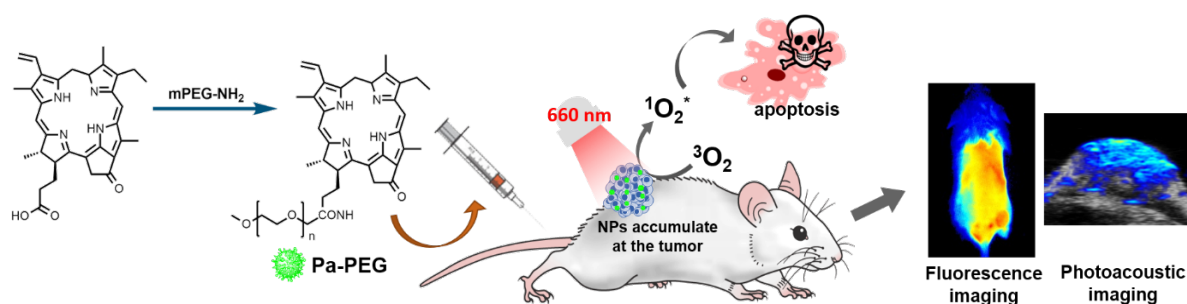


Figure 1. The targeted NPs at the tumor are exposed to NIR light to generate singlet oxygen that can kill the cancerous cells.

Keywords: Pa-PEG Nanoparticles, Ultra-small Size, Dual-modal Imaging, Photodynamic Therapy, Renal Clearance

References

1. M. Ethirajan, Y. Chen, P. Joshi and R. K. Pandey, *Chem. Soc. Rev.*, **2011**, *40*, 340–362.
2. L. Cheng, D. Jiang, A. Kamkaew, H. F. Valdovinos, H. J. Im, L. Feng, C. G. England, S. Goel, T. E. Barnhart and Z. Liu, *Adv Funct Mater*, **2017**, *27*, 1702928.

In silico and *in vitro* studies of chalcones as potent anticancer agents with EGFR tyrosine kinase

Kanyani Sangpheak^a, Kiattawee Choowongkamon^b, Chompoonut Rungnim^c, Warinthon Chavasiri^d, Peter Wolschann^e, and Thanyada Rungrotmongkol^{g,h,*}

^a Program in Biotechnology, Faculty of Science, Chulalongkorn University, Bangkok, Thailand

^b Department of Biochemistry, Kasetsart University, Bangkok, Thailand.

^c Nanoscale Simulation Laboratory, National Nanotechnology Center, National Science and Technology Development Agency, Pathum Thani, Thailand

^d Natural Products Research Unit, Department of Chemistry, Faculty of Science, Chulalongkorn University, Bangkok, Thailand.

^e Department of Pharmaceutical Technology and Biopharmaceutics, University of Vienna, Austria

^g Structural and Computational Biology Research Group, Department of Biochemistry, Faculty of Science, Chulalongkorn University, Bangkok, Thailand

^h Ph.D. Program in Bioinformatics and Computational Biology, Faculty of Science, Chulalongkorn University, Bangkok, Thailand

*Email: thanyada.r@chula.ac.th

The epidermal growth factor receptor (EGFR, Fig. 1) is one of molecular targets for anticancer therapy. It is overexpressed in many human cancer cells including non-small cell lung, breast, head and neck, bladder, ovarian carcinoma and especially human epidermoid carcinoma cell lines (A431) cancer cell lines [1]. Chalcone (1,3-diphenyl-2-propen-1-one) is a phenolic compound abundant in edible plant and is considered to be a precursor of flavonoids. The pharmaceutical activities of chalcones such as anti-proliferative, antioxidant, anti-inflammatory and anti-cancer activities have been reported [2]. Some chalcone derivatives were found to inhibit EGFR. In this study, cell-based and enzyme assays were used for screening potent compounds from the 47 synthesized chalcones. The MTT assay were used for investigating their cytotoxicity against A431. As a result, the chalcone 2a inhibits A431 cancer cells and EGFR activity with IC_{50} values of 9.89 ± 1.91 and 13.15 ± 1.46 μ M, respectively. For Erlotinib, it inhibits A431 cell lines and EGFR activity with IC_{50} values of 0.62 ± 0.11 μ M and 24.91 ± 1.53 nM. However, compound 2a shows less cytotoxicity toward the human embryonic fibroblast than commercial drug, erlotinib. In addition, the binding pattern between potent chalcones and EGFR tyrosine kinase was investigated by Molecular dynamics simulation. The observed ligand-protein interactions from molecular dynamics study affirm that the binding pattern of this chalcone similar to erlotinib.

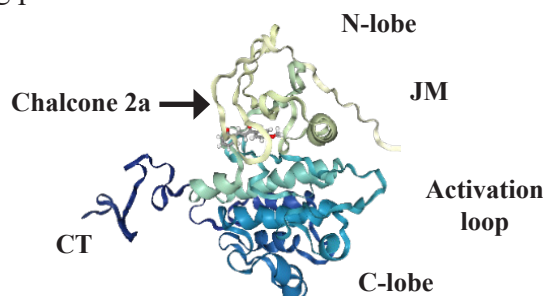


Figure 1. Docked structure of chalcone 2a in the binding site of EGFR tyrosine kinase domain

Keywords: Chalcones, Anticancer activity, EGFR kinase assay, MTT assay, Computational simulations

References

1. Chen, L., et al., Eur J of Med Chem, **2017**, 138, 689-697.
2. Mahapatra, D. K.; Bharti, S. K.; Asati, V., Eur J of Med Chem, **2015**, 98, 69-114.

Alpha Mangostin-Loaded Nanostructured Lipid Carriers as Innovative Veterinary Medicine for Non-surgical Castration of Male Animals

**Jakarwan Yostawonkul^a, Suvimol Surassmo^a, Katawut Namdee^a, Mattaka Khongkow^a, Chatwalee Boonthum^b,
Uracha Rungsardthong Ruktanonchai^a, Suppawiwat Ponglowhapan^b, and Teerapong Yata^{a*}**

^aNational Nanotechnology Centre (NANOTEC), National Science and Technology Development Agency,
Pathumthani, Thailand

^bDepartment of Obstetrics, Gynaecology and Reproduction, Faculty of Veterinary Science, Chulalongkorn University,
Bangkok, Thailand

*e-mail: Teerapong@nanotec.or.th

Uncontrolled reproduction in free-roaming companion animals (cats and dogs) has become the crisis in many countries (including Thailand). The development and application of an effective and affordable approach for animal contraception would have an enormous advantage over the current surgical intervention which suffers from surgical risks including risks of anesthesia, bleeding and/or surgical wound infection. The main purpose of this study was to develop and evaluate a novel herbal-based sterilant for non-surgical castration of male animals. Specifically, we investigated the feasibility of nanostructured lipid carriers encapsulating α -mangostin derived from mangosteen (*Garcinia mangostana* L) pericarp extract (AM-NLC) as a potential non-surgical method of contraception by using *in-vitro* mouse testicular cells, a cat *ex-vivo* testicular explants obtained from castrated testes as well as *in vivo* study in puberty rats. AM-NLC was produced through a hot homogenization technique. Our results showed that the negatively charged particle of AM-NLC was nano-sized with a narrow polydispersity index (PDI) and stable under the accelerated storage conditions. AM-NLC exhibited antiproliferative activity towards spermatogonium cells. It induced apoptosis in the cells. In addition, AM-NLC exhibited anti-inflammatory activities in lipopolysaccharide-activated macrophages. Abnormal anatomy of seminiferous tubule was noted following treatment of testicular explant with AM-NLC. Promisingly, a single dose administration of AM-NLC significantly reduced testicular size of puberty rats after one month intra-testicular injection. There was no clinical sign of inflammation such as redness, swelling, pain observed in experimental animals. Testicular ultrasound examinations of rats treated with AM-NLC showed focal hypoechoic lesions and heterogeneity of the testicular parenchyma. In conclusion, this nanomedicine-based sterilant would be a promising platform that may be considered as an alternative to surgical castration in male animals in order to address this health and welfare in free-roaming animals on a large scale.

Keywords: Alpha-mangostin, Nanostructured lipid carrier (NLC), Castration, Apoptosis.

Synthesis and Cytotoxicity of Cadmium Telluride Quantum Dots in *Leptospira*

Kanlaya Prapainop^{a,b,*}, Yotsakorn Tantiapibalkun^a, Toemsak Srihirin^{b,c}, and Galayanee DOUNGCHAWEE^{d,e}

^aDepartment of Biochemistry, Faculty of Science, Mahidol University

^bSchool of Materials science and Innovation, Faculty of Science, Mahidol University

^cDepartment of Physics, Faculty of Science, Mahidol University

^dDepartment of Pathobiology Faculty of Science, Mahidol University

^eFaculty of Medical Technology, Mahidol University

*e-mail: kanlaya.pra@mahidol.edu

Cadmium telluride quantum dots have been applied in various biological imaging due to its unique fluorescence properties and their versatility to be functionalized with other biomolecules¹. Even though the quantum dots exhibit excellent properties for biological applications, there are concerns of its toxicity. Several studies have investigated the potential cytotoxicity in different human cell lines and animal models^{2,3}. However, there is very limited information on the toxicity of the quantum dots to bacteria especially pathogenic bacteria such as leptospira. The leptospira can cause common life-threatening disease worldwide that affect both human and animals called Leptospirosis⁴. Therefore, results of the toxicity are essential for understanding the mechanism of the toxicity and also for future applications of the quantum dots to the leptospira. In this study the cadmium telluride quantum dots were successfully synthesized via aqueous route system with addition of mercaptosuccinic acid (MSA) as a stabilizing agents. The obtained quantum dots (CdTe-MSA) were characterized by fluorescence spectroscopy which showed maximum emission wavelength at 547 nanometer. This CdTe-MSA were incubated with leptospira at different concentrations (0-900 nM) and monitor the cytotoxicity effects from both behavior and cell growth under dark field microscope. Different concentrations and incubation times affected to cell death and cell movement differently. These results suggested that the cytotoxicity of the CdTe-MSA are dose and time dependence. Therefore, future applications of the CdTe-MSA to leptospira should be carefully performed to provide appropriate concentrations and time to the bacteria.

Keywords: Quantum dots, *Leptospira*, Cytotoxicity, Imaging

References

1. J. Tian, R. Liu, Y. Zhao, Q. Xu, S. Zhao, *J. Colloid Interface Sci*, **2009**, 336, (2), 504-509.
2. T. Zhang, Y. Hu, M. Tang, L. Kong, J. Ying, T. Wu, Y. Xue, Y. Pu, *Int. J. Mol. Sci*, **2015**, 16, (10), 23279-23299
3. M. Wang, J. Wang, H. Sun, S. Han, S. Feng, L. Shi, P. Meng, J. Li, P. Huang, Z. Sun, *Int. J. Nanomedicine*, **2016**, 11, 2319-2328
4. G.Doungchawee, D. Sutdan, K. Niwatayakul, T. Inwisai, A. Sitthipunya, N. Boonsathorn, T. Sakulterdkiat, W. Sirawaraporn, V. Thongboonkerd, *Sci. Rep.* **2017**, 7, 2309.

Identification of Circulating Long Non-Coding RNA Reference Genes and Cancer Biomarkers from Serum of Cervical Cancer Patients

Tawin Iempridee^{a,*}, Suphachai Wiwithaphon^a, Kitiya Piboonprai^a, Pornpitra Pratedrat^a, Phattharachanok Khumkhong^a, Deanpen Japrungrung^a, Sasithon Temisak^b, Somsak Laiwejpithaya^c, Pattama Chaopotong^c, Tararaj Dharakul^d

^a*National Nanotechnology Center (NANOTEC), National Science and Technology Development Agency, Pathum Thani, Thailand*

^b*National Institute of Metrology (NIMT), Pathum Thani, Thailand*

^c*Department of Obstetrics and Gynecology, Faculty of Medicine Siriraj Hospital, Mahidol University, Bangkok, Thailand*

^d*Department of Immunology, Faculty of Medicine Siriraj Hospital, Mahidol University, Bangkok, Thailand*

*e-mail: tawin@nanotec.or.th

Circulating lncRNA has attracted considerable attention as a novel class of noninvasive biomarkers for diagnosing cancers. However, little is known about their suitability as biomarkers for cervical cancer. Here, we profiled and validated lncRNA expression from serum of cervical cancer patients and controls using microarrays and RT-qPCR. We identified lncRNAs RP11-204K16.1, XLOC_012542, and U6 small nuclear RNA as the most stable reference genes for data normalization. These genes were suitable also for samples from different age groups or with hemolysis. Additionally, we discovered lncRNAs AC017078.1 and XLOC_011152 as candidate biomarkers, whose expression was down-regulated in cervical cancer. Our findings could aid research on circulating lncRNAs and contribute to the development of minimally invasive diagnostic tests for cervical cancer.

Keywords: reference genes, circulating RNA, long non-coding RNA, serum, diagnostic biomarker, cervical cancer

MED-O-010

Development of Biosensor Cells for Anti-aging Compounds Screening from Natural Products

Phattharachanok Khumkhong^{a,*}, Kitiya Piboonprai^a, Mattaka Khongkow^a, Apichart Suksamran^b, Udom Asawapirom^a, Tawin Iempridee^a

^aNational Nanotechnology Center (NANOTEC), National Science and Technology Development Agency, Pathum Thani, Thailand

^bDepartment of Chemistry, Faculty of Science, Ramkhamhaeng University, Bangkok, Thailand

*e-mail: phattharachanok.khu@ncr.nstda.or.th

Aging is a key driver in major chronic diseases including cardiovascular disease, neurodegeneration and cancer, negatively affecting both health and wellbeing. P16^{INK4A} is considered a biomarker for cellular senescence whose expression increases during chronological aging. Thus, a compound capable of downregulating p16^{INK4A} expression may rejuvenate aged cells and return them to their younger states. In this study, we developed biosensor cells for anti-aging compound screening based on the p16^{INK4A} promoter driving an expression of nano-luciferase. We infected human embryonic kidney cells (HEK-293) with recombinant lentivirus and selected for stable clones using RFP and puromycin selection. The biosensor cells were functional and responsive to both pro-aging and anti-aging compounds, with EX-527 (SIRT1 inhibitor) and SRT-1720 (SIRT1 activator) induced and inhibited promoter activity, respectively. Of 48 purified compounds from Thai herbs, we discovered a novel compound 036 as the most effective agent in decreasing p16^{INK4A} promoter activity, approximately 38-fold more potent than resveratrol. Treatment of aged primary human dermal fibroblasts with 1 μ M of the compound 036 for 3 days significantly reduced a number of positive aged cells by 54.4% as compared to 33% inhibition by 10 μ M resveratrol based on senescence-associated β -galactosidase staining. Taken together, our study demonstrates the utility of p16^{INK4A}-nanoluc biosensor cells for discovering new bioactive compounds which may serve as a stepping stone towards developing new anti-aging products in the future.

Keywords: P16^{INK4a}, Senescence, Anti-aging, Biosensor cells

Occupational Exposure Risks of Engineered Nanomaterials in Relation to Toxicology

Bey Fen Leo^{1,2}, Tuerxun Duolikun², Norzulaika Binti Mohamed Azmi², Kiew Lik Voon³, Chung Lip Yong⁴,
Alexandra E. Porter⁵, Mary P. Ryan⁵, Mohd Rafie Bin Johan²

¹Faculty of Medicine, University of Malaya, 50603 Kuala Lumpur, Malaysia

²Nanotechnology and Catalysis Research Center (NANOCAT), Institute of Postgraduate Studies, University of Malaya, 50603 Kuala Lumpur, Malaysia

³Department of Pharmacology, Faculty of Medicine, University of Malaya, 50603 Kuala Lumpur, Malaysia

⁴Department of Pharmacy, Faculty of Medicine, University of Malaya, 50603 Kuala Lumpur, Malaysia

⁵Department of Materials and London Centre for Nanotechnology, Imperial College London, Exhibition Road, London SW7 2AZ, UK

The widespread use of engineered nanomaterials (ENMs) in various consumer products, ranging from electronic and photonic devices to textiles, food storage containers, and antiseptic and antibacterial sprays, has raised concerns about their long-term stability and potential adverse effects on human health[1]. For this reason, there is a need to assess the interaction of ENMs with biological systems for early prediction of their cytotoxicity. Adequate physicochemical characterization of ENMs prior to the toxicity assessment and selection of appropriate doses in toxicological studies are paramount to correlate their properties with biological action. In the context of respirable NPs, the interactions with both lung lining fluid components and local cell populations will determine the effects on cell metabolism and lung function [2]. Our studies aim to highlight the need to consider the interaction of ENMs with different sizes and surface coatings, access the pulmonary tissues which can be linked to the pulmonary's disease. Interaction of ENMs with pulmonary cells, as well as their uptake, cytotoxicity and processing inside cells were investigated using different correlative imaging techniques. In order to manipulate and optimise particular NPs features with favourable bio-availability and bio-distribution, not only NP uptake into cells, but also a fundamental understanding of the NPs-protein complex is necessary. To design safe and functional nanomaterials or nano-enabled products, safe-by-design concept was also discussed in this study.

References

1. Park, J., Lim, D.H., Lim, H.J., Kwon, T., et al. *Chem. Commun*, 47, 15 (2011) page 4382 –page 4384.
2. Leo, B.F., Chen, S., Kyo, Y., Herpoldt, K.L., et. al. . *Environ. Sci. Technol*, 47, 19 (2013) page 11232 –page 11240.

Atomic Structure of Cobalt Doped Copper Ferrite Thin Film

Thiha Soe^{a,*}, Arthit Jityen^a, Teerakorn Kongkaew^a, Kittitit Subannajui^a, Asawin Sinsarp^b, Tanakorn Osotchan^{a,b}

^a School of Material Science and Innovation, Faculty of Science, Mahidol University, Rama VI Road, Bangkok, Thailand.

^b Department of Physics, Faculty of Science, Mahidol University, Rama VI Road, Bangkok, Thailand.

*e-mail: thihasoel263@gmail.com

Copper ferrite (CuFe_2O_4) has been well known because of its interesting physical properties, and it has been used as a candidate for many applications such as Li-ion storage, gas sensors, catalysts, and magnetic devices. Copper ferrite (CuFe_2O_4) structure is of significant importance in the context of engineered materials and their structure development due to the natural superlattice structure. In this work, copper ferrite (CuFe_2O_4) nanostructures with cobalt doped were prepared on glass substrate by spin-coating technique. The mixture of copper and iron nitrate at various ratios were used to prepare thin film at room temperature and then post-annealed at 500°C in air up to 5 hours. The nanostructures of fabricated thin films are characterized by x-ray diffraction (XRD), x-ray photoelectron spectroscopy (XPS) and field emission scanning electron microscope (FE-SEM). The surface morphology and chemical composition of nanostructure in thin film form can be extracted from the FE-SEM and XPS, respectively due to their surface sensitivities. The property modification by cobalt doping in copper ferrite (CuFe_2O_4) thin film was systematically investigated for various mixing ratio and post-anneal temperatures. It was found that the XPS spectra of oxygen 1s peak exhibited the significant change for modified atomic arrangement of nanostructure thin film after long annealing time.

Keywords: Copper Ferrite, Spin Coating, Cobalt Doped.

References

1. T.Kongkaew, K.Sakurai, *Chem.Lett.* **2017**, *46*, pp.1493-1496.
2. V.Jeseentharani, M.George, B.Jeyaraj, A.Dayalan, K.S.Nagaraja, *J.Exp. Nanosci.* **2013**, *8*, pp.358-370.

Nano-Flower Structure of Indium and Gallium doped Zinc Oxide Powder

Tin Htet Htet Lynn^{a*}, Arthit Jityen^a, Kritsanu Tivakornsasithorn^b, Rawat Jaisutti^c, Tanakorn Osothchan^{a,b}

^a*School of Material Science and Innovation, Faculty of Science, Mahidol University, Rama VI Road, Bangkok, Thailand.*

^b*Department of Physics, Faculty of Science, Mahidol University, Rama VI Road, Bangkok, Thailand.*

^c*Department of Physics, Faculty of Science and Technology, Thammasat University, Pathum Thani, Thailand.*

*e-mail: tinhtethtetlynn@gmail.com

Flower-like zinc oxide nanostructures have been successfully fabricated by various methods such as chemical vapor deposition, vapor phase transport deposition, thermal evaporation, hydrothermal, sol-gel and template growth methods. Zinc oxide doped with indium and gallium can demonstrate the potential utilization in electronic application for its semiconductor characteristic and the nanostructure of this doped material can enhance its property. In this study, indium and gallium doped zinc oxide nano-structures were prepared by ease method of hydrothermal process, which can well control the morphologies of zinc oxide nanostructure. The concentration percentage of dopants including indium and gallium were varied up to the limitation of synthesis. The dependence on doping content of indium and gallium on the particle morphologies and specific surface area of the samples was investigated systematically. The atomic arrangement and surface properties of synthesized samples were studied according to the measured results obtained by x-ray diffraction, x-ray photoelectron spectroscopy, field emission scanning electron microscope and Brunauer-Emmett-Teller measurement. According to the results, the obtained sample nanostructures are in the size of hundred nanometers with the shape in sheet-like and/or needle-like flower structures. However, the nano-flower structure is found to be disappeared beyond some specific high percentage of the dopant above 15%. The amount of doped indium and gallium are also found in XPS measurement and the substitution of doped atoms in zinc oxide crystal system are also showed in XRD investigation.

Keywords: Nano-flower, Zinc oxide nanopowder, Indium doped zinc oxide, Gallium doped zinc oxide

References

1. E.Pál, I.Dekany, *Colloids Surf.,A*. **2008**, *318*, pp. 141-150.
2. S. F. Du, *Key Eng.Mater.* **2007**, *336-338*, pp. 2041-2043.
3. S. Baruah, J. Dutta, *Sci.Technol.Adv.Mater.* **2009**, *10*, pp.1-18.
4. Z. L.Wang, *J.Phys.:Condens.Matter.* **2004**, *16*, pp. 829–858.

Hydrothermal Growth of ZnO Nanostructures using Sodium Hydroxide as Source of Hydroxyl Ion

Nontakoch Siriphongsapak^a, Somyod Denchitcharoen^{a*}, Pichet Limsuwan^a

^a*Department of Physics, Faculty of Science, King Mongkut's University of Technology Thonburi*

**e-mail: led_material@hotmail.com*

In this work, ZnO nanostructures were hydrothermally grown on silicon and ITO/glass substrates with AZO seed layer. The chemical agents to grow nanostructures were zinc nitrate and sodium hydroxide as precursors of zinc and hydroxyl ions, respectively. The molar ratios of zinc to hydroxyl ions were varied to be 1:1, 1:2, 1:3 and 1:4 with and without hexamine. Moreover, the ZnO nanorods were subsequently grown on ZnO nanostructures which were fabricated with molar ratio of 1:4. Then, all samples were characterized by FESEM, XRD and UV-vis to study the morphology, crystalline quality and optical property, respectively. The results showed that the morphology of nanostructures was highly dense and uniform when hydroxyl ions were obtained from sodium hydroxide. When the concentrations of hydroxyl ions were varied, they affected the diameter and surface density of nanostructures. Finally, the ZnO nanorods showed high uniformity on ZnO nanostructure. The estimated surface area of ZnO nanorods on nanostructures was more than that of ZnO nanorods on seed layer.

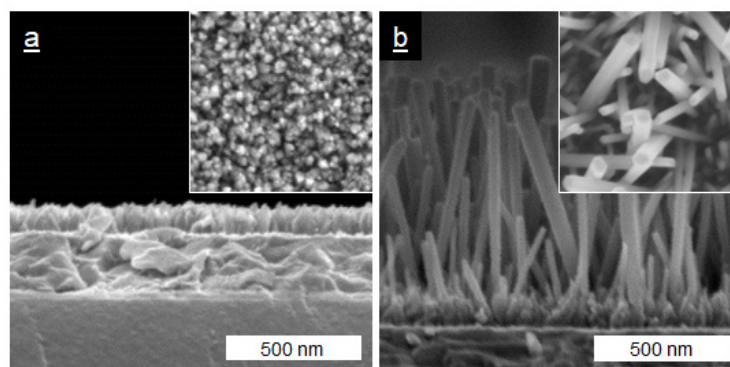


Figure 1. (a) ZnO nanostructures and (b) ZnO nanorods on ZnO nanostructures.

Keywords: ZnO Nanorods, ZnO Nanostructures, Hydrothermal

Ion transport in Composite Gel Electrolyte Based on Cellulose Acetate for Electrochemical Applications

Chuleekorn Chotsuwan*, Udom Asawapirom, Suwimon Boonrungrsriman, Aroonsri Ngamaroonchote, Thanakorn Jiemsakul, Kanpitcha Jiramitmongkon

National Nanotechnology Center (NANO TEC), National Science and Technology Development Agency (NSTDA), Pathumthani 12120, Thailand

*e-mail: chuleekorn@nanotec.or.th

The performance of electrochemical devices such as sensors, supercapacitors, and electrochromics depends on charge transport in a bulk layer and an interface layer. The kinetics of ion transport of electrolytes in bulk and to the surface of an active layer directly impacts the performance and efficiency of these devices. Electrolytes have been developed toward gel and solid to increase its stability under an application of external applied voltage and to decrease an interfacial resistance between the contact of electrolyte and an active layer. Previously, our group successfully designed gel electrolyte systems based on natural polymers [1,3] and nanoparticles [2,4]. In these systems, we showed that ions can move effectively in polymer or in nanoparticle channel networks. To expand the scope of our electrolyte systems, we are investigating composite film electrolytes consisting of polymers based on cellulose acetate incorporating nanomaterials. Characterization of this new composite gel electrolyte system included viscosity, conductivity, morphology, diffusion and dynamic process of ion transport to a conductive polymer film on an ITO substrate. It is found that composite gel electrolyte formed a linking network resulting in a highly viscous gel with a viscosity of 982.1 mPa.s and a conductivity of $4.39 \pm 0.30 \text{ mS cm}^{-1}$ at 25°C suitable for electrochemical device applications.

Keywords: Composite Gel Electrolyte, Cellulose Acetate, Nanomaterials, Ions Transport

References

1. A. Ngamaroonchote, C. Chotsuwan* *J. of Applied Electrochemistry* **2016**, 46:5, 575-582.
2. C. Chotsuwan*, S. Boonrungrsriman, T. Chokanarojwong, S. Dongbang. *J. of Solid State Electrochemistry* **2017**, 21:3011-3019.
3. Composition of gel electrolyte of potassium chloride based agarose for sensing with an electrode and the preparation of the gel electrolyte. C.Chotsuwan. Petty patent application number 1703001530, Thailand
4. Gel electrolytes based on ammonium salt for electrochemical devices and preparation methods of gel electrolyte. C.Chotsuwan. Petty patent application number 1603000584, Thailand

Coumarin Probe for Selective Detection of Fluoride Ions in Water

Kantapat Chansaenpak^{a,*}, Anyanee Kamkaew^b, Oratai Weeranantanapan^c, Khomson Suttisintong^a and Gamolwan Tumcharern^a

^aNational Nanotechnology Center, National Science and Technology Development Agency, Thailand Science Park, Pathum Thani 12120, Thailand

^bSchool of Chemistry, Institute of Science, Suranaree University of Technology, Nakhon Ratchasima 30000, Thailand

^cSchool of Preclinical Sciences, Institute of Science, Suranaree University of Technology, Nakhon Ratchasima 30000, Thailand

*e-mail: kantapat.cha@nanotec.or.th

Fluoride (F^-) is commonly added in many commercial products associating with oral hygiene due to its important role in tooth decay prevention. However, an excess fluoride uptake in human can cause adverse health effects such as dental/skeletal fluorosis, bone fractures, and bone cancer. Recently, high fluoride levels in drinking water have been linked to neurodevelopmental disabilities in children.¹ These harmful health effects have sparked increasing attention in the development of fluoride sensors in water samples. In this work, we have developed new coumarin probes for fluoride ion detection through a fluoride-mediated desilylation triggering fluorogenic reaction (Figure 1).² In addition, we have introduced a hydroxyl moiety into the silyl-capped coumarin backbone in order to improve its hydrophilicity that enhance its capability to detect fluoride in aqueous phase. Gratifyingly, this probe is hydrolytically stable in aqueous systems, can be dissolved in aqueous solution up to 100 μ M without aggregation effects and possesses distinct fluorescence enhancement toward fluoride. It also exhibited high fluoride-selectivity over several anions and a satisfactory limit of detection of 0.044 ppm. Finally, this compound was successfully employed in the detection fluoride levels in the fluoride-spiked water samples, such as tap water and river water, with significant analytical accuracy (less than 5% error).

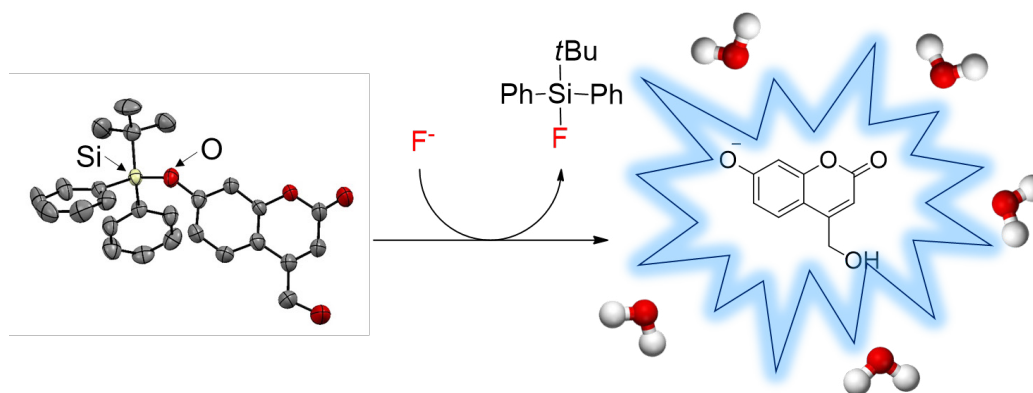


Figure 1. A fluoride-mediated desilylation triggering fluorogenic reaction of a coumarin probe presented in this work.

Keywords: Coumarin; Chemosensor; Fluoride; Drinking water; Fluorescence

References

1. P. Grandjean, P. J. Landrigan, *Lancet Neurol.* **2014**, *13*, 330-338.
2. K. Chansaenpak, A. Kamkaew, O. Weeranantanapan, K. Suttisintong, G. Tumcharern, *Sensors*, **2018**, *18*, 2042.

Top-Down and Sensitive In₂O₃ Nanoribbon Field Effect Transistor Biosensor Chips Integrated with On-Chip Gate Electrodes toward Point of Care Applications

Noppadol Aroonyadet*

National Nanotechnology Center, 111 Thailand Science Park, Pathum Thani 12120 THAILAND

*e-mail: noppadol@nanotec.or.th

Nanomaterial based field effect transistors (FET) have drawn attentions from researchers all around the globe due to their high sensitivity for detection of biomolecules (i.e. proteins, antibodies, nucleic acid strands, viruses etc.). Bottom-up nanomaterials yield ultrasensitive devices, but are challenging to achieve highly uniform properties and even assembly on the substrate. To overcome these struggles, the top-down nanoribbon concept has been proposed to fabricate transistors with high scalability and uniform device properties using conventional microelectronic facilities as shown in Figure 1 a-d. In₂O₃ was selected as the promising nanoribbon material because of its stability in buffer solution, intrinsic semiconducting property, high electrical performance, and lower cost than silicon on insulator (SOI) wafers [1]. In₂O₃ nanoribbon FET biosensors have been demonstrated for high sensitivity in detection of p24 proteins at 20 fg/ml and troponin I protein at 0.1 pg/ml, biomarkers for human immunodeficiency virus (HIV) infection and acute myocardial infraction (AMI), respectively as shown in Figure 1 e-h. They have better limit of detection (LOD) than commercial enzyme link immunosorbent assay kits about 3-5 orders of magnitude [1-2]. The on-chip gate electrode has been integrated on to the biosensor chip (Figure 1 a) to replace the external Ag/AgCl electrode to increase portability and to push this platform toward the point-of-care application [2].

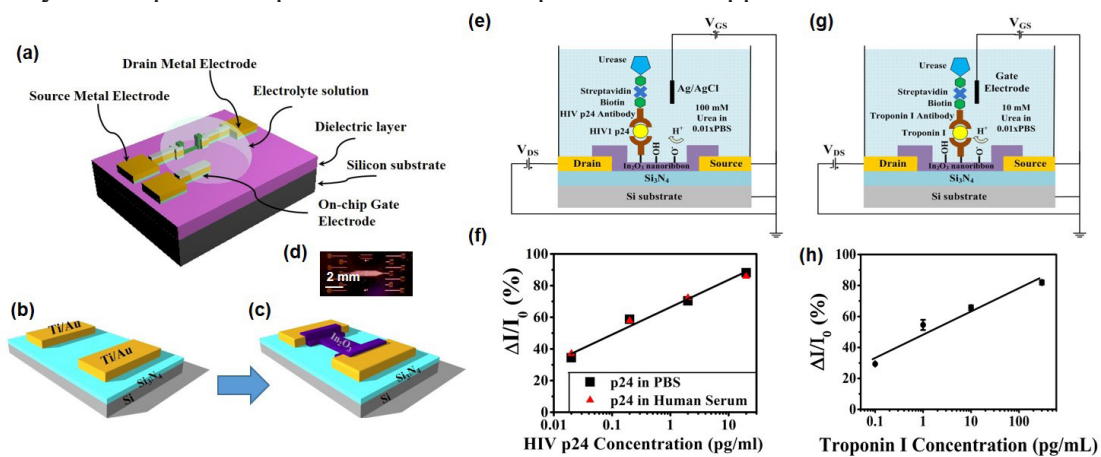


Figure 1 (a) Schematic diagram of an In₂O₃ nanoribbon FET biosensor (b) and (c) Fabrication process for metal electrode and nanoribbon deposition, respectively (d) A photograph of an In₂O₃ nanoribbon FET chip (e) and (f) Schematic diagram and average sensing responses of HIV1 p24 protein detection (g) and (h) Schematic diagram and average sensing responses of troponin I protein detection

Keywords: Nanoribbon Biosensor, On-Chip Gate Electrode, FET Biosensor, In₂O₃ Nanoribbon

References

- 1 N. Aroonyadet, X. L. Wang, Y. Song, H. T. Chen, R. J. Cote, M. E. Thompson, R. H. Datar and C. W. Zhou, *Nano Letters* 2015, 15, 1943-1951.
2. N. Aroonyadet, W. Jeamsaksiri, A. Wisitsoraat and A. Tuantranont, *Nanotechnology* 2018.

A Simplistic Approach into Colorimetric Sialic Acid Determination Based on Boronic Acid and Un-functionalized Gold Nanoparticles

Titilope John Jayeoye,^{a,b} Wilairat Cheewasedtham,^b Chatchai Putson,^{c,d} Thitima Rijiralai^{a,b,*}

^aDepartment of Chemistry and Center of Excellence for Innovation in Chemistry, Faculty of Science, Prince of Songkla University, Hat Yai, Songkhla 90112, Thailand.

^bAnalytical Chemistry and Environment Research Unit, Division of Chemistry, Department of Science, Faculty of Science and Technology, Prince of Songkla University, Pattani 94000, Thailand.

^cDepartment of Physics, Faculty of Science, Prince of Songkla University, Songkhla, 90112, Thailand

^dCenter of Excellence in Nanotechnology for Energy (CENE), Songkhla 90112, Thailand

*thitima.r@psu.ac.th

A novel, simple and highly sensitive colorimetric method is developed for the Sialic acid detection. The detection strategy was based on aggregation of a buffered and un-functionalized gold nanoparticles (AuNPs) through the sequential addition of 3-aminophenyl boronic acid (3-APBA) and sialic acid (SA). Under the optimum conditions, the absorbance ratios (A_{700}/A_{520}) increases with SA concentrations, with an assay time of 5 minutes, the fastest amongst developed colorimetric methods for SA.

The AuNPs color transited between red to purple and finally to blue as SA concentration increases. Selectivity of the developed assay was investigated against different carbohydrates. The practical potentiality of the developed method was demonstrated by carrying out SA detection in simulated human saliva sample and a satisfactory recovery of 98.7-106.0 % was achieved.

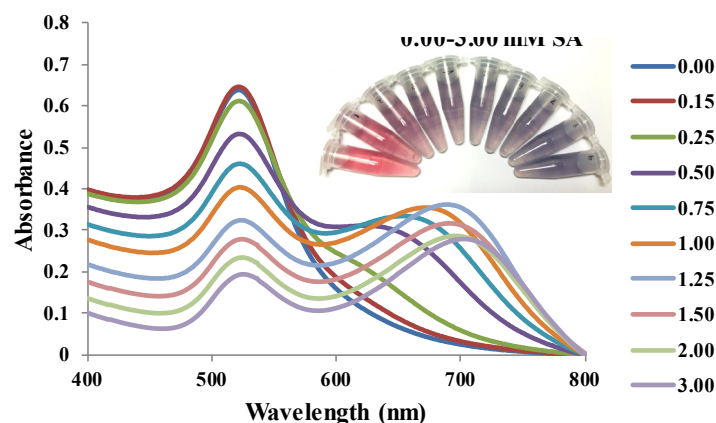


Figure 1: UV-vis absorption spectra of buffered AuNPs colloidal solution under a sequential addition of optimized concentration of 3-APBA and different concentrations of SA (0.00-3.00 mM). Inset shows the photographic images.

Keywords: Sialic acid, Gold nanoparticles, Colorimetric detection, 3-aminophenyl boronic acid, simulated human saliva

References

1. M. Crook, M. Haq, P. Tutt, *Clin Biochem.* **1993**, 26, 449–454.
2. Y. Zhou, D. Hui, L. Lantao, L. Jing, X. Maotian, *Biosens Bioelectron.* **2014**, 60, 231–236.

Design and Synthesis of New Heavy Metal Ions Fluorescence Sensors and Their Applications in Commercial Products and Living Cell

Anuwut Petdum^a, Pattanawit Swanglap^a, Jitnapa Sirirak^a, Adisri Charoenpanich^c, Waraporn Panchan^b, Somboon Sahasithiwat^b, Vinich Promarak^d, Thanasat Sooksimuang^b, Nantanit Wanichacheva^{a,*}

^a Department of Chemistry, Faculty of Science, Silpakorn University, Nakhon Pathom, 73000, Thailand

^b National Metal and Materials Technology Center (MTEC), Pathumthani, 12120, Thailand

^c Department of Biology, Faculty of Science, Silpakorn University, Nakhon Pathom, 73000, Thailand

^d School of Molecular Science and Engineering, Vidyasirimedhi Institute of Science and Technology (VISTEC), Thailand

*e-mail: wanichacheva.nantanit@gmail.com

Contaminations of heavy metal ions in cosmetic, food, beverage and environment can lead to various health problems of humans and animals, hence sensors with high selectivity and low detection limit for heavy metal ions are required to prevent the contamination outbreaks. Accordingly, designing and synthesizing of fluorescent sensors for the determination of heavy metal ions have become a goal in our research group. Up to date, several fluorescent sensors for heavy metal ions have been successfully developed. For example, Hg²⁺ fluorescent sensor was recently developed via fluorescent resonance energy transfer (FRET), the sensor illustrated very large Stokes shift up to 176 nm. The sensor could be used to selectively detected Hg²⁺ by monitoring the “turn on” fluorescent change as well as the visually chromogenic change of the sensor from greenish-yellow to orange. Additionally, new Ag⁺ fluorescent sensor was synthesized. This sensor not only provided highly selective “off-on” fluorescent switch toward Ag⁺, but also could be used for detection of silver nanoparticles (AgNPs) with simply one-step sample pretreatment. Therefore, the sensor could benefit measurement of AgNPs levels in the consumer products and the environment. In addition, the dual-analytes fluorescent sensor for Cu²⁺ or Zn²⁺ have also been recently developed, the sensor could provide highly selective determination of Cu²⁺ or Zn²⁺ in different medium and different emission wavelengths. All of these developed fluorescent sensors exhibited high selectivity respond for each metal over the interfering metal ions. Importantly, the detection limits (3σ/slope) of these sensors were lower than the recommended value in drinking water for the United State Environmental Protection Agency (U.S. EPA) and World Health Organization (WHO). Furthermore, our results indicated that the developed sensors were highly tolerant to the interferences from the matrix of real samples such as drinking water (sensors for Hg²⁺, Cu²⁺ and Zn²⁺), skin lightening cream (Hg²⁺ sensor) and living cells (sensors for Hg²⁺, Cu²⁺ and Zn²⁺).

Keywords: Fluorescence Spectroscopy, Fluorescent sensor, High Selectivity, Heavy metal ions

References

1. A. Petdum, W. Panchan, P. Swanglap, J. Sirirak, T. Sooksimuang, N. Wanichacheva, *Sens. Actuators, B.* **2018**, *259*, 862–870.
2. A. Petdum, W. Panchan, J. Sirirak, V. Promarak, T. Sooksimuang, N. Wanichacheva, *New J. Chem.* **2018**, *42*, 1396–1402.
3. S. Sakunkaewkasem, A. Petdum, W. Panchan, J. Sirirak, A. Charoenpanich, T. Sooksimuang, N. Wanichacheva, *ACS Sens.* **2018**, *3*, 1016–1023.
4. T. Sooksimuang, W. Panchan, N. Wanichacheva, S. Sakunkaewkasem, A. Petdum, patent application number 1501003213, June 10, **2015**.
5. T. Sooksimuang, W. Panchan, K. Kwanplod, N. Wanichacheva, A. Petdum, patent application number 1701005852, September 29, **2017**.

Comparison of Methane Gas Sensing of Zinc Oxide Film and Tin Oxide Film

Veronica M. Mercado^a, Emmanuel A. Florido^{a*}

^aInstitute of Mathematical Sciences and Physics, University of the Philippines Los Baños, Los Baños, Laguna, Philippines

*e-mail: eaflorido@up.edu.ph

Zinc oxide (ZnO) film was fabricated by successive ionic layer adsorption and reaction (SILAR) with 200 cycles of alternate dipping in sodium zincate solution and hot water bath maintained at 90°C. The film was annealed at 300°C and later sensitized using palladium chloride (PdCl₂). The methane gas sensing response of the fabricated film was compared to that of tin oxide (SnO₂) commonly used in commercial methane gas sensors such as the MQ4. Analytical grade methane was supplied from standard methane gas canisters. The required amount of calibrated gas was injected to an airtight chamber containing the sensors using a gas syringe. The sensors were tested using two concentration ranges: 10 to 60 ppm and 618 to 5000 ppm. The ZnO/Pd film exhibited a sensitivity of 1 mV per 10 ppm while the SnO₂ film sensor showed a sensitivity of 0.8 mV per 10 ppm in the 618 to 5000 ppm. In the 10 to 60 ppm range the ZnO/Pd film had a sensitivity of 1mV per ppm. The SnO₂ sensor failed to show gas sensitivity and had low correlation between voltage output and concentration and in the low concentration range.



Figure 1 Gas sensing set-up showing airtight gas chamber (middle), Arduino microcontroller board (foreground), and syringe pump with valve (top).

Keywords: Zinc oxide, Tin oxide, Sensor, Successive ionic layer adsorption and reaction (SILAR), Sensitivity

References

1. W. S. Reeburgh, *Treatise on Geochemistry*. 2003, 4, 65-69
2. A. Nwanya, P.R. Deshmukh, R. Osuji, M. Maaza, C.D. Lokhande, F. Ezema, *Nano-Composite Thin Film*. 2014, 671-677.
3. P.K. Basu, P. Bhattacharyya, N. Saha, H. Saha, S. Basu, *Sensors and Actuators B Chemical*. 2008, 133(2), 357-363.
4. A.M. Gibb, *New Media Rt, Design, and the Arduino Microcontroller: A Malleable Tool*. Thesis for Master of Science. Pratt Institute. 2010.
5. E. Gertz, P. Di Justo, *O'Reilly Media, Inc.* 2012, 1-79.
6. V. Jain, *Engineers Garage*. 2012. Information on: <https://www.engineersgarage.com/insight/how-gas-sensor-works>

Polydiacetylene/Zinc-Aluminium Layered Double Hydroxides Nanocomposites with Reversible Thermochromism

Sarawut Kingchok^a, Patsaya Anukunwithaya^b, Kritapas Laohhasurayatin^b, Nisanart Traiphol^{c,e}, Rakchart Traiphol^{a,d,*}

^aLaboratory of Advanced Polymers and Nanomaterials, School of Materials Science and Innovation, Faculty of Science, Mahidol University at Salaya, Phuttamonthon 4 Road, Nakhon Pathom 73170, Thailand

^bNational Nanotechnology Center (NANO TEC), National Science and Technology Development (NSTDA), Pathum Thani 12120, Thailand

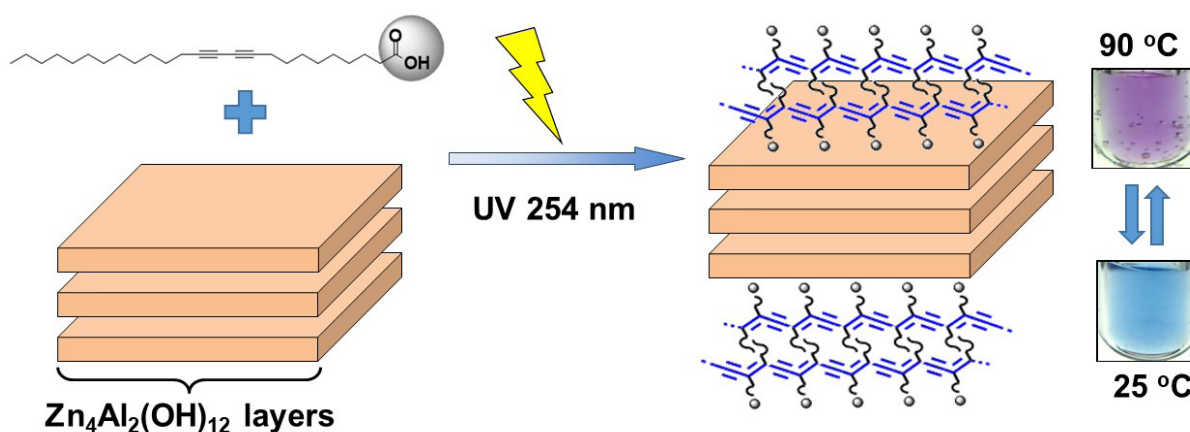
^cLaboratory of Advanced Chromic Materials, Department of Materials Science, Faculty of Science, Chulalongkorn University, Bangkok 10330, Thailand

^dNANO TEC-MU Excellence Center of Intelligent Materials and Systems, Faculty of Science, Mahidol University, Rama 6 Road, Ratchathewi, Bangkok 10400, Thailand

^eCenter of Excellence on Petrochemical and Materials Technology, Chulalongkorn University, Bangkok 10330, Thailand

*e-mail: rakchart.tra@mahidol.ac.th

Polydiacetylene (PDA)-based materials are known to exhibit color transition under external perturbation *i.e.* thermal, mechanical and chemical stimulus. As a consequence, these materials have been continuously developed for sensing applications. Normally, the commercial PDA materials show irreversible color transition after thermal perturbation. In this work, we introduce a new method for preparing PDA materials with reversible thermochromism. The diacetylene (DA) monomer, 10,12-Pentacosadiynoic acid (PCDA), was simply mixed with zinc-aluminium layered double hydroxides (ZnAl-LDH) in aqueous suspension. After incubation at low temperature, PDA/ZnAl-LDH nanocomposite was obtained via photopolymerization process. This method facilitates the interfacial interactions between poly(PCDA) molecules and ZnAl-LDH particles which promote the reversible thermochromism process (Scheme 1.). The ratio of PDA/ZnAl-LDH and pH of suspension were systematically varied. At suitable condition, the resultant nanocomposite exhibited reversible blue-to-purple color transition at 90°C. Origins of this behavior are explored by utilizing various techniques including Fourier-transform infrared spectroscopy (FT-IR) and X-ray diffraction (XRD).



Scheme 1. show the interfacial interaction between Poly(PCDA) and ZnAl-LDH particles and their reversible thermochromism

Keywords: Polydiacetylene; Layered Double Hydroxide; Thermochromism; Nanocomposite

Effects of Group I (Alkali) Metal Cations on Self-assemblies and Color-transition Behaviors of Polydiacetylene

Ma Theint^a, Nisanart Traiphol^{b,c}, Rakchart Traiphol^{a,d,*}

^aLaboratory of Advanced Polymers and Nanomaterials, School of Materials Science and Innovation, Faculty of Science, Mahidol University at Salaya, Phuttamonthon 4 Road, Salaya, Nakhon Pathom 73170, Thailand

^bLaboratory of Advanced Chromic Materials, Department of Materials Science, Faculty of Science, Chulalongkorn University, Bangkok 10330, Thailand

^cCenter of Excellence on Petrochemical and Materials Technology, Chulalongkorn University, Bangkok 10330, Thailand

^dNANOTECH-MU Excellence Center on Intelligent Materials and Systems, Faculty of Science, Mahidol University, Rama 6 Road, Ratchathewi, Bangkok 10400, Thailand

*e-mail: rakchart.tra@mahidol.ac.th (R. Traiphol).

Polydiacetylene (PDA) is a well-known conjugated polymer for its color-transition behavior upon exposure to thermal, chemical, mechanical, and UV light stimuli. This property allows utilization of PDA in various sensing applications. To realize its full potential, the ability to control color-transition behavior of PDA is essential. In this study, we introduce the simple and easy approach for fine tuning color-transition behavior of PDA by metal cations addition. The diacetylene (DA) monomer, 10,12-pentacosadynoic acid, is simply mixed with Group I alkali metal cations (M^+) such as Li^+ , Na^+ , K^+ , Cs^+ in aqueous suspension. The electrostatic interaction of positive metal cation (M^+) and carboxylic/carboxylate head group alters local interactions within the PDA- M^+ assemblies. Thus, the self-assembled behavior of PDA is improved and the yields of PDA are significantly increased. In addition, the color-transition behaviors of PDA- M^+ can be systematically tuned upon exposure to various stimuli such as pH, organic base, solvent, surfactant, UV light, and temperature. Moreover, the size and concentration of metal cations affect its colorimetric response and properties. The interactions of PDA- M^+ system are investigated through various techniques such as Fourier-transform infrared spectroscopy (FT-IR) and X-ray diffraction (XRD).

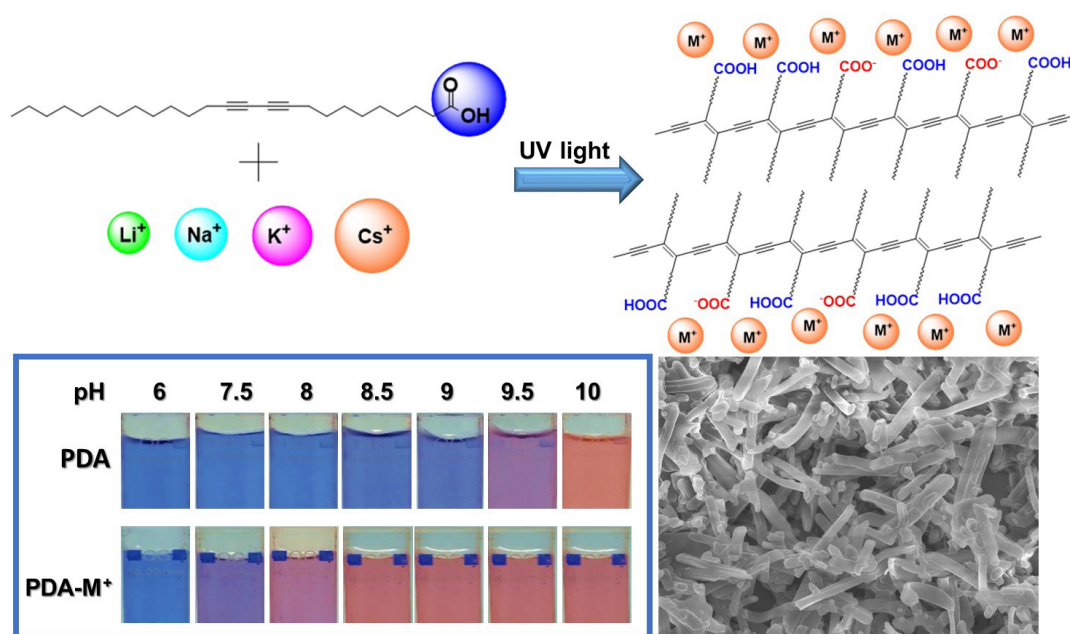


Figure 1. Incorporation of metal cations into PDA assemblies allows fine tuning of color-transition behavior.

Keywords: Polydiacetylene; Chromatic Sensor; Cation Additive, Self-assembly

The Effect of Alkaline Intercalant on Birnessite Structure towards Hydrazine Oxidation Mechanism and Sensing Application

Phatsawit Wuamprakhon^a, Atiweena Krittayavathananon^a, Soracha Kosasang^a, Nattapol Ma^a, Thana Maihom^{a,c}, Jumras Limtrakul^b, Montree Sawangphruk^a,

^a Department of Chemical and Biomolecular Engineering, School of Energy Science and Engineering, Vidyasirimedhi Institute of Science and Technology, Rayong 21210, Thailand

^b Department of Materials Science and Engineering, School of Molecular Science and Engineering, Vidyasirimedhi Institute of Science and Technology, Rayong 21210, Thailand

^c Laboratory for Computational and Applied Chemistry, Department of Chemistry, Faculty of Science and Center for Advanced Studies in Nanotechnology and Its Applications in Chemical, Food and Agricultural Industries, Kasetsart University, Bangkok 10900, Thailand

*e-mail address: montree.s@vistec.ac.th

An idea using a cation intercalated into a layer compound as a charge transport carrier in electrochemical systems has long been exploited in energy conversion and energy storage applications. Among layer structures, a birnessite-type MnO_2 has received considerable research attention as a heterogeneous catalyst and an energy storage material. Their interlayers are separated by water molecules and alkali cations for charging balance. By changing the cations, their layered structure and space must be altered impacting the electrochemical performance¹, however, their mechanism are still unclear. This work opens up the rationale behind the alkali cations' work in the MnO_2 birnessite structure towards the hydrazine oxidation via a combination between density functional theory (DFT) calculation with experimental studies. By varying the different intercalants (Li^+ , Na^+ , K^+ , Rb^+ and Cs^+), the standard heterogeneous electron transfer rate constant (k^0) of smallest cation size, Li^+ intercalant, significantly increases by 2.0 fold higher than Cs^+ intercalant. For testing the practical use in sensing application, the hydrazine sensor is also evaluated via measuring the limit of detection (LOD) value, selectivity and real-world detection.

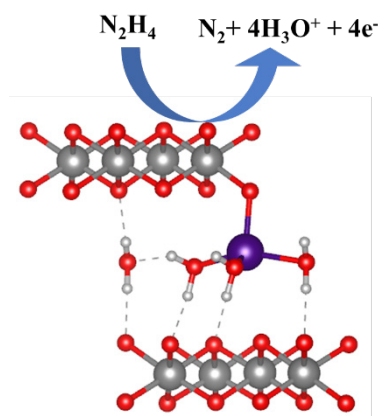


Figure 1. Schematic illustration for hydrazine oxidation on birnessite manganese oxide.

Keywords: Intercalated cation, birnessite, heterogeneous electron transfer rate constant, DFT calculation

References

1. P. Wuamprakhon, A. Krittayavathananon, S. Kosasang, N. Ma, T. Maihom, J. Limtrakul, M. Sawangphruk, *Chem Comm* 2018, 54, 8575-8578.

Highly Sensitive Detection of Ractopamine Using Surface-Enhanced Raman Scattering Based Lateral Flow Immunosensor

Sirin Sittivanichai, Suwussa Bamrungsap, Natpapas Wiriyachaporn, Pimporn Roeksrungruang, Chayachon Apiwat, Weerakanya Maneepprakorn*

National Nanotechnology Center (NANOTEC), National Science and Technology Development Agency (NSTDA), Pathumthani 12120, Thailand.

**e-mail: weerakanya@nanotec.or.th*

The highly sensitive lateral flow immunochromatographic assay (LFA) based on the use of surface-enhanced Raman scattering (SERS) for detection of ractopamine, β -agonist compounds used as repartitioning agents in livestock, was developed. Gold nanostar (AuNS) with multi-arms and surface's roughness features which allow the labelling of more biological moieties on their surfaces and better SERS performance were used as the signal reporter in this system. In this assay, AuNS was labelled with the Raman reporter molecule (4-aminothiophenol, ATP) and monoclonal antibody (MAb) specific to ractopamine. The assay reaction at the test area is based on the competitive immune-reaction between free ractopamine in the sample and ractopamine-bovine serum albumin immobilized at test area for binding with AuNS-antibody conjugate. The SERS based LFA developed in this work can not only provide the colorimetric immunoassay by visual detection but also the quantitative analysis by Raman signal measurement. This system shows high sensitivity and no cross reactivity to other β -agonist (clenbuterol and salbutamol) with the cut-off value of 1 ng/mL and the detection threshold of 0.01 ng/mL based on visual detection and Raman detection, respectively. Based on Raman signal detection, our SERS based-LFA shows highly sensitivity toward the conventional LFA. SERS based-LFA proposed in this work could be further applied for detection of other β -agonists and other forms of samples such as meats, urine, animal feed, etc.

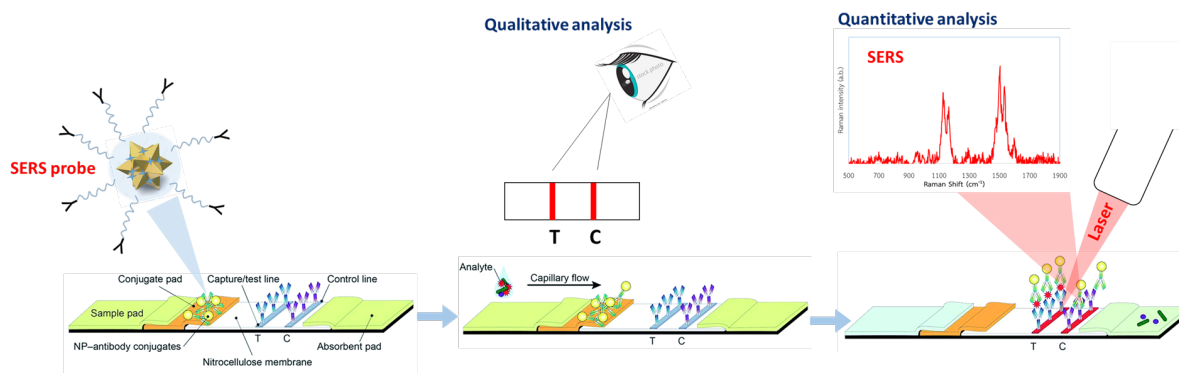


Figure 1. Principle of SERS based-LFA

Keywords: Gold nanostar, Ractopamine, SERS, immunoassay, β -Agonist

Gas Response of SILAR Fabricated Zinc Oxide Thin Film to Ammonia and Methane Gas at Room Temperature

Christopher T. Estandarte^{a*}, Emmanuel A. Florido^a

^aUniversity of the Philippines Los Baños

*e-mail: ctestandarte@up.edu.ph

The gas response of Zinc oxide (ZnO) thin films to ammonia and methane gas have been studied in the present work. The ZnO thin films were fabricated by successive ionic layer adsorption reaction (SILAR) technique then annealed at 400°C for 2 hours. Three types of films were produced, unsensitized ZnO film, Pd sensitized ZnO film (Pd-ZnO) and Mn sensitized ZnO film (Mn-ZnO). The sensitization on the films was done via dipping technique. These films were exposed to ammonia (NH₃) and methane (CH₄) gas using three concentrations; 667ppm, 1333ppm, 2000ppm. The effect of varying gas concentrations on the gas response of the sensor has been investigated. Results show that the sensitivity of the unsensitized film to methane gas is 2.46/10,000ppm while its sensitivity to ammonia gas is 0.49/10,000ppm. Results show that the unsensitized film was more sensitive to methane gas compared to ammonia gas. All the three films also showed higher gas response to ammonia compared to methane.

Keywords: Zinc oxide, Thin film, SILAR, Gas response, Gas sensor

References

1. S. Roy, H. Saha, C.K. Sarkar. *Int. J. on Smart Sensing & Int. Syst.* 2010, 3,(4), 605-620.
2. L.A.Patil, L.S. Sonawane, D. Patil. *J. of Mod. Phys.* 2011, 2(10), 1215-1221.
3. P. Mitra, S. Mondal,(2013). *Prog. in theo. and app. Phys.* 2013, 1, 17-31.
4. P. Mitra, A.K. Mukhopadhyay. *Bull. of the Polish Acad. of Sci-Tech. Sci.*, 2007, 55(3), 281-285.

Styryl-BODIPY as Fluorescent Probe for Gold(III) Ion in Aqueous Media

Suthikorn Jantra^a, Mongkol Sukwattanasinitt^a and Sumrit Wacharasindhu^{a,*}

^aThailand Nanotec-CU Center of Excellence on Food and Agriculture, Department of Chemistry, Faculty of Science, Chulalongkorn University Bangkok 10330, Thailand

*e-mail: sumrit.w@chula.ac.th

Fluorescent probes are great tools for visualization of analytes in aqueous solution. Although several probes perform well with green emission, a probe with longer wavelength is desirable. In this study, boron-dipyrromethene (BODIPY)-based fluorescent probe **SB** (Figure 1. Chemical Structure of **SB**) has been developed. **SB** has two styryl groups anchored to the BODIPY pyrrole rings by Knoevenagel condensation to extend the emission wavelength into the red region. In aqueous media, the probe could response to Au(III) ion selectively, demonstrating colorimetric change from blue to purple and fluorometric change from red to orange. Fluorescent intensity at 594 nm upon excitation at 540 nm was enhanced up to 7 folds within 2 hours in the presence of excess Au(III) ion. The reaction consisted of several oxidation steps and oxidative intermediates were observed by mass spectrometry.

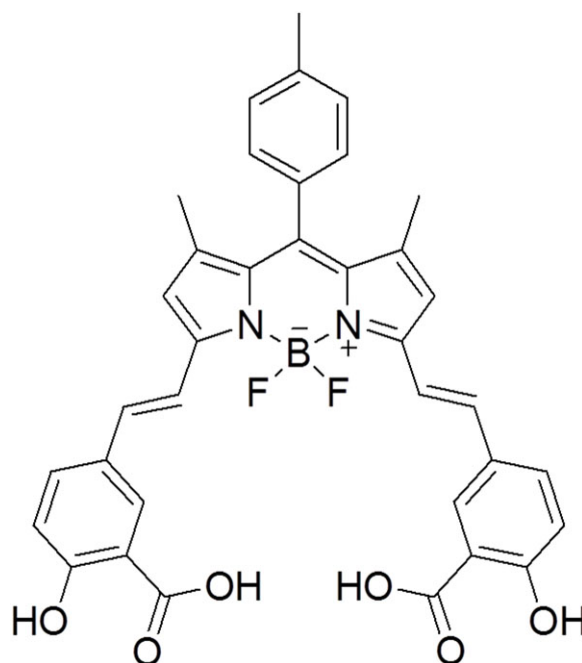


Figure 1. Chemical Structure of **SB**

Keywords: Sensor, BODIPY, Gold, Knoevenagel

Two-biosensor Platforms Based on Graphene Quantum Dots *via* Enzymatic Reaction for Photoluminescence Detection of Organophosphate Pesticide

Chonticha Sahub^a, Boosayarat Tomapatana^{a*}, Jonathan W. Steed^{b*}

^aDepartment of Chemistry, Faculty of Science, Chulalongkorn University, Bangkok, 10330, Thailand.

E-mail: tboosayarat@gmail.com

^bDepartment of Chemistry, University of Durham, South Road, DH1 3LE, UK.

E-mail: jon.steed@durham.ac.uk

Two-biosensor platforms based on graphene quantum dots (GQDs) *via* enzymatic reactions have been successfully developed for the determination of organophosphate pesticides (OPs). A first platform consisting of GQDs and active enzyme, **GQDs/Enz** platform is simply fabricated in an aqueous solution, while the second platform is continuously developed in well-defined model of hydrogels for the improvement of enzymatic stability and especially easy to be used for OPs sensing. Based on the concept, H_2O_2 generated *in situ* by the active enzymatic reactions of acetylcholinesterase and choline oxidase enables to react with GQDs resulting in photoluminescence (PL) quenching of GQDs at 467 nm. The PL recovery of GQDs was observed in the presence of organophosphate due to enzymatic inhibition process. Apparently, the PL changes of GQDs reasonably correspond to the amount of pesticide. The detection limits of **GQDs/Enz** platform towards dichlorvos was 0.78 μM in aqueous solution. Furthermore, the novel incorporation of GQDs and enzyme into hydrogels enables to significantly enhance the photoluminescence of GQDs and effectively improve the detection limit of dichlorvos pesticides. Two-biosensor platforms served as a promising photoluminescence affinity biosensor for specific detection of H_2O_2 and OPs.

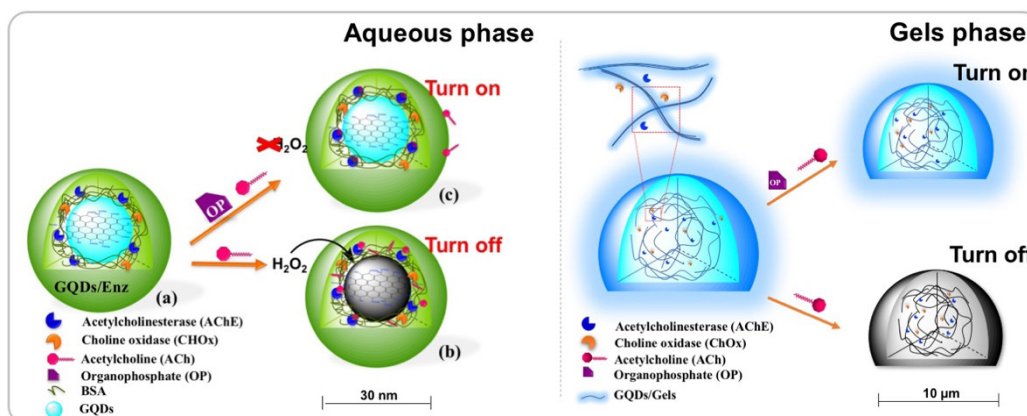


Figure 1. GQDs/Enz biosensor in aqueous and gels phase

Keywords: Graphene quantum dots, Enzymatic reaction, Organophosphate pesticide, Hydrogels

Chemically Modified Tip-Enhanced Raman Scattering (TERS) for Enantiomeric Discrimination

Thanyada Sukmanee^{a,c}, **Kanet Wongravee**^{a,b}, **Yasutaka Kitahama**^c,
Sanong Ekgasit^{a,b}, **Prompong Pienpinijtham**^{a,b*}, **Yukihiro Ozaki**^{c*}

^a Sensor Research Unit, Department of Chemistry, Faculty of Science, Chulalongkorn University

^b National Nanotechnology Center of Advanced Structural and Functional Nanomaterials, Department of Chemistry, Faculty of Science, Chulalongkorn University

^c Department of Chemistry, School of Science and Technology, Kwansei Gakuin University

*e-mail: prompong.p@chula.ac.th, ozaki@kwansei.ac.jp

This work presents a use of chemically modified tip-enhanced Raman scattering (TERS) to discriminate enantiomers *via* changes in hydrogen-bonding interaction between a probe molecule and analytes. The surface of silver tip is modified by *para*-mercaptopyridine (*p*MPY) through Ag–S bond. The efficiency of *p*MPY for enantiomeric recognition is evaluated using pure enantiomers of 2-octanol, α -methylbenzylamine and 2-amino-1-propanol. According to the formation of N–H⁺ in the pyridyl group of *p*MPY (Figure 1), the *p*MPY-modified tip interacts with each enantiomer to form the different hydrogen-bonded complexes enforced by a charge transfer process. The difference in molecular orientation of complexes is associated with the difference in energy states, which reflect to the relative intensities of Raman bands from *p*MPY. The relative Raman intensity of the C–C stretching with protonated and deprotonated nitrogen (1615 and 1577 cm⁻¹) can be used to discriminate the enantiomers. The enantiomeric excess (ee, %) shows that the *p*MPY-modified tip can be used to monitor (S)-enantiomer of 2-amino-1-propanol in the mixture with (R)-enantiomer, when % ee is greater than 50 %.

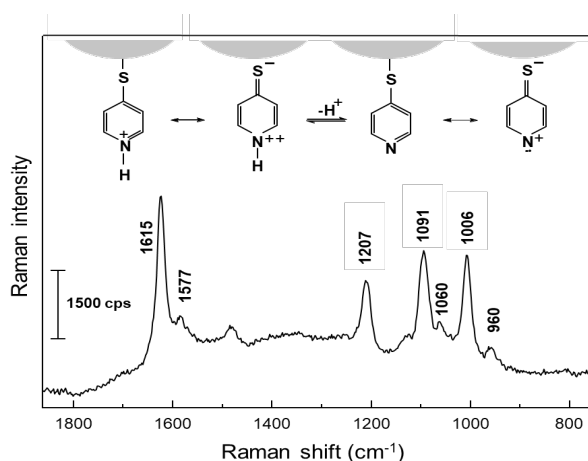


Figure 1. TERS spectrum of *p*MPY on silver tip. The inset shows the resonance forms of *p*MPY on silver surface.

Keywords : Charge transfer, Enantiomeric recognition, Hydrogen bonding, Tip-enhanced Raman scattering

References

1. Y. Wang, W. Ji, H. Sui, Y. Kitahama, W. Ruan, Y. Ozaki, B. Zhao, *J. Phys. Chem. C* 2014, *118*, 10191-10197.
2. Y. Wang, Z. Yu, X. Han, H. Su, W. Ji, Q. Cong, B. Zhao, Y. Ozaki, *J. Phys. Chem. C* 2016, *120*, 29374-29381.
3. J. A. Baldwin, B. Vlčková, M. P. Andrews, I. S. Butler, *Langmuir* 1997, *13*, 3744-3751.
4. J. Hu, B. Zhao, W. Xu, B. Li, Y. Fan, *Spectrochim Acta A Mol Biomol Spectrosc* 2002, *58*, 2827-2834.
5. Z. Wang, L. J. Rothberg, *J. Phys. Chem. B* 2005, *109*, 3387-3391.

Fluorescence-based Aptasensor for Albumin Detection in Urine

Wireeya Chawjiraphan^{a*}, Chayachon Apiwat^a, Naiyana Poottasane^b, Deanpen Japrun^a

^aNational Nanotechnology Center (NANO TEC), National Science and Technology Development Agency (NSTDA), Thailand Science Park, Pathumthani, Thailand

^bThammasat University Hospital, Thammasart University, Pathumthani, Thailand

*e-mail: wireeya.cha@nanotec.or.th

Albuminuria refers to moderately raised albumin levels in urine, which is resulted from functional impairment and pathological changes of the renal. Determination of albuminuria is the early predictor for renal disease and progression of chronic kidney problem. A fluorescence-base aptasensor was developed for the determination of albumin in urine comparing with the standard automate instrument. The specificity, linearity, stability and similarity were evaluated. The fluorescent signal and albumin concentration in 15 urine samples was investigated. The signal was linearly increased in concentration range between 0.01 and 1.5 mg/mL, revealed linear regression was 0.983 ($y = 5.5495X + 14.75912$). Albumin concentration detected from aptasensor has significant positive correlation ($r = 0.844$, $p < 0.01$) compared to standard protocol. Normalize fluorescence intensity of human albumin was found to be closely related to bovine albumin, which were 0.4 μmol and 0.6 μmol respectively. We also analyzed the sequences similarity of human albumin compared to other species in the context of their potential cross-reactivity. The sequence showed a similarity very similar to bovine albumin. The albumin detection aptasensor was determined to be as good as a automate detection instrument. This aptasensor may be consider as routine albumin detection in clinical samples for early detection of renal dysfunction.

Keywords: Albumin, Urine, Aptasensor, Kidney disease

References

1. G. Fanali, A. di Masi, V. Trezza, M. Marino, M. Fasano, P. Ascenzi, *Mol Aspects Med.* **2012**, 33, 209-290.
2. A. Levey, J. Coresh, *Lancet.* **2012**, 379, 165-180.
3. A. Webster, E. Nagler, R. Morton, P. Masson, *Lancet.* **2016**, 389, 1238-1252.
4. KDOG/National Kidney Foundation, *J. Kidney International Supplements.* **2017**, 7, 1-59.
5. C. Apiwat, P. Luksirikul, P. Kankla, P. Pongprayoon, K. Treerattakoon, K. Paiboonsukwong, S. Fuchareon, T. Dharakul, D. Japrun, *Biosens Bioelectron.* **2016**, 82, 140-145.
6. Higashimoto, S. Yamagishi, K. Nakamura, T. Matsui, M. Takauchi, Noguchi, H. Inoue, *Microvasc Res.* **2007**, 74, 65-69.
7. C. Lu, H. Yang, C. Zhu, X. Chen, G. Chen, *Angew. Chem. Int. Ed.* **2009**, 48, 4785-4787.
8. R. Nurdiansyah, M. Rifa'I and N. Widodo, *J. Taibah Univ Med Sc.* **2016**, 11, 243-249.

In silico study of gold nanoparticle uptake into mammalian cell: interplay of size, shape, and surface charge

Thodsaphon Lunnoo^a, Jirawat Assawakhajornsak^b and Theerapong Puangmali^{a,*}

^{a,*}*Department of Physics, Faculty of Science, Khon Kaen University, Khon Kaen 40002, Thailand*

^b*Department of Physics, King's College London, Strand, London, WC2R 2LS, United Kingdom*

**e-mail: theerapong@kku.ac.th*

The study of interactions between Au nanostructures and living cells is a fundamental aspect that can be applied for the promising applications in nanomedicine. In the present work, we performed coarse-grained molecular dynamics (MD) simulations to observe the internalization pathways of Au nanostructures (nanosphere, nanocage, nanorod, nanoplate, and nanohexapod) into an idealized mammalian plasma membrane at an unprecedented level of complexity. Compared with the simple lipid bilayer model consisting of two lipid species, the different cellular uptake pathways of the AuNP were found. We highlight that the complexity of the lipid bilayer models plays an important role in the uptake pathway of nanoparticles (NPs). The permeability of aggregated AuNPs was much less than the NP counterpart. Spherical AuNPs showed pronounced size and surface charge dependence in their translocation through the plasma membrane. The translocation rates of different Au nanostructures were also evaluated and we found that Au nanohexapod exhibited highest cellular uptake. Understanding the interrelationship between size, shape, surface charge, and aggregation of Au nanostructures provides a clear view on the design of Au nanostructures for developing new diagnostic strategies and drug delivery.

Keywords: Plasma membrane, Internalization pathways, Drug delivery

References

1. N. Shikha, S. Radhakrishna, *Langmuir*. **2011**, 28, 17666-17671.
2. C. Eun Chul, X. Jingwei, W. Patricia A, X. Younan, *Nano Letters*. **2009**, 9, 1080-1084.
3. K. Yang, Y.-Q. Ma, *Nature Nanotechnology*. **2010**, 5, 579-583.
4. X. Quan, C. Peng, D. Zhao, L. Li, J. Fan, J. Zhou, *Langmuir*. **2017**, 33, 361-371,

Velocity Autocorrelation Function as a Fast Estimation of Diffusion Coefficients

Nithinart Chitpong^a, Anintaya Khamkanya^b, Satakhun Bunbuchachai^{c,*},
and Teeranan Nongnual^{c,*}

^aDepartment of Textile Engineering, Faculty of Engineering, Rajamangala University of Technology Thanyaburi, Pathumthani, 12110, Thailand

^bDepartment of Industrial Engineering, Faculty of Engineering, Thammasat University, Pathumthani, 12120, Thailand

^cDepartment of Chemistry, Faculty of Science, Burapha University, Chonburi, 20130, Thailand

*e-mail: teeranan.no@buu.ac.th

Nanoscale trajectories of a mobilizing particle can be observed by using single particle tracking based on super-resolution fluorescent microscopy. Traditionally, the mean-squared displacement method generates averaged particle displacements at different lag time, resulting the scale of particle movement in terms of diffusion coefficients. Alternatively, the velocity autocorrelation function based on the Green-Kubo equation was proposed for the calculation of the diffusion coefficients. Herein, three-dimensional trajectories of particles undergoing free diffusion were generated by using the random-walk simulations. Consequently, the diffusion coefficients were then measured by a set of written computational algorithms. It was found that the resulting diffusion coefficients determined from both methods are significantly indifferent. Moreover, the velocity autocorrelation function algorithm implemented with the fast Fourier transform dramatically reduces the computational time by an order of magnitude comparing to the conventional mean-squared displacement. The results suggest that the velocity autocorrelation function could be a promising approach in kilohertz-framerate experiments or real-time single particle tracking applications, due to its high reliability and fast computational calculations.

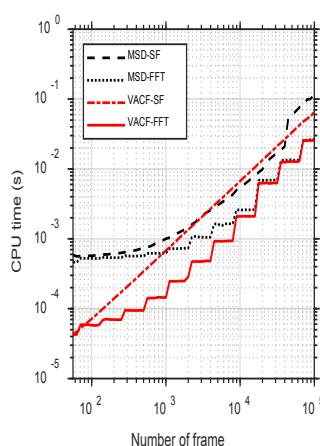


Figure 1. Comparison of the estimated CPU time for calculating the particle diffusion coefficients by using mean-squared displacement (MSD) and velocity autocorrelation function (VACF), each written in the straight-forward algorithm (SF) or combined with the fast Fourier transform (FFT).

Keywords: velocity autocorrelation function, mean-squared displacement, diffusion coefficient, real-time particle tracking

References

1. T. Schmidt, G. J. Schütz, W. Baumgartner, H. J. Gruber, H. Schindler *Proc. Natl. Acad. Sci. U.S.A.* **1996**, *93*, 2926-2929.
2. J. Gelles, B. J. Schnapp, M. P. Sheetz *Nature* **1988**, *331*, 450-453.
3. C. Kural, H. Kim, S. Syed, G. Goshima, V. I. Gelfand, P. R. Selvin *Science* **2005**, *308*, 1469-72.

Effect of Electrolyte Additives on the Stability and Electrochemical Performance of Lithium-Sulfur Batteries

Salatan Duangdangchote^a, Atiweena Krittayavathananon^a, Nutthaphon Phattharasupakun^a, Poramane Chiochan^a, and Montree Sawangphruk^{a,*}

^aDepartment of Chemical and Biomolecular Engineering, School of Energy Science and Engineering, Vidyasirimedhi Institute of Science and Technology, Rayong 21210, Thailand

*e-mail: montree.s@vistec.ac.th

Soluble lithium polysulfide intermediates dissolving in the electrolyte during the charge/discharge cycles is one of the major issues making the rapid capacity decays of lithium-sulfur batteries. Moreover, the formation of lithium dendrites at metal anodes during cycling can be grown, passed through the separator, and contacted with the cathode leading to the short circuit. To overcome these issues, electrolyte additives, are typically used to control the lithium dendrite growth via reacting with electrolyte compounds to form the stable solid-electrolyte interphase (SEI) layers above the metallic anode, in which these SEI layers is believed to control the dendrite¹. On the cathode, the additive anions can be used to trap the lithium polysulfides species resulting from lewis acid-base reactions. This protective layer is formed in several steps with complex mechanisms; different anions additives dominates in different pathways of the mechanism². This investigates that the role of additives in both cathode and anode sides of lithium-sulfur batteries is still unclear. Herein, this work was investigated the mechanism of the electrolyte additive with different anions (i.e., chalcogen and halide groups) in the lithium-sulfur battery cell and their performances via using the density functional theory (DFT) calculations along with the experimental study. By varying anions, the mechanism of SEI formation at the anode and the binding capabilities of lithium polysulfides intermediate at the cathode will be informed in this work. We hope that this should be a useful information in term of the effect of the anion additives that can enhance performance and safe operation of lithium-sulfur batteries.

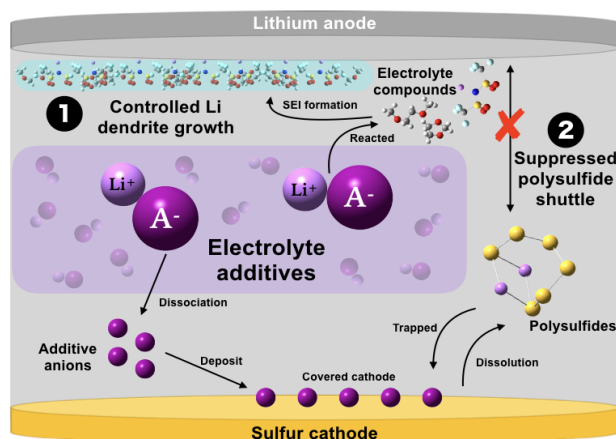


Figure 1. Schematic of the effect of the electrolyte additive over the cathode and the anode of lithium-sulfur battery.

Keywords: DFT, Electrolyte Additives, SEI, Lithium Polysulfides Intermediates

References

1. Chen, L.; Shaw, L. L. *J. Power Sources* **2014**, *267*, 770-783.
2. Lili, W.; Yusheng, Y.; Nan, C.; Yongxin, H.; Li, L.; Feng, W.; Renjie, C. *Adv. Funct. Mater.* **2018**, *0* (0), 1800919.

Surface Plasmon Resonance Sensor using Thin Film of Aluminium—a Theoretical Study

Kunal Sharma^a, Dr. Tanujjal Bora^{a,b}, Dr. Gabor L. Hornyak^{a,b}

^a*Nanotechnology, Industrial Systems Engineering, School of Engineering and Technology, Asian Institute of Technology, PO Box 4, Klong Luang, Pathumthani – 12120, Thailand*

^b*Center of Excellence in Nanotechnology, Asian Institute of Technology, PO Box 4, Klong Luang, Pathumthani – 12120, Thailand*

Surface Plasmon Resonance (SPR) is the characteristic shown by metallic nanoparticles when they interact with light of particular wavelength. SPR has been popular with gold and silver, but it can be exhibited by other inexpensive metals as well, such as aluminium (Al). Advantages with Al is that, it is inexpensive compared to gold and silver, high abundance in earth crust and uniquely shows SPR in ultraviolet region (wavelength < 0.400 μm), unlike gold and silver that show SPR absorption in visible region. In this work, the application of inexpensive Al as a potential SPR sensor is demonstrated. The sensor output is estimated by using finite element analysis (FEA) method. A 25 nm thin film of Al is deposited on a borosilicate glass substrate (refractive index 1.517) and a p-polarized light is shined on the Al thin film and reflectance of the system is recorded. Due to the SPR absorption, the Al thin film exhibited a sharp drop in reflectance at a particular wavelength, which is a function of the film thickness. Sensor is first tested with a test solution composed of pure water with refractive index 1.33, for which the SPR reflectance drop was observed at 0.336 μm . A red-shift in the SPR reflectance (from 0.336 μm to 0.394 μm , shown in Figure) was recorded when the refractive index of the test medium was varied from 1.33 to 1.35, inferring that Al also exhibits SPR effect which can be suitable for sensing in ultraviolet region. Although aluminium has lesser stability than gold because of its high oxidizing properties, by coating it with metallic oxides like alumina, life of Al thin film can be significantly increased.

Figure 1. Reflectance spectra calculated for a 25 nm thick Al thin film deposited on glass substrate showing a red-shift in the SPR absorption band in UV region as function of increasing refractive index of the surrounding medium.

Keywords: Surface Plasmon Resonance, Sensor, Aluminium, Ultraviolet, Finite Element Analysis.

Theoretical Study on Diels-Alder Reaction of Furan and Methyl Acrylate over Lewis Acidic Sn-BEA Zeolite

Veerachart Paluka^{a,b}, Chompunuch Warakulwit^{a,b*}, Thana Maihom^{c*}

^aDepartment of Chemistry, Faculty of Science, Kasetsart University, Bangkok 10900, Thailand

^bNANOTEC Center of Excellence for Nanoscale Materials Design for Green Nanotechnology and Center for Advanced Studies in Nanotechnology for Chemical, Food and Agricultural Industries, Kasetsart University, Bangkok 10900, Thailand

^cDepartment of Chemistry, Faculty of Liberal Arts and Science, Kasetsart University, Kamphaeng Saen Campus, Nakhon Pathom 73140, Thailand

*e-mail: faastnm@ku.ac.th (M. Thana), fscicpn@ku.ac.th (C. Warakulwit)

Herein, we apply density functional theory calculations to study the Diels-Alder (DA) reaction of furan and methyl acrylate over Lewis acidic Sn-BEA zeolite compared to the uncatalyzed reaction. With the contribution of zeolite active site, the activation free energy of DA was 16.8 kcal/mol lower than the uncatalyzed system. We also investigate the influence of Li cation exchange Sn-BEA (Li-Sn-BEA) on the studied reaction. We find that Li-Sn-BEA can reduce the activation barrier of about 2 kcal/mol relative to that in Sn-BEA. This result can be explained by the FMO analysis, which reveals a higher electrophilic character of the adsorbed methyl acrylate in the case of Li-Sn-BEA compared to Sn-BEA one.

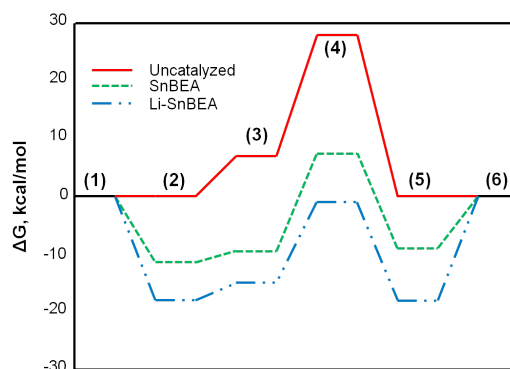


Figure 1. Free energy profiles for the DA reaction of furan and methyl acrylate over Sn-BEA, Li-Sn-BEA and the gas phase uncatalyzed system.

Keywords: Diels-Alder Reaction, Zeolites, Sn-Substituted BEA, Li-Exchanged Sn-BEA

References

1. A. Prasertsab, T. Maihom, M. Probst, C. Wattanakit, J. Limtrakul, *Inorg Chem*, **2018**, *57*, 6599-6605.
2. T. Salavati-fard, S. Caratzoulas, R. F. Lobo, D. J. Doren, *ACS. Catal.* **2017**, *7*, 2240–2246.

Carbon-doped Boron Nitride Nanosheet as a Promising Metal-free Catalyst for NO Reduction: DFT Mechanistic Study

Tanabat Mudchimo^a, Supawadee Namuangruk^b, and Siriporn Jungstittiwong^{a*}

^aDepartment of Chemistry, Faculty of Science, Ubon Ratchathani University, Ubon Ratchathani, Thailand

^bNational Nanotechnology Center (NANOTEC), National Science and Technology Development Agency (NSTDA), Pathum Thani, Thailand

*e-mail: siriporn.ubu@gmail.com

Currently, metal-based catalysts are commonly used to convert highly toxic gases like NO molecules into less toxic gases, such as N₂O molecules through the process of reduction reaction that has a low activation energy (E_a) and high efficiency. Due to the high cost, environmental hazards and limited supply of metal-based catalysts, development of metal-free catalysts that are low cost and environmentally friendly has increased. For this research, NO reduction mechanism using the carbon-doped boron nitride nanosheets (CBNs) as a metal-free catalyst was investigated by density functional theory (DFT). For the NO reduction mechanism, the dimer mechanism pathway was investigated using the following equation: $2\text{NO} \rightarrow \text{N}_2\text{O} + \text{O}_{\text{ad}}$. In addition, the catalytic activity of carbon atom substitution onto BNs for NO reduction was studied. The results showed that the *trans*-(NO)₂ structure of C_NBNs (D5) is a potentially crucial intermediate with thermodynamically and kinetically favorable, in which the calculated rate-determining step along the most energetically favorable pathway is 0.62 eV. Hence, our results presented here suggest that C_NBNs can be a highly active metal-free material in NO removal, which will reduce NO into environmentally friendly gases.

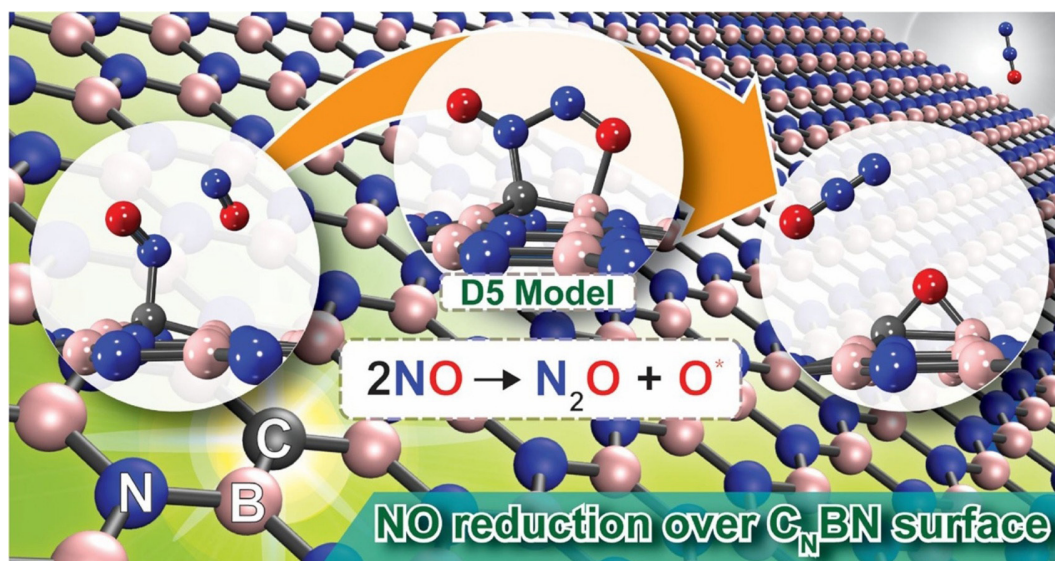


Figure 1. The most favorable pathway for NO reduction mechanism on carbon-doped boron nitride

Keywords: Metal-free catalyst, Carbon-doped boron nitride, NO reduction mechanism, Density functional theory

References

1. M. Tanabat, N. Supawadee, K. Nawee, and J. Siriporn, *Applied Catalysis A, General*. **2018**, 557, 79–88.

Structure-activity Relationship on Pyridine-amine Nickel Complexes for Polyethylene Polymerization: Theoretical Study

Pongsakorn Chasing^a, Phornphimon Maitarad^{a,b*}, Liyi Shi^b, Dongsong Zhang^b, Hongmin Wu^b, Vinich Promarak^{a*}

^a School of Molecular Science and Engineering, Vidyasirimedhi Institute of Science and Technology, Rayong 21210, Thailand.

^b Research Center of Nanoscience and Technology, Shanghai University, Shanghai 200444, PR China.

*e-mail: pmaitarad@shu.edu.cn, vinich.p@vistec.ac.th

Structure–activity relationship (SAR) approach was applied to comprehend the effects on catalytic activities of polyethylene polymerization on a set of pyridine-amine nickel complexes with various substituents. Molecular descriptors of both electronic and steric properties were investigated by the density functional theory calculations. The multiple linear regression analysis was then used to derive the relationship between the PE activity (dependent variable, $\ln(A)$) and catalysts' structural properties (independent variables). The best SAR model showed a good correlation with $R^2 = 0.92$, residual sum of square = 0.079 and predictive sum of square = 0.538. The obtained SAR model is $\ln(A) = -32.673(\text{N-charge}) - 0.114(\text{Rotatable bonds}) - 17.848$. Thus, N-charge of pyridine and rotatable bonds properties could be used to relate the single-site pyridine-amine Ni catalysts and their PE activities. Alternatively, it indicated that the more negative charge of N and the less rotatable bond would increase the PE catalytic performance. In summary, this finding is useful to guide the idea for further designing on pyridine-amine nickel complexes aiming to enhance the polyethylene polymerization.

Keywords: Single-site Catalyst, Metallocene, Polyethylene, QSAR, DFT.

References

1. S. Zai, H. Gao, Z. Huang, H. Hu, H. Wu and Q. Wu, *ACS Catalysis*, **2012**, *2*, 433-440.
2. T. Le, V. C. Epa, F. R. Burden and D. A. Winkler, *Chem Rev*, **2012**, *112*, 2889-2919.
3. V. Cruz, S. Martinez, J. Martinez-Salazar, D. Polo-Cerón, S. Gómez-Ruiz, M. Fajardo and S. Prashar, *Polymer*, **2007**, *48*, 4663-4674.
4. V. Cruz, J. Ramos, A. Muñoz-Escalona, P. Lafuente, B. Peña and J. Martinez-Salazar, *Polymer*, **2004**, *45*, 2061-2072.
5. W. Yang, J. Yi, Z. Ma and W.-H. Sun, *Catal. Commun.*, **2017**, *101*, 40-43.

ACKNOWLEDGMENTS

This work was supported by Vidyasirimedhi Institute of Science and Technology (VISTEC) with both funds and equipments. Thanks for support from the Thailand Research Fund (RTA6080005) and Research Center of Nano Science and Technology, Shanghai University. We would like to thank NANOTECH, Thailand Sci Park for cluster computer and software supports. PM and LS would like to thank the Shanghai Municipal Science and Technology Commission of Professional and Technical Service Platform for Designing and Manufacturing of Advanced Composite Materials (16DZ2292100).

Equivalent Circuit Parameters of Hybrid Quantum-Dot Solar Cells

Unchittha Prasatsap^a, Suwit Kiravittaya^{a,*},

Thanaphat Rakpaises^b, Nanthaphop Sridumrongsak^b, Aniwat Tандаechanurat^b

Visittapong Yordsri^c, Chanchana Thanachayanont^c

Chanyanuch Chevintulak^d, Supachok Thainoi^d, and Somsak Panyakeow^d

^a *Advanced Optical Technology (AOT) Laboratory, Department of Electrical and Computer Engineering, Faculty of Engineering, Naresuan University, Phitsanulok 65000, Thailand*

^b *International School of Engineering (ISE), Faculty of Engineering, Chulalongkorn University, Bangkok, 10330, Thailand*

^c *National Metal and Materials Technology Center (MTEC), National Science and Technology Development Agency (NSTDA), Pathumthani 12120, Thailand*

^d *Semiconductor Device Research Laboratory, Department of Electrical Engineering, Faculty of Engineering, Chulalongkorn University, Bangkok, 10330, Thailand*

*e-mail: suwitki@gmail.com

Hybrid quantum-dot (QD) solar cells have been fabricated and experimentally investigated [1]. Cross-sectional transmission electron microscopic (TEM) image of a hybrid QD sample is shown in Fig. 1(a). A simple equivalent circuit model (Fig. 1(b)) is applied to explain electrical characteristics of the fabricated solar cells. Measured and fitted I-V curves are shown in Fig. 2. The experimental results can be well fitted with the relation [2]:

$$I_{cell} = \frac{1}{R_s} \frac{nkT}{q} W \left[\frac{q}{nkT} \frac{I_o R_s}{(1 + R_s / R_{sh})} \exp \left[\frac{q}{nkT} \frac{V_{cell} + R_s (I_o + I_{ph})}{(1 + R_s / R_{sh})} \right] + \frac{V_{cell} / R_{sh} - (I_o + I_{ph})}{1 + R_s / R_{sh}} \right]$$

where I_{cell} and V_{cell} are current and voltage across the cell, W is the Lambert W function, I_{ph} is the photocurrent, I_o is the reverse saturation current, n is the diode ideality factor, kT/q is the thermal voltage, R_{sh} is the shunt resistance and R_s is the series resistance. We have developed the curve fitting method with five fitting parameters (I_{ph} , I_o , n , R_{sh} , and R_s). The extracted parameter values can be discussed and related to the physical structure of solar cells.

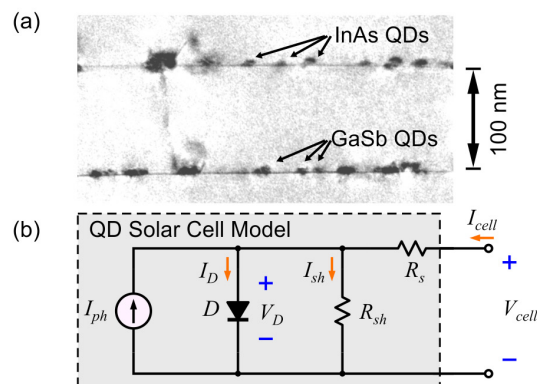


Figure 1. (a) TEM image of hybrid QD structure consisted of hybrid type-I InAs QDs and type-II GaSb QDs. (b) Equivalent circuit model of a solar cell.

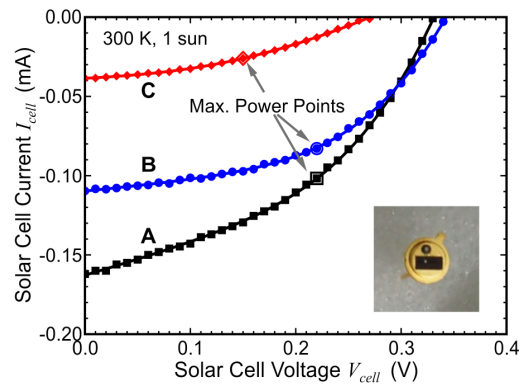


Figure 2. I-V characteristics of three hybrid QD solar cells (A: type I on top of type II, B: type II on top of type I, and C: 3 pairs of type I on type II). The lower right inset shows a photo of the investigated sample.

Keywords: Quantum Dot, Solar Cell, Current-Voltage Characteristics, Curve Fitting, Circuit Model

References

1. T. Rakpaises *et al.*, World Conference on Photovoltaic Energy Conversion (WCPEC 2018), 10-15 Jun. 2018.
2. S. Sriphan, S. Kiravittaya, S. Thainoi, S. Panyakeow, *Adv. Mater. Res.* **2015**, *1103*, 129-135.

The Reactivity and Selectivity of Ni(111) for Propane Dehydrogenation to Produce Propylene

Tinnakorn Saelee^a, Supawadee Namuangruk^b, Nawee Kungwan^{a*}, Anchalee Junkaew^{b*}

^aDepartment of Chemistry, Faculty of Science, Chiang Mai University, Chiang Mai 50200, Thailand ^bNational Nanotechnology Center (NANOTEC), National Science and Technology Development Agency, Pathumthani, 12120, Thailand

*e-mail: anchalee@nanotec.or.th, naweekung@gmail.com

Propylene, the important raw material for a variety of products such as propylene oxide, acrylonitrile and alcohols, can be produced via propane dehydrogenation (PDH) using high effective catalyst. To date, platinum- (Pt-) based catalyst is widely used for PDH process. Due to the high reactivity of alkane reaction on Ni catalyst and good stability at high temperatures as well as lower price than Pt-based catalyst, the Ni is a promising candidate for PDH reaction. However, the reaction mechanism of PDH on Ni catalyst is still unclear. In this study, mechanisms of PDH and side reactions are theoretically investigated on Ni(111) surface. For PDH reaction, the dehydrogenation of propane to form 1-propyl intermediate before undergoing to propylene formation is more feasible than that of 2-propyl because of more kinetic favourable of PDH reaction and more thermodynamic stable of 1-propyl on Ni(111) surface. Moreover, the side reaction of C-C bond cracking cannot be taken place during PDH process. Understanding of the reaction mechanisms of PDH and side reactions on Ni(111) surface is useful for designing and developing the better selective Ni catalyst by increasing the reactivity of propylene desorption and inhibiting the side reaction of C-C bond cracking and deep dehydrogenation.

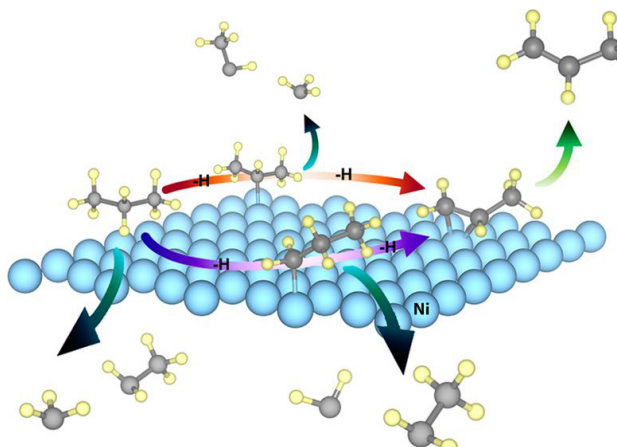


Figure 1. All proposed mechanisms of PDH and side reaction on Ni(111) surface

Keywords: propane dehydrogenation; C-C bond cracking; Ni(111) surface; DFT; propylene

References

1. M.-L. Yang, Y.-A. Zhu, C. Fan, Z.-J. Sui, D. Chen, X.-G. Zhou, *J. Mol. Catal. Chem.* **2010**, 321, 42-49
2. T. Saelee, S. Namuangruk, N. Kungwan, A. *J. Phys. Chem. C.* **2018**, 122, 14678-14690
3. Z. Yan, D.W. Goodman, *Catal. Lett.* **2012**, 142, 517-520
4. M.-L. Yang, J. Zhu, Y.-A. Zhu, Z.-J. Sui, Y.-D. Yu, X.-G. Zhou, D. Chen, *J. Mol. Catal. Chem.* **2014**, 395, 329-336



Poster

Simple and Selective Colorimetric Detection for Fumonisin B1 in Corn Samples

Thaksinan Chotchuang,^{a,b} Titilope John Jayeoye,^{a,b} Wilairat Cheewasedtham,^b Thitima Rujiralai,^{a,b*}

^aDepartment of Chemistry and Center of Excellence for Innovation in Chemistry, Faculty of Science, Prince of Songkla University, Hat Yai, Songkhla 90112, Thailand.

^bAnalytical Chemistry and Environment Research Unit, Division of Chemistry, Department of Science, Faculty of Science and Technology, Prince of Songkla University, Pattani 94000, Thailand.

*e-mail: thitima.r@psu.ac.th

A novel, simple and highly sensitive colorimetric method is developed for determination of fumonisin B1. The system is based on aggregation of cysteamine-capped gold nanoparticles (cyst-AuNPs) in the presence of the hydrolyzed fumonisin. It was found that the color of gold nanoparticles changed from red to blue with increasing fumonisin concentration. The absorbance ratio (A_{675}/A_{520}) was linear with fumonisin concentrations in the range of 2.0 to 12.0 ppb ($R^2 = 0.9937$). Under the optimum experimental conditions, the sensor achieved a detection limit of 1.73 ppb by the naked eye. The selectivity of cyst-AuNPs probe for fumonisin B1 was also investigated in the presence of other interferences, while the real applicability was demonstrated on corn samples.

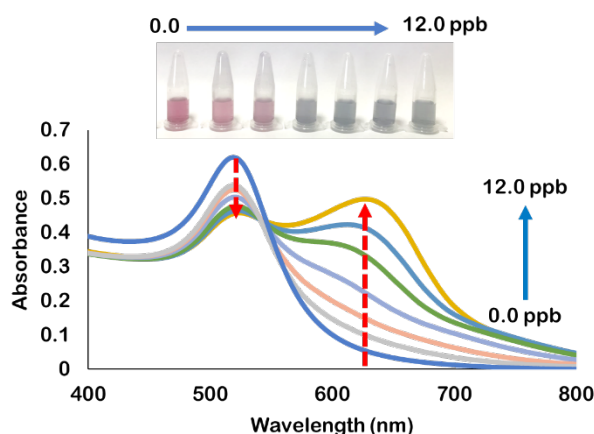


Figure 1 Sensitivity of cyst-AuNPs to different concentrations of fumonisin B1.

Keywords: Fumonisin, Gold nanoparticles, Colorimetry, Spectrophotometry

References

1. R. Assunção, E. Vasco, B. Nunes, S. Loureiro, C. Martins, P. Alvito, *Food Chem. Toxic.* **2015**, *86*, 274-281.
2. Y. Zhou, H. Dong, L. Liu, M. Li, K. Xiao, M. Xu, *Sens. Actuators B: Chem.* **2014**, *196*, 106-111.

Physicochemical Studies of Turmeric Nanoemulsions Using Different Sources of Turmeric Extracts

**Plernta Sukjarernchaikul^a, Sirinat Jearanai^a, Kunat Suktham^a, Onuma Ketchart^a, Benchaporn Meemuk^a,
Tirapote Rattana-amron^a, Jayanant Iemsam-arng^{a,*},**

^aNational Science and Technology Development Agency, Thailand

*e-mail: jayanant@nanotec.or.th

Background: Turmeric is generally used in various therapeutic products because of its renowned pharmaceutical properties, especially for gastrointestinal benefits as well as its abundant source found in many regions. As a result, different origin of turmeric might affect the product quality. This study aimed to evaluate both physical and chemical characteristics of turmeric extracts from different sources by preparing in the form of nanoemulsions.

Methods: Dynamic light scattering (DLS), atomic force microscopy (AFM) and Wilhelmy plate technique were applied to investigate the surface properties of nanoemulsions. Differential scanning calorimetry (DSC) was utilised to examine crystallization characteristics during a change of temperature. Liquid chromatography-tandem mass spectrometry (LC-MS/MS) was used to quantify the content of curcuminoids and its stability during certain storage time.

Results: Different source of turmeric extracts provided dissimilar particle diameter ranging from 70 to 300 nm and zeta potential varied from -12 to -9 mV. Surface tension of each source was similar with value around 30mN/m. DSC result showed unique peak for each turmeric extract and each nanoemulsion formulation. LC-MS/MS revealed that turmeric extracts from different sources have different amount of curcuminoids content. For the stability assessment, each encapsulated turmeric extract was stable at 4°C and at room temperature for 4 months.

Conclusions: This study could imply that source of turmeric extracts should be concerned in the production process because each source has distinctive property which provides different physical and chemical characteristics when encapsulated into turmeric nanoemulsions.

Keywords: Turmeric, Curcumin, Curcuminoids, Nanoemulsions

Production and Characterization of Encapsulated Proteins from the Giant River Prawn

**Siwapech Sillapaprayoon^{a,b}, Nichanun McMillan^c, Wanwisa Srinuanchai^a, Rujira Sukhampa^d,
Issara Sramala^{a*}, Satita Tapaneeyakorn^{b*}**

^a*Nano Agro and Food Innovation Laboratory, NANOTEC, NSTDA, Thailand 12120*

^b*Nanomolecular Target Discovery Laboratory, NANOTEC, NSTDA, Thailand 12120*

^c*Department of Aquaculture, Faculty of Fisheries, Kasetsart University, Thailand 10900*

^d*Department of Biology, Faculty of Science and Technology, Suan Sunandha Rajabhat University Thailand 10300*

**e-mail: issara@nanotec.or.th, satita@nanotec.or.th*

Giant river prawn is one of the most valuable commercial aquatic species in Thailand. It shows a sexually dimorphic growth pattern where males grow much faster and consequently reach a larger size at harvest than females. Therefore, all-male cultures significantly give more profitable to farmers than either all-female or mixed cultures. Androgenic glands are male-specific tissues and able to induce male differentiation in several crustaceans, including giant river prawn. Here, we constructed an expression plasmid to express proteins from the androgenic glands. The protein expression was optimized and purified by Ni²⁺ affinity chromatography. The purified protein fractions were pooled and dialysed in 1XPBS, pH7.2. The dialysed proteins were quantified by Bradford method and characterized by Western blot. Furthermore, the proteins were encapsulated in phospholipids. Size, shape and charge of encapsulated proteins were determined by dynamic light scattering and TEM. The encapsulated proteins will be further used to produce all-male population of the prawn.

Keywords: Androgenic gland, All-male culture, Encapsulation, Giant river prawn

Formulation and in vitro Evaluation of Bile Salt-Based NPs for Controlled Release of Essential Oils in Gastrointestinal Tract

Somrudee Keawmarun^a, Mattaka Khongkow^a, Teerapong Yata^a, and Katawut Namdee^{a*}

^aNational Nanotechnology Centre (NANOTEC), National Science and Technology Development Agency, 111 Thailand Science Park, Paholyothin Rd., Klong Luang, Pathumthani, 12120, Thailand

**e-mail: katawut@nanotec.or.th*

The essential oils (EOs) of thyme (*Thymus vulgaris* L.) and bark of cinnamon (*Cinnamomum zeylanicum*) have been widely used for medical purposes with their antioxidants and antibacterial properties. Consumption of EOs has been used as a food supplement to improve human gut health without using any anti-biotics. However, stabilities and properties of these EOs have been shown to diminish due to a severe condition of our gastrointestinal tract. In order to improve these benefit of EOs, nanoencapsulation for oral delivery should be applied. Nanotechnology such as nanoemulsion (NE) has been implicated as a drug delivery system for pharmaceuticals and been reported as a suitable system for EO encapsulation.

In this research, we formulated and characterized nanoemulsion containing combined cinnamon and Thyme essential oils with natural inspired surfactant, bile salts. These included an investigation of nanoparticles stability and their ability to tolerate the acid-base conditions in the GI tract. The properties of potential antimicrobial activity of these NEs were also evaluated using agar dilution method.

We found that, the obtained NEs were approximately 100-150 nm in size with 0.2 in PDI. An addition of bile salts into NE formulation was able to increase these essential oil stabilities in GI tract compared to NE without bile salt formula. Finally, NE containing essential oils were further validated for their antibacterial activities against gastrointestinal microorganisms. The minimum bactericidal concentration (MBC) of Thyme oil and cinnamon oil was approximately 0.25-0.5 mg/ml. Together, all of these results suggest that the use of bile salts in the combination of nanoencapsulation could potentially enhance functions and improve stabilities of essential oils using for oral administrating applications.

Keywords: Essential oils, Nanoemulsion, Bile salt, Surfactant, Anti-biotics

Stability of Curcumin Loaded Nanoparticles Compared to Nanoemulsions under Thermal Processing and Storage Conditions

Thanida Chuacharoen*

Faculty of Science and Technology, Suan Sunandha Rajabhat University,

1 U Thong Nok Rd, Dusit, Bangkok 10300, Thailand

**e-mail: thanida.ch@ssru.ac.th_*

To date, curcumin loaded nano-formulations: nanoemulsions and nanoparticles have been proposed for food uses with the purpose of improving physiological characteristics and enhancing stability. The comparative effect between nanoemulsions and nanoparticles on preventing the deterioration of curcumin from processing conditions and storage with food matrix, which causes physical and chemical stability changes of nanocarriers is lacking in the literature and is addressed in this study. Curcumin loaded nanoemulsions (Cur-NE) and nanoparticles (Cur-NP) stabilized with a combined lecithin and Tween 80 were synthesized at the same level of surfactant concentration (Figure 1). Both systems were subjected to thermal processing conditions (63°C for 30 min referred as pasteurization and 95°C for 10 min referred as sterilization) and stored at 4°C and room temperature for 15 days to investigate the physical and chemical stabilities of two nanocarriers relevant to commercial applications. Results showed that nanoparticles protected curcumin against degradation better under thermal treatments, while the surface charge of nanoemulsion system dramatically decreased under thermal conditions. The effect of nanoparticles on curcumin stability was less pronounced after 15 days of storage compared with the nanoemulsion systems. In the presence of milk, nanoemulsions and nanoparticles had the potential to inhibit lipid oxidation, as indicated by an antioxidant activity and an insignificant color change of the fortified milk was found after storage for 5 days. This study provides insights which can help decide the use of nanoparticles or nanoemulsions suitable for delivering of curcumin as a food additive in different commercial food products.

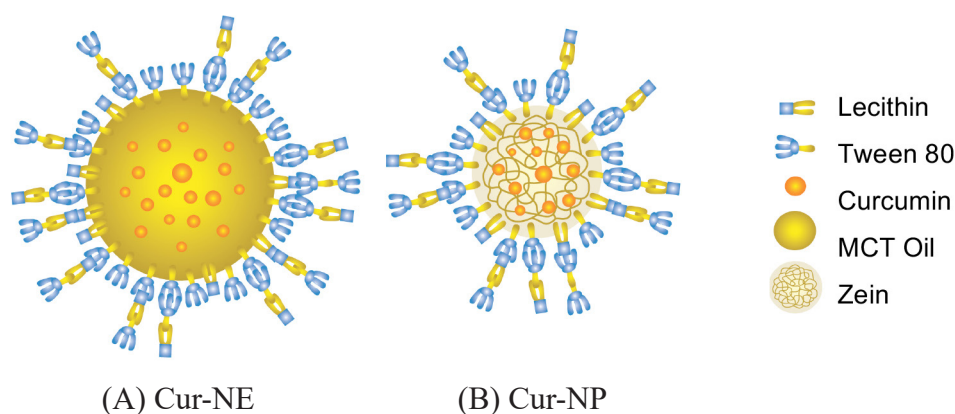


Figure 1. Schematic structures of (A) curcumin-loaded nanoemulsion (Cur-NE) and (B) curcumin-loaded zein nanoparticle (Cur-NP): interaction among surfactants, core materials, and curcumin compounds

Keywords: Curcumin, Nanoemulsions, Nanoparticles, Functionality, Stability

Colorimetric Sensor for Shrimp Spoilage

Thanawan Nitikriengkrai^a, Radchada Buntam^{a*}, Suchanan Leelahawong^b, Pakin Wonglohaphan^b, Wisarut Nitiruangjaras^b, Chatuporn Sawatruksa^b

^aDepartment of Chemistry, Faculty of Science, Silpakorn University, Nakhon Pathom 73000, Thailand.

^bDepartment of Chemistry, Mahidol Wittayanusorn School, Nakhon Pathom 73170, Thailand.

*e-mail: radchadab@yahoo.com

Freshness is one of the main quality concerns for shrimp, fish and meat processing, marketing and consumption. Among these, shrimp is the most favored among the consumers even its short shelf life. The shrimp spoilage produces a very unpleasant odor composed of a variety of volatile amines and some other compounds including hydrogen sulfide. The key to monitor the spoilage is to detect the volatile amines. Combining Cu^{2+} , an effective amine binder, with chitosan was attempted as an optical sensor for shrimp spoilage. Various film fabrications were performed by mixing 25 mL of chitosan solution in 3% (w/v) acetic acid solution with 15 mL of 0.050 M copper(II) chloride solution. The mixture was stirred to obtain the clear solution, subsequently poured into petri dish and dried to yield a green transparent and smooth film. The film was preliminarily tested against the gaseous ammonia. The film color changed from green to blue. The visible absorption of the films before and after ammonia adsorption was recorded. The maximum absorption of the film before and after ammonia adsorption was observed at 814 and 624 nm respectively. This blue shift corresponds to the larger crystal field splitting of the copper ammine complex. The film was applied to detect the shrimp freshness. 80 g of adult brackish water shrimp was placed in each of six plastic boxes (11.5 cm (w) x 11.5 cm (l) x 6.8 cm (h)) with two films attached to each lid. The shrimps and films were kept in closed boxes at room temperature. Two films from each box were taken for visible absorption analyses at different time interval: 4, 8, 12, 16, 20, 24 hours. After 8 hours, the blue color appeared at the edge of the film indicating the appearance of amine from the shrimp spoilage. The black color of sulfide complex of copper appeared after the films were kept in shrimp box for 16 hours. However, the black color disappeared after the films were left in the open air for a few hours due to the weak binding between H_2S and Cu^{2+} . The maximum absorption at 625 nm was observed for the films after being left in the box for 24 hours.

Keywords: Chitosan film, Amine sensor, Shrimp spoilage

References

1. R. Grau, A. J. Sánchez, J. Girón, E. Iborra, A. Fuentes and J. M. Barat, *Food Res. Int.* **2011**, *44*, 331-337.
2. M. K. Morsy, et al, *Food Control* **2016**, *60*, 346-352.
3. X. Huang, J. Xin, J. Zhao, *J. Food Eng.* **2011**, *105*, 632-637.

Development of Mucoadhesive Nanovaccine Against *Flavobacterium Columnare* for Immersion Vaccination in Farmed Tilapia

Sirikorn Kitiyodom¹, Suvimol Surassmo², Katawut Namdee², Kunat Sukthum², Channarong Rodkhum³, Noppadon Pirarat¹ and Teerapong. Yata^{2*}

¹Wildlife Exotic and Aquatic Pathology-Special Task Force for Activating Research, Department of Pathology, Faculty of Veterinary Science, Chulalongkorn University, Bangkok 10330, Thailand,

²National Nanotechnology Center, Pathum Thani 12120, Thailand and ³Department of Microbiology, Faculty of Veterinary Science, Chulalongkorn University, Bangkok 10330, Thailand

*e-mail: nopadonpirarat@gmail.com, teerapong@nanotec.or.th

Tilapia (*Oreochromis niloticus*) has become one of the most important fish in aquaculture. Bacterial infection caused by *Flavobacterium columnare*, the causative agent of columnaris disease, has been now identified as one of the most serious infectious diseases in farmed tilapia and cause major financial damage to the producers of tilapia fish. Among the effective prevention and control strategies, vaccination is one of the most effective approach. As the surface of living fish is covered by mucus and directly associated with the mucosal immunity, we therefore hypothesized that the efficacy of killed vaccines could be enhanced by nanoencapsulation technology in combination with incorporation of mucoadhesive characteristic. In this study, we prepared chitosan-complexed nanovaccines through emulsification and homogenization techniques followed by coating with mucoadhesive polymer chitosan. The physiochemical properties of chitosan-complexed nanovaccine were analyzed, and their mucoadhesive characteristics and immune response against model antigen were also evaluated. The analysis of hydrodynamic diameter and zeta-potential also suggested the successful modification of nanovaccines by chitosan. The chitosan modified nanovaccines were positively charged and the overall diameter also increased. The prepared vaccines were nano-sized and spherical as confirmed by transmission electron microscopy (TEM). *In vivo* mucoadhesive study demonstrated the excellent affinity of the chitosan-complexed nanovaccines toward fish gills as confirmed by bioluminescence imaging, fluorescent microscopy, and spectrophotometric quantitative measurement. Following vaccination with the prepared nanovaccines by immersion 30 mins, the challenge test was then carried out 60 days post-vaccination and resulted in 90% mortalities in the control. The relative per cent survival (RPS) of vaccinated fish was calculated at 89 for mucoadhesive nanovaccine. Our results also suggested that uncomplexed nanovaccines failed to protect fishes from columnaris infection, which is consistent with the mucoadhesive assays showing that naked vaccines were unable to bind to mucosal surfaces. In conclusion, we could use this system to deliver antigen preparation to the mucosal membrane of tilapia fishes and obtained a significant increase in survival compared to controls, suggesting that targeting mucoadhesive nanovaccines to the mucosal surface could be exploited as an effective method for immersion vaccination. This research is supported by Thailand Graduate Institute of Science and Technology Scholarship, NSTDA research grant SCA-CO-2560-4578-TH.

Keywords: immersion vaccination, chitosan, Columnaris disease, tilapia.

The Cinnamon Oil Nanoparticles in pH-responsive Microsphere as an Antibiotic Alternative Against Food-borne Pathogens

Naiyaphat Nittayasut¹, Katawut Namdee¹, Mattaka Khongkow¹, Nararat Kotcharat¹, Jakarwan Yostawonkul¹, Suwimon Boonrungsiman¹, Suvimol Surassmo¹, Sasithon Temisak² and Teerapong Yata^{1,*}

¹National Nanotechnology Centre (NANOTEC), National Science and Technology Development Agency, Pathum Thani 12120, Thailand

²Bio Analysis Group, Chemical Metrology and Biometry Department, National Institute of Metrology (NIMT), Pathumthani, Thailand

*e-mail: teerapong@nanotec.or.th

Cinnamon essential oil exhibits strong *in vitro* antimicrobial activity against several common bacterial foodborne pathogens; however, oral administration of essential oils has limited practicality due to their high volatility, odor, fast decomposition, and poor bioavailability in the lower intestines. The main objective of this study was to develop a method for targeted delivery and sustained release of essential oils in the gastrointestinal tract by using a double encapsulation system. Cinnamon oil was used as a model essential oil to prepare nanoparticle via the phase inversion composition technique (low energy method). The prepared nanoparticles were then encapsulated in microparticles using alginate-calcium chloride system. The obtained particles were designed as cinnamon oil nanoparticle-in-microspheres. Their stability was investigated in simulated gastrointestinal fluid. The particles were also physicochemically characterized and biologically evaluated as an antibacterial agent against food-borne pathogens. Our results showed that under simulated gastrointestinal conditions, the cinnamon oil nanoparticle-encapsulated microparticles exhibited good gastric resistance and sustained release in intestinal fluids. They also exhibited good anti-bacterial activity against important food-borne pathogens namely, *Escherichia coli* O157:H7, *Pseudomonas aeruginosa*, *Salmonella typhi*, *Salmonella enterica*, *Staphylococcus aureus*, and *Vibrio cholerae*. *V. cholera* was shown to be more sensitive to microbeads as determined from minimum Bactericidal Concentrations (MBC) amounting to 25 mg/mL of microbeads, as compared to the corresponding values of 62.5 determined for *E. coli* O157:H7 and *P. aeruginosa*. In conclusion, the innovation as presented here is an improved version of cinnamon oil encapsulated in the nanoparticle-in-microsphere which serves as a promising candidate as an anti-bacterial agent for decontamination of food-borne pathogens in the gastrointestinal tract.

Keywords: essential oils, controlled release, nanotechnology, microencapsulation and antimicrobials

Synthesis of Poly(aryleneethynylene)s Using Palladium Supported on Calcium Carbonate as Heterogeneous Catalyst

Nopparat Thavornsin^a, Paitoon Rashatasakhon^a, Mongkol Sukwattanasinitt^a and Sumrit Wacharasindhu^{*a}

^aNanotec-CU Center of Excellence on Food and Agriculture, Department of Chemistry, Faculty of Science, Chulalongkorn University, Bangkok 10330, Thailand.

*e-mail: sumrit.w@chula.ac.th

An inexpensive and commercially available heterogeneous catalyst palladium supported on calcium carbonate (Pd/CaCO₃) is used for the synthesis of poly(aryleneethynylene)s (PAE)s having low metal contamination via Sonogashira coupling polymerization. The optimized condition investigation reveals that the use of 10 mol% of Pd/CaCO₃ together with commercially available and inexpensive reagents can catalyze C-C coupling polymerization between aryldiethyne and a variety of aryl diiodides/dibromides at 80 °C to provide corresponding PAEs in excellent yields (79-100%). A panel of PAEs is generated with high molecular weight (M_w) ranging from 6.1 to 44.2 kDa along with polydispersity index (PDI) varying from 1.5 to 3.8. The catalytic activity of our Pd/CaCO₃ was compared with classical heterogeneous, Pd/C and homogeneous catalyst Pd(PPh₃)₄. The results show comparable catalytic activity in term of turn over number (TON). Importantly, resulting polymer from Pd/CaCO₃ catalyzed reaction exhibits much less Pd and Cu contamination (1.9 and 3.4 ppm, respectively) in comparison to products from Pd/C and homogeneous catalyst Pd(PPh₃)₄ catalyzed reaction.

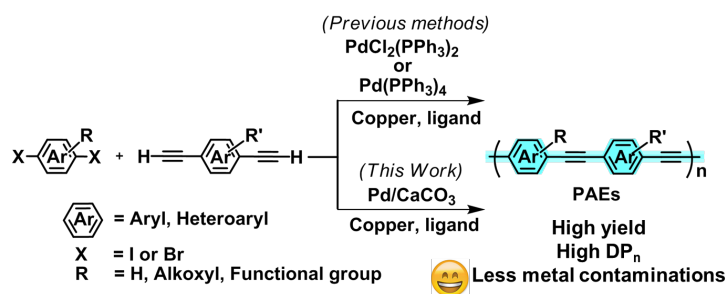


Figure 1: Synthetic methods for PAEs

Keywords: Poly(aryleneethynylene)s, Heterogeneous catalyst, Sonogashira coupling, Metal contamination

References

1. L. Yin and J. Liebscher, *Chem. Rev.*, **2007**, *107*, 133-173.
2. T. Saetan, C. Lertvachirapaiboon, S. Ekgasit, M. Sukwattanasinitt and S. Wacharasindhu, *Chem. Asian J.*, **2017**, *12*, 2221-2230.
3. N. Thavornsin, M. Sukwattanasinitt, S. Wacharasindhu, *Polym. Chem.*, **2014**, *5(1)*, 48-52.

The Catalyzing the Catalytic Hydrogen Transfer of Furfural to Furfuryl Alcohol over Lewis Acid Beta Zeolite

Anittha Prasertsab^a, Thana Maihom^{b*}, Bundet Boekfa^c and Piti Treesukol^d

^a Department of Chemistry, Faculty of Liberal Arts and Science, Kasetsart University, Kamphaeng Saen Campus, Nakhon Pathom 73140, Thailand

*e-mail: faastnm@ku.ac.th

The conversion of furfural to furfuryl alcohol via the catalytic hydrogen transfer (CTH) over alkali and alkali earth exchanged Lewis acid BEA zeolites had been investigated by using density functional calculations. The reaction mechanism proceeded in 3 steps, (I) the dissociation OH bond of *i*-propanol, (II) the hydrogen transfer from *i*-propanol to furfural carbonyl carbon and (II) production of furfuryl alcohol. The calculation results showed that the second step was a rate-determining step. The Zr-BEA was more efficient for catalyzing the studied reaction than Sn-BEA one based on the activation barrier and the reaction rate. Moreover, we also found that the catalytic activity of various cation-exchanged Zr-BEA zeolite was in a sequence of Mg > Ca > Be > Li > Na > K.

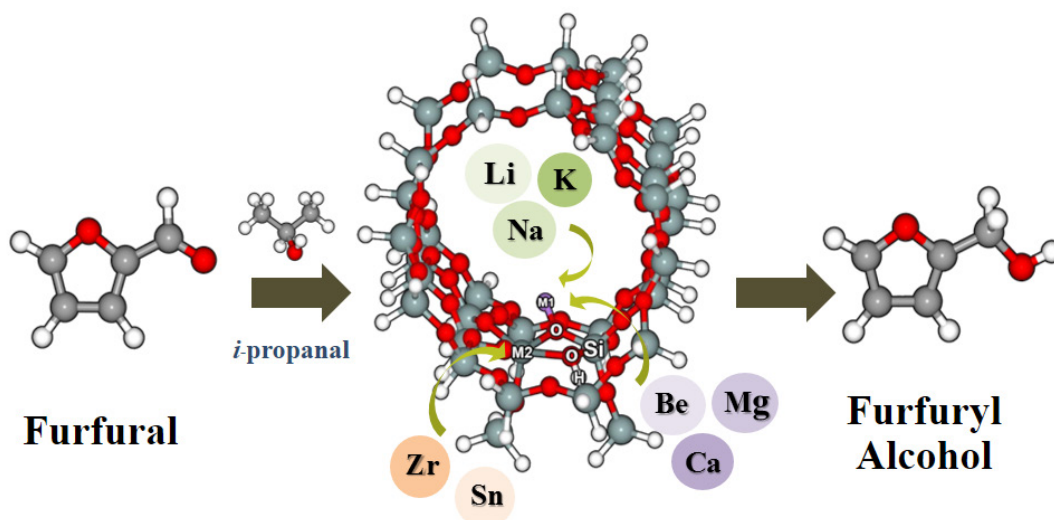


Figure 1. Pathway of the conversion furfural to furfuryl alcohol via CTH reaction

Keywords: Furfural, Furfuryl Alcohol, Catalytic hydrogen transfer (CTH), Zeolites

References

1. Prasertsab, A., Maihom, T., Probst, M., Wattanakit, C., and Limtrakul, J., *Inorg Chem*, **2018**, *57*, 6599-6605.
2. Koehle, M., and Lobo, R. F., *Catal. Sci. Technol.*, **2016**, *6*, 3018-3026.

Synthesis of Bagasse Ash-Derived Silica-Aluminosilicate Composite for Methanol Adsorption

Preeyaporn Ruengrung^a, Pasitchote Jongkraivut^a, Waleeporn Donphai^{a,b}, and Metta Chareonpanich^{a,b,*}

^a*KU-Green Catalysts Group, Department of Chemical Engineering, Faculty of Engineering, Kasetsart University, Bangkok 10900, Thailand*

^b*Nanocatalysts and Nanomaterials for Sustainable Energy and Environment Research Network of NANOTEC, Kasetsart University, Bangkok 10900, Thailand*

*e-mail: fengmic@ku.ac.th

This work aimed to study the syntheses of Al-MCM-41 (with template), silica-aluminosilicate (without template) and ZSM-5 zeolite by using bagasse ash as a silica source. These adsorbents were applied for methanol adsorption abilities. The adsorption conditions were as follows: adsorption temperature, 40 °C; operating pressure, 1 bar; carrier gas, N₂; and total gas flow rate, 30 ml/min. It was found that ZSM-5 zeolite exhibited the excellent methanol adsorption ability. The maximum methanol adsorption capacity of ZSM-5 zeolite obtained from the breakthrough curve was 1.3 and 1.8 times higher than those of Al-MCM-41 (with template) and silica-aluminosilicate (without template), respectively. Morphology and breakthrough curve of ZSM-5 zeolite were shown in figure 1. From this work, it can be concluded that ZSM-5 zeolite shows the excellent performance in methanol adsorption due to its higher specific surface area, micropore volume and proper pore characteristics compared to those of Al-MCM-41 (with template) and silica-aluminosilicate (without template). Based on the monetary unit, silica-aluminosilicate (without template) composite showed an outstanding potential as a low-cost solid waste-derived adsorbent compared to those of Al-MCM-41 (with template) and ZSM-5 zeolite.

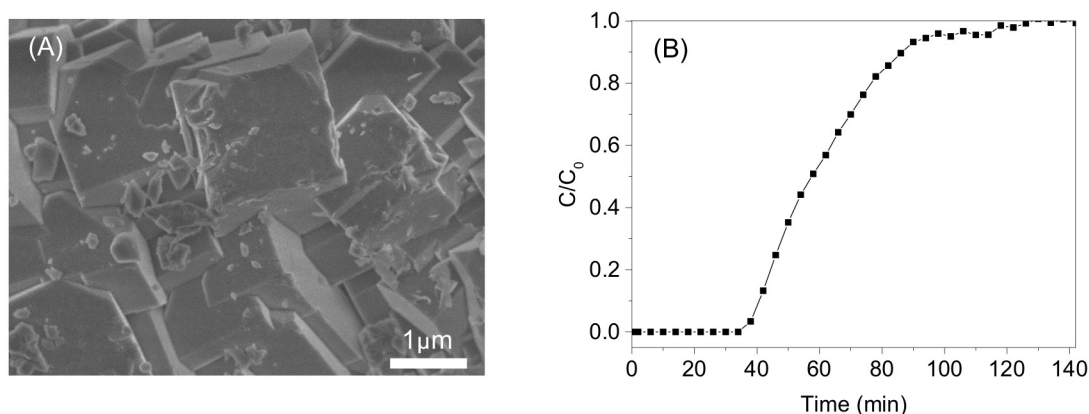


Figure 1. (A) SEM of ZSM-5 zeolite, and (B) breakthrough curve for methanol adsorption on ZSM-5 zeolite.

Keywords: Adsorption, Methanol, ZSM-5, Silica-aluminosilicate

References

1. C. Sriakkarin, W. Umchoo, W. Donphai, Y. Poo-arporn, and M. Chareonpanich, *Catalysis Today. Sustainable production of methanol from CO₂ over 10Cu-10-Fe/ZSM-5 catalyst in a magnetic field-assisted packed bed reactor.* **2018**, 314, 114-121.

Synthesis of Silica-aluminosilicate as a Support from Bagasse Ash

Orrakanya Phichairatanaphong^a, Patsara Trumpangparn^a, Metta Chareonpanich^{a,b} and Waleeporn Donphai^{a,b,*}
^{a,b,*}*KU-Green Catalysts Group, Department of Chemical Engineering, Faculty of Engineering, Kasetsart University, Bangkok 10900, Thailand*

^b*Nanocatalysts and Nanomaterials for Sustainable Energy and Environment Research Network of NANOTECH, Kasetsart University, Bangkok 10900, Thailand*

**e-mail: fengwod@ku.ac.th*

Thailand is an agricultural country, a lot of wastes are produced from agricultural industrial process. The utilization of waste has been a good concept for both the environment and economy. Bagasse ash is a biowaste produced from sugar industrial process which is one of the important industries in Thailand. In this research, bagasse ash was used as a raw material for mesoporous silica-aluminosilicate synthesis because of its high silica content. The method of silica extraction in form of sodium silicate and the synthesis conditions with different $\text{SiO}_2/\text{Al}_2\text{O}_3$ ratios (∞ , 7.5, 10, 15, 20) were investigated. For the silica extraction method, the extraction processes were compared between the fusion with sodium carbonate and the alkali fusion method. After this process, sodium silicate was used as a silica source for mesoporous silica-aluminosilicate synthesis via sol-gel method. As the results, the fusion with sodium carbonate method at 850°C gave the highest efficiency of silica extraction which was 94.66%. For mesoporous silica-aluminosilicate synthesis with different $\text{SiO}_2/\text{Al}_2\text{O}_3$ ratios, it was found that in the case of without alumina, the silica had a hexagonal structure and the highest surface area. When alumina was added into the framework, the hexagonal structure was destroyed and the surface area of samples were decreased, as shown in Figure 1.

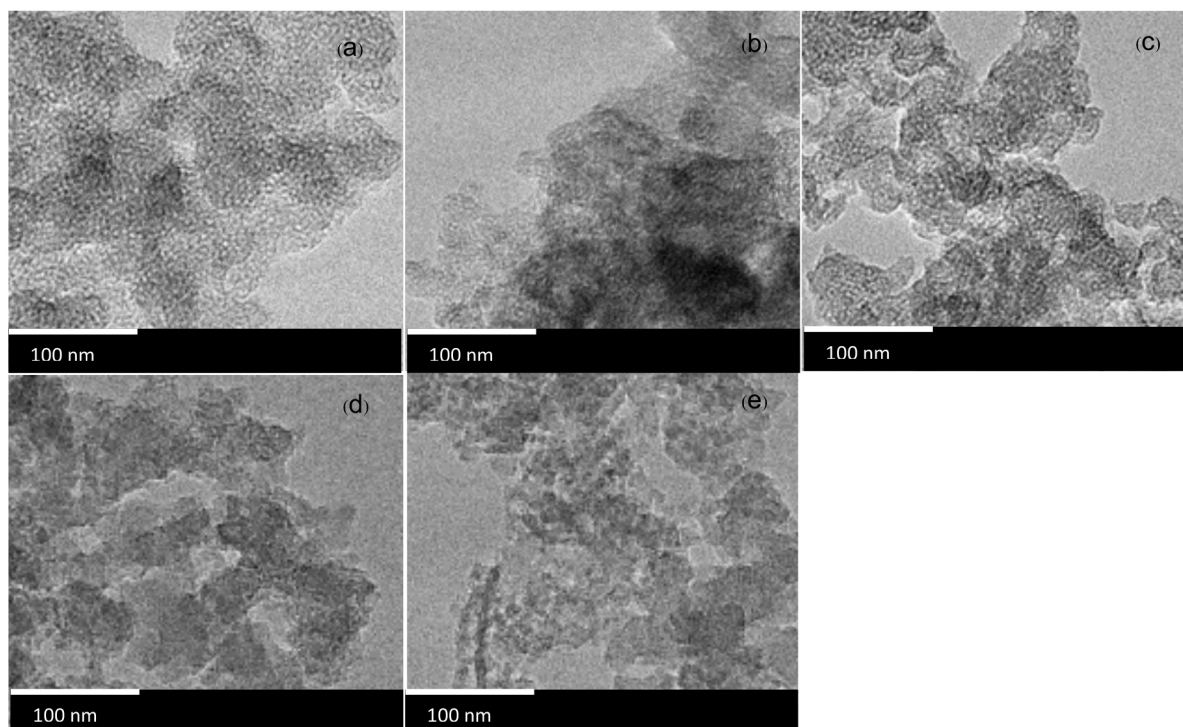


Figure 1. TEM images of mesoporous silica-aluminosilicate with different $\text{SiO}_2/\text{Al}_2\text{O}_3$ ratios (a) ∞ , (b) 20, (c) 15, (d) 10 and (e) 7.5.

Keywords: Bagasse Ash, Sodium Carbonate, Sodium Silicate, Silica-Aluminosilicate

References

1. N. Nazriati, H. Setyawan, S. Affandi, M. Yuwana, S. Winardi, *Journal of Non-Crystalline Solids*. **2014**, *400*, 6–11.

Highly Efficient Metals-Modified Hierarchical MFI Zeolite for Selective Oxidation of Alcohols

Marisa Ketkaew^a, Duangkamon Suttipat^a, Wannaruedee Wannapakdee^a, Pannida Dugkhuntod^a, Kachaporn Saenluang^a, Pinit Kidkhunthod^b and Chularat Wattanakit^{a,*}

^aDepartment of Chemical and Biomolecular Engineering, School of Energy Science and Engineering, Institute of Science and Technology, Rayong, 21210, Thailand

^bSynchrotron Light Research Institute (Public Organization), 111 University Avenue, Muang District, Nakhon Ratchasima, 30000 Thailand

*e-mail: Chularat.w@vistec.ac.th

The selective oxidation of alcohols to aldehydes is of great importance for the organic synthesis in both academic and industrial issues. Among them, aromatic aldehydes are important intermediates for the preparation of various fine chemicals, therefore, their effective production has been widely investigated. The liquid phase oxidation of benzyl alcohol to benzaldehyde was chosen as a model reaction to study the catalytic performances of Pt supported on zeolite nanosheets catalysts¹ due to various potential applications of benzaldehyde ranging from cosmetics, perfumery, food, dye stuff, agrochemical to pharmaceutical industries². Owing to cost effectiveness and environmental concerns, a molecular oxygen and cerium oxide or ceria (CeO_2) were used as an oxidant and oxygen carrier in the reaction, respectively. The effect of CeO_2 which could accelerate the mobility of lattice oxygen on the catalytic performance has been systematically investigated. Interestingly, the synergic effect of Pt and CeO_2 can greatly enhance the catalytic performances. Benzaldehyde yield almost 100 % can be achieved over the Pt supported on CeO_2 -zeolite nanosheets, whereas the yield of benzaldehyde obtained from the conventional catalyst was less than 40 %. The zeolite nanosheets not only can increase the fraction of exposed active sites because of its unique high surface area that can prevent the aggregation of Pt and CeO_2 nanoparticles, but also affect the oxidation state of CeO_2 . The presence of high content of trivalent Ce compound (Ce^{3+}) on zeolite nanosheets benefits to the oxidation reaction³. Furthermore, the tunable Si to Al ratio of zeolite catalysts can also significantly improve the catalytic performance, leading to the reduction of the Pt nanoparticles size, due to the improved relative strength of interactions of the Pt precursor and the support⁴.

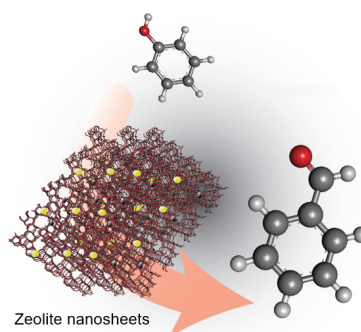


Figure 1. Schematic illustration of selective oxidation of benzyl alcohol to benzaldehyde.

Keywords : Selective Oxidation of Alcohol, Zeolite Nanosheets, Benzyl alcohol to Benzaldehyde.

References

1. W. Wannapakdee, C. Wattanakit, V. Paluka, T. Yutthalekha and J. Limtrakul, *RSC Advances* **2016**, *6*, 2875-2881.
2. R. Marotta, I. Di Somma, D. Spasiano, R. Andreozzi and V. Caprio, *Chemical engineering journal* **2011**, *172*, 243-249.
3. A. Makdee, P. Unwiset, K. C. Chanapattharapol and P. Kidkhunthod, *Materials Chemistry and Physics* **2018**, *213*, 431-443.
4. J. Chen, Q. Zhang, Y. Wang and H. Wan, *Advanced Synthesis & Catalysis* **2008**, *350*, 453-464.

Bimetallic Pt-Ru over Hierarchical H-ZSM5 Nanosheets for Mild Hydrodeoxygenation (HDO) of Lignin-Derived Compounds

S. Salakhum,^a T. Yutthalekha,^a S. Shetsiri, and C. Wattanakit^{a,*}

^a Department of Chemical and Biomolecular Engineering, School of Energy Science and Engineering, Vidyasirimedhi Institute of Science and Technology, Rayong, 21210, Thailand

*e-mail: chularat.w@vistec.ac.th

The demand of energy usage has been increasing dramatically. A lot of effort has been put into finding a sustainably renewable energy. One of the most promising alternative and renewable energies such as bio-oils, which can be obtained from pyrolysis of lignocellulosic biomass, has become greatly interesting. However, bio-oils cannot be used as fuels directly because of its poor quality such as low heating value, high corrosive, high viscosity and low stability. This behavior relates to the presence of high level of oxygenate compounds in bio-oils.¹ In order to use the bio-oils as fuels, oxygen need to be removed. Hydrodeoxygenation (HDO) is one of the most important processes for the bio-oil upgrading due to the removal of oxygen content.² However, this process has been successfully operated under high H₂ pressures (4–5 MPa).³ Therefore, the development of catalysts for the HDO of lignin-derived compounds operated under mild conditions is still a great challenge.⁴ In the present study, we report the hydrodeoxygenation of 4-propylphenol as a model bio-oil compound. The reaction was operated at mild condition (383 K at 1 atm). The ratio between the noble metals (Pt/Ru ratio), Si/Al ratio of zeolite, as well as the hierarchical porous system were also systematically investigated. The results show that the bimetallic Pt-Ru/HZSM-5 nanosheets exhibited a very high yield of cyclohexane (100 %). The reason of the high activity relates to the synergistic effect of bimetallic and hierarchical structures. The hierarchical structure not only provides the improvement of the diffusion limitation of bulky molecules but also enhances the dispersion of small bimetallic nanoparticles on zeolite supports.

Keywords: Bio-oil Upgrading, Hydrodeoxygenation, Bimetallic Pt-Ru, Hierarchical Structure

References

1. L. Wang, J. Zhang, X. Yi, A. Zheng, F. Deng, C. Chen, Y. Ji, F. Liu, X. Meng and F.-S. Xiao, *ACS Catal.*, 2015, **5**, 2727-2734.
2. Y. Wang, J. Wu and S. Wang, *RSC Adv.*, 2013, **3**, 12635-12640.
3. H. W. Lee, S. H. Park, J.-K. Jeon, R. Ryoo, W. Kim, D. J. Suh and Y.-K. Park, *Catal. Today*, 2014, **232**, 119-126.
4. Ohta, H.; Yamamoto, K.; Hayashi, M.; Hamasaka, G.; Uozumi, Y.; Watanabe, Y., *ChemComm.* **2015**, *51* (95), 17000-17003.

Hydrogenation of CO₂ to Methanol Using Atomically Precise Ruthenium-Gold Containing Cluster Deposited on TiO₂

Siriluck Tesana^{a,b}, Alex Yip^c, Vaibhav Bhugra^{b,d}, Thomas Nann^{b,d},
Chris Ridings^e, Gunther Andersson^c and Vladimir Golovko^{a,b,*}

^a School of Physical and Chemical Sciences, University of Canterbury, New Zealand.

^b The MacDiarmid Institute for Advanced Materials and Nanotechnology, Wellington, New Zealand.

^c Department of Chemical and Process Engineering, University of Canterbury, New Zealand.

^d School of Chemical and Physical Sciences, Victoria University of Wellington, New Zealand.

^e Flinders Centre for Nanoscale Science and Technology, Flinders University, Adelaide, Australia.

*e-mail: vladimir.golovko@canterbury.ac.nz

Due to the significant increase in worldwide CO₂ emissions, the transformation of CO₂ into value-added products (methanol *etc.*) has attracted considerable attention over the past decades.¹ The challenge in CO₂ conversion is the high thermodynamic stability of CO₂ leading to the high energy barrier for breaking the C=O bond.² In this work, the hydrogenation of CO₂ catalysed by bimetallic cluster Ru₃AuPPh₃Cl(CO)₁₀ supported on TiO₂ was studied for the first time. The successful deposition of the clusters on TiO₂ was confirmed using diffuse reflectance UV-vis spectroscopy, microwave plasma atomic emission spectrometry and X-ray photoelectron spectroscopy. The catalytic test was carried out in a liquid phase in a batch Parr reactor under moderate conditions (185°C, 19 hr) in the presence of CO₂ (30 bar) and H₂ (10 bar). The weight % of metal loading was varied from 0.08 wt% to 5.0 wt%. The partial removal of protecting ligands after cluster deposition achieved via calcination (200°C under vacuum for 2 hr) allowed a better access to metal active sites resulting in higher activity. The catalyst exhibited the superior catalytic activity in CO₂ hydrogenation to methanol compared to other catalysts reported in the literature.³ The crystal structures of the cluster used in this work are shown in **Figure 1**.



Figure 1. Crystal structure of Ru₃AuPPh₃Cl(CO)₁₀ cluster.

Keywords: Ruthenium-Gold Cluster, Atomically Precise, TiO₂, CO₂ Hydrogenation

References

1. S.G. Jadhav, P.D. Vaidya, B.M. Bhanage, J.B. Joshi, *Chem. Eng. Res. Des.* **2014**, *92*, 2557-2567.
2. A. Vourros, I. Garagounis, V. Kyriakou, S.A.C. Carabineiro, F.J. Maldonado-Hódar, G.E. Marnellos, M. Konsolakis, *J. CO₂ Util.* **2017**, *19*, 247-256.
3. M. D. Porosoff, B. Yan, J. G. Chen, *Energy Environ. Sci.* **2016**, *9*, 62-73.

Pd Nanoparticles Immobilized on Individual Calcium Carbonate Plate Derived from Mussel Shell Waste: An Eco-Friendly Catalyst for Copper-Free Sonogashira and Suzuki Coupling Reactions

Trin Saetan^a, Sukumaporn Chotnitikornkun^a, Chutiparn Lertvachirapaiboon^b, Sanong Ekgasit^b, Mongkol Sukwattanasinitt^a, and Sumrit Wacharasindhu^{*a}

^aNanotec-CU Center of Excellence on Food and Agriculture, Department of Chemistry, Faculty of Science, Chulalongkorn University, Bangkok 10330, Thailand

^bDepartment of Chemistry, Faculty of Science, Chulalongkorn University, Bangkok 10330, Thailand

*e-mail: of the Sumrit.w@chula.ac.th

In this work, Asian green mussel shell waste (*Perna viridis*) is disintegrated into individual calcium carbonate plates (ICCPs). ICCPs is used as a supporting material for a heterogeneous palladium catalyst. Palladium nanoparticles (3–6 nm) are deposited with good dispersion on the ICCP surface, as shown in X-ray diffraction and scanning electron microscopy results. The catalytic performances of the Pd/ICCP was explored for copper-free Sonogashira and Suzuki coupling reactions under green reaction conditions. The Sonogashira cross-coupling reaction took place successfully for the cross-coupling of various aryl iodide and phenyl acetylene with K_2CO_3 as base, ethanol as solvent and good reusability during 3 cycles. In the case of Suzuki coupling reaction, using potassium carbonate in aqueous solvent in the presence of 2 mol% of Pd/ICCP at 40 °C can catalyse the Suzuki cross-coupling reaction between aryl bromides and iodides with various electron-donating and electron-withdrawing groups to couple with arylboronic acid to give coupling products in good to excellent isolated yields without remaining starting materials. Moreover, the prepared Pd/ICCP catalyst also could be reused up to seven times with NMR yield more than 85% with a little Pd metal leaching content. The main features of this prepared catalyst consist of abundant, inexpensive and green catalytic support, no using external ligand in the reaction condition as well as its high reusability.

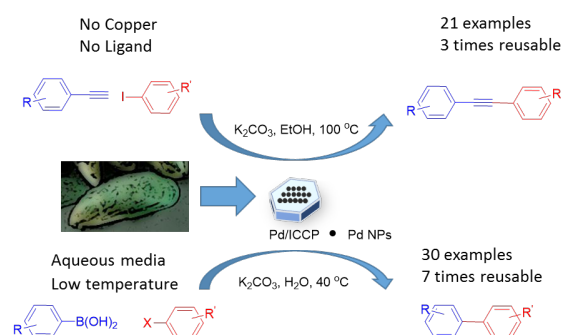


Figure 1. Graphical abstract

Keywords: Mussel shell, Pd/ICCP, Heterogeneous catalyst, Sonogashira reaction, Suzuki reaction.

References

1. C. Lertvachirapaiboon, T. Jirapisitkul, P. Pienpinijtham, K. Wongravee, C. Thammacharoen, S. Ekgasit, *J Mater Sci* **2014**, *49*, 6282-6289.
2. T. Saetan, C. Lertvachirapaiboon, S. Ekgasit, M. Sukwattanasinitt, S. Wacharasindhu, *Chemistry – An Asian Journal* **2017**, *12*, 2221-2230.

Color Tuning in Two Series of Lanthanide Coordination Polymers Base on Hydrazide Ligand

Chatphorn Theppitak^a, Winya Dungkeaw^b Filip Kielar^c and Kittipong Chainok^{d*}

^a *Division of Chemistry, Faculty of Science and Technology, Thammasat University, Thailand*

^b *Department of Chemistry, Faculty of Science, Maharakham University, Thailand*

^c *Department of Chemistry, Faculty of Science, Naresuan University, Thailand*

^d *Materials and Textile Technology, Faculty of Science and Technology, Thammasat University, Thailand*

**e-mail: kc@tu.ac.th*

Two novel series of one-dimensional lanthanide coordination polymers $[\text{Ln}(\text{Bz})_3(\text{Bzz})(\text{H}_2\text{O})] \cdot \text{H}_2\text{O}$ (**1Ln**; Ln = Pr, Nd, Sm, Eu, Gd, Tb, Dy, Er; Bz = benzoate; Bzz = benzohydrazide) and $[\text{Ln}_3(\text{Bz})_9]$ (**2Ln**; Ln = Eu, Tb, Dy, Er), were synthesized and characterized by single crystal X-ray diffraction to determine their structure. Polymer **1Ln** crystallizes in a monoclinic space group $P2_1/c$ and displays a 1D chain structure in which the Bz ligand acts as monodentate and bridging ligand to coordinate with Ln(III) ions, while the Bzz ligand adopts only a bidentate chelating ligand through the carbonyl oxygen atom and one hydrazide nitrogen atom. Each 1D chain is connected by water of crystallization through intermolecular $\text{N}-\text{H} \cdots \text{O}$ and $\text{O}-\text{H} \cdots \text{O}$ hydrogen bonds to yield a 3D supramolecular network. Polymer **2Ln** crystallizes in a monoclinic space group $P2_1/n$ and features a 1D ribbon like chain structure constructed by the Bz ligands are linked the adjacent Ln(III) ions in the bidentate-chelating and tridentate bridging-chelating modes. The ribbon chains interact *via* $\pi \cdots \pi$ stacking interactions between adjacent Bz ligands, forming a 3D supramolecular architecture. The effect of intermolecular interactions on the solid state architectures of these polymers was investigated. Moreover, outstanding tunable photoluminescence was successfully realized by codoping Eu/Tb or Eu/Tb into analog Gd compounds.

Keywords: Lanthanide, Coordination Polymers, Hydrazide, Photoluminescence

Test Cell for Electrical Double-Layer Capacitor

Jedsada Manyam^{a*}

^a*National Nanotechnology Center, NSTDA, 111 Thailand Science Park, Phahonyothin Road, Khlong Nueng, Khlong Luang, PathumThani 12120 Thailand*

**e-mail: jedsada@nanotec.or.th*

Swagelok union has been traditionally used as a body of an electrochemical test cell in lithium-ion battery or capacitor research. A conventional Swagelok cell may possess poor reproducibility due to unintended variation in compressive force applied to a cell in each assembly. A test cell associated with a range of pressure can produce considerable uncertainty in quantification of electrochemical properties such as capacitance and resistance of a cell. Here, the new feature has been introduced to a Swagelok test cell, in which it has capability to determine spring pressure inside a body, thus making every assembly almost identical. The new test cell was implemented to a symmetric electrical double layer capacitors. A full cell setup composed of 10-mm diameter activated charcoal electrodes, separator, and aqueous electrolyte. Data of 15 repeating assembly were collected from charge-discharge galvanostatic and electrical impedance spectroscopic measurements. The results showed that standard deviations for gravimetric capacitance and internal resistance values for the prototype were 5.7 Ohm.cm² and 0.98 F/g, respectively, at the nominal pressure of 5 kgf/cm². The errors were approximately 3-fold and 2-fold smaller than those examined using a conventional designed test cell, showing significant improvement in both reliability of the assembly and accuracy of cell evaluation. In summary, it is suggested that experimental setup for electrochemical cell measurement must be taken care, and in this case the value of pressure applied on a cell should be reported together with other measurable cell characteristics.

Keywords: Swagelok union, Electrochemical cell, Capacitor

Revealing Charge Carrier Dynamics of Co_3O_4 Film by Transient Absorption Spectroscopy (TAS)

Ponart Aroonratsameruang, Pichaya Pattanasattayavong

*Department of Materials Science and Engineering, School of Molecular Science and Engineering,
Vidyasirimedhi Institute of Science and Technology (VISTEC), Rayong 21210, THAILAND
e-mail: pichaya.p@vistec.ac.th*

Spinel cobalt oxide (Co_3O_4) nanomaterials have been applied as a catalytic electrode for photoelectrochemical water splitting devices due to its p-type behavior and simple preparation.¹⁻³ However, Co_3O_4 shows a poor electrical conductivity which retards the device performance. Understanding the photophysics and dynamics of charge carrier generation of Co_3O_4 are therefore essential to improve its performance. The major obstacle which reduces the electronic conductivity or the number of conducting electrons is the presence of trap states with energies deep in the band gap. Probing the carrier dynamics and trap states requires an advanced technique as the processes are fast and can have multiple steps.

In this work, transient absorption spectroscopy (TAS) was employed to observe the presence of trap states in Co_3O_4 film which was prepared by electrodeposition method. The experimental results show that there are two main photo-induced absorption regions at 810 and 830 nm which might be two trap states aligning in Co_3O_4 bandgap. Moreover, this advanced spectroscopy provides the carrier dynamics of electrodeposited Co_3O_4 film and the timescale of the charge relaxation is on the order of a few microseconds. Furthermore, we also performed in-situ TAS of the Co_3O_4 electrode in working conditions in order to study carrier dynamics of nanomaterials at different biases in electrochemical cell. Revealing the photophysics of Co_3O_4 by TAS will be beneficial to optimize its charge transport for achieving high device performance.

- (1) Mao, Y.; Li, W.; Liu, P.; Chen, J.; Liang, E. Topotactic Transformation to Mesoporous Co_3O_4 Nanosheet Photocathode for Visible-Light-Driven Direct Photoelectrochemical Hydrogen Generation. *Mater. Lett.* **2014**, *134*, 276–280.
- (2) Yang, H.; Jin, Z.; Liu, D.; Fan, K.; Wang, G. Visible Light Harvesting and Spatial Charge Separation over the Creative Ni / CdS / Co_3O_4 Photocatalyst. *J. Phys. Chem. C* **2018**.
- (3) Ebadi, M.; Mat-Teridi, M. A.; Sulaiman, M. Y.; Basirun, W. J.; Asim, N.; Ludin, N. A.; Ibrahim, M. A.; Sopian, K. Electrodeposited P-Type Co_3O_4 with High Photoelectrochemical Performance in Aqueous Medium. *RSC Adv.* **2015**, *5* (46), 36820–36827.

A Feasibility of Developing Crosslinked Poly(acrylic acid) for Use as a Solid Adhesive Electrolyte in Electrochromic Glasses

Thannarasmī Khunsriya Samerpak^{a,d}, Jatuphorn Wootthikanokkhan^{b*}, and Khomson Suttisintong^c

^aThe Joint Graduate School of Energy and Environment, King Mongkut's University of Technology Thonburi, Bangkok, Thailand

^bDivision of Materials Technology, School of Energy, Environment and Materials, King Mongkut's University of Technology Thonburi, Bangkok, Thailand

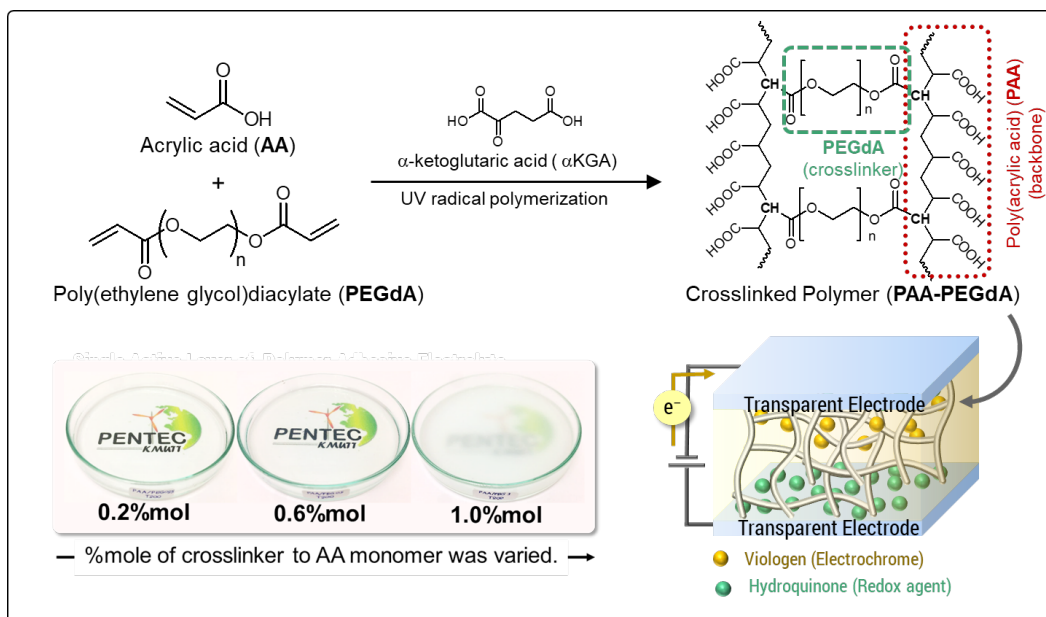
^cFunctional Nanomaterials and Interfaces Laboratory, National Nanotechnology Center, National Science and Technology Development Agency, Pathum Thani, Thailand

^dCenter of Excellence on Energy Technology and Environment, PERDO, Bangkok, Thailand

*e-mail: jatupharn.woo@kmutt.ac.th

Electrochromic (EC) windows are normally comprised of 5 layers which are (i) transparent electrode, (ii) electrochromic layer, (iii) electrolyte layer, (iv) ion counter layer, and (v) transparent electrode. Notably, liquid electrolyte is commonly used due to its high ion conductivity. However, this led to a short lifetime and leakage problems of the device. Attempts have been made to replace the liquid electrolyte with solid materials such as Ta₂O₃. However, fabrication process of EC based on this solid electrolyte is still complex and difficult to be scaled up. In this study, rather than using the metal oxide as an electrolyte, a feasibility of developing a transparent polymeric adhesive for use as electrolyte in EC has been explored. Specifically, poly(acrylic acid) (PAA) crosslinked with poly(ethylene glycol)diacrylate (PEGdA) was prepared. The aim of this work was to investigate the effect of polymeric crosslinking agent concentration on optical, mechanical and electrical properties of the materials. From our preliminary study, the optimum concentration of poly(ethylene glycol) diacrylate that yielded the crosslinked PAA product (PAA-PEGdA) with high optical transparency was 0.6 %mol. Further works have yet to be carried out in order to examine ion conductivity, tensile properties and peel strength of the materials using Cyclic Voltammetry (CV) and Universal Testing Machine (UTM), respectively. Our ongoing work focuses on an application of the polymeric adhesive electrolyte containing viologen and hydroquinone, as an all-in-one, single active layer for EC fabrication via lamination with electrodes.

Keywords: Viologen, Poly(acrylic acid), Poly(ethylene glycol), Electrochromic, Adhesive, Electrolyte



Parametric Study on the Synthesis of Ni Nanochains for Cermet Selective Solar Absorbers by Chemical Reduction Method

Piyarach Srimara^a, Thatchai Chevapruck^b, Tanyakorn Muangnapoh^{c*}, Pisist Kumnorkaew^c, Paravee Vas-Umnuay^{a*}

^aCenter of Excellence in Particle Technology, Department of Chemical Engineering, Faculty of Engineering, Chulalongkorn University, Thailand

^bDepartment of Materials Engineering, Faculty of Engineering, Kasetsart University, Bangkok, 10900, Thailand

^cNanofunctional Coating Laboratory, National Nanotechnology Center (NANOTEC), National Science and Technology Development Agency, 111 Thailand Science Park, Phahonyothin Rd., Khlong Nueng, Khlong Luang, Pathumthani 12120, Thailand

*e-mail: Paravee.V@chula.ac.th/ Tanyakorn.Mua@nanotec.or.th

Nowadays, the use of various nanostructured materials are favored in applications of concentrating solar power (CSP)¹ systems. Solar absorber, which is one of an important layer in a multilayered coating, is used to convert sunlight into thermal electric power due to its selective properties. Recently, Ni nanochain² solar absorbers have received many attractions because they offer maximized absorption and minimized thermal radiation losses. However, only few detailed investigations on the effects of morphology and structure of Ni nanochain on the selective absorber properties have been reported. Therefore in this work, the synthesis of Ni nanochains via a chemical reduction method³, the parametric study on the effects of synthesis conditions and the fabrication of Ni nanochain-Al₂O₃ cermet coating as the selective solar absorber via convective deposition⁴ method are presented. The scope of this work is to investigate the following parameters including (1) pH of precursor solution for Ni nanochain ranging from 7.0 – 11.0, and (2) concentration of Ni nanochain in Al₂O₃ matrix ranging from 0.10 - 1.70 M. These parameters are expected to strongly affect the size and shape of synthesized Ni nanochains (as shown in figure 1) as well as the morphology of the fabricated cermet coating, which will ultimately affect the optical properties, *i.e.* absorptance and emittance. Characterization of the morphology and structure of Ni nanochain and cermet coating is performed using scanning electron microscopy (SEM) and X-ray diffraction (XRD), respectively. In addition, emissometer is used to measure the thermal emissivity, and UV-Vis-NIR spectrophotometer is used to measure the reflectance of the film. The goal of this work is to optimize the operating parameters in order to obtain the maximum absorptance and the minimum emittance, which will be suitable for solar selective absorbing coating applications.

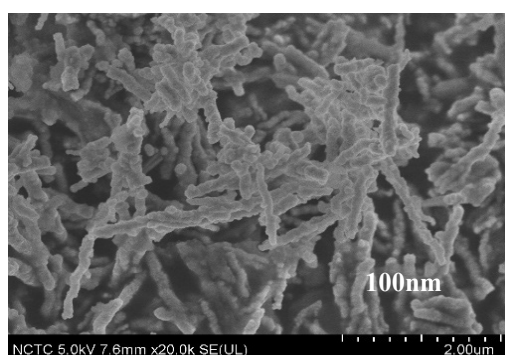


Figure 1. SEM image of Ni nanochains synthesized at pH of 11.

Keywords: Solar selective absorbers, Convective deposition, Cermet, Ni nanochain-Al₂O₃

References

1. H.L. Zhang, J.Baeyens, J.eve, G.Caceres. *Renew Sust Energ Rev.* **2013**, 22, 1-16.
2. X. Wang, H. Li, X. Yu, X. Shi, J. Liu. *Appl. Phys.* **2012**, 101, 3-7.
3. N.R. Roselina, A. Azizan, K. Hyie, A. Jumahat, M.A. Bakar. *Procedia Engineering.* **2013**, 68, 1-6.
4. P. Kumnorkaew, Y. Ee, N. Tansu, J. F. Gilchrit. *Langmuir.* **2008**, 24, 12150-12157.

Improving Charge Transport in CuSCN Hole Transport Layer by Anti-Solvent Treatment and Application in High-Efficiency Organic Solar Cells

Pimpisut Worakajit^a, Pichaya Pattanasattayavong^{a,*}

^aDepartment of Materials Science and Engineering School of Molecular Science and Engineering
Vidyasirimedhi Institute of Science and Technology (VISTEC) Rayong 21210, Thailand

*e-mail: pichaya.p@vistec.ac.th

Copper(I) thiocyanate (CuSCN) is a wide band gap transparent p-type semiconductor with remarkable potential as a hole transporting material. Low-temperature, solution processability is another advantage of applying CuSCN in large-area electronic applications.¹ CuSCN was recently reported to use as a hole transport layer in organic photovoltaic (OPVs) and organic light emitting diodes (OLEDs) in order to replace the conventional materials such as PEDOT:PSS. Interestingly, CuSCN devices exhibit higher efficiency than PEDOT:PSS.²⁻³ However, the development of CuSCN as hole transport layer is still in the early stage and further optimization is expected to improve performance, especially by improving the charge transport properties within CuSCN film which is the fundamental factor to control device efficiency.

Here, we report on adjusting film morphology by anti solvent treatment that leads to improved hole transport in the films. The common solvents were applied in a second spin coating step, using as an anti-solvent including Acetone (Ace), Methanol (MeOH), Isopropanol (IPA) and Tetrahydrofuran (THF). The resultant films were highly transparent in visible and NIR region similar to an untreated film. In addition, film morphology was observed using atomic force microscopy (AFM). The results show that CuSCN film treated by Ace, IPA and THF exhibit better film quality than the other because of smaller grain size and reducing root mean square roughness (RMS). These smoother films enhance the transport of charge carriers as proved by five times increasing of CuSCN thin-film transistor mobility. Thus, anti-solvent method appear to be a remarkable approach to enhance OPVs devices efficiency.

Keywords: Copper(I) thiocyanate, CuSCN, Solution-processed, Charge Transport, Organic Photovoltaic

References

1. P. Pattanasattayavong, V. Promarak, T. D. Anthopoulos, *Adv. Electron. Mater.* 2017, 3, 1.
2. N. Yaacobi-Gross, N. D. Treat, P. Pattanasattayavong, H. Faber, A. K. Perumal, N. Stingelin, D. C. Bradley, P. N. Stavrinou, M. Heeney, T. D. Anthopoulos, *Adv. Energy Mater.* **2015**, 5, 1.
3. N. Wijeyasinghe, A. Regoutz, F. Eisner, T. Du, L. Tsetseris, Y. H. Lin, H. Faber, P. Pattanasattayavong, J. Li, F. Yan, M. A. McLachlan, D. J. Payne, M. Heeney, T. D. Anthopoulos, *Adv. Funct. Mater.* 2017, 27, 1.

New Wide Band Gap Inorganic Semiconductor tin(II) Thiocyanate [Sn(NCS)₂] as Its Application in Organic Solar Cell

Jidapa Chaopaknam^a, Chayanit Wechwithayakhlung^a, Pichaya Pattanasattayavong^{a,*}

^aDepartment of Materials Science and Engineering School of Molecular Science and Engineering

Vidyasirimedhi Institute of Science and Technology (VISTEC) Rayong 21210, Thailand

*e-mail: pichaya.p@vistec.ac.th

Polymeric metal thiocyanates are introduced as a new class of semiconductors with unique electronic properties of the metal centers combined with wide band gaps from bonding with the thiocyanate ligand. One example is copper(I) thiocyanate (CuSCN) which is an excellent transparent p-type semiconductor and has already shown a great potential in electronic application particularly thin film transistors (TFTs), perovskite solar cells (PSCs), organic solar cells (OSCs), and organic light emitting diodes (OLEDs).^{1,2,3} Herein, we introduce tin(II) thiocyanate [Sn(NCS)₂] as another inorganic coordination polymer semiconductor. Sn(II) compounds show promising applications in opto/electronic devices due to its electronic structure, for example, SnO is an excellent p-type oxide with high hole mobility.⁴ It is of great interest to study the properties of Sn(NCS)₂ and its applications in electronic devices.

Sn(NCS)₂ was synthesized and solution-processed into thin films by spin coating. Film annealing can be carried out at temperatures below 80°C, showing compatibility with organic layer processing and plastic substrates. As part of this study, optical, chemical, and morphological characterization was performed. Absorption spectrum of SnSCN₂ also demonstrated absorption in UV region which related to high transparency of SnSCN₂ thin film in visible and NIR region. The chemical composition of Sn(NCS)₂ thin film was confirmed by X-ray photoelectron spectroscopy (XPS). Atomic force microscopy (AFM) presented morphology and roughness of Sn(NCS)₂ film. The result shows that the film had high smoothness (RMS = 7.5 nm.) and excellent film quality. In addition, organic solar cells were fabricated using either P3HT:PC70BM or PBDTTT-EFT:PC70BM as the active light-absorbing layer and employing Sn(NCS)₂ as the hole transport layer. Device fabrication currently investigates the deposition parameters to optimize the device efficiency.

In conclusion, Tin thiocyanate was demonstrated as one of the new p-type material based on thiocyanate ligand which exhibits remarkable properties and a potential to use in OPVs. Further studies are required to understand charge transport mechanism and investigate new electronic applications.

Keywords : Tin(II) Thiocyanate [Sn(NCS)₂], P-type Semiconductor, Hole Transport Layer, Organic Solar Cells

References

1. P. Pattanasattayavong, V. Promarak, T. D. Anthopoulos, *Adv. Electron. Mater.* **2017**, 3, 1.
2. N. Yaacobi-Gross, N. D. Treat, P. Pattanasattayavong, H. Faber, A. K. Perumal, N. Stingelin, D. C. Bradley, P. N. Stavrinou, M. Heeney, T. D. Anthopoulos, *Adv. Energy Mater.* **2015**, 5, 1.
3. N. Wijeyasinghe, A. Regoutz, F. Eisner, T. Du, L. Tsetseris, Y. H. Lin, H. Faber, P. Pattanasattayavong, J. Li, F. Yan, M. A. McLachlan, D. J. Payne, M. Heeney, T. D. Anthopoulos, *Adv. Funct. Mater.* **2017**, 27, 1.
4. Z. Wang, P. K. Nayak, J. A. Caraveo-Frescas, H. N. Alshareef, *Adv. Mater.* **2016**, 28, 3831.

A Fast Route to Synthesis Hybrid Perovskite $\text{CH}_3\text{NH}_3\text{PbI}_3$ by using Acetone as Iodine Reduction Agent during Methyl Ammonium Iodide Preparation

Phitsamai Kamonpha^{a,c}, Jintara Padchasri^a, Usa Sukkha^b, Narong Chanlek^c, Saroj Rujirawat^a, Rattikorn Yimnirun^d

^a*School of Physics, Institute of Science, Suranaree University of Technology, Nakhon Ratchasima, 30000, Thailand*

^b*Synchrotron Light Research Institute (Public Organization), 111 University Avenue, Muang District, Nakhon Ratchasima 30000, Thailand*

^c*King Mongkut's Institute of Technology Ladkrabang Prince of Chumphon Campus, Chumphon 86160, Thailand*

^d*School of Energy Science and Engineering, Vidyasirimedhi Institute of Science and Technology, Rayong 21210, Thailand*

*e-mail: phitsamai.own1993@gmail.com

The emerging of perovskite solar cell has attracted much interests in the synthesis and characterization of hybrid perovskite materials related to methylammonium iodide (MAI) due to various interesting properties. In this work, a faster way to synthesis hybrid perovskite $\text{CH}_3\text{NH}_3\text{PbI}_3$ from MAI precursor is reported. It is found that the synthesis time for MAI synthesis can be shorten by four times, from 48 h to 12 h by changing the reduction agent from dimethylformamide (DMF) to acetone. The MAI precursors from different solvents were used to synthesis hybrid perovskite $\text{CH}_3\text{NH}_3\text{PbI}_3$ powders by solid state method with varying conditions. The characterizations by X-ray Diffraction (XRD), Infrared Spectroscopy (IR) and X-ray absorption spectroscopy (XAS) shown that the characteristic quality of hybride perovskite $\text{CH}_3\text{NH}_3\text{PbI}_3$ powders from acetone and DMF are comparable thus confirm the effective of the new préparation route.

Keywords: Methyl ammonium iodide, Hybrid perovskite

References

1. Yanbo Li, J. Phys. Chem. Lett. 2015, 6, 493–499
2. Zhang , Energy Environ. 2014, focus 3, 354–359
3. Nam Joong Jeon, Nature material, 2014, VOL 13 ,897-903
4. Lee, M. M. Science. 2012, 338,643-647
5. Heo, J. H., Nature Photon. 2013, 7, 486-491
6. Nam Joong Jeon, J. Am. Chem. Soc. 2013, 135, 19087–19090
7. Sneha A. Kulkarni, Tom Baikie, Pablo P. Boix, Natalia Yantara, J. Mater. Chem. A, 2014, 2,9221-9225
8. Woon Seok Yang, Science 2017,356, 1376–1379
9. N. J. Jeon, Nature 2015, 517,476–480
10. Weidong Xu, Nano Lett. 2016, 16, 4720–4725
11. McGehee, M. D. Nature 2013, 501, 323–325.
12. Jeffrey A. J. Am. Chem. Soc. 2014, 136, 758–764

Cattail Flower-Derived High Surface Area Mesoporous Activated Carbons by Alkali Activation

Parncheewa Udomsap^{a,b*}, Nuwong Chollacoop^b and Apiluck Eiad-ua^a

^aCollege of Nanotechnology, King Mongkut's Institute of Technology Ladkrabang, Bangkok 10520, Thailand

^bNational Metal and Materials Technology Center, National Science and Technology Development Agency, Pathumthani 12120, Thailand

*e-mail: parncheu@mtec.or.th

A highly functionalized carbonaceous material (hydrochar) was obtained by means of the hydrothermal carbonization (200 °C for 2 h) of biomass, Cattail flower. This product contains around 50-60% of the carbon originally present in the biomass. In order to modify the pore structure, the hydrochars were further activated chemically using KOH, K₂CO₃, NaOH and Na₂CO₃ with heat treated at 900 °C for 2 h under N₂ atmosphere. The changes of the pore structure and surface chemistry of activated carbon were investigated in terms of nitrogen adsorption-desorption isotherm, scanning electron microscope and fourier transform infrared spectroscopy. The BET surface areas and total pore volumes of all activated carbon dramatically increased as compared to the carbon without activation (24 m²g⁻¹ and 0.02 cm³g⁻¹). The activated carbon by Na₂CO₃ presented the highest surface area and total pore volume of 1341 m²g⁻¹ and 0.79 cm³g⁻¹, respectively. While, KOH, K₂CO₃ and NaOH activation produced the carbon with the similar surface area and total pore volume which are in the range 740-880 m²g⁻¹ and 0.47-0.58 cm³g⁻¹, respectively. Moreover, the mesopore volume fractions of all sample obviously increased. The mesopore volume to total pore volume ratio ($V_{\text{meso}}/V_{\text{total}}$) of carbon activated by KOH, K₂CO₃, NaOH and Na₂CO₃ was 0.71, 0.47, 0.72 and 0.62 which were higher than the commercial activated carbon (0.29). In addition, alkali hydroxides activation presented significant higher the $V_{\text{meso}}/V_{\text{total}}$ ratio than the alkali salts activation. The high surface area mesoporous activated carbon can be used as catalyst support which enhance the catalytic activity of the catalyst.

Keywords: Activated carbon, Mesoporous, Alkali activation, Cattail flower

References

1. I. Isil Gurten, M. Ozmak, E. Yagmur, Z. Aktas, *Biomass Bioenerg.* **2012**, 37, 73-81.
2. T. Song, J-M. Liao, J. Xiao, L-H. Shen, *New Carbon Mater.* **2015**, 30, 156-166.
3. J. Su, J.-S. Chen, *Micropor. Mesopor. Mat.* **2017**, 237, 246-259.
4. A. Jain, R. Balasubramanian, M. P. Srinivasan, *Chem. Eng. J.* **2016**, 283, 789-805.
5. D. Prahas, Y. Kartika, N. Indraswati, S. Ismadji, *Chem. Eng. J.* **2008**, 140, 32-42.

A Polycalicene Family as Potential Molecular Wires

Thawalrat Ratanadachanakin^{a(*)}, Willard E. Collier^{b(*)}

^aFaculty of Science, Maejo University, Sansai, Chiang Mai, 50290, Thailand

^bDepartment of Chemistry, College of Arts and Sciences, Tuskegee University, Tuskegee, AL, 36088, USA

*e-mail: thawalrat4@gmail.com, wcollier@tuskegee.edu

Polycalicenes are an intriguing region of chemical space that includes many non-benzenoid aromatic compounds. While calicene **1** (shown in Figure 1) has yet to be synthesized, a few simple polycalicenes are known and have been shown to be aromatic [1-3]. The structures and aromaticities of polycalicenes **2-4** (shown in Figure 1) were investigated as part of an effort to discover new molecular wire candidates. The aromaticities of **2-4** were evaluated using the nucleus independent chemical shift (NICS) criterion of aromaticity. The NICS values and NMR chemical shifts of calicene, benzene, cyclopentadienyl anion, and cyclopropenyl cation were calculated as references. All geometries and NMR properties are reported at B3LYP/6-31+g(d,p) level of theory. We will discuss the structures and aromaticities of polycalicenes **2-4** and their potential as molecular wires.

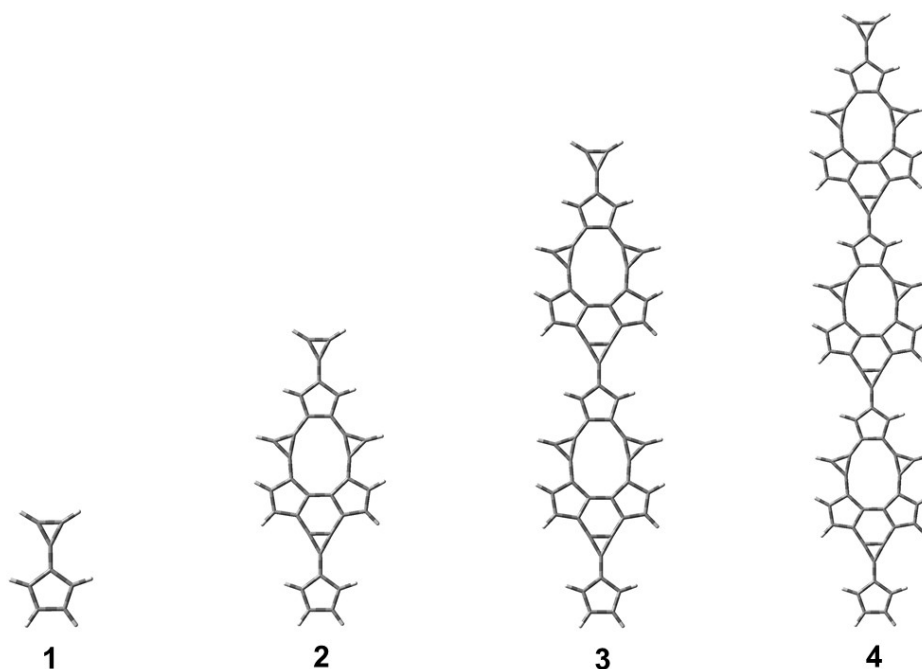


Figure 1. A Polycalicene Family

Keywords: Calicene, Polycalicenes, Aromaticity, NICS

References

1. Z. Yoshida, *Pure & Appl. Chem* **1982**, *54*, 1059-1074.
2. S. Yoneda, M. Shibata, S. Kida, Z. Yoshida, Y. Kai, K. Miki, N. Kasai, *Angew. Chem. Int. Ed. Engl.* **1984**, *23*, 63-64.
3. Y. Sugimoto, M. Shibata, S. Yoneda, Z. Yoshida, Y. Kai, K. Miki, N. Kasai, T. Kobayashi, *J. Am. Chem. Soc.* **1986**, *108*, 7032-7038.

The Preparation and Characterization of SiO₂ Films by Spray Coating Technique for Radiative Cooling Glass Application

Khamin Praweerawat^{a,b}, C. Muangphat^{a,c,*}, C. Luangchaisri^{a,b}

^a Smart Materials Laboratory (SMaL), King Mongkut's University of Technology Thonburi, Bangkok, Thailand

^b Department of Physics, Faculty of Science, King Mongkut's University of Technology Thonburi, Bangkok, Thailand

^c Division of Materials Technology, School of Energy, Environment, and Materials, King Mongkut's University of Technology Thonburi, Bangkok, Thailand

*e-mail: chivarat.mua@kmutt.ac.th

Radiative cooling glass is a new type of energy saving glass products that can prevent incoming heat flux through the window by changing near-infrared radiation into transparency window wavelength and release back to the environment. Transparency window wavelength is the wavelength from 8 to 13 microns that is called mid-infrared region (MIR). This MIR region does not interact with the atmosphere and can penetrate to space directly. Therefore, radiative cooling glass is not only able to save energy in buildings, but it also reduces urban heat island effect. Silicon dioxide (SiO₂) film is a component in radiative cooling glass that is employed as an absorption layer to absorb the MIR wavelength and transfer to other layers.

This study investigates the surface morphology and optical properties of SiO₂ film on glass substrate at various coating conditions. A mixture solution of tetraethyl orthosilicate (TEOS), DI water and ethanol was sprayed through the nozzle with different concentration and volume at ambient atmosphere. Optical microscope results show the higher concentration of TEOS gives the rougher surface of SiO₂ film due to the formation and the accumulation of SiO₂ particles, as show in Fig.1. However, UV-Vis spectroscopy results show that the concentration of TEOS and the thickness of SiO₂ film do not influence on the percent transmittance of SiO₂ films.

transmittance of SiO₂ films.

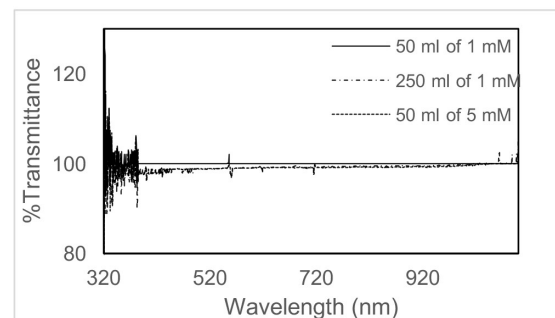
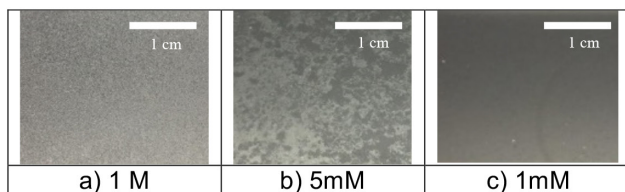


Figure 1. Optical microscope images show the morphology of SiO₂ films using the different concentration of TEOS solution a.) 1 M, b.) 5 mM and c.) 1 mM

Figure 2. Percent transmittance of 50 ml of 1 mM, 250 ml of 1 mM and 50 ml of 5 mM SiO₂ films.

Keywords: Radiative cooling glass, Silicon dioxide (SiO₂) film, Spray coating technique

The Effect of Ratio and Porous Structure of NiO/TiO₂ Composite Film for Increasing Efficiency of Dye Sensitized Solar Cell

K. Nakayama^a, C. Muangphat^b, C. Luangchaisri^{c*} and K. Praweerawat^c

^aDepartment of Mathematics and Physics, Faculty of Natural Science, Kanazawa University, Ishikawa, 9201164, Japan.

^bDivision of Material Technology, School of Energy, Environmental and Materials, King Mongkut's University of Technology Thonburi, Bangkok, 10140, Thailand.

^cDepartment of Physics, Faculty of Science, King Mongkut's University of Technology Thonburi, Bangkok, 10140, Thailand.

*e-mail: chumphon.lua@kmutt.ac.th

Spray Pyrolysis Technique (SPT) has been applied for preparing many kinds of thin films because this technique offers a lot of advantages such as inexpensive cost, uncomplicated process and large scale production. Therefore, SPT is used for making 100 % TiO₂ and NiO/TiO₂ composite films in this report. NiO/TiO₂ composite film is getting attention to be used as a compact layer in Dye Sensitized Solar Cell (DSSC) because NiO can be used as a hole collector and a barrier for energy recombination properties. 5:95, 10:90 of NiO/TiO₂ composite films and 100 % TiO₂ film were studied in this report. NiO/TiO₂ composite films were prepared by using 300 ml and 600 ml of a mixture solution of Titanium tetraisopropoxide (Ti(OCH(CH₃)₂)₄), ethanol, acetyl acetone and nickel nitrate hexahydrate powder (Ni(NO₃)₂·6H₂O). The mixture solutions were sprayed at a constant air pressure at 1 bar at 400 °C. 100 % TiO₂ and NiO/TiO₂ composite films show low contact angles and the contact angles decrease with increasing the amount of solution or the film thickness, as shown in Fig 1.

However, the low contact angle of pure TiO₂ and NiO/TiO₂ composited films do not result from the hydrophilic property, but it is effect of the columnar structure of films. As shown in Fig 2, the columnar structure of 100 % TiO₂ and the 10:90 NiO/TiO₂ composite film were observed using Field-Emission Scanning Electron Microscope (FE-SEM). Cross-Sectional FE-SEM images show that the thickness of NiO/TiO₂ decrease with increasing the ratio of NiO. Therefore, the droplet of water can go through the columnar structure to the bottom of substrate, as shown in Fig 3. For this reason, the columnar structure and thickness of TiO₂ and NiO/TiO₂ films can increase the contact area between the compact layer and dye for increasing DSSCs efficiency.

Keywords: NiO/TiO₂ composite film, Spray pyrolysis, Porous structure, Dye sensitized solar cell

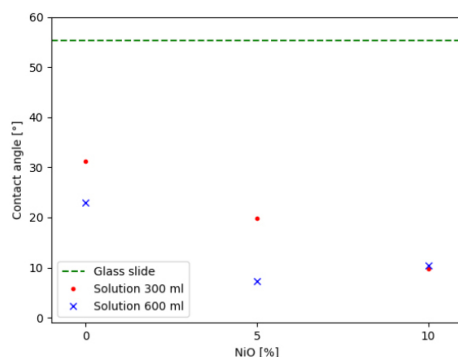


Figure 1. The relationship between the contact angle and the ratio of NiO. The points show the volume of solution 300 ml and cross marks show 600 ml at 100 % TiO₂, 5:95 and 10:90 NiO/TiO₂ composite films, respectively. The dashed line indicates the contact angle on the glass substrate

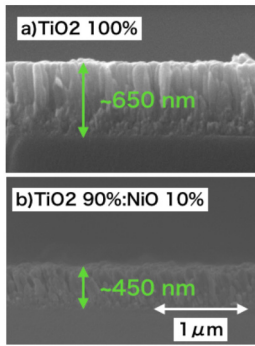


Figure 2. Cross-section images show the thickness a) 100 % TiO_2 and b) 10 :90 NiO/TiO_2 prepared using 600 ml solution

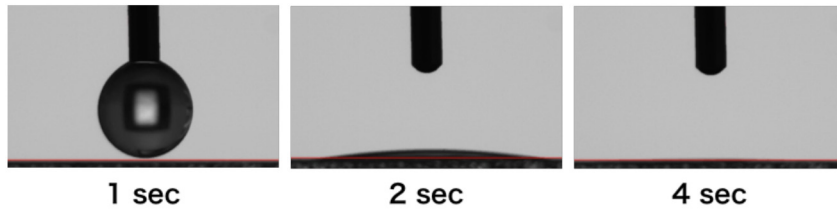


Figure 3. The movement of a water droplet on 100 % TiO_2 prepared using 600 ml solution

References

1. S. Wahyuningsih et al., **2018**, IOP Conf. Ser.: Mater. Sci. Eng. 333 012032
2. Y. Ku et al., 2011, Journal of Molecular Catalysis A: Chemical 349 20–27
3. C.-S. Chou et al., **2011**, Advanced Power – Technology 22 31-42

Activated Carbon from Palm Fiber via Microwave Assisted KOH Activation as Alternate Catalyst Supporter

Napat Kaewtrakulchai^a, Kajornsak Faungnawakij^b, Apiluck Eiad-Ua^{a*}

^aCollege of Nanotechnology, King Mongkut's Institute of Technology Ladkrabang, Bangkok 10520, Thailand

^bNational Nanotechnology Center (NANOTEC), National Science and Technology Development Agency (NSTDA), 111 Thailand Science Park, Phahonyothin rd., Khlong Nueng, Khlong Luang, Pathum Thani 12120, Thailand

*e-mail: apiluck.ei@kmitl.ac.th

The present study explores the variability of agricultural residues for activated carbon production. Activated carbon were prepared from pineapple fiber (PF) efficaciously using potassium hydroxide (KOH) activation (1:2 impregnation ratio, KOH:C, w/w) in a microwave heating system. The effects of experimental variables (i.e. microwave powers and activation times) on the properties and production yields of these obtained activated carbons under different conditions were comprehensively evaluated. KOH activation using microwave heating system was accomplished at 450 to 800 W for 4, 6, 8 and 10 min. The production yields were continuously decreased via an increase of both microwave powers and activation times. The lowest production yield was obtained at 800 W microwave power, and highest activation time of 10 min. Nonetheless, the highest specific surface areas of PF activated carbon found at 700 W for 6 min were approximately 991.46 m²/g and total pore volume of 0.46 cm³/g. Also, the PF activated carbons have mainly microporous structure.

Keywords: Palm fiber, Activated carbon, KOH activation

References

1. I. Okman, S. Karagöz, T. Tay, M. Erdem, Applied Surface Science, 2014, 293, 138–142.
2. H. Saygılı, F. Güzel, Y. Onal, Journal of Cleaner Production, 2015, 93, 84-93.
3. K.Y. Foo, B.H. Hameed, Bioresource Technology, 2012, 116, 522–525.
4. S.S. Lam, R.K. Liew, Y.M. Wong, P.N.Y. Yek, N.L. Ma, C.L. Lee, H.A. Chase, Journal of Cleaner Production, 2017, 162, 1376-1387.
5. E.K. İu, C. Akmil-Baßsar, Advanced Powder Technology, 2015, 26, 811–818.

Effect of Substrate Temperature on GaAs Nanowires Growth Directly on Si (111) Substrates by Molecular Beam Epitaxy

Kay Khaing Oo^a, Samatcha Vorathamrong^a, Somsak Panyakeow^a, Piyasarn Praserttham^b, and Somchai Ratanathamphan^{a*}

^a*Semiconductor Device Research Laboratory, Department of Electrical Engineering, Faculty of Engineering, Chulalongkorn University, Bangkok 10330, Thailand*

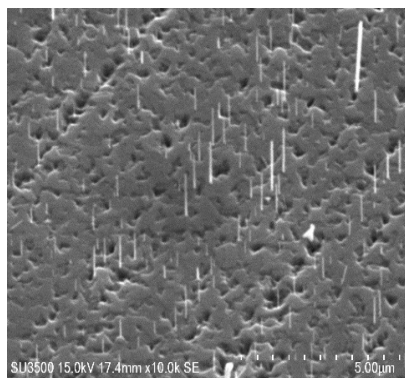
^b*Center of Excellence on Catalysis and Catalytic Reaction Engineering, Department of Chemical Engineering, Faculty of Engineering, Chulalongkorn University, Bangkok 10330, Thailand*

*e-mail: rsomchai@chula.ac.th

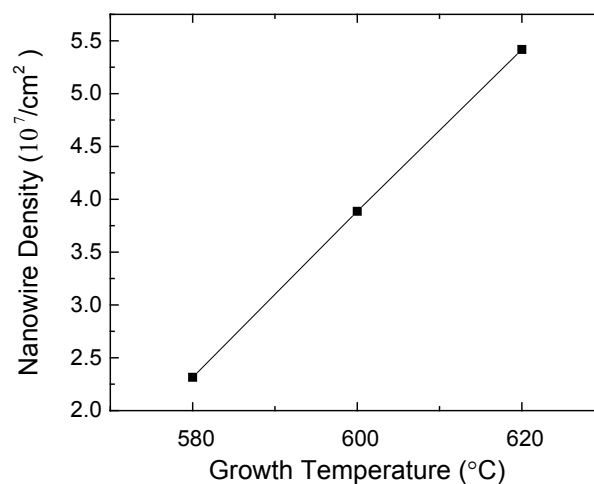
We have demonstrated the growth of GaAs nanowires directly on Si (111) substrates by Ga-assisted technique using molecular beam epitaxy. The growth processing are droplet forming and nanowire growth. In this work, the droplet forming and nanowire growth are performed at the same substrate temperature. The effect of substrate temperature while droplet forming with growth on the GaAs nanowire structural properties is investigated by Scanning Electron Microscope (SEM) and X-ray diffraction. The nucleation of GaAs nanowires strongly depends on the substrate temperature. The results show that the density, length, and diameter of GaAs nanowires relate to the substrate temperature. Some of results are shown in Fig 1.

Acknowledgment This work is supported by NSTDA, AOARD and AUD-SEED/Net

Keywords : GaAs, Nanowires, Si substrate, Molecular Beam Epitaxy, Scanning Electron Microscopy



(a)



(b)

Figure 1. (a) SEM image of GaAs nanowire grown at 620 °C and (b) Graph for nanowire density as a function of substrate temperature

Preparation of Three-Dimensional PolyAspAm(EDA/EA)/TA-Graphene Aerogel Containing Silver NPs and the Antibacterial Property

Dat Quoc Dang^a, Bo Wang^a, Milene Tan^b and Ji-Heung Kim^{a*}

^aDepartment of Chemical Engineering, Sungkyunkwan University, 16419 Suwon, Korea

^bDepartment of Chemistry, University of Fribourg, 1700 Fribourg, Switzerland.

*e-mail: kimjh@skku.edu

The increased use of medical devices combined with the emergence of new multi-drug resistant bacteria has focused the research on biomaterials-related infections. Silver has already been proven to be effective against bacterial infections even at low concentration (0.1-10 ppm). It has been demonstrated that smaller sizes of Ag nanoparticles (NPs) show better antibacterial activities. However, small sizes of AgNPs tend to aggregate in the process of preparation, which leads to remarkable loss of their antibacterial properties. Three-dimensional (3D) polymeric hydrogel or graphene with the large accessible surface area of graphene sheets and highly porous structures can be used as a supporting matrix which can promote immobilization and maximize the loading of noble-metal NPs. In addition, the aggregation problem of AgNPs can be minimized and even prevented. Tannic acid (TA) is a specific form of tannin, a type of polyphenol, can reduce not only graphene oxide (GO) to graphene but also reduce Ag ions to AgNPs without the need for any reducing reagents. Here, we present a synthetic poly(amino acid), specifically polyaspartamide, modified by ethylenediamine and ethanolamine, PolyAspAm(EDA/EA), which was mixed with TA and GO to fabricate ultralight 3D graphene hybrid aerogel. This 3D graphene aerogel with TA-mediated AgNPs has potential as a new antibacterial material for a wide range of industrial and clinical applications.

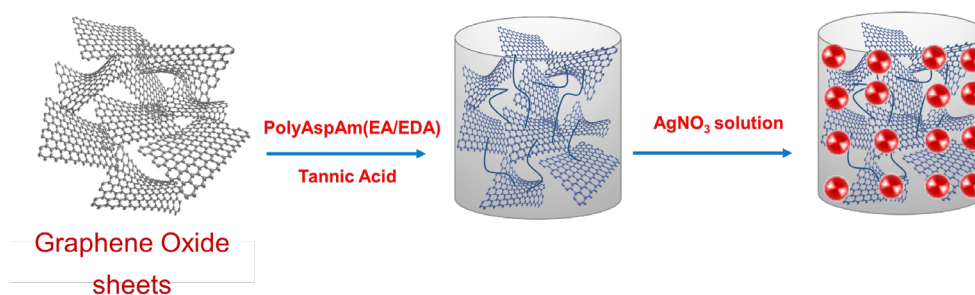


Figure 1. Silver nanoparticle embedded graphene/polymer hybrid aerogel

Keywords: Graphene aerogel, Tannic acid, Polyaspartamide, Silver nanoparticle, Antibacterial

Biocompatibility and Bone Sensing Technology of Graphene Oxide Nanomaterial

Artit Ramdongbang and Sirinrath Sirivisoot*

*Biological Engineering Program, Faculty of Engineering, King Mongkut's University of Technology Thonburi,
Bangkok 10140, Thailand*

**e-mail: sirinrath.sir@kmutt.ac.th*

Graphene oxide (GO) is one of popular nanomaterials used in various new applications for biomedical treatments. GO consists of carbon atoms and oxygen containing functional groups (such as hydroxyl, epoxy, carbonyl, and carboxyl groups), which lead to coexisting of its hydrophobic and hydrophilic properties [1][2]. Hence, GO has a remarkable biocompatibility and high electrical conductivity. In this study, titanium surface was fabricated using anodization method for creating TiO₂ nanotube array. Then electrodeposition method was performed for GO coating on anodized titanium. The solution of GO was used at the concentrations of 150 µg/ml and 200 µg/ml in electrodeposition process. The GO electrodeposited samples at the concentration of 200 µg/ml were observed clearly the morphology of GO coating on the samples using scanning electron microscopy. On anodized titanium, TiO₂ nanotube array was appeared with the diameter at about 50 nm. The investigation of elements with energy dispersive X-ray spectrometry confirmed a presence of carbon, oxygen and titanium after surface modifications. The GO electrodeposited samples had a significant increase of elemental percentage of carbon. A biocompatibility assay on the GO electrodeposited samples was tested with pre-osteoblast cells to determine cell adhesion and spreading after four hours of cultures. The results indicated that the GO electrodeposited on conventional titanium had a significant improvement of cell density on the samples. Pre-osteoblast cells were well spread on the GO electrodeposited on both conventional and anodized titanium. Moreover, the GO electrodeposited on anodized titanium (GO-ATi) was applied in the form of working electrode to test an electron transfer at the sample surface in electrochemical system. The GO-ATi working electrodes detect an electron transfer (oxidation-reduction) in the presence of osteocalcin protein (bone extracellular matrix proteins), thus, the GO-ATi has a potential to be used in bone sensing technology. The results of biocompatibility studies and electrochemical analysis in this study show a capability of using GO-ATi in point-of-care diagnostic and orthopedic applications.

Keywords: Graphene oxide, Bone growth sensing, Osteocalcin

References

1. Wang, G., Wang, B., Park, J., Yang, J., Shen, X., and Yao, J., 2009, "Synthesis of Enhanced Hydrophilic and Hydrophobic Graphene Oxide Nanosheets by a Solvothermal Method", **Carbon**, Vol. 47, No. 1, pp. 68-72.
2. Lee, J., Kim, J., Kim, S., and Min, D.-H., 2016, "Biosensors Based on Graphene Oxide and Its Biomedical Application", **Advanced Drug Delivery Reviews**, Vol. 105, No., pp. 275-287.

Novel Sulfonamido Spirobifluorenes as off-on Fluorescent Sensors for Mercury(II) Ion and Glutathione

Komthep Silpcharu^a, Mongkol Sukwattanasinitt^a, Paitoon Rashatasakhon^{a,*}

^aDepartment of Chemistry, Faculty of Science, Chulalongkorn University, Bangkok 10330, Thailand

**e-mail: paitoon.r@chula.ac.th*

Novel spirobifluorene derivatives containing two and four sulfonamide groups are successfully synthesized from the commercially available bromo-9,9'-spirobifluorene by Sonogashira couplings. These compounds exhibit excellent selective fluorescent quenching by Hg(II) in DMSO/HEPES buffer mixture with three-time-noise detection limits of 8.4 to 94.7 nM. A static sensing mechanism is formulated by the data from ¹H-NMR and UV-Vis spectroscopy, as well as the observation of the Tyndall effect. Satisfactory results are obtained from comparing experiments using these sensors and ICP-OES. The reversibility of these sensors is demonstrated by a complete fluorescence restoration upon addition of EDTA or L-glutathione. The application as a turn-on sensor for L-glutathione is demonstrated in a quantitative analysis of three samples of L-glutathione supplement drinks.

Keywords: Fluorescent sensors, Glutathione, Mercury ion, Spirobifluorene, Sulfonamide.

A Binder-Free and Sustainable Lignin Composite Electrode for Energy Storage Applications

Saowaluk Chaleawert-umpon^{a*} and Clemens Liedel^b

^aNational Nanotechnology Center, 111 Thailand Science Park, Pathumthani 12120, Thailand

^bDepartment of Colloid Chemistry, Max Planck Institute of Colloids and Interfaces, Research Campus Golm, 14476 Potsdam, Germany

*e-mail: saowaluk@nanotec.or.th

Electrochemical energy storage using lignin as renewable electrode material is a cheap and sustainable approach for future batteries and supercapacitors.¹⁻³ Further significant environmental impact is caused by fluorinated binders,^{4,5} which are most widely used for electrode fabrication. We propose a new route to fabricate a binder-free composite electrode from Kraft lignin in a combination with conductive carbon as a promising alternative electrode for energy storage applications. By crosslinking the lignin with glyoxal (glyoxalated lignin), a high molecular weight lignin is obtained to enhance both properties: electroactive compound and binder in composite electrodes.⁶

To better understand desired lignin properties for energy storage, we investigate lignin-carbon composites in a three-electrode system by cyclic voltammetry and analyze charge storage contributions in terms of electrical double layer (EDL) and redox reactions. The influence of annealing temperature, amount of glyoxal, and means of electrode fabrication is evaluated to improve stability and charge storage capacity. A total capacity of 80 mAh g⁻¹ at a discharge rate of 0.2 A g⁻¹ is obtained in stable electrodes without fluorinated binder additives. The resulting binder-free lignin carbon composite electrodes are stable in conventional organic electrolytes. A primary lithium battery was tested resulting in a discharge capacity of 250 mAh g⁻¹ at a discharge rate of 2 A g⁻¹. Thus, these electrodes are promising as more stable, sustainable and more environmentally benign devices for energy storage applications.

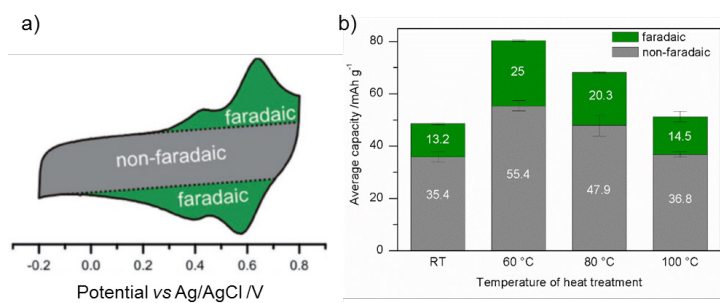


Figure 1. a) Cyclic voltammogram of glyoxalated lignin composite electrode measured at 5 mV s⁻¹ in 1 M HClO₄ with indicated contributions by faradaic and non-faradaic processes to charge storage and b) capacity of glyoxalated lignin based electrodes at which lignin was treated with glyoxal at various temperatures for processing crosslinking on the electrode film.

Keywords: Energy Storage, Lignin Composite Electrode, Glyoxalated lignin, Binder-free Electrode

References

1. S. Admassie, F.N. Ajjan, A. Elfwing, O. Inganäs, *Mater. Horiz.* **2016**, *3*, 174-185.
2. G. Milczarek, O. Inganäs, *Science* **2012**, *335*, 1468-1471.
3. G. Milczarek, *Langmuir* **2009**, *25*, 10345-10353.
4. S.L. Chou, Y. Pan, J.Z. Wang, H.K. Liu, S.X. Dou, *Phys. Chem. Chem. Phys.* **2014**, *16*, 20347-20359.
5. P. Martins, A.C. Lopes, S. Lanceros-Mendez, *Prog. Polym. Sci.* **2014**, *39*, 683-706.
6. S. Chaleawert-umpon and C. Liedel, *J. Mater. Chem. A* **2017**, *5*, 24344-24352.

Investigation of Osteopontin Protein and Gene Expression on Graphene Oxide Electrodeposited Titanium Implants

Pichayada Techaniyom and Sirinrath Sirivisoot*

Biological engineering Program, Faculty of Engineering, King Mongkut's University of Technology Thonburi

**e-mail: sirinrath.sir@kmutt.ac.th*

Orthopedic implants are manufactured for replacement or support of damaged bones and joints. This study is aimed to understand the process of osteoblast differentiation on graphene oxide electrodeposited on titanium implants. In the previous study, bone forming cells (MC3T3-E1 cells) or pre-osteoblasts cells were cultured onto a modified surface of titanium by anodization and electrodeposition of graphene oxide, and then calcium mineralization on the samples was investigated. The effects of such surface modifications to osteopontin protein and gene expression by osteoblasts were evaluated in this study by flow cytometry and quantitative reverse transcription-polymerase chain reaction (qRT-PCR) method. Osteopontin protein and gene expression were observed after MC3T3-E1 cells were cultured on polystyrene (PS), graphene oxide coated on polystyrene (GO), anodized titanium (ATi), and graphene oxide coated on anodized titanium (ATiGO). The protein expression was detected with an indirect immunofluorescence staining using flow cytometer after MC3T3-E1 cells were cultured on the samples for 14 and 21 days. The results showed that the relative fluorescence intensity (RFI) of osteopontin in MC3T3-E1 cells on ATiGO was significantly higher than that on PS and GO at day 14. Conversely, at day 21, the RFI of osteopontin in cells on ATiGO was significantly decreased, but, the RFIs of osteopontin on PS and GO were significantly increased. Moreover, the expression of *Spp1* gene which expressed osteopontin protein was investigated on the samples by qRT-PCR at day 14 and 21. However, the results of gene expression of secreted phosphoprotein 1 (*Spp1*) showed that the expression from cells cultured on ATiGO at day 21 is higher than that at day 14, which did not match with the results from flow cytometry. Importantly, the results of osteopontin protein and gene expression at day 14 and 21 suggested that ATiGO could accelerate osteoblasts to secrete osteopontin protein during cell differentiation.

Keywords: Graphene oxide, Anodized Titanium, Osteopontin, Differentiation

Electrochemical Characterization of Graphene Oxide Modified Electrodes Fabricated by Electrophoretic Deposition

Lalida Suppaso and Sirinrath Sirivisoot*

Biological Engineering Program, Faculty of Engineering, King Mongkut's University of Technology Thonburi, Bangkok 10140, Thailand

**e-mail: sirinrath.sir@kmutt.ac.th*

Graphene oxide (GO) has been widely used due to its unique chemical structure, promising its composites with good electronic, thermal, electrochemical, and mechanical properties. An electrophoretic deposition technique is a method that can deposit GO on the surface of conductive substrates. With this method GO can be used to modify a working electrode, and increasing its sensitivity for sensor applications [1-2]. This work reported electrochemical performance of working electrode, GO electrodeposited on anodized titanium (ATi) substrate, when controlling applied voltages (5, 10, 20 V) and duration (5, 10, 30 min) during electrodeposition process. Cyclic voltammetry was carried out to characterize the GO electrodeposited on ATi substrates (ATiGO) in a three-electrode system at a scan rate of 100 mV/s. The $\text{Fe}^{2+/3+}$ redox results revealed that the oxidation peak at ATiGO, which had GO electrodeposited at 20 V and 10 min, was higher in current density than that at ATiGO, which had GO electrodeposited at 5 V (5, 10, 30 min), 10 V (5 and 10 min), and 20 V (5 and 30 min). However, the reduction peak at ATiGO, which had GO electrodeposited at 20 V and 10 min, was highest in current density. The results in this study provide a preliminary data for fabrication of a bone-growth detecting sensor on-chip which has ATiGO as a modified electrode. Such sensor can help an early diagnosis for physicians in detecting bone ingrowth juxtaposed to orthopedic implants in patients.

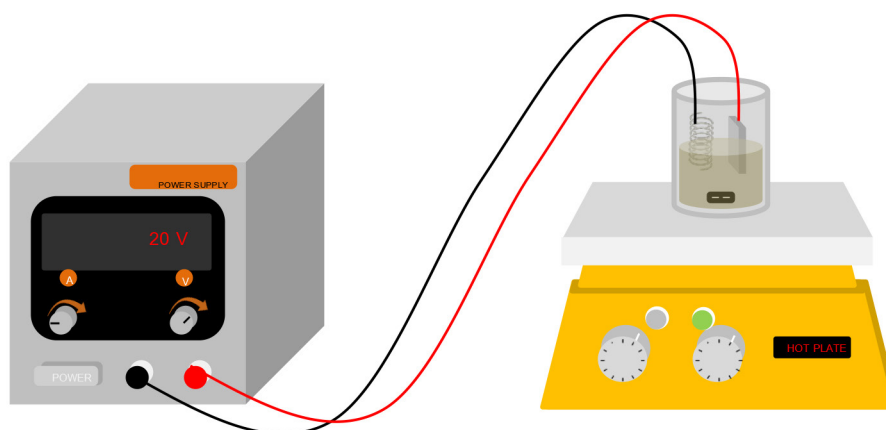


Figure 1. Electrophoretic Deposition of Graphene Oxide

Keywords: Anodized Titanium, Cyclic Voltammetry, Electrodeposition, Graphene Oxide, Redox Couple

References

1. M. Z. H. Khan, *J. Nanomaterials*. **2017**, Apr. 2017, 1-11.
2. S. Pruneanu, A. R. Biris, F. Pogacean, C. Socaci, M. Coros, M. C. Rosu, F. Watanabe, and A. S. Biris. *J. Electrochimica Acta*. **2015**, 154, 197-204.

A Simple and Eco-Friendly Method for Preparation of Tryptophan Intercalated Zinc Aluminium/Layered Double Hydroxide

Patsaya Anukunwithaya^a and Kritapas Laohhasurayotin^{a,*}

^aNational Nanotechnology Center (NANOTEC), National Science and Technology Development Agency (NSTDA), Pathumthani, 12120, Thailand

*e-mail: kritapas@nanotec.or.th

Intercalation of organic molecule in nano-interlayer of 2D structure – layered double hydroxide (LDH) has been known to be challenging. The zwitter ionic structure of amino acid like tryptophan (Trp) does not favor the anionic interlayer of LDH, this simple ion-exchange process may not be appropriated in adding such molecule into the LDH structure. Co-precipitation and other harsh environments, i.e. strong pH and high temperature have been reported for intercalating amino acid in LDH. We develop a new approach omitting extreme condition, but instead employ simple and eco-friendly ion-exchange process to successfully place Trp molecule in the LDH interlayer. This incorporation is evidenced by x-ray diffraction (XRD) analysis which exhibits the expansion of basal space from 0.88 nm of pristine ZnAl-LDH (NO₃⁻ form) to 1.92 nm of expected ZnAl-LDH (Trp form). Further scanning electron microscopic (SEM) analysis displays the sheet-like morphology of the product convincing that LDH still retains its original structure. Fourier transform infrared (FT-IR) was used to investigate the presence of carboxylic group and aromatic side chain of Trp molecule (Fig.1). Intercalation aspect differed from surface adsorption of Trp molecule was also confirmed from thermogravimetric analysis (TGA).

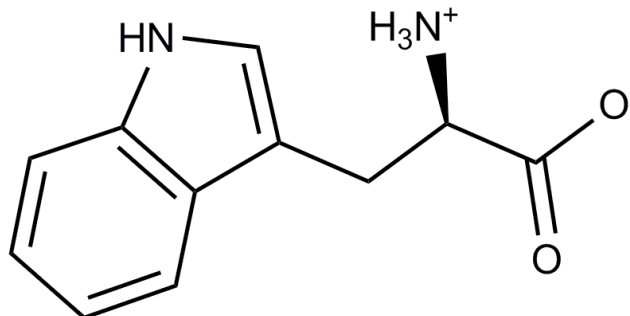


Figure 1. molecular structure of Tryptophan (Trp)

Keywords: ZnAl, LDH, Trp, intercalated

References

1. P. Koilraj, K. Sasaki, K. Srinivasan, *J. of Mater. Chem. A* **2017**, 5, 14783-14793.
2. G. Choi, J.-H. Yang, G.-Y. Park, A. Vinu, A. Elzatahry, C. H. Yo, J.-H. Choy, *Eur. J. Inorg. Chem.* **2015**, 925-930.
3. S. Aisawa, Y. Ohnuma, K. Hirose, S. Takahashi, H. Hirahara, E. Narita, *Appl. Clay Sci.* **2005**, 28, 137-145.

Study of Butyl-Substituted Diquaternary Cations as Organic Structure Directing Agents in Synthesis of Pentasil Zeolites

Veerachart Paluka^{a,b}, Sye Hoe Keoh^c, Watcharop Chaikittisilp^c, Atsushi Shimojima^d, Chompunuch Warakulwit^{a,b,*}, Jumras Limtrakul^c, and Tatsuya Okubo^e

^aDepartment of Chemistry, Faculty of Science, Kasetsart University, Bangkok 10900, Thailand

^bNANOTECH Center of Excellence for Nanoscale Materials Design for Green Nanotechnology and Center for Advanced Studies in Nanotechnology for Chemical, Food and Agricultural Industries, Kasetsart University, Bangkok 10900, Thailand

^cDepartment of Chemical System Engineering, The University of Tokyo, 7-3-1 Hongo, Bunkyo-ku, Tokyo 113-8656, Japan

^dDepartment of Applied Chemistry, Faculty of Science and Engineering, Waseda University, 3-4-1 Ohkubo, Shinjuku-ku, Tokyo 169-8555, Japan.

^eDepartment of Materials Science and Engineering, School of Molecular Science and Engineering, Vidyasirimedhi Institute of Science and Technology, Rayong 21210, Thailand

*e-mail: okubo@chemsys.t.u-tokyo.ac.jp (T. Okubo,) fscicpn@ku.ac.th (C. Warakulwit)

Butyl-substituted diquaternary phosphonium (Bu_6 -diquatP- n) and ammonium (Bu_6 -diquatN- m) cations were synthesized and used as organic structure directing agents (OSDAs) for the synthesis of pentasil zeolites. The obtained zeolite samples were characterized by X-ray powder diffraction (XRD), scanning electron microscopy (SEM) and solid-state cross-polarization magic-angle spinning carbon-13 nuclear magnetic resonance (CP/MAS ^{13}C -NMR) spectroscopy. The results show that changing of the cation type (phosphonium and ammonium cations) affects the phase selectivity in the hydrothermal synthesis of zeolites. For Bu_6 -diquatP- n and Bu_6 -diquatN- m cations, the formation of zeolites was successfully obtained when the numbers of methylene groups between the cation moieties (n or m) are between 5-10 and 6-9, respectively. Nevertheless, it was found in the both cases that with n or m of lower than 8, the MFI zeolite are typically obtained while the formation of MEL zeolites is favored when n or $m \geq 8$. Changing of cation type (P and N) also influences on the product morphology, and in turn, the textural properties of the synthesized MFI zeolites. While it does not influence on the product morphology when MEL zeolites are formed.

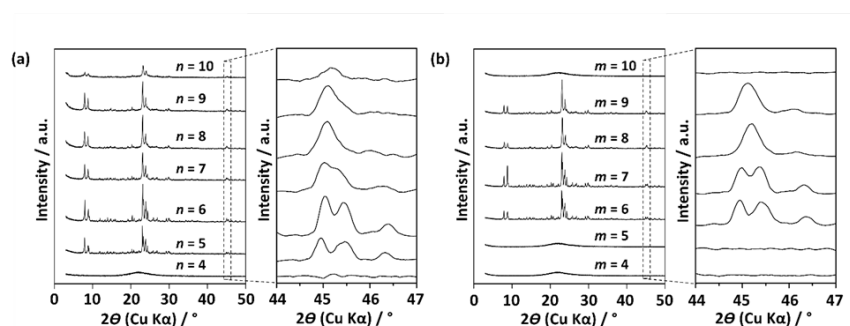


Figure 1. XRD patterns of the products synthesized by using (a) Bu_6 -diquatP- n and (b) Bu_6 -diquatN- m , where $n = m = 4$ -10 as the OSDAs.

Keywords: Diquaternary Cations, Diquaternary Phosphonium Cation, Pentasil Zeolites, MEL, MFI

References

1. S. H. Keoh, W. Chaikittisilp, K. Muraoka, R. R. Mukti, A. Shimojima, P. Kumar, M. Tsapatsis, T. Okubo, *Chem. Mater.* **2016**, *28*, 8997–9007.
2. W. Chaikittisilp, Y. Suzuki, R. R. Mukti, T. Suzuki, K. Sugita, K. Itabashi, A. Shimojima, T. Okubo, *Angew. Chem. Int. Ed.* **2013**, *52*, 3355–3359.

Long-term Efficacy of Self-Disinfecting Coating by Nanomaterial for Decrease Incidence of Infectious Disease

Pawinee Siritongsuk^{a,b}, Rina Patramanon^{a,b*}

^a Department of Biochemistry, Faculty of Science, Khon Kaen University, Thailand

^b Protein and Proteomics Research Center for Commercial and Industrial Purposes, Khon Kaen University, Khon Kaen 40002, Thailand

*E-mail: narin@kku.ac.th

Infectious disease is a worldwide problem. Microbes that cause infectious disease can be found in atmosphere or contaminated on material surfaces. This research aims to develop long-term self-disinfecting coating and low toxicity to human and environment. This is water-based polyurethane that is composed of silver nanocomposite (AgNCs) of silver nanoparticles (AgNPs) and chitosan. AgNPs were tested against 10^5 CFU/mL of *Escherichia coli*, *Vibrio cholerae*, *Staphylococcus aureus* and methicillin-resistant *Staphylococcus aureus* (MRSA) by a serial dilution method. The minimum inhibitory concentration (MIC) and minimum bactericidal concentration (MBC) values are 32-128 $\mu\text{g/mL}$ and 0.156 $\mu\text{g/mL}$, respectively. These MIC and MBC concentration were chosen to use in AgNCs synthesis. These AgNCs were then developed into water-based polyurethane that was the formula of coating agent. The antimicrobial test of coating material was performed and showed that *S.aureus* was reduced to 96.87% when compared to the uncoated surface. If we successfully achieve the purpose of our research, this may be help preventing and reducing the risk of infection.

Keywords: Infectious disease, self-disinfecting coating, silver nanocomposite, water-based polyurethane

References

1. Guo, L., W. Yuan, Z. Lu and C. M. Li (2013). "Polymer/nanosilver composite coatings for antibacterial applications." *Colloids and Surfaces A: Physicochemical and Engineering Aspects* 439: 69-83.
2. Lichter, J. A., K. J. Van Vliet and M. F. Rubner (2009). "Design of antibacterial surfaces and interfaces: polyelectrolyte multilayers as a multifunctional platform." *Macromolecules* 42(22): 8573-8586.
3. Dongwei W., W. Sun, Weiping Q., Yongzhong Y., X. Mac (2009). "The synthesis of chitosan-based silver nanoparticles and their antibacterial activity." *Carbohydrate Research* 344: 2375-2382.
4. Qianqian Z., Jingwei H., J. Shen, Jindun L. and Y. Zhang (2015). "Long-lasting antibacterial behavior of a novel mixed matrix water purification membrane." *J. Mater. Chem. A* 3: 18696-18705

Red Organic Light Emitting Diodes Based on Benzothiadiazole-Thiophene Core Fluorescent Materials Dope with CBP host

Chaiyon Chaiwai,^a Teadkai Kaewpuang,^b Pongsakorn Chasing,^a Taweesak Sudyodsuk^a and Vinich Promarak^{a}**

^a Department of Material Science and Engineering, School of Molecular Science and Engineering, Vidyasirimedhi Institute of Science and Technology, Rayong 21210, Thailand

^b School of Chemistry, Institute of Science, Suranaree University of Technology, Nakhon Ratchasima 30000, Thailand

* vinich.p@vistec.ac.th

Organic light-emitting diodes (OLEDs) are the next-generation technology for lighting applications because of homogeneous illumination, high efficiency and low energy consumption. This work focuses on red-OLEDs using benzothiadiazole-thiophene core fluorescent materials, namely BT1 and BT2. The results show that red-OLEDs (ITO/PEDOT:PSS/BT1 or BT2/TPBi/LiF:Al) which made from BT1 and BT2 demonstrate electro-luminescence (EL) in red region with maximum external quantum efficiency (EQE) around 0.97% and 0.41% respectively. For doped devices (ITO/PEDOT:PSS/BT1 or BT2 in CBP/TPBi/LiF:Al), the suitable doping concentration of 20 wt% in CBP host exhibited improved maximum EQE around 2.15%, and 1.64% for BT1 and BT2, respectively.

Keywords: red-OLEDs, fluorescent material, Benzothiadiazole-Thiophene, CBP host

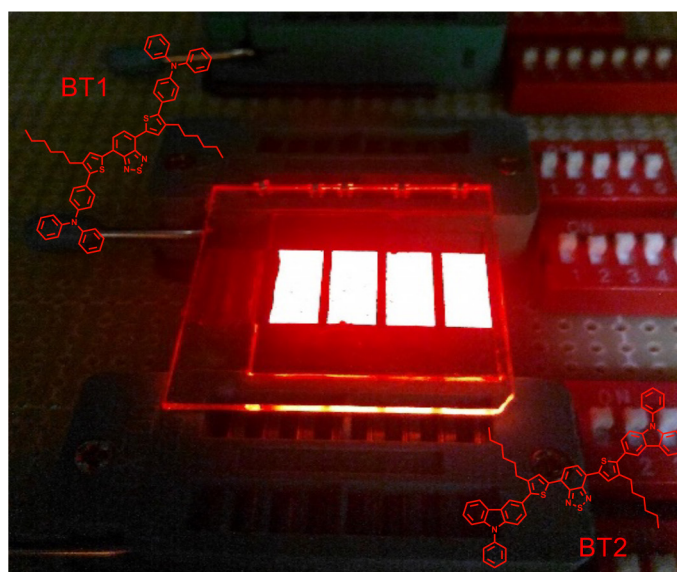


Figure 1. Chemical structure of BT1, BT2 and red-OLEDs device image

Guest Exchange in Soft Porous Zinc(II) Supramolecular Compounds

**Siripak Jittirattanakun^a, Nanthawat Wannarit^a, Winya Dungkaew^b,
Kittipong Chainok^{c,*}**

^a*Division of Chemistry, Faculty of Science and Technology, Thammasat University, Thailand*

^b*Department of Chemistry, Faculty of Science, Maharakham University, Thailand*

^c*Materials and Textile Technology, Faculty of Science and Technology, Thammasat University, Thailand*

**e-mail: kc@tu.ac.th*

A soft porous supramolecular compound, $[\text{Zn}(\text{NCS})_2\text{L}_2] \cdot 2\text{MeOH}$, (**Zn·MeOH**), (where L = N-(2'-pyridylmethylene)-2,3-dimethylaniline) was synthesized. Compound **Zn·MeOH** is stable up to 250 °C and flexible to external stimuli, showing reversible single-crystal-to-single-crystal transformations in response to methanol, ethanol and isopropanol, as demonstrated by X-ray crystallography, infrared spectroscopy, thermogravimetric analysis. In-depth analyses on these soft crystalline materials revealed that the crystal structure stability is primarily due to strong interactions of weak intermolecular forces and not dependent on the size of guest solvent molecules, as confirmed by Hirshfeld surface analyses.

Keywords: Soft Porous, Supramolecular, Zinc(II)

Electrochemical Portable Mini-Potentiostat for Graphene Electrochemical Sensors

Patraporn Tanawattanaprasert^a, Kessararat Ugsornrat^{a*}, Assawapong Sappat^b, Patiya Patsakorn^b, Chakrit Sriprachuabwong^b, and Adisorn Tuantranont^b

^aDepartment of Industrial Physics and Medical Instrumentation, King Mongkut's University of Technology North Bangkok, Bangkok, Thailand

^bThailand Organic and Printed Electronics Innovation Center (TOPIC), National Electronics and Computer Technology Center, Pathumthani, Thailand

*e-mail: kessararat.u@sci.kmutnb.ac.th

This research studied about development of mini-potentiostat to analyze minimal reagent consumption for graphene electrochemical sensors. Mini-Potentiostat was designed with electronics circuits and was fabricated by using integrated circuit and was controlled with microcontroller. Mini-potentiostat was tested for graphene electrochemical sensors the end of T-junction electrowetting on dielectric (EWOD) as digital microfluidic which used for merging droplets to move the droplets to three detectors for analysis. The sensors consist of a screen-printing electrode : a graphene-carbon working electrode, graphene-carbon counter electrode and a silver/silver chloride reference electrode. For analysis, the mini-potentiostat was demonstrated to tested for electrochemical detector for minimal reagent consumption with ferri-ferrocyanide. The concentration of reagent was varied from 2, 4, 6, 8, and 10 μM .

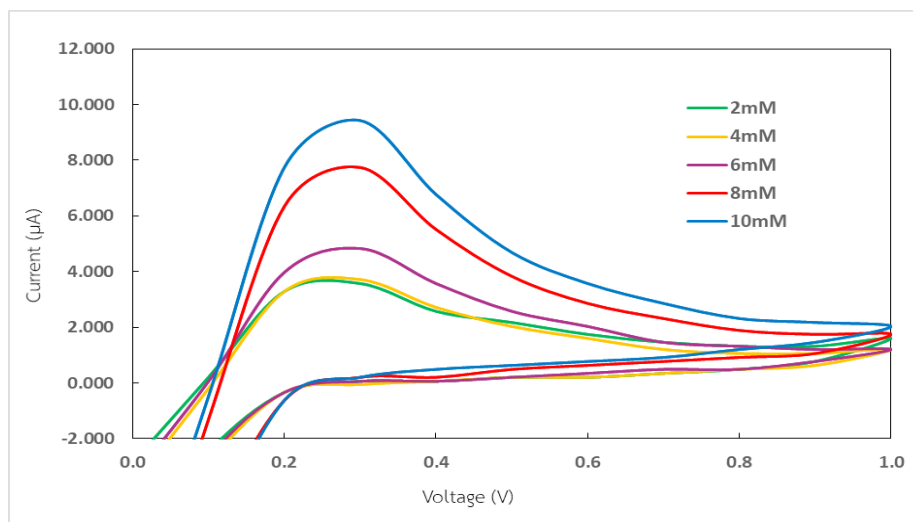


Figure 1. The various current with different scan rate of ferri-ferrocyanide

Keywords: Electrochemical sensors, Mini-Potentiostat, Graphene

References

1. P. H. John. and A. W. Stephen, *Trends in Analytical Chemistry*. **1997**, *16*, 89-103.
2. Y. Keiichiro, C. V. Mun delanji, and T. Eiichi, *Sensors*. **2016**, *16*, 1-16.
3. O.D.Renedo, M.A.Alonso-Lomillo, and M.J. Martinez, *Talanta*. **2007**, *73(2)*, 202-219.
4. W. Joseph, *Chemical Review*. **2008**, *108(2)*, 814-825

Fingerprinting Seamless Single-Walled Carbon Nanotube Junctions and Diameter Modulation: Are SWNT Continuous with Different Diameters?

Theerapol Thurakitseree^{a,*}, Christian Kramberger^b, Pisith Singjai^c, and Shigeo Maruyama^{d,e}

^a Program in Applied Physics, Faculty of Science, Maejo University, Chiang Mai, Thailand

^b Research Group Physics of Nanostructured Materials, Faculty of Physics, University of Vienna, Vienna, Austria

^c Department of Physics and Materials Science, Chiang Mai University, Chiang Mai, Thailand

^d Department of Mechanical Engineering, School of Engineering, University of Tokyo, Tokyo, Japan,

^e National Institute of Advanced Industrial Science and Technology, Tsukuba, Japan

*e-mail: theerapol@mju.ac.th

Structure control such as diameter changes along single-walled carbon nanotubes (SWNTs) can be achieved in arrays of vertically aligned (VA-) SWNTs by switching the feedstock during growth in chemical vapor deposition (CVD) process^{1,2}. The local nature of the macroscopic transition from one diameter to another is then questioned as one can either envisage seamless transitions or discontinuous individual SWNTs. From our previous study³, the nanotube connection between tube-to-tube has been observed with the majority of discontinuous. However, seamless nanotubes could be also traced by migration of gas molecules stored inside the small interior. Here, we demonstrate that encapsulated molecules can serve as markers to doubtlessly identify seamless interconnections in macroscopic samples. A migration of nitrogen molecules inside continuous SWNTs is observed by bulk scale measurements on double-layered SWNT array synthesized from different carbon/nitrogen feedstocks. The existence of N₂ molecules at the top of the SWNT array proves continuous SWNTs throughout double layered arrays with different diameters as shown in Figure 1.

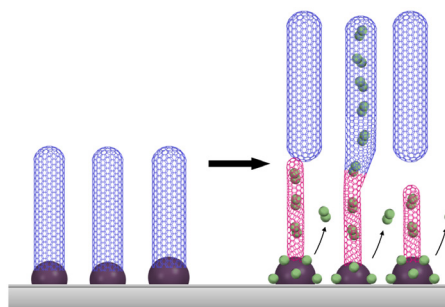


Figure 1. The diameter of single-walled carbon nanotubes could be modulated during the nanotube growth, while the nanotube junctions could be either continuous or discontinuous connections.

Keywords: Single-walled carbon nanotube, Encapsulated nitrogen, Connected junction, Diameter reduction

References

1. R. Xiang, Z. Zhang, K. Ogura, J. Okawa, E. Einarsson, Y. Miyauchi, J. Shiomi, S. Maruyama, *Jpn. J. Appl. Phys.* **2008**, *47*, 1971–1974.
2. T. Thurakitseree, C. Kramberger, A. Kumamoto, S. Chiashi, E. Einarsson, S. Maruyama, *ACS Nano* **2013**, *7*, 2205–2211.
3. T. Thurakitseree, C. Kramberger, S. Maruyama, *Nanoscale* **2018**, *10*, 14579.

A Study on the Performance of Digital Microfluidic Microchip with NrGO Electrochemical Detector Fabricated by Screen Printing Method

Thanakrit Thanacharoenchanaphas^a, Paleerak Keerat^a, Kessararat Ugsornrat^{a*}, Chakrit Sriprachuabwong^b, Patiya Patsakorn^b, Assawapong Sappat^b, Nithi Atthi^c, Tawee Pogfai^b, and Adisorn Tuantranont^b

^aDepartment of Industrial Physics and Medical Instrumentation, King Mongkut's University of Technology North Bangkok (KMUTNB), Bangkok, Thailand

^bThailand Organic and Printed Electronics Innovation Center (TOPIC), National Electronics and Computer Technology Center (NECTEC), Pathumthani, Thailand

^cThai Microelectronics Center (TMEC), National Electronics and Computer Technology Center (NECTEC), Pathumthani, Thailand

*e-mail: kessararat.u@sci.kmutnb.ac.th

In this research, a performance of graphene digital microfluidic microchip with N-doped reduced graphene oxide (NrGO) electrochemical detector that fabricated by screen printing method was studied. The microchip comprised with an integrated single plate of electrowetting on dielectric (EWOD) and electrochemical sensing on single plate substrate. In this time, EWOD electrodes were designed as close-pack space electrode arrays that comprises of thirty square electrodes arranged in a T-junction configuration for merging buffer reagent and analyze chemical droplets. Whereas three electrochemical sensing electrodes that comprises of NrGO graphene-carbon working/counter and silver reference lines are located at the end of T-junction to sense the mixing of analyze chemical droplets. Both parts were fabricated by screen printing technique. The performance of electrochemical detection of microfluidic chip was characterized by using mini-potentiostat for minimal hydrogen peroxide (H_2O_2) reagent consumption. The concentration of H_2O_2 was varied at 20, 40, 60, 80 and 100 μM . The current-voltage (I_g - V_g) characteristic shown that I_g has increased by increasing a V_g . The threshold voltage of microfluidic chip is higher than 0.3 V. The I_g (@ $V_g = 1.0$ V) has increased from 0.2 to 2.0 μA by increased a concentration of H_2O_2 from 20 to 100 μM . This means, NrGO electrochemical detector fabricated by low-cost screen printing method was found to significantly improve the sensitivity of graphene digital microfluidic microchip.

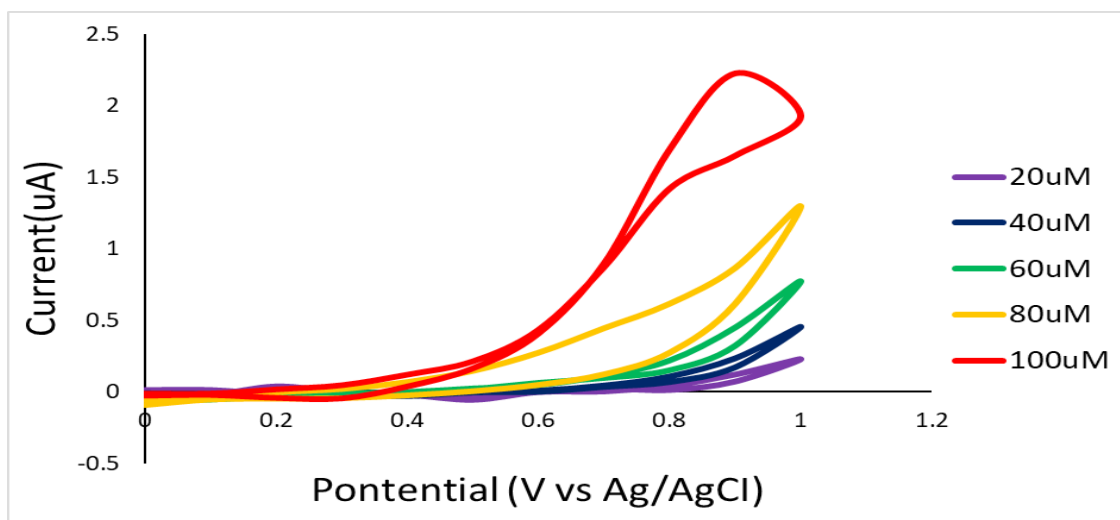


Figure 1. The I-V characteristics of graphene digital microfluidic microchip NrGO electrochemical detector in H_2O_2 reagent fabricated by screen printing method.

GRA-P-04

Keywords: Digital Microfluidics, Electrochemical Detector, Graphene, NrGO, Screen printing

References

1. A. Wisitsoraat, C. Karuean, K. Wong-ek, D. Phokharatkul, P. Sritongkham and A. Tuantranont, *Sensors*. **2009**, *9*, 8658-8668.
2. J. Noiphung, T. Songjaroen, W. Dungchai, C. S. Henry, O. Chailapakul and W. Laiwattanapaisal, *Analytica Chimica Acta*. **2013**, *78*, 39-45.
3. Y. Keiichiro, C. V. Mun delanji and T. Eiichi, *Sensors*. **2016**, *16*, 1-16.
4. P. H. John. and A. W. Stephen, *Trends in Analytical Chemistry*. **1997**, *16*, 89-103.
4. O.D.Renedo, M.A.Alonso-Lomillo, and M.J. Martinez, *Talanta*. **2007**, *73(2)*, 202-219.

The Effects on Proliferation and Differentiation of Bone-Forming Cells using Electrodeposited Graphene Oxide

Pacharabhorn Tanurat and Sirinrath Sirivisoot*

Biological Engineering Program, Faculty of Engineering, King Mongkut's University of Technology Thonburi, Bangkok 10140, Thailand

**e-mail: sirinrath.sir@kmutt.ac.th*

Graphene oxide (GO) coating on biomaterial surfaces have been increasingly studied because GO improves biocompatibility of biomaterials [1], [2]. This study showed the results from pre-osteoblast proliferation and cell differentiation assays on commercial pure titanium (Ti), anodized titanium (ATi), GO electrodeposited on Ti, and GO electrodeposited on ATi. The results showed that the GO electrodeposited on ATi samples had significantly increased the proliferation of MC3T3-E1 cells after 3 and 5 days of cultivation when compared with ATi and Ti samples. Cell differentiation of MC3T3-E1 was evaluated for calcium deposition, total protein, and alkaline phosphatase (ALP) activity at day 7, 14, and 21 of cultivation. The results showed that the GO electrodeposited on ATi samples had significantly highest in ALP activity and total protein at day 7, 14, and 21. Furthermore, calcium deposition on the GO electrodeposited on ATi samples was significantly highest at day 14 and 21 of cultures. Importantly, the use of GO electrodeposited on ATi can improve pre-osteoblast proliferation and differentiation in a standard cell culture, suggesting that this material has a potential to be used as an alternative biomaterial for bone implants.

Keywords: Biocompatibility, Graphene oxide, Titanium dioxide nanotube array

References

1. A.M. Pinto, I.C. Gonçalvesb, and F.D. Magalhães, *Colloids and Surfaces B: Biointerfaces*, **2013**, Vol. 111, pp. 188-202.
2. Y. Ma, J. Hana, M. Wang, X. Chen, and S. Jia, *Journal of Materiomics*, **2018**, Vol. 4, pp.108-120.

Materials for Sustain Release of Antibiotics in Bone Spacer

Pongpat Oungeun^a, Rojrit Rojanathanes^b, Supasorn Wanichweacharungruang^{a,*}

^a*Department of Petrochemistry and Polymer Science, Faculty of Science, Chulalongkorn University, Phayathai road, Pathumwan Bangkok 10330, Thailand*

^b*Department of Chemistry, Faculty of Science, Chulalongkorn University, Phayathai road, Pathumwan Bangkok 10330, Thailand*

**e-mail: supason.p@chula.ac.th*

Bone spacer is a device developed to temporarily insert into the body to treat infected tissue caused by bone replacement. Burst release of antibiotics from normal bone spacer not only limit their ability to clear infection but also cause tissue inflammation. Therefore, here we have fabricated bone spacers containing antibiotic-loaded nano- and microparticles, and study their antibiotic release character. Various polymeric particles were investigated. Vancomycin and erythromycin were used as hydrophilic and hydrophobic model drugs, respectively. Rice granules and calcium citrate particles were selected to encapsulate vancomycin because these materials are soluble in the medium of water and poly (lactic-co-glycolic acid) particles and ethyl cellulose particles were selected to encapsulate erythromycin because these materials are soluble in the medium of ethanol. In addition, All of these materials have selected for this study are compatible with human tissue. Drug loading in each particle type was investigated through the quantification of unencapsulated drug using UV-VIS spectrophotometer at 287 nm and 207 nm for vancomycin and erythromycin, respectively. Then the drug-loaded particles were impregnated into poly (methyl methacrylate) bone spacer. Antibiotics released from the obtained bone spacer into PBS buffer pH 7.4 was monitored at 37 celcius by analyzing the release medium using UV-VIS spectrophotometry. The results of vancomycin encapsulation showed that rice granule showed the percent of encapsulation efficiency (%EE) 70% and calcium citrate particles encapsulated 20%. In case of erythromycin encapsulation, poly (lactic-co-glycolic acid) particles showed percent encapsulation efficiency 90% and ethyl cellulose particles encapsulated 60%. For the results of antibiotics released in 7 days. In case of vancomycin, adding vancomycin directly in bone spacer showed the initial burst release 2.06 mg. While rice granules particles decreased the initial burst release of antibiotics down to 1.36 mg but calcium citrate increased the initial burst release of antibiotics up to 7.93 mg. In case of erythromycin, adding erythromycin directly in bone spacer showed the initial burst release 6.59 mg. After erythromycin encapsulation in poly (lactic-co-glycolic acid) particles and ethyl cellulose particles the initial burst release increased up to 13.26 and 15.62 mg, respectively. However, calcium citrate particles and ethyl cellulose particles released the amount of drug highest in each type of drugs after passed 7 days.

References

1. Stevens, C. M., Tetsworth, K. D., Calhoun, J. H., & Mader, J. T. An articulated antibiotic spacer used for infected total knee arthroplasty: a comparative in vitro elution study of Simplex® and Palacos® bone cements. *J Orthop Res.* 2005, 23(1), 27-33.
2. Kelm, J., Regitz, T., Schmitt, E., Jung, W., & Anagnostakos, K. In vivo and in vitro studies of antibiotic release from and bacterial growth inhibition by antibiotic-impregnated polymethylmethacrylate hip spacers. *Antimicrob Agents Chemother.* 2006, 50(1), 332-335.
3. DeSilva, G. L., Fritzler, A., & DeSilva, S. P. Antibiotic-impregnated cement spacer for bone defects of the forearm and hand. *Tech Hand Up Extrem Surg.* 2007, 11(2), 163-167.

Keywords: Bone spacer, Antibiotic release, Drug encapsulated particles

Development of Nanoparticles Containing *Litsea Glutinosa* and *Centella Asiatica* as a Promising Active Ingredient in Hair Care Product.

Supatchaya Jaemsai^a, Chutikorn Phungbun^a, Pichaporn Bunwatcharaphansakun^a and Mattaka Khongkow^{*a}

^aNational Nanotechnology Centre (NANOTECH), National Science and Technology Development Agency, 111 Thailand Science Park, Paholyothin Rd., Klong Luang, Pathumthani, 12120, Thailand

*e-mail: mattaka@nanotec.or.th

The Mucilage of *Litsea glutinosa* leaves has been widely used as a conventional medicinal herb to induce hair growth. It has been reported that the treatment of this mucilage stimulates the proliferation of human follicle dermal papilla cells (HFDPC). This research, we found that water-extracted mucilage induced HFDPC proliferation was noticeably higher than those of Minoxidill, a widely used in enhanced hair growth. Exhibitionally, this suggests a potential effect of mucilage as a hair growth stimulator. The *Centella asiatica* leaves, also known as centella has been used traditionally in medicine and cosmeceutical applications. The aqueous extract of centella has been shown to exhibit anti-inflammatory activity to increase the strength of scalp and hair. To develop delivery system and improve cell penetration, we prepared LipoNiosome nanoparticle containing 1-2% of each extract or mixed two extracts in the combination with phospholipid, nonionic surfactants, cholesterol and tocopherol by homogenization. The obtained LipoNiosome particles, were smooth globular in their morphology with particle size in range of 100-130 nm and polydispersity index (PDI) in range of 0.20-0.30. Interestingly, the nanoparticles containing mucilage extract (MU) showed a significant increase in HFDPC proliferation higher than those of extract. Additionally, the centella extract encapsulating particles (CA) exhibited significantly stronger anti-inflammation activity than that of centella extract. These results suggest that formulation of LipoNiosome encapsulating combined mucilage and centella extracts is able to improve a potential effect of these compounds on hair growth and hair strength induction. Successfully, nanoparticle formulation containing mucilage and/or centella extracts potentially provide a very promising candidate using as an active ingredient in hair care products.

Keywords: *Litsea glutinosa*, *Centella asiatica*, Nanoparticles, Induce hair growth

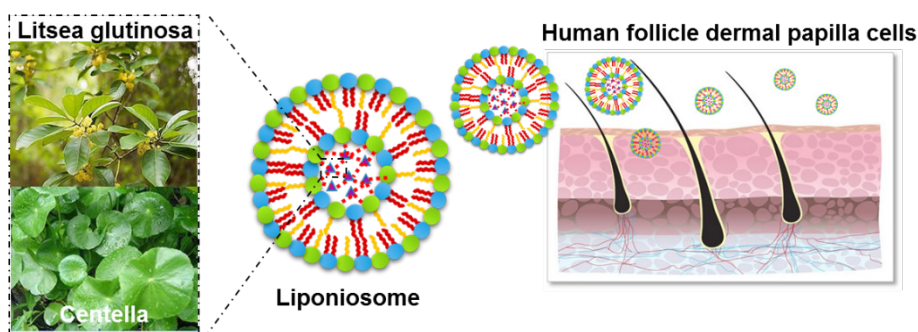


Figure 1. Nano-encapsulation of *L. glutinosa* and *C. asiatica* leaves for increasing of hair strength and anti-inflammation

Formulation and Characterization of Lipiosome Encapsulating Fenugreek Extract for Cosmeceutical Usages

Waleewan Eaknai*, Phichaporn Bunwatcharaphansakun, Mattaka Khongkow, Sasikarn Chaisri, Chutikorn Phungbun, Suwimon Boonrunsi, and Ubonthip Nimmannit

National Nanotechnology Center (NANOTEC), National Science and Technology Development Agency, Pathumtani, Thailand

*e-mail: waleewan@nanotec.or.th

Trigonella foenum-graecum L. or fenugreek has been widely used to increase postnatal lactation and possessed various biological activities¹. In this work, we present a novel role and delivery system of fenugreek extract for cosmeceutical application. Briefly, the ethanolic extract of fenugreek seed powder from Herbal Acharn's Home Co., Ltd was examined its biological activity, including DPPH radical scavenging ($IC_{50} = 1.20 \pm 0.02$ mg/mL) and anti-collagenase activity ($IC_{50} = 0.57 \pm 0.02$ mg/mL). We observed that the extract exhibits a novel cosmetic properties with a low in its physical stability. Therefore, nano-encapsulation was applied to resolve this problem². Lipiosome encapsulating fenugreek extract was formulated and kept at 4°C, 25°C and 40°C for three months to investigate its stability. The highly stable oval-shaped nanoparticles were obtained by the formation of phospholipid bilayers with an entrapment of fenugreek extract in the middle. The particle size was approximately 167.93-270.38 nm by DLS measurement. The percentage of entrapment efficiency (%EE) was 44.02-49.18% by UHPLC quantification using rutin as a standard marker. For cytotoxicity of these particles, MTT was performed and found that the lipiosome containing fenugreek was able to improve cell viability compared to blank lipiosome. All of these results suggest that lipiosome encapsulating fenugreek extract could be used as a new potential active anti-aging agent for cosmetic products.

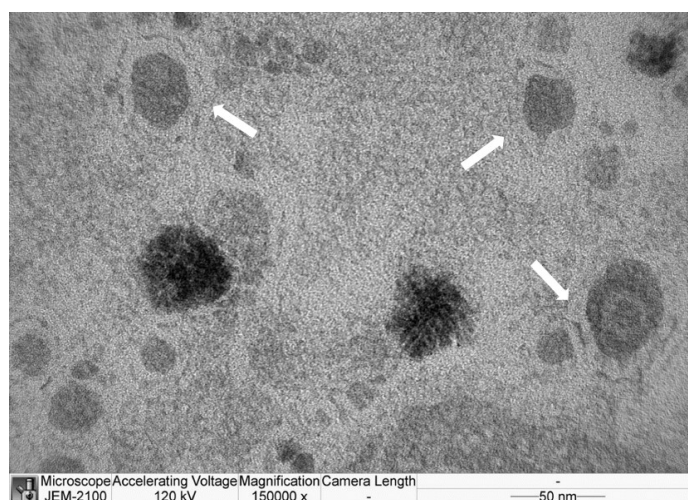


Figure 1. TEM image of lipiosome of fenugreek extract

Keywords: Fenugreek, Lipiosome, Anti-collagenase, Anti-aging, Rutin

References

1. S. A. Wani, P. Kumar, J. Saudi Soc Agri Sci. 2016, 17, 97-106.
2. M. Vinceković, M. Viskić, S. Jurić, J. Giacometti, D. B. Kovačević, P. Putnik, F. Donsi, F. J. Barba, A. R. Jambrak, Trends Food Sci Technol. 2017, 69, 1-12

Effect of Nanoparticle Containing Butterfly pea as an Active Ingredient for Hair Treatment

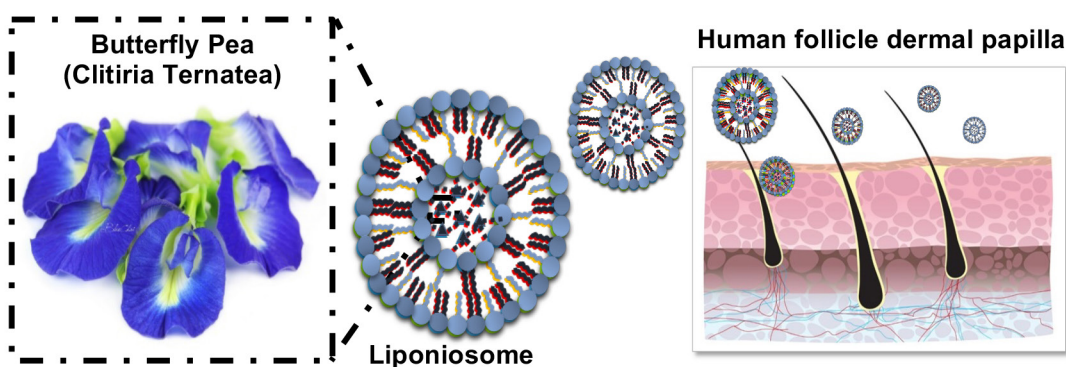
Angkana Jantimaporn,¹ Supatchaya Jaemsai,¹ Mattaka Khongkow,^{*1}

¹National Nanotechnology Centre (NANOTEC), National Science and Technology Development Agency, 111 Thailand Science Park, Paholyothin Rd., Klong Luang, Pathumthani, 12120, Thailand

*e-mail: mattaka@nanotec.or.th

Butterfly Pea (*Clitoria Ternatea*) is known as a Thai traditional ingredient in cosmetics, generally used for hair treatment. The benefit of butterfly pea is promoting hair growth, reducing hair loss and preventing grey hair. The active compound of butterfly pea is anthocyanin which exhibits antioxidant activity. Nowadays, nanotechnology is widely used to improve stabilities and abilities of phytochemical extracts in cosmeceutical products.

Our Nano-cosmeceutical laboratory has been developing nanoparticle containing butterfly pea. Therefore, this research focuses on cytotoxicity and bioactivities of this nanoparticle in primary human follicle dermal papilla cells (HFDPC). We found that nanoparticle containing butterfly pea showed low toxic to HFDPC. Moreover, it exhibited an inductive effect on tyrosinase activity in melanocytes (B16F10), which subsequently induce melanin production. Additionally, nanoparticle containing butterfly pea could stimulate proliferation of H₂O₂-induced cytotoxicity in HFDPC, higher than those of butterfly pea extract, suggesting a protective effect of this nanoparticle containing butterfly pea against free radical. All of these results demonstrated that formulation of nanoparticle containing butterfly pea is able to improve antioxidant property of the extract and can be used as a good active ingredient for hair care products



Keywords: Butterfly pea, Human follicle dermal papilla, Nanoparticle, Antioxidant

QM/MM Study on Cleavage Mechanism Catalyzed by NS2B/NS3 Serine Protease of Zika virus

Bodee Nutho,^a Adrian Mulholland,^b and Thanyada Rungrotmongkol^{c,d,*}

^a Program in Biotechnology, Faculty of Science, Chulalongkorn University, Bangkok, Thailand

^b Centre for Computational Chemistry, School of Chemistry, University of Bristol, U.K.

^c Structural and Computational Biology Research Group, Department of Biochemistry, Faculty of Science, Chulalongkorn University, Bangkok, Thailand

^d Ph.D. Program in Bioinformatics and Computational Biology, Faculty of Science, Chulalongkorn University, Bangkok, Thailand

*Email: thanyada.r@chula.ac.th

Zika virus (ZIKV), a mosquito-borne flavivirus, was originally isolated from sentinel rhesus monkey in the Zika Forest of Uganda in 1947. The virus is transmitted to humans by *Aedes* species mosquitoes. The recent evidences have revealed that this virus is now associated with serious pathological disorders including microcephaly in newborns and Guillain-Barré syndrome in adults. Up to now, there is no currently available vaccine or therapeutic drug for preventing or controlling ZIKV infection. One of the attractive drug-targets for ZIKV treatment is the nonstructural (NS)2B/NS3 serine protease that processes viral polyprotein during infection. Here we have used a hybrid Quantum Mechanics and Molecular Mechanics (QM/MM) umbrella sampling simulation at the PM6/ff14SB level of theory to investigate the acylation step of the reaction catalyzed by the enzyme. The obtained results reveal that proton transfer from S135 to H51 and nucleophilic attack on the substrate by S135 occur in a concerted manner. The rate determining step is considered as the tetrahedral intermediate formation with an energy barrier of ~ 10.0 kcal·mol⁻¹. In addition, single-point energy QM/MM calculations on the BH&HLYP-D3/6-31G(d)/ff144SB optimized geometries were carried out at the SCS-(L)MP2/(aug)-cc-pVTZ/ff14SB and L-CCSD(T)/(aug)-cc-pVTZ/ff14SB to correct the potential energy surfaces. The average values of computed activation energies at the SCS-LMP2/(aug)-cc-pVTZ/ff14SB of 17.8 ± 1.2 kcal·mol⁻¹ and L-CCSD(T)/(aug)-cc-pVTZ/ff14SB of 16.3 ± 1.4 kcal·mol⁻¹ are in good agreement with the experimental data. Therefore, the ability of the QM/MM presented here could be informative and useful for further designing of NS2B/NS3 inhibitors based on transition state analogues.

Keywords: Enzyme catalysis, NS2B/NS3 serine protease, QM/MM reaction mechanism, Zika virus

References

1. Phoo, W. W., Li, Y., Zhang, Z., Lee, M. Y., Loh, Y. R., Tan, Y. B., Ng, E. Y., Lescar, J., Kang, C., and Luo, D., *Nat. Commun.*, **2017**, 7, 1-8.
2. Lee, H., Ren, J., Nocadello, S., Rice, A. J., Ojeda, I., Light, S., Minasov, G., Vargas, J., Nagarathnam, D., Anderson, W. F., Johnson, M. E., *Antiviral res.*, **2017**, 139, 49-58.

Lignin-Based Bioadhesive for Skin Retention of Topically Applied Compounds

Nutthanit Thumrongsiri^a, Thanisorn Mahatnirunkul^a, Thitikorn Chomtong^a, Udom Asawapirom^a,
Nattika Saengkrit^{a*}

^a National Nanotechnology Center, Pathum Thani 12120, Thailand

*e-mail: nattika@nanotec.or.th

Lignin is one of the most well-known biomass by-products obtained from pulp and paper production industries. The utilization of lignin has still been challenging due to its varied, complex chemical structure and unique morphology. Recently, various studies have reported about the novel uses of lignin in cosmetic and medical applications. In this study, we aimed to synthesize lignin nanoparticle (LiNPs) and modify its surface to enhance the adherence of nanoparticle on skin. Lignin nanoparticles could be used to carry active compounds for topical delivery in order to prevent skin penetration of loaded compounds. The synthesis of LiNPs started from dissolving alkali lignin in acetone:water (9:1 v/v) and subsequently introduced lignin solution into the water system through syringe filter. In order to improve particle bioadhesive property, poly (vinyl) alcohol (PVA) was employed as a coating materials. Different concentrations of PVA were prepared for coating on LiNP surfaces with a weight ratio of lignin:PVA at 1:1. Physicochemical of LiNPs was characterized using dynamic light scattering (DLS). LiNP morphologies were observed under scanning electron microscope (SEM). The result indicated that the average size of LiNPs was approximately 153 nm with a highly negatively charge -32 mV. Coating of PVA induced the increasing of particle sizes and charges. Meanwhile, SEM images revealed the spherical and discrete nanoparticles. The bioadhesive property was confirmed in ex vivo using pig skin as a model. LiNPs labelled with rhodamine fluorescence dye were applied on fresh pig skin. The result was investigated under fluorescence microscope after skin cross sections. At 2 h post-incubation, higher signal intensities of fluorescence were observed from the skin treated by PVA coated LiNPs compared with LiNP. The result suggested that PVA coated LiNPs could be retarded on skin stratum corneum. In conclusion, these PVA coated LiNPs would be potential alternative nanocarriers for non-skin penetration purpose. The delivery system is practical for encapsulation of UV filters to avoid accumulation of compounds in the body.

Keywords: Lignin, Lignin nanoparticles, Nanoperticles, Bioadhesive

References

1. Yang, F.; Lewis, J.; Girardi, M.; Saltzman, W. M. A Sunblock Based on Bioadhesive Nanoparticles *Nature materials*. **2015**, 14, 1278–1285
2. Lievonon M, Valle-Delgado JJ, Mattinen M-L, Hult E-L, Lintinen K, Kostianen MA, et al. Simple process for lignin nanoparticle preparation. *Green Chemistry*. 2016;18:1416–1422.

Herbal Medicine-Loaded Nanostructure Lipid Carrier (NLC) for Topical Delivery System: Physicochemical and Bioactivity Properties

Narin Paiboon, Kunat Suktham, Jakarwan Yostawonkul, Jayanant Iemsam-arng, and Suvimol, Surassmo*

National Nanotechnology Centre (NANOTECH), National Science and Technology Development Agency, Pathumthani, Thailand.

*e-mail: suvimol@nanotec.or.th

Herbal medicines have been widely used in the field of medicinal, pharmaceutical and cosmeceutical since ancient times. In this research, six crude herbal extracted including Galangal, Turmeric, Phlai, Jewel Vine, Sappan wood and Black ginger were investigated in their biochemical and biological properties which revealed high anti-inflammation, high anti-oxidation and low cytotoxicity against human skin fibroblast (CRL-2522). Due to the poor solubility of these herbal extracted, nanostructured lipid carriers (NLCs) was performed to encapsulate active ingredient of herbal medicines extracted via high energy method. The average particle size of herbal encapsulated NLCs was in the range of 72-124 nm with negatively charged (more than -35 mV). Encapsulation efficiency of herbal-loaded NLCs which determined in each active component (curcumin, gingerol and sabinene) was dependent to the amount of herbal extracted and it remained stable after 4 month at accelerate condition (45°C). Anti-inflammatory properties via COX-1 and COX-2 assay demonstrated more than 70% anti-inflammation for MH1 (70.76±0.01, 99.67±0.04) , MH6 (75.57±0.39, 100±0.01) and MH7 (72.24±0.02, 82.72±0.02) formulations could be observed and these herbal-loaded NLC showed high anti-oxidation activity by nitrite scavenging comparable to free herbal extracted. *In vitro* cytotoxic activity against CRL-2522 and RAW 264.7 cell lines revealed time-dependent effect of herbal-loaded NLCs. MH6 and MH7 formulations showed low toxicity than MH1 against CRL-2522 and RAW 2564.7 cells after 48 h of incubation. All result suggested that herbal NLCs contained a mixtures of 0.05% (w/w) galangal, 0.05% (w/w) turmeric and 0.05% (w/w) phlai extracted could be the optimum formulation. These result demonstrated the ability of NLCs to encapsulated natural herbal extracted with maintained their unique biological and biochemical functions. Taken together, this would be found the beneficial effect of herbal medicines encapsulated NLCs having a profound future potential for topical delivery system.

Keywords: Herbal medicines, Nanostructure lipid carriers, Topical delivery system, Anti-inflammation,



References

1. V. Mamillapalli, A Malyada Atmakuri, P. Khantamneni, *Asian J Pharm.* 2016, 10, 12-21
2. B.V Bonifácio, P.B. da Silva, M.A. dos Santos Ramos, K.M.S. Negri, T.M. Bauab, M. Chorilli, *Int J Nanomedicine*, 2014, 9, 1-15

Antibacterial Synergistic of Ceftazidime with Silver Nanoparticles as a Possible Alternative for Treatment of Melioidosis

Sathit Malawong^{a,b}, Saengrawee Thammawithan^{a,b}, Rina Patramanon^{a,b*}

^a Department of Biochemistry, Faculty of Science, Khon Kaen University, Khon Kaen, 40002, Thailand

^b Protein and Proteomics Research Center for Commercial and Industrial Purposes, Khon Kaen University, Khon Kaen 40002, Thailand

*e-mail: narin@kku.ac.th

Melioidosis, an infectious disease which is caused by Gram-negative bacteria named *Burkholderia pseudomallei* (*BP.*). This bacteria is widespread in the soil and surface water in Southeast Asia and northern Australia. Most cases of melioidosis (85%) result in acute infections from recent bacterial exposure. Presently, there is no vaccine against melioidosis and it can be fatal if not treated with a specific antibiotic regimen, which typically includes the third-generation cephalosporin, ceftazidime (CAZ). However, in present study, some clinical isolates of *BP.* reveal their resistance to ceftazidime both in vitro and in vivo. To resolve this problem, we evaluated antibacterial agent which has synergistic effect between CAZ and silver nanoparticles (AgNPs) against 2 isolates of *BP.* including *BP.* 1026b and *BP.* 316c that are CAZ-non-resistant isolate and CAZ-highly resistant isolate, respectively. Synergistic antibacterial effects were evaluated by the fractional inhibitory concentration (FIC) index and the fractional bactericidal concentration (FBC) index, which were obtained by the plate count of micro-dilution checkerboard method. The result from antimicrobial test found that minimum inhibitory concentration (MIC) and minimum bactericidal concentration (MBC) values of CAZ against *BP.* 1026b are 4 and 64 $\mu\text{g/mL}$ while *BP.* 316c are 128 and 512 $\mu\text{g/mL}$. Likewise, the MIC and MBC of AgNPs against *BP.* 1026b are 8 and 16 $\mu\text{g/mL}$ while *BP.* 316c are 16 and 32 $\mu\text{g/mL}$. Interestingly, combination effect of CAZ and AgNPs against *B. pseudomallei* 1026b exhibit synergistic antimicrobial effects at 1 and 2 $\mu\text{g/mL}$ that was 4-fold lower in the combination of both agents than using each agent alone while *B. pseudomallei* 316c exhibit synergistic antimicrobial effects of CAZ and AgNPs at 16 and 4 $\mu\text{g/mL}$ that was 8-fold lower in the combination of both agents than using each agent alone. In addition, kinetic time-killing studies were performed using micro-dilution plate count at concentrations of their FIC and the result were found that at the combination condition could reduce the growth of both bacterial isolates within 30 min but could not completely reduce the bacterial growth. These results indicated that the combination between CAZ and AgNPs show strongly synergistic effect to these bacteria. This finding provides an advantage in delivering robust solutions of clinically-relevant synergistic antibiotics for possible alternative for treatment of melioidosis. In the future work, we will further study about AgNPs in the aspects of cytotoxicity and bacterial resistance to fulfil more selectivity and biocompatibility which can be served as the effective antibacterial agents in medical applications.

Keywords: Synergistic, Combination, Silver nanoparticles, Melioidosis, *Burkholderia pseudomallei*

References

1. D. Limmathurotsakul, S. Wongratanacheewin, N. Teerawattanasook, G. Wongsuvan, S. Chaisuksant, P. Chetchotisakd, W. Chaowagul, Nicholas P. J. Day, and Sharon J. Peacock. Am. J. Trop. Med. Hygiene. 2010, 82(6), 1113–1117.
2. W. Joost Wiersinga, Harjeet S. Virk, Alfredo G. Torres, Bart J. Currie, Sharon J. Peacock, David A. B. Dance and D. Limmathurotsakul. Nat Rev Dis Primers. 2018, 4, 1-22.

Anisotropic Silver Nanoparticles, an Alternative Treatment as the Effective Antimicrobial Agents

Saengrawee Thammawithan^{a,b}, Rina Patramanon^{a,b*}

^a Department of Biochemistry, Faculty of Science, Khon Kaen University, Khon Kaen, 40002, Thailand

^b Protein and Proteomics Research Center for Commercial and Industrial Purposes, Khon Kaen University, Khon Kaen 40002, Thailand

*e-mail: narin@kku.ac.th

Silver nanoparticles (AgNPs) are known as the effective antibacterial agent. The antimicrobial effect of AgNPs depends on physical properties including their shape and size. In this research, we evaluated antibacterial activity and cytotoxic effect of both AgNPs and anisotropic AgNPs which have difference in size and shape. The AgNPs were synthesized by chemical method and the colloidal solution showed yellow color then such AgNPs were added into H₂O₂ to obtain anisotropic AgNPs. The result from characterization by TEM found that AgNPs with yellow solution showed average sizes of 5 nm in spherical shape while anisotropic AgNPs with orange solution showed average sizes of 30 nm in mix shapes of spherical, triangular and hexagonal nanoplates. The antibacterial activity by the microdilution plating method found that minimum inhibitory concentration (MIC) and minimum bactericidal concentration (MBC) values of AnNPs against *E.coli* O157/H7 and *S.aureus* ATCC25923 are in the range of 1-8 µg/mL and 2-16 µg/mL, respectively. In a similar way, the MIC and MBC value of anisotropic AgNPs against *E.coli* O157:H7 and *S.aureus* ATCC 25923 are in the range of 2-16 µg/mL and 2-32 µg/mL, respectively. For the cytotoxicity, the result exhibited that AgNPs showed an IC₅₀ of 30.80±14.67 µg/mL and 17.70±13.67 µg/mL on cell line of keratinocyte and fibroblast while anisotropic AgNPs showed an IC₅₀ of 65.39±13.84 µg/mL and 65.39±13.84 µg/mL in the same cell with AgNPs testing. From these results reveal that antimicrobial activity of AgNPs and anisotropic AgNPs is slightly different but cytotoxic effect of AgNPs show more cytotoxic than anisotropic AgNPs in both types of cell line. These finding suggest that both AgNPs types is efficient antimicrobial agent against bacteria, especially anisotropic AgNPs is safer for using in living organisms.

Keywords: Silver nanoparticles, Anisotropic silver nanoparticles, Antimicrobial, Cytotoxicity

References

1. P. V. Dong, C. H. Ha, L. T. Binh and J. Kasbohm. Int Nano Lett. 2012, 2-9
2. T. Parnklang, C. Lertvachirapaiboon, P. Pienpinijtham, K. Wongravee, C. Thammacharoen and S. Ekgasit. RSC Adv. 2013, 3, 12886–12894.
3. X. Zheng, Y. Peng, X. Cui and W. Zheng. Mater Lett. 2016, 173, 88–90.
4. M. Vedhanayagam, M. Nidhin, N. Durai Pandey, N. D. Naresh, G. Jaganathan, M. Ranganathan, M. S. Kiran, S. Narayan, B. U. Nair, K. J. Sreeram. Int J Biol Macromol. 2017, 99, 655–664.
5. F. J. Osonga, A. Akgul, I. Yazgan, A. Akgul, R. Ontman, V. M. Kariuki, G. B. Eshuna and O. A. Sadik. RSC Adv. 2018, 8, 4649-4661.

Synthesis and Determination of Stability Constant of *Meso*-2,3-Dimercaptosuccinic Acid for Complexation with Zinc Oxide Nanoparticles

Poonyawee Keattanong^{a,*}, Sujittra Srisung^a and Nootcharin Wasukan^b

^aDepartment of Chemistry, Faculty of Science, Srinakharinwirot University, Sukhumwit 23, Wattana District, Bangkok 10110, Thailand

^bNational Nanotechnology Center, National Science and Technology Development Agency (NSTDA), 111 Thailand Science Park, Khlong Luang, Pathum Thani 12120, Thailand

*e-mail: gs581110107@swu.ac.th

The current growth of nanotechnology was the cause of more using nanomaterial in various industries. Therefore, human is more likely to get various nanoparticles in everyday life. The vast majority causes little ill effect, and go unnoticed, but occasionally an accumulation will cause appreciable harm to the organism. Nowadays, various Zinc Oxide nanoparticles (ZnONPs) have been developed as a commodity such as sunscreens, food additives, rubber manufacture, and electronic materials^{1,2}. With the wide application of ZnONPs, concern has been raised about its unintentional health. For example, an increase in the amounts of free radicals or reactive oxygen species (ROS) in the body³. Chelating agent such as *meso*-2,3-dimercaptosuccinic acid (DMSA) have been widely used in the treatment of heavy metal such as Mercury (Hg), Lead (Pb) and Arsenic (As). Due to DMSA is a reasonably safe, ideally effective in removing several toxic metals (especially lead), Additional rounds increased excretion of toxic metal. Many studies of DMSA for a chelator heavy metal poisoning and stability on heavy metal with DMSA. The aim of this study was to evaluate the efficacy of DMSA for treatment ZnONPs and compared with other metals. We synthesized and characterized ZnONPs and DMSA-ZnONPs complex by UV-Vis spectrophotometer, Fourier Transform Infrared (FTIR) and scanning electron microscope (SEM). We found that ZnONPs and ZnONPs-DMSA complex were synthesized by expedient method, save time and cheap were in nanoscale with white powder. Moreover, we determined the ratio and the stability constant of DMSA-ZnONPs complex and DMSA complex with other heavy metal by UV-Vis titration method and benesi hildebrand equation⁴. We found that the ratio of ZnONPs : DMSA is 1 : 2 as well as mainly complex of DMSA with other heavy metal in this study. For the stability of metal chelates of the DMSA were in order Cr(III) > Zn (II) > Cu(II) > ZnONPs > Fe(III) > Fe(II) > Ni (II). Then, we predict the structure of complex by thiol group (-SH) and carboxylic group (-COOH) of DMSA react with metal. The results were indicated efficiency and stability of DMSA in therapeutic chelating agents as antidotes for metal poisoning.

Keywords: DMSA, ZnONPs, Complexes, Synthesis, Stability constant

References

1. D. Li, H. Haneda. *Chemosphere*. **2003**, *51*, 129–137.
2. M. Rittner. *J. Am. Ceram. Soc.* **2002**, *81*, 33–36.
3. T. Brunner, P. Wick, P. Manser. *Environ. Sci. Technol.* **2006**, *40*, 4374–4381.
4. A Tella, J. Obaleye, G. Obiyenwa. *J. Pharm Res.* **2011**, *4(1)*, 241-244.

Comparison of Photocatalytic Property of Metal Oxides/Silica Nanofibers Fabricated by Different Processes

Papada Natsathaporn, Ratchapol Jenjob and Daniel Crespy*

Department of Materials Science and Engineering, School of Molecular Science and Engineering, Vidyasirimedhi Institute of Science and Technology, 21210 Rayong, Thailand

**e-mail: daniel.crespy@vistec.ac.th*

Contamination of organic pollutants in water is global critical issue caused by draining insufficiently treated wastewater to water resources. Degradation of organic pollutants using metal oxides photocatalyst nanofibers has been investigated as promising method to efficiently remove organic pollutants from wastewater.¹ Moreover, 1D-structured metal oxides photocatalyst nanofibers are also environmental friendly because they can be easily separated from medium. Herein, metal oxides/silica nanofibers were synthesized using different processes including electrospinning of polymer solution containing metal salts and silica nanoparticles² as well as electrospinning of polymer containing silica nanoparticles that was further crosslinked and soaked in solutions of metal salts. Calcination of metal salts/silica nanofibers in air was required for all samples to simultaneously remove the polymer, sinter silica nanoparticles, and nucleate metal oxides. Morphology, phase and elemental analysis of metal oxides/silica nanofibers with different preparations were studied using scanning electron microscope (SEM), powder X-ray diffraction (XRD) and inductively coupled plasma optical emission spectrometry (ICP-OES). Photodegradation of a model dye was performed under UV-irradiation at room temperature to compare photocatalytic activity of metal oxides/silica nanofibers obtained by different preparations.

Keywords: Electrospinning, Metal oxide, Nanofiber, Photocatalyst.

References

1. J. Mu, B. Chen, M. Zhang, Z. Guo, P. Zhang, Z. Zhang, Y. Sun, C. Shao, Y. Liu, *ACS Appl. Mater. Interfaces* **2011**, 4 (1), 424–430.
2. N. Horzum, R. Muñoz-Espí, G. Glasser, M. Demir, K. Landfester, D. Crespy, *ACS Appl. Mater. Interfaces* **2012**, 4 (11), 6338–6345.



SAF-P-01

Silver Nanoparticles Lead to Antibiotic Resistance in Bacteria

Chitrada Kaweeteerawat, Preeyawis Na Ubol, Sanirat Sangmuang, Sasitorn Aueviriyavit and Rawiwan Maniratanachote

National Nanotechnology Center (NANOTECH), National Science and Technology Development Agency (NSTDA), 111 Thailand Science Park, Phahonyothin Road, Khlong Luang, Pathum Thani 12120, Thailand.

Silver nanoparticles (AgNPs) are widely used for decades for antimicrobial and antifouling applications. However, information on the bacterial impact and environmental toxicity of the particles is not comprehensive. Here, we report that AgNPs lead to growth inhibition and oxidative stress in the bacteria *Escherichia coli* and *Staphylococcus aureus*, with half-maximal inhibitory concentrations of 15 and 11 mg/L, respectively. Surprisingly, bacteria pre-exposed to AgNPs exhibit increased resistance towards antibiotics with diverse mechanisms of action (ampicillin, penicillin, chloramphenicol and kanamycin). The minimal inhibitory concentration (MIC) and minimal biocidal concentration (MBC) increased by 100 – 300%. We also show that AgNPs pre-treated bacteria exhibit less permeable membranes, lower levels of oxidative stress, decreased membrane potential and elevated levels of intracellular ATP. *In vitro* incubation with plasmid DNA revealed the potential for AgNPs to catalyze DNA strand scission. Bacterial reverse mutation assay (Ames test) show that AgNPs are mutagenic agents. Overall, the results suggest that AgNPs lead to antibiotics resistance in bacteria by mean of genetic mutation. These results highlight a potential consequence of the incidental exposure of bacteria to AgNPs in the environment, and underscore the need to regulate the use and disposal of silver nanoparticles in industry and consumer products.

Resonance Rayleigh Scattering Nano-Sensor for Hg²⁺ Detection Based on Hg²⁺- DNA Complex Induced Gold Nanorods Aggregation

Sawinee Ngermpimai^a, Piyaporn Matulakun^a, Saowapak Teerasong^b, Theerapong Puangmali^a, Atcha Kopwithaya^c, Apiwat Chompoosor^{d,*}

^aMaterials Science and Nanotechnology Program, Faculty of Science, Khon Kaen University, Khon Kaen 40002, Thailand

^bDepartment of Chemistry and Applied Analytical Chemistry Research Unit, Faculty of Science, King Mongkut's Institute of Technology Ladkrabang, Bangkok 10520, Thailand

^cNational Electronics and Computer Technology Center, 112 Thailand Science Park, Pathumthani 12120, Thailand

^dDepartment of Chemistry, Faculty of Science, Ramkhamhaeng University, Bangkok 10240, Thailand

*e-mail: apiwat@ru.ac.th

Mercuric ion (Hg²⁺) is a highly toxic metal that is harmful to human health even at very low concentrations [1]. Analytical current methods are conventionally employed for trace analyses of Hg²⁺ [2]. However, to achieve a very low detection limit, hyphenated techniques have been suggested. A resonance Rayleigh Scattering (RRS) technique is a highly-sensitive simplicity and rapidness in performance for the determination of certain inorganic and organic [3]. In this work, RRS method was developed for monitoring Hg²⁺ concentration using positively charged gold nanorods (GNRs) and thymine-rich single-stranded DNA (ssDNA). In the presence of Hg²⁺, a conformation of ssDNA can change from a random coil to a rigid hairpin structure via thymine–Hg²⁺–thymine coordination. The hairpin DNA has a high density of negative charges leading to extensive aggregation of GNRs that can enhance the RRS intensity. The intensity of RRS at 550 nm ($\lambda_{\text{ex}} = \lambda_{\text{RRS}}$) was observed by spectrofluorometer to detect the concentration of Hg²⁺. This proposed method demonstrated a detection limit of 0.23 nM, which is lower than the maximum mercury contaminant level required by US Environmental Protection Agency. The reproducibility of the developed sensor exhibited good precision with 3.1% relative standard deviation. The present assay can be completed in a single step within 5 min and has good selectivity for Hg²⁺. Furthermore, this method is a simple and rapid assay for quantification of Hg²⁺, involving in-situ mixing and sensing in a one-pot solution.

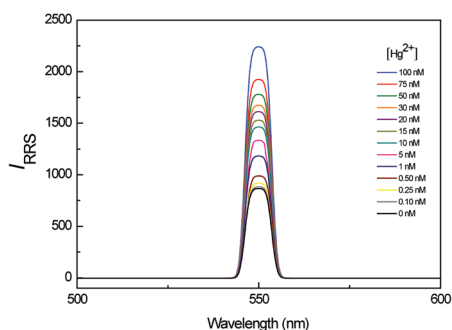


Figure 1. The RRS responses of the nanosensor after addition of various concentrations of Hg²⁺.

Keywords: Aggregation, Gold nanorods, Hg²⁺, Resonance Rayleigh scattering, ssDNA, Tap water

References

1. A. Renzoni, F. Zino, E. Franchi, *Environ. Res.* **1998**, 77, 68–72.
2. H. Louie, C. Wong, Y.J. Huang, S. Fredrickson, *Anal. Methods.* **2012**, 4, 522–529.
3. Z.F. Gao, W.W. Song, H.Q. Luo, N.B. Li, *Biosens. Bioelectron.* **2015**, 65, 360–365.

Gold Nanoparticle-Based Colorimetric Aptasensor for Rapid Detection of 8-Oxo-Dg in Urine

**Piyaporn Matulakul^a, Chadamas Sakonsinsiri^b, Apiwat Chompoosor^c,
Theerapong Puangmli^{a,*}**

^aMaterials Science and Nanotechnology, Department of Physics, Faculty of Science, Khon Kaen University, Khon Kaen 40002, Thailand.

^bDepartment of Biochemistry, Faculty of Medicine, Khon Kaen University, Khon Kaen 40002, Thailand.

^cDepartment of Chemistry, Faculty of Science, Ramkhamhaeng University, Bangkok 10240, Thailand.

*e-mail: Theerapong@kku.ac.th

Cholangiocarcinoma (CCA) or a bile duct cancer is prevalently found in the northeast region of Thailand [1]. CCA is characterized by its late diagnosis and poor prognosis with primary sclerosing cholangitis and high-cost detection [2]. Therefore, there is an urgent need to develop an efficient and easy-to-use detection method for a detection of CCA. 8-Oxo-7, 8-dihydro-2'-deoxyguanosine (8-oxo-dG), an oxidized form of guanosine residues in DNA which is a result of oxidative damage of the genome [3], is a biomarker for CCA detection. In this work, gold nanoparticle-based colorimetric aptasensor has been developed for the detection of 8-oxo-dG in urine. The development of a proposed aptasensor can be divided into two main parts. The difference of each part is the length of ssDNA aptamers. Two ssDNA sequences was used in the present study. The former is obtained from the literature (5'-GCG GGC GAT CGG CGG GGG GTG CGT GCG CTC TGT GCC AGG GGG TGG GAC AGA TCA TAT GGG GGT GCT-3'), whereas the latter is obtained from a computer simulation (5'-GTG CGT GCG CTC TGT GCC AGG GGG TGG GAC AGA TCA TAT-3') developed in our research group. To apply our aptasensor in urine, the optimization of the solution with a phosphate buffer was performed. The aptamers can absorb onto citrate-capped gold nanoparticle (AuNPs), and can be stabilized by electrostatic repulsion and steric hindrance under high salt concentrations. Upon binding with the target molecules, aptamer can specifically bind with 8-oxo-dG and forms a four-stranded tetraplex structure (G-quadruplex) [4], and intramolecular hydrogen bonds between guanines resulting in an aptamer-8-oxo-dG complex in the solution. The aptamer can no longer protect AuNPs from aggregation under high salt concentrations. Thus, the colour of the solution is changed from red to purple. The quantity of 8-oxo-dG can be obtained by UV-VIS spectroscopy. Based on this principle, this sensor could be applied for colorimetric aptasensor which is easy to use, low cost, and rapid detection.

Keywords: Aptamer, Aptasensor, Gold nanoparticle, G-quadruplex

References

1. P. Saichua, A. Yakovleva, C. Kamamia, A R. Jariwala, J. Sithithaworn, B. Sripa, P J. Brindley, T. Laha, E. Mairiang, C. Pairojkul, N. Khuntikeo, J. Mulvenna, P.Sithithaworn, and J M. Bethony, *PLOS Negl. Trop. Dis.* **2015**, 9.
2. R. Thanan, M. Murata, S. Pinlaor, P. Sithithaworn, N. Khuntikeo, W. Tangkanakul, Y. Hiraku, S. Oikawa, P. Yongvanit, and S. Kawanishi. *Cancer Epidemiol. Biomark. Prev.***2008**, 17(3), 518–24.
3. E.S. Stovgaard, H.E. Poulsen, K. Broedbaek, A. Weimann, *Free Radic. Biol. Med.* **2011**, 51(8), 1473–1479.
4. C. Wang, Y S. Xue, J H. Zhou, B. Qian, Q M. Wang, Y S. Yin, J C. Zhao, H. Liu, H. Wang, J and S D Liu. *Biosens. Bioelectron.* **2014**, 58, 2 – 26.

A Simple Paper-based Surface-enhanced Raman Scattering (SERS) for Cancer Cell Detection

Pimporn Reoksrungruang¹, Tararaj Dharakul², Suwussa Bamrungsap^{1*}

¹National Nanotechnology Center (NANOTEC), National Science and Technology Development Agency (NSTDA), Pathum Thani, 12120, Thailand. ²Department of Immunology, Faculty of Medicine Siriraj Hospital, Mahidol University, Bangkok, 10700, Thailand.

*e-mail: suwussa@nanotec.or.th

Surface-enhanced Raman scattering (SERS) is a technique that enhances Raman scattering of particular molecules absorbed onto a rough metal surface. Recently, SERS demonstrates potential applications in bioanalytical and biomedical research. Cancer detection using a simple paper-based SERS platform was herein demonstrated. A plasmonic paper was fabricated by immersing plain filter paper into a solution of gold nanorods (AuNRs) for use as a SERS substrate. The images from scanning electron microscope (SEM) confirmed absorption of AuNRs throughout the plasmonic paper without aggregation. This plasmonic paper enhanced signal of the Raman reporter, 4-meraptobenzoic acid, by an enhancement factor (EF) of 10^6 - 10^8 . HT-29, a colorectal cancer cell line that highly expresses epithelial cell adhesion molecule (EpCAM) served as the target cells and fibroblast which is a non-EpCAM expressing cell was used as negative control. The target HT-29 cells and fibroblast were then dropped on the plasmonic paper followed by SERS measurement. Due to structural and metabolic changes, cancer cells yield pattern of SERS spectra which is dominated in protein (~ 760 cm^{-1} , ~ 1175 - 1177 cm^{-1} , ~ 1553 - 1555 cm^{-1} and ~ 1618 - 1620 cm^{-1}) and nucleic acids (~ 1578 - 1585 cm^{-1} and ~ 1450 - 1550 cm^{-1}), while the fibroblast provided strong lipid characteristic bands at ~ 1350 cm^{-1} . This investigation indicated that this simple paper-based SERS platform can be applied to differentiate cancer and normal cells which is feasible for further cancer detection.

Keywords: Surface-enhanced Raman scattering (SERS), Plasmonic paper, Cancer cell detection

Carbon Nanofibers Prepared via C_2H_2 - CO_2 Reaction over Eggshell Waste with Gold Nanoparticles for H_2O_2 Detection

Malinee Niamlaem^{ab}, Chompunuch Warakulwit^{a,b*}, Chaiyan Boonyuen^{a,b}, Winyoo Sangthong^b, Jumras Limtrakul^c

^aDepartment of Chemistry, Faculty of Science, Kasetsart University, Bangkok 10900, Thailand

^bNANOTEC Center of Excellence for Nanoscale Materials Design for Green Nanotechnology and Center for Advanced Studies in Nanotechnology for Chemical, Food and Agricultural Industries, Kasetsart University, Bangkok 10900, Thailand

^cDepartment of Materials Science and Engineering, School of Molecular Science and Engineering, Vidyasirimedhi Institute of Science and Engineering, Rayong 21210, Thailand

*e-mail: fscicpn@ku.ac.th

Carbon nanofibers (CNFs) were prepared via the oxidative dehydrogenation of C_2H_2 by CO_2 with the aim to utilize CO_2 , reducing greenhouse gas emissions. Eggshell waste was used as environment-friendly supporting material for the CNF synthesis. The obtained fibers were then deposited by gold nanoparticles, encapsulated by polyvinylpyrrolidone (PVP) and 4-dimethylaminopyridine (DMAP) (1:4) or Au-(P1:D4) via electrostatic self-assembly without any pretreatment of carbon surfaces. After the deposition of Au-(P1:D4), the obtained hybrid materials were deposited on a glassy carbon electrode (GCE) and used for the electrochemical experiments without using any binders. The Au-(P1:D4)/CNFs/GCE materials show good voltammetric response for H_2O_2 reduction. The electrode with the fibers prepared at $400^\circ C$ (Au-(P1:D4)/CNFs-400/GCE) exhibits good sensing performance, leading to a wide linearity range for H_2O_2 detection from $5 \mu M$ to 23 mM and the low detection limit of $0.33 \mu M$ ($S/N = 3$). Furthermore, its selectivity evaluated by some co-existing compounds with H_2O_2 in the real biological sample, including ascorbic acid (AA), acetaminophen (AP), citric acid (CA), glucose, and uric acid (UA), is good. The results reveal that CNFs prepared by C_2H_2 - CO_2 reaction, using eggshell waste support, are attractive alternative and environment-friendly materials for H_2O_2 -selective detection, which is significant important in biological systems.

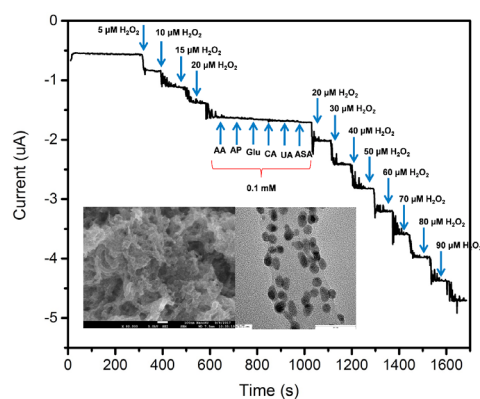


Figure 1. Chronoamperometric response of the Au-(P1:D4)/CNFs-400/GCE (inset: SEM and TEM images) to the successive additions of H_2O_2 , followed by additions of interference.

Keywords: Carbon Nanofibers, Eggshell Waste, Gold Nanoparticles, Oxidative Dehydrogenation, Hydrogen Peroxide Detection

References

1. P. Pannopard, C. Boonyuen, C. Warakulwit, Y. Hoshikawa, T. Kyotani and J. Limtrakul, *Carbon* **2015**, *94*, 836-844.
2. C. Warakulwit, S. Yadnum, V. Paluka, O. Phuakkong, M. Niamlaem, K. Pongpaisanseree, S. *Chemical Engineering Journal* **2015**, *278*, 150-158.

Non-invasive Measurement of Liver Disease for Monitoring Health Status by Using Electronic Nose

Tanthip Eamsa-ard^a, Thara Seesaard^b, Taya Kitiyakara^{c,*} and Teerakiat Kerdcharoen^{d,e,*}

^a *Materials Science and Engineering Programme and Center of Nanoscience and Nanotechnology, Faculty of Science, Mahidol University, Bangkok 10400, Thailand*

^b *Department of Physics, Faculty of Science and Technology, Kanchanaburi Rajabhat University, Kanchanaburi 71190, Thailand*

^c *Division of Gastroenterology and Hepatology, Faculty of Medicine Ramathibodi Hospital Mahidol University, Bangkok, Thailand*

^d *Department of Physics, Faculty of science, Mahidol University, Bangkok 10400, Thailand*

^e *Research Network of NANOTEC at Mahidol University, National Nanotechnology Center, Thailand*

**email: tayakiti@googlemail.com, teerakiat@yahoo.com*

Nowadays, medical researchers are increasingly interested in the detection of odor biomarkers for screening, diagnosis and monitoring of diseases. This is due in part to its rapid analysis and non-invasive methodology, which makes its applications quite attractive for various clinical arenas. In this work, we proposed an electronic nose (e-nose) technology that has been developed to detect and discriminate odorous molecules from the exhaled breath in order to indicate the health status of its owner. The sensing materials are based on 8 commercial metal oxide semiconductors (TiO₂, SnO₂, etc.) and 8 nanocomposites of non-conductive polymer with functionalized single-walled carbon nanotubes (f-SWCNTs) sensors that are sensitive to a broad range of volatile organic compounds, such as ammonia, sulfides, alcohol and hydrocarbons, sufficiently to cover the chemical species contained in the human exhaled breath. We have developed nanocomposite gas sensors, which were shown to be capable to discriminate between the sample groups of hepatocellular carcinoma (HCC) patients and healthy control subjects. The electronic nose system has been designed and fabricated to be suitable for exhaled breath detection. The obtained results as analyzed by the principal component analysis (PCA) have demonstrated that the e-nose has a potential to discriminate the patterns of exhaled breath odor from healthy controls and HCC patients. In the future, this approach may become very useful in clinical application to serve as a non-invasive device for screening patients with early-stage liver cancer.

Keywords: Non-invasive methodology, Electronic nose, Chemical sensor, Hepatocellular carcinoma, Volatile organic compounds, Cancer.

References

1. R. F. Machado, D. Laskowski, O. Deffenderfer, T. Burch, S. Zheng, P. J. Mazzone, T. Mekhail, C. Jennings, J. K. Stoller, J. Pyle, J. Duncan, R. A. Dweik and S. C. Erzurum, "Detection of lung cancer by sensor array analyses of exhaled breath," *American Journal of Respiratory and Critical Care Medicine*, **2005**, vol. 171, pp. 1286-1291.
2. T. Seesaard, C. Khunarak, T. Kitiyakara and T. Kerdcharoen, "Development of an electronic nose for detection and discrimination of exhaled breath of hepatocellular carcinoma patients," *IEEE International Conference on Systems, Man, and Cybernetics (IEEE SMC 2012)*, **2012**.
3. T. Seesaard, S. Kladsomboon, P. Lorwongtragool, T. Kitiyakara and T. Kerdcharoen, "Health Status Monitoring by Discrimination of Exhaled Breath with an Electronic Nose," *IEEE International Conference on Biomedical Engineering International Conference (IEEE BMEicon 2012)*, **2012**.
4. U. Tisch, I. Schlesinger, R. Ionescu, M. Nassar, N. Axelrod, D. Robertman, Y. Tessler, F. Azar, A. Marmur, J. Aharon and H. Haick, "Detection of Alzheimer's and Parkinson's disease from exhaled breath using nonmaterial based sensors," *Nanomedicine*, **2013**, vol. 8, pp. 43-56.
5. X. Sun, K. Shao and T. Wang, "Detection of volatile organic compounds (VOCs) from exhaled breath as noninvasive method for cancer diagnosis," *Analytical and Bioanalytical Chemistry*, **2016**, vol. 408, pp. 2759-2780.
6. T. Eamsa-ard, T. Seesaard, T. Kitiyakara, and T. Kerdcharoen, "Screening and discrimination of Hepatocellular carcinoma patients by testing exhaled breath with smart devices using composite polymer/carbon nanotube gas sensors", *IEEE International Conference on Biomedical Engineering International Conference (IEEE BMEicon 2012)*, **2012**.

Detecting Urinary Volatile Compounds by Electronic Nose for Early Diagnosis of Diabetes

**Mon Myat Swe^a, Tanthip Eamsa-ard^a, Phuntsho Choden^a, Thara Seesaard^b,
Chutintorn Sriphrapradang^{c,*} and Teerakiat Kerdcharoen^{d,e,*}**

^a *Materials Science and Engineering Programme and Center of Nanoscience and Nanotechnology,
Faculty of Science, Mahidol University, Bangkok, Thailand*

^b *Department of Physics, Faculty of Science and Technology, Kanchanaburi Rajabhat University, Kanchanaburi 71190, Thailand*

^c *Division of Endocrinology and Metabolism, Faculty of Medicine Ramathibodi Hospital,
Mahidol University, Bangkok 10400, Thailand*

^d *Department of Physics, Faculty of science, Mahidol University, Bangkok 10400, Thailand*

^e *Research Network of NANOTEC at Mahidol University, National Nanotechnology Center, Thailand*

*e-mail: chutins@gmail.com, teerakiat@yahoo.com

Diabetes is a chronic disease in which the metabolic disorders can lead to the lack of insulin which burns glucose for energy. According to International Diabetes Federation (IDF), 371 million people in the world are suffering from diabetes and 187 million of them do not even notice themselves. Patients can only know when they do blood screening at hospital. Increasing glucose level in diabetic patients is difficult to control if they cannot accept the proper treatment. As a consequence, it may lead to heart disease, kidney failure and blindness. Thus, diabetes patients should be diagnosed at home early. We developed an electronic nose which is suitable for early diagnosis and healthcare monitoring along the life. The metal oxide gas sensors (MQ-8, TGS 2444, TGS 823, TGS 2600, TGS 2603, TGS 2610, TGS 825 and TGS 2602) and polymer/functionalized SWCNT nanocomposite gas sensors (Poly (4-styrenesulfonic acid)/SWCNT, Poly (acrylic acid)/SWCNT, Poly (4-styrenesulfonic acid) solution/SWCNT and Polyvinyl alcohol/SWCNT) were applied for two different types of electronic nose. Both types of electronic nose were performed with six urinary volatile compounds commonly found in diabetes mellitus such as ammonia, ethyl methyl ketone, butyric acid, acetic acid, acetone and water as the first test, and with real urine samples from healthy people and type II diabetic patients as the second test. The gas sensors could show the high response to the volatile organic compounds in the urine of diabetes patients. Moreover, the electronic nose systems were able to classify between urinary odors from healthy people and diabetic patients by using principal component analysis (PCA). In addition, these electronic nose systems have potential to be useful as painless and comfortable diabetes detection in the near future.

Keywords: Diabetes, Urinary Volatile Compounds, Electronic Nose, Gas Sensors

References

1. J.B. Yu, H.G. Byun, M.S. So and J.S. Huh, "Analysis of diabetic patient's breath with conducting polymer sensor array," *Sensors and Actuators B*, **2005**, vol. 108, pp. 305-308.
2. P. Lorwongtragool, A. Wisitsoraat and T. Kerdcharoen, "An electronic nose for amine detection based on polymer/SWNT-COOH Nanocomposite," *Journal of Nanoscience and Nanotechnology*, **2011**, vol.11, pp. 1-6.
3. S. Siyang, C. Wongchoosuk, and T. Kerdcharoen, "Diabetes diagnosis by direct measurement from urine odor using electronic nose," in Biomedical Engineering International Conference (BMEiCON), **2012**, pp. 1-4.
4. P. Lorwongtragool, E. Sowade, N. Watthanawisuth, R. R. Baumann, T. Kerdcharoen, "A novel wearable electronic nose for healthcare based on flexible printed chemical sensor array," *Sensors*, **2014**, vol. 14, pp. 19700-19712.
5. S. Canivell and R. Gomis, "Diagnosis and classification of autoimmune diabetes mellitus," *Autoimmunity Reviews*, **2014**, vol. 13, pp. 403-407.

SEN-P-05

6. L. Capelli, G. Taverna, A. Bellini, L. Eusebio, N. Buffi, M. Lazzeri, et al., “Application and uses of electronic noses for clinical diagnosis on urine samples: A Review,” **2016** , vol. 16, pp. 1708.
7. T. Seesaard, C. Sriphrapadang, T. Kitiyakara, and T. Kerdcharoen “Self-Screening for diabetes by sniffing urine samples based on a hand-held electronic nose,” in Biomedical Engineering International Conference (BMEiCON), **2016**, pp.1-4.
8. P. Choden, T. Seesaard, U. Dorji, C. Sriphrapadang and T. Kerdcharoen, “Urine odor detection by electronic nose for smart toilet application,” in International Conference on Electrical Engineering/ Electronics, Computer, Telecommunications and Information Technology (ECTI-CON) ,**2017**, pp.190-193.
9. P. Choden, T. Seesaard, T. Eamsa-ard, C. Sriphrapadang and T. Kerdcharoen, “Volatile urine biomarkers detection in type II diabetes towards use as smart healthcare application,” in International Conference on Knowledge and Smart Technology, **2017**, pp.178-181.

A Label-Free Electrochemical Origami Paper-Based Immunoassay for C-Reactive Protein Detection in Human Serum

Suchanat Boonkaew^a, Sudkate Chaiyo^a, Sakda Jampasa^a, Sirirat Rengpipat^b, Weena Siangproh^d and Orawon Chailapakul^{a,*}

^aElectrochemistry and Optical Spectroscopy Center of Excellence (EOSCE), Department of Chemistry, Chulalongkorn University, Pathumwan, Bangkok, 10330, Thailand

^bDepartment of Microbiology, Faculty of Science, Chulalongkorn University, Pathumwan, Bangkok, 10330, Thailand

^cNational Center of Excellence for Petroleum, Petrochemicals, and Advanced Materials, Chulalongkorn University, Pathumwan, Bangkok, 10330, Thailand

^dDepartment of Chemistry, Faculty of Science, Srinakarinwirot University, Bangkok, 10110, Thailand

*e-mail: corawon@chula.ac.th

An origami paper-based label-free electrochemical immunoassay for C-reactive protein (CRP) detection has been developed. Origami paper-based analytical device (*o*PAD) was designed to combine the multiple steps of the electrode modification into a single device¹. A conductive graphene-modified screen-printed carbon electrode (G/SPCE) was employed to enhance the sensitivity of detection. Gold nanoparticle (AuNP) was first electrodeposited onto the G/SPCE, followed by a self-assembled monolayer (SAM) of L-cysteine (L-cys). The anti-CRP was then covalently immobilized onto the modified electrode via EDC/NHS chemistry. Cyclic voltammetry (CV) and scanning electron microscopy (SEM) were also applied to verify the successful modification of the electrode. The presence of CRP was determined by measuring the charge-transfer resistance (R_{ct}) changes between electrode surface and a redox couple $[\text{Fe}(\text{CN})_6]^{3-/4-}$ using electrochemical impedance spectroscopy (EIS). Under the optimal conditions, the CRP concentration was detected in the range of 0.05-100 $\mu\text{g/mL}$, and the limit of detection (LOD) of 46.67 ng/mL ($S/N=3$) was obtained. Furthermore, this developed sensor was successfully applied to determine CRP in a certified human serum. This proposed immunosensor demonstrates a simple, low-cost, and disposable sensor which can be possibly used as an alternative method for various biological detections and point-of-care monitoring.

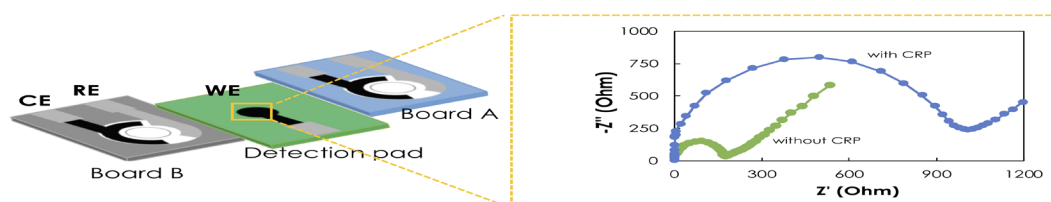


Figure1. The design of the *o*PAD electrode

Keywords: C-reactive protein (CRP), microfluidic paper-based analytical devices (μ -PADs), Graphene, Screen-printed carbon electrode (SPCE), Electrochemical impedance spectroscopy

References

1. C. Ma, W. Li, Q. Kong, H. Yang, Z. Bian, X. Song, J. Yu, M. Yan, 3D origami electrochemical immunodevice for sensitive point-of-care testing based on dual-signal amplification strategy. *Biosensor and bioelectronics*. **2015**, *63*, 7-13.

Development of Low-cost Sleep Monitoring Systems

Shongpun Lokavee^a, Worakot Suwansathit^b, Visasiri Tantrakul^{b*}, and Teerakiat Kerdcharoen^{c,d*}

^aMaterials Science and Engineering Programme and Center of Intelligent Materials and Systems (CIMS),
Faculty of Science, Mahidol University, Bangkok 10400, Thailand

^bSleep Disorder Center and Pulmonary and Critical Care, Ramathibodi Hospital, Mahidol University, Bangkok,
10400, Thailand

^cDepartment of Physics, Faculty of Science, Mahidol University, Bangkok 10400, Thailand

^dResearch Network of NANOTEC at Mahidol University, National Nanotechnology Center, Thailand

*e-mail: vtantrakul@gmail.com, teerakiat@yahoo.com

This work introduces a smart sleep care system based on pressure sensors embedded within a pillow sheet that can be used to measure relevant sleep parameters without restraint to a human. This system consists of an array of pressure sensors, wireless network devices based on low-cost ZigBee technology to digitize and transmit the pressure data to desktop computer or display devices, and software to analyze and classify body movements. We have demonstrated this system by evaluating the quality of breathing and sleep efficiency based on detection of the frequency of head movement during the night, which are then classified using a newly developed classification algorithm. The characteristic breathing patterns are explained by the change of the head pressure distribution on the pillow due to the lifting and lowering of the thorax movement. A slightly slower frequency variation in the same head region caused by breathing effect is measured to get respiration signal. We have found that the body movement frequency is different among individuals during sleep. Here, we have shown that the quality of sleep can be characterized and distinguished by correlations of the breathing rates separated by lifting and lowering of the thorax motion. The results were compared with the gold standard measurement scheme, such as the laboratory polysomnogram (PSG), for reasonable validity in assessing sleep physiology of health and disease. In summary, this smart pillow has a high efficiency as an alternative approach not only for determining respiration rates, but also for identifying breathing patterns that can be used to identify sleep-related breathing disorders. Furthermore, the smart pillow can be used in home environment for long term monitoring without any supervision from trained professionals.

Keywords: Smart pillow, Polysomnogram, ZigBee technology, Wireless sensor network.

References

1. R. Morais, M. A. Fernandes, S. G. Matos, C. Serodio, P.J.S.G. Ferreira, and M.J.C.S. Reis, "A ZigBee multi-powered wireless acquisition device for remote sensing applications in precision viticulture," *Comp. Electron. Agric. J.*, vol. 62, pp. 94-106, 2008
2. S. Lokavee, W. Suwansathit, V. Tantrakul, and T. Kerdcharoen, "Unconstrained detection of respiration rate and efficiency of sleep with pillow-based sensor array," *International Conference on Electrical Engineering/Electronics, Computer, Telecommunications and Information Technology (ECTI-CON)*, 2014.
3. T. Watanabe and K. Watanabe, "Noncontact Method for Sleep Stage Estimation," *IEEE Transactions on Biomedical Engineering*, vol. 51, no 10, 2004.
4. C. Apetrei, I.M. Apetrei, S. Villanueva, J.A. de Saja, F. Gutierrez-Rosales, and M.L. Rodriguez-Mendez, "Combination of an e-nose, and e-tounge and an e-eye for the characterization of olive oils with different degree of bitterness", *Analytica Chimica Acta*, vol. 663, pp. 91-97, 2010.
5. W. Chen, X. Zhu, T. Nemoto, Y. Kanemitsu, K. Kitamura, K Yamakoshi, "Unconstrained detection of respiration rhythm and pulse rate with one under-pillow sensor during sleep," *Med Biol Engin Comp*, vol. 43 pp. 306-312, 2005.
6. S. J. Redmond and C. Heneghan, «Cardiorespiratory-Based Sleep Staging in Subjects With Obstructive Sleep Apnea,» *IEEE Transactions on Biomedical Engineering*, vol. 53, no. 3, 2006.

Innovative Colorimetric Sensor for Detection of Chloramine by Using Nano Sodium Iodide in Amylose Helix

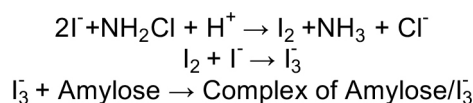
Athicha Santilinn^a, Natprawee Patthayawij^a, Napat Sajjamongkol^a and Kiattipoom Rodpun^{*a}

^aMahidol Wittayanusorn School, Salaya, Phutthamonthon, Nakorn Pathom, 73170, Thailand

*e-mail: mart@mwit.ac.th

Chloramine in swimming pools is generated by the reaction of free chlorine with the amine compounds such as urine and sweat. Chloramine can irritate to the eyes and also cause smell of swimming pools.¹ Accordingly, the excess amount of chloramine in swimming pools is the crucial issue to change the pool water. However, the general test which has been employed for swimming pools is to measure the total chlorine value which is a sum of free chloride and chloramine. If the total chlorine exceeded the standard limit, the pool water will be drained for new water replacement. Since the total chlorine value is included with the free chloride not only chloramine, this general method might waste water at an earlier time for water replacement.

This work, therefore, aims to innovate the colorimetric sensor for the direct detection of only chloramine for further application of controlling chloramines in swimming pools. In the literature, it was found that iodide ion in the presence of amylose can react with chloramine to form a blue complex of amylose/triiodide as following reactions.^{2,3}



Due to the advantageous nature of nanotechnology, it is well known that nanoscale materials can provide various fascinating properties. In our case, sodium iodide which is a starting material of iodide ion was scaled down to nano sodium iodide in the purpose of enhancing rate reaction as well as effective visual color for application as the colorimetric sensor. Herein, amylose helix was then utilized as a template to encapsulate sodium iodide as stable nanocomposites through straightforward method.⁴

To create the simple chemical sensor test kit for chloramine check-up in swimming pools, nano sodium iodide in amylose helix was prepared as a coated strip vial. Note that the amount of nano sodium iodide in the vial test kit is the limited amount that can completely reacted with the exact amount of chloramine which is equal to the maximum permission value of chloramine in swimming pools. In water sampling procedures, Berthelot's reagent was also used as a final key factor for analysis by the test kit. After the unknown water was filled in to the strip vial, Berthelot's reagent would be subsequently added to the water sample. The sample water containing chloramine of less than or equal the maximum permission value would appear blue color of amylose/triiodide complex (chloramine was completely consumed). In contrast, if the water containing chloramine exceeded the limit value, the chloramine residue which was remained after the reaction with the limiting nano sodium iodide would react with Berthelot's reagent and turn the sample water to green color.⁵

Keywords: Colorimetric Sensor, Chloramine, Nano Sodium Iodide

References

1. G. Moore, E. Calabrese and M. McGee, *Journal of Environmental Science and Health* **1980**, *15*, 239-258.
2. K. Kumar, R. Day and D. Margerum, *Inorg. Chem.* **1986**, *25*(24), 4344-4350.
3. W. R. Morrison and B. Laiglelet, *Journal of Cereal Science* **1983**, *1*(1), 9-20.
4. Z. Zaheer, E. Aazam and S. Hussain, *RSC Advances* **2016**, *6*(65), 60513-60521.
5. R. Harfmann and S. Crouch, *Talanta* **1989**, *36*(1-2), 261-269.

Electrochemical Investigation on the Interaction of L-cysteine with Lysozyme-functionalized rGO/MnO₂/PPy Composite.

Ibrar Alam^a, Piyapong Asanithi^{b*}, Benchaporn Lertanantawong^c

a. Department of Nanoscience and Nanotechnology, King Mongkut's University of Technology Thonburi, Thailand.

b. * Department of Physics, King Mongkut's University of Technology Thonburi, Thailand.

c. Department of Biomedical Engineering, Faculty of Engineering, Mahidol University, Thailand.

*e-mail: piyapong.asa@mail.kmutt.ac.th

The biological interactions of nanomaterial have attracted great interest because of their wide applications in biosensors, medical diagnostics and imaging [1]. Here we studied the interaction of L-cysteine and lysozyme-functionalized rGO/MnO₂/PPy composite (GMP). Preparation of GMP nanocomposite, characterization with SEM and FT-IR, deposition, and electrochemical measurement were carried out. Then, 130 μL of 5 mg/mL lysozyme was deposited on GMP by carrying out CV with scan rate of 0.05 V/s for 10 cycles and no oxidation peak was observed (Fig 1b, blue line). Next, lysozyme was cleared with a tissue paper and CV was carried out for 130 μL of PBS with 20 cycles to improve the stability of the deposited lysozyme. An oxidation peak was observed with V=0.595V, I=5.67 μA (Fig 1b, red line). Afterward, for investigating the interaction and the order of deposition we dropped 10 μL of 5mg/mL L-cysteine to the PBS. When the L-cysteine in the PBS solution interact with lysozyme deposited on the GMP, a peak of V=0.958V, I=66.5 μA was observed. Most probably this peak comes from the tryptophan residues occurring in the active site of lysozyme that may get expose to solution due to some configurational changes as a consequence of interaction [1, 2]. The interactions may be electrostatic, van der Waals and hydrophobic interactions. By changing the order of deposition on GMP i.e. 130 μL L-cysteine was deposited by carrying out 10 cycles of CV, it was then cleared with a tissue paper and CV was carried out for 130 μL of PBS with 20 cycles. An oxidation peak was observed with V=0.577V, I=6.51 μA (Fig 1c, black line). Afterward, for studying the interaction we dropped 10 μL of 5mg/mL lysozyme to the PBS and no clear oxidation peak was observed (Fig 1c, red line). This means that by changing the order of deposition i.e. depositing the L-cysteine on GMP may avoid its interaction with lysozyme present in the PBS solution. Our composite may be a potential candidate for investigating the interactions of amino acid with lysozyme.

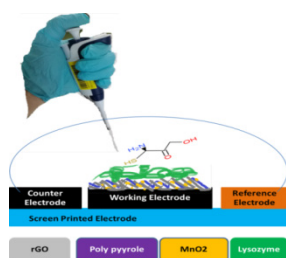


Figure 1a.

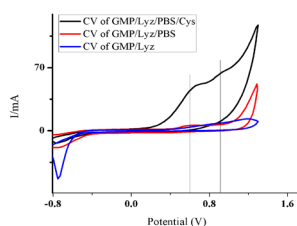


Fig. 1b

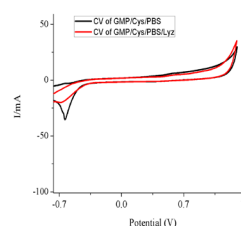


Fig. 1c

Figure 1a: Schematic abstract for functionalizing the surface of printed electrode. **1b:** CV of lysozyme-functionalized GMP interacting with L-cysteine. **1c:** CV of L-cysteine-functionalized GMP interacting lysozyme.

Keywords: Cyclic Voltammetry, Graphene, L-cysteine, Lysozyme, Manganese Oxide, Polypyrrole



SEN-P-10

References

1. F. Shi, S. Liu, & X. Su, *New Journal of Chemistry*, **2017** *41*, 4138-44.
2. S. Prasanth, D. R. Raj, R. K. Thomas, T. V. Vineeshkumar, & C. Sudarsanakumar, *RSC Advances*, **2016**, *6*, 105010-20.

Acknowledgement: We acknowledge financial support from “The Petchra Pra Jom Klao Doctoral Scholarship”, KMUTT, for Ph.D. study of Mr. Ibrar Alam. And we also acknowledge “Theoretical and Computational Science Center (TaCS), KMUTT for providing printing materials.

Novel Lanthanide Coordination Polymers as Luminescent Probes for Small Organic Sensing

Suwadee Jiajaroen^a, Winya Dungkaew^b, Filip Kielar^c, Kittipong Chainok^{d*}

^a*Division of Chemistry, Faculty of Science and Technology, Thammasat University, Thailand*

^b*Department of Chemistry, Faculty of Science, Maharakham University, Thailand*

^c*Department of Chemistry, Faculty of Science, Naresuan University, Thailand*

^d*Materials and Textile Technology, Faculty of Science and Technology, Thammasat University, Thailand*

**email: kc@tu.ac.th*

Two new luminescent lanthanide coordination polymers of a general formula $[\text{Ln}(\text{Br}_4\text{tp})_{1.5}(\text{MeOH})_3]_n$, where Ln = Eu (**1**), Tb (**2**), were synthesized from the self-assembly reactions between lanthanide(III) nitrate hexahydrate and tetrabromoterephthalic acid ($\text{H}_2\text{Br}_4\text{tp}$) in mixed methanol/water solution under solvothermal conditions. The single crystal X-ray diffraction analysis revealed that both compounds are isostructural and crystallize in the monoclinic space group $C2/c$, featuring a 2D layered structure constructed from $\{\text{Ln}_2\text{O}_2\}$ dimers bridged through the carboxylate groups of Br_4tp ligands. A 3D supramolecular structure is generated through hydrogen bonding and π - π interactions between the layers. In the solid-state, compounds **1** and **2** display bright red and green emission, respectively, at room temperature. Interestingly, **1** possesses a luminescence “turn-on” (enhancement) response to isopropanol, whereas **2** prominent “turn-off” (quenching) responses for ethyl acetate, suggesting that they may be excellent candidates for potential photonic materials.

Keywords: coordination polymers, lanthanide, luminescent probes, sensors

Anti-Aggregation of 2-Mercaptoethanesulfate Modified Silver Nanoplates for Detection of Phosphate on Paper-Based Device

Chanika Pinyorospatum^a, Poomrat Rattanarat^a, Weena Siangproh^b and Orawon Chailapakul^{a,c,*}

^a *Electrochemical and Optical Spectroscopy Center of Excellence (EOSCE), Department of Chemistry, Faculty of Science, Chulalongkorn University, 254 Phayathai Road, Pathumwan, Bangkok 10330, Thailand.*

^b *Department of Chemistry, Faculty of Science, Srinakharinwirot University, 114 Sukhumvit 23, Wattana, Bangkok 10110, Thailand.*

^c *Center of Excellence on Petrochemical and Materials Technology, Chulalongkorn University, 254 Phayathai Road, Pathumwan, Bangkok 10330, Thailand.*

*e-mail: corawon@chula.ac.th

A novel method for phosphate detection has been developed and proposed on paper-based device. The method utilized thiol functional group (2-mercaptoethane sulfate) modified silver nanoplates for the colorimetric detection. Europium ion (Eu^{3+}) was used for aggregation of modified silver nanoplates and binding of phosphate ion¹. In the presence of Eu^{3+} , the color of modified silver nanoplates on the paper-based device changes from pink to violet. When phosphate ion presences together with Eu^{3+} , the color of modified silver nanoplates remains unchanged. This is because modified silver nanoplates are undergone anti-aggregation. These colors can be observed by the naked eye. The integration of this method and paper device provides rapid and inexpensive mean for monitoring of phosphate. The optimization conditions and effect of interferences on the colorimetric detection of phosphate were studied. Using optimal conditions, the linearity was found to be $0.0326 - 0.9893 \mu\text{g}$ ($1.65 - 49.47 \text{ ppm}$) of phosphorus and the detection limit as low as $0.5507 \mu\text{g}$ ($\text{S/N}=3$). Finally, the method was applied to real soil samples collected from 3 different soil layers. The results from real samples showed the satisfactory and good agreement between the proposed method and standard UV-visible spectrophotometry using molybdenum blue assay.

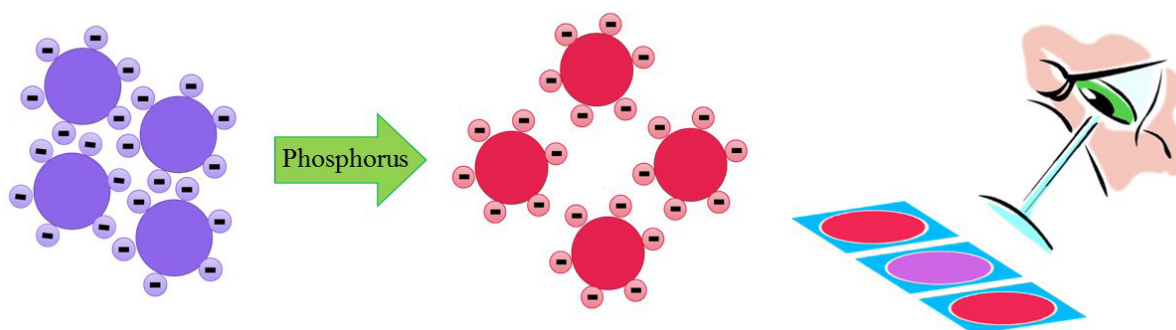


Figure 1. Schematic for detection of phosphate on paper-based device

Keywords: Phosphate, modified silver nanoplates, paper-based device, colorimetric method

References

1. Liu, W.; Du, Z.; Qian, Y.; Li, F., A specific colorimetric probe for phosphate detection based on anti-aggregation of gold nanoparticles. *Sensors and Actuators B: Chemical* 2013, 176, 927-931.

Preparation of Reversible Thermochromic Polydiacetylene/ Zn^{2+} Nanocomposites in Aqueous Suspension and their Colorimetric Responses to Chemical Stimuli

Jirapa Rueangsuwan^a, Nisanart Traiphol^{b,c}, Rakchart Traiphol^{a,d,*}

^aLaboratory of Advanced Polymers and Nanomaterials, School of Materials Science and Innovation, Faculty of Science, Mahidol University at Salaya, Phuttamonthon 4 Road, Salaya, Nakhon Pathom 73170, Thailand

^bLaboratory of Advanced Chromic Materials, Department of Materials Science, Faculty of Science, Chulalongkorn University, Bangkok 10330, Thailand

^cCenter of Excellence on Petrochemical and Materials Technology, Chulalongkorn University, Bangkok 10330, Thailand

^dNANOTECH-MU Excellence Center on Intelligent Materials and Systems, Faculty of Science, Mahidol University, Rama 6 Road, Ratchathewi, Bangkok 10400, Thailand

*e-mail: Rakchart.tra@mahidol.ac.th (R. Traiphol)

Polydiacetylene (PDA) is one of the conjugated polymers that has become an immense interest of chromic sensing material due to its chromatic property. When PDA is exposed to various external stimuli such as mechanical stresses (mechanochromism), temperature (thermochromism), pH (ionochromism), the structural change results in color transition. Normally, the commercially available PDAs show irreversible blue-to-red thermochromism. Our group recently introduces a new class of materials by incorporating of zinc oxide (ZnO) nanoparticles into PDA assemblies. We have found that PDA/ZnO nanocomposites exhibit the high color stability and fully reversible thermochromism with controllable color-transition temperature. In this continuing study, we demonstrate a simple method for achieving reversible thermochromic PDA-based materials, which involves mixing with zinc ions (Zn^{2+}) in aqueous medium. The ratios between PDAs and Zn^{2+} ions and pH of suspension are systematically varied. We have found that reversible thermochromism is achieved at PDA: Zn^{2+} ratio of 2:1 and pH above 9. Scanning electron microscopy observes well-ordered nanocrystal growth at this condition. The obtained PDA/ Zn^{2+} nanocomposite exhibits reversible blue-to-purple color transition at 90 °C. The colorimetric response of the nanocomposites upon exposure to various kinds of chemical stimuli including acids, bases, and solvents is also investigated. Fourier transform infrared spectroscopy, X-ray diffraction and other techniques are used to explore the molecular origins of this behavior.

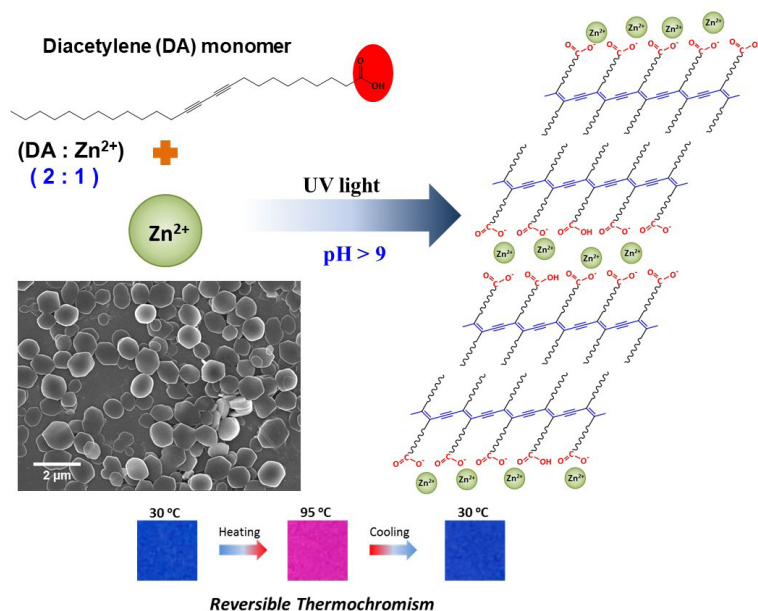


Figure 1. Incorporation of Zn^{2+} ions into PDA assemblies at PDA: Zn^{2+} ratio of 2:1 and pH above 9 exhibits reversible thermochromic property.

Keywords: Polydiacetylene, Nanocomposites, Thermochromism, Chemical Stimuli

Selectivity Encapsulation of *Zingiber Cassumunar* Roxb. Oil by Beta-Cyclodextrin Derivatives

Auraya Manaprasersak^a and Thitinun Karpkird^{a,*}

^aDepartment of Chemistry, Faculty of Science, Kasetsart University, Bangkok 10900, Thailand

*e-mail: fscitnm@ku.ac.th

Zingiber Cassumunar Roxb. (Plai) is a medical plant widely cultivated in Asia and its essential oil has been reported for several biological activities, such as anti-inflammatory, anti-microbial and anti-oxidant effects. In this work, the essential oil was extracted from Plai by steam distillation with 0.32% yield. (*E*)-4-4-(3',4'-dimethoxyphenyl)butadiene (DMPBD), (*E*)-4-4-(3',4'-dimethoxyphenyl)but-3-ene-1-ol (compound D) and terpinen-4-ol were reported as the major components. The components of Plai oil were investigated by GC-MS. It was found that sabinene, terpinen-4-ol and DMPBD were detected as the major components for 23, 20 and 30%. The three types of beta-cyclodextrins (CDs) i.e. beta-cyclodextrin (bCD), 2-hydroxypropyl-beta-cyclodextrin (HPbCD) and citric acid crosslinked beta-cyclodextrin (pbCD) were used to form the inclusion complexes with Plai oil to increase the aqueous solubility, selectivity and anti-analgesic properties. The ratio of CDs and plai oil was varied. The amount of terpinen-4-ol and DMPBD were detected by GC-MS. The result showed that terpinen-4-ol was fitted to bCD whereas HPbCD showed the highest loading efficiency for DMPBD. The pbCD showed the lowest selectivity both terpinen-4-ol and DMPBD. As the results, the different types of CDs showed the different selectivity for inclusion complex formation with major component in Plai oil. The separation of terpinen-4-ol and DMPBD can be done by using CD inclusion complexes. The anti-analgesic property of plai oil and its complexes will be further studied.

Keywords: *Zingiber Cassumunar* Roxb., plai oil, cyclodextrin, encapsulation, essential oil

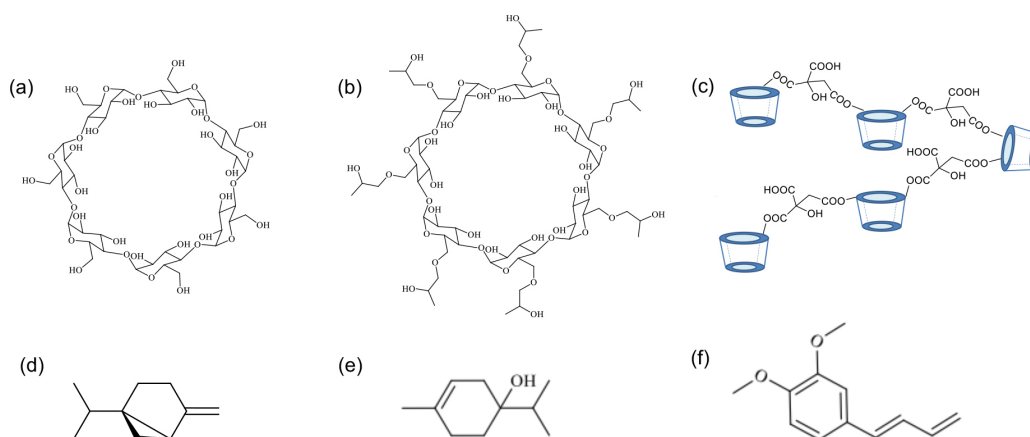


Figure 1 Structure of (a) beta-cyclodextrin (bCD), (b) 2-hydroxypropyl-beta-cyclodextrin (HPbCD), (c) citric acid crosslinked beta-cyclodextrin (pbCD), (d) sabinene, (e) terpinen-4-ol and (f) (*E*)-4-4-(3',4'-dimethoxyphenyl)butadiene (DMPBD)

References

1. J. Leelarungrayub, J. Manorsoi, A. Manorsoi, A. *Int. J. Nanomed.* **2017**, *12*, 2469.
2. P. Pithayanukul, J. Tubprasert, M. Wuthi-Udomlert, *Phytother. Res.* **2007**, *21*, 164.
3. W. Chaiyana, S. Anuchaperrda, P. Leelaporn, R. Phongpradist, H. Viernsterin, M. Mueller, *AAPS PharmSciTech.* **2017**, *18*, 1332.

Effective Fluorescence Probes Based on Nanomicelles for Specific Determination of Long-Chain Aldehydes

Piyanan Pranee, Boosayarat Tomapatanaget*

Department of Chemistry, Faculty of Science, Chulalongkorn University, Bangkok, 10330, Thailand

**e-mail: tboosayarat@gmail.com*

Long-chain aldehyde compounds such as hexanal, heptanal, octanal and nonanal are regarded as potential biomarkers of many diseases for biomedical applications. Furthermore, hexanal is served as the important quality indicators of fat and oil products due to the oxidation reaction during manufacturing processes. Apart from hydrophobic tails of long-chain hydrocarbon and hydrophilic heads of aldehyde functional group, we expected that aldehydes should perform as surfactants to form the self-assembling organized nanomicelle. In this research, the nanomicellar probes towards aldehyde compounds have been achieved. As our the concept, the incomplete micelle, which was prepared by cetyltrimethylammonium bromide (CTAB) and co-surfactant (S2) upon the challenge optimizing task, could be induced to form the complete nanomicelle by long-chain aldehyde as a target analyte by self-assembling organized nanomicelle. The fluorescence intensity at 542 nm of hydrazine-functionalized fluorescent dye incorporated in incomplete micelle was enhanced upon the addition of long-chain aldehyde. This sensing platform served as a high selectivity of self-assembling micellar sensor toward long-chain aldehydes. Moreover, the fluorescence enhancement of dye-doped micelle is proportional to the amounts of long-chain aldehyde added. The reaction time of probes was completed within 20 min in PBS buffer pH 7.4 with the limit of detection (LOD) of 74.38, 80.38, 80.98 and 64.09 μM for hexanal, heptanal, octanal, and nonanal, respectively. Consequently, this nanomicelle system offers the promising determination of the long-chain aldehydes detection and a benefit for easy checking in real samples.

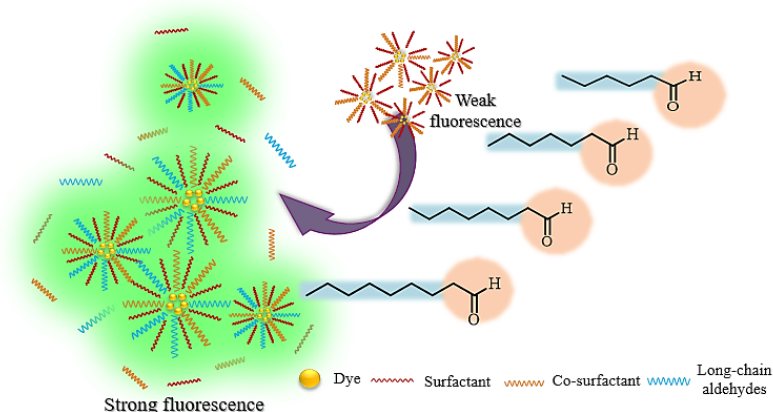


Figure1. Conceptual design of fluorescent micellar probe for long-chain aldehydes sensing

Keyword: Long-chain aldehydes; micelle; fluorescence; nanomicelle, self-assembly

References

1. Tang, Y.; Kong, X.; Liu, Z.-R.; Xu, A.; Lin, W., *Analytical Chemistry* 2016, 88 (19), 9359-9363.
2. Mukherjee, K.; Chio, T. I.; Gu, H.; Banerjee, A.; Sorrentino, A. M.; Sackett, D. L.; Bane, S. L., *ACS Sensors* 2017, 2 (1), 128-134.

Theoretical Study of CO₂ Hydrogenation on Cd₄/TiO₂ Catalyst

Jittima Meeprasert^a, Guanna Li^a and Evgeny Pidko^{a*}

^a Inorganic Systems Engineering, Chemical Engineering Department, Delft University of Technology, Van der Maasweg 9, 2629 HZ Delft, The Netherlands

* e-mail: e.a.pidko@tudelft.nl

The conversion of CO₂ into valuable chemicals received much attention in the recent years in the field of renewable energy. However, due to the high thermodynamic and kinetic stability of CO₂ its efficient and selective conversion is a challenge under normal conditions.¹⁻³ Recent experimental work has found that Cd nanoparticles supported on TiO₂ allows reducing CO₂ with H₂ and obtain high conversions along with exceptional methanol selectivities. These findings inspired us to carry out a computational study on the mechanism of CO₂ hydrogenation over a model Cd₄/TiO₂ catalyst to unravel the key factors controlling the CO₂ reduction reactivity and methanol selectivity. Our preliminary results indicate the crucial role of the interface sites between the nanoparticle and the support for the reaction. The H₂ dissociation is slightly endothermic and proceeds at such interface sites. For the CO₂ hydrogenation, two main reaction pathways have been identified: (1) the reversed water-gas shift (RWGS) pathway, and (2) the formate pathway. We found that methanol formation is highly exothermic which is in agreement with the experimental observation. The competitive reaction pathways of methanol formation and CO production were also investigated.

Keywords: CO₂ hydrogenation, TiO₂, cadmium, DFT

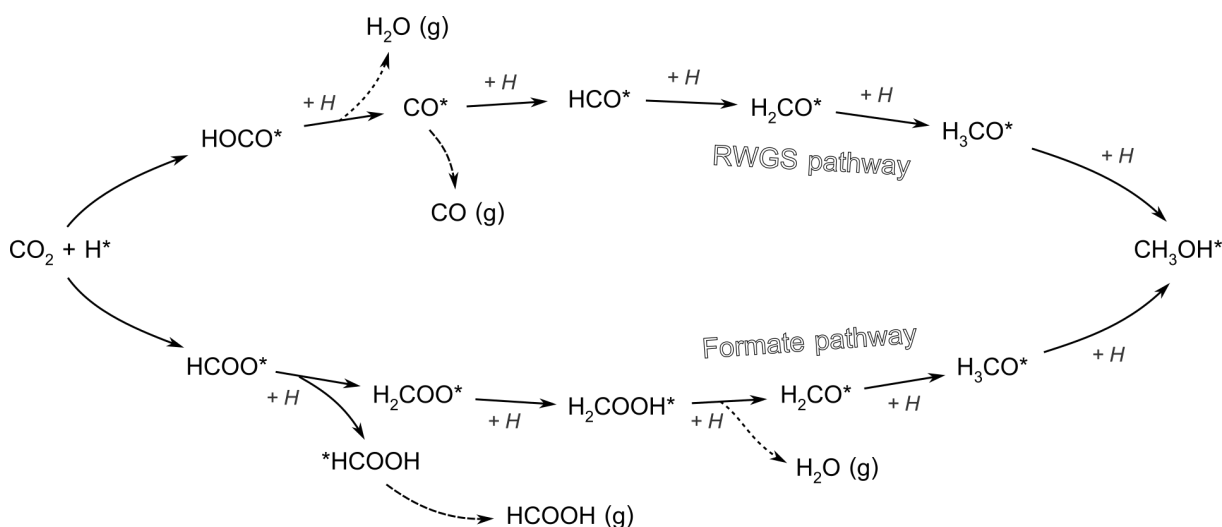


Figure. Proposed reaction pathways of CO₂ hydrogenation to CO, HCOOH and CH₃OH

References

1. S. Kattel, P. Liu, J. G. Chen, *J. Am. Chem. Soc.* **2017**, *139*, 9739-9754
2. P. Schlexer, H. T. Chen, G. Pacchioni, *Catal Lett.* **2017**, *147*, 1871-1881
3. Y. Li, S. H. Chan, Q. Sun, *Nanoscale.* **2015**, *7*, 8663-8683

First-Principles Study of Electron Transport in α - V_2O_5 Cathode Materials for Li-ion Batteries

Panuwat Wathaisong^{a,b} and Suwit Suthirakun^{a,b,*}

^aSchool of Chemistry, Institute of Science, Suranaree University of Technology, Nakhon Ratchasima 30000, Thailand

^bCenter of Excellence in Advanced Functional Materials, Suranaree University of Technology, Nakhon Ratchasima 30000, Thailand

*e-mail: suthirak@sut.ac.th

Lithium-ion batteries (LIBs) are widely used as energy storage to supply power for portable electronic devices. Vanadium pentoxide (V_2O_5) has proved to be a promising candidate as cathode materials for LIBs because of its high energy density and good safety.¹ However, key issues in this material are its low electronic conductivity and slow electrochemical kinetics.^{2,3} In order to improve the performance of the V_2O_5 cathode, one needs to understand at its most fundamental mechanism of the electron movement in the V_2O_5 material. Thus, the transport property of electron polarons in α - V_2O_5 was computationally studied employing density functional theory with Hubbard-U corrections (DFT+U). This method is used to compute the electronic and atomic structures of polarons localized on V ions, and the barrier for polaron hopping in stoichiometric V_2O_5 and Li-inserted V_2O_5 . The calculated results show a high degree of anisotropy in polaron mobilities, both within the bilayer sheets and across the van der Waals (vdW) gaps in the stoichiometric V_2O_5 system. The presence of Li-ion decreases the degree of anisotropy in polaron mobilities and stabilize the polaron migration across the vdW gaps. Nevertheless, having Li-ion in the lattice increases the effective barrier of polaron migration in all considered directions when compared with those in the stoichiometric V_2O_5 system.

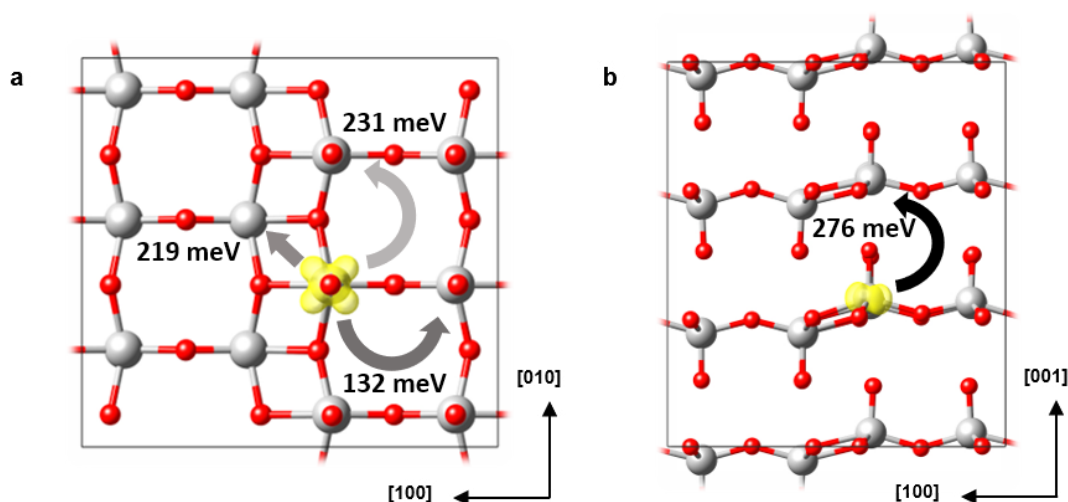


Figure 1. Polaron hopping directions and their hopping barriers a) within the V_2O_5 layer and b) across a van der Waal gap.

Keywords: Lithium-ion batteries, Vanadium pentoxide, DFT+U, Electron transport

References

1. J. B. Goodenough, K.-S. Park, *J. Am. Chem. Soc.* **2013**, *135*, 1167-1176.
2. L. R. De Jesus, G. A. Horrocks, Y. Liang, A. Parija, C. Jaye, L. Wangoh, J. Wang, D. A. Fischer, L. F. J. Piper, D. Prendergast and S. Banerjee, *Nat. Commun.* **2016**, *7*, 12022.
3. W. Yang, T. Katsunori, L. Kyoungcho and C. Guozhong, *Adv. Funct. Mater.* **2006**, *16*, 1133-1144.

Excited State Proton Transfer (ESPT): Theoretical Study on Principal Photophysics of New Chromophores, Fluorescent Molecular Probes and Luminescent Materials

Nawee Kungwan

Department of Chemistry, Faculty of Science, Chiang Mai University, Chiang Mai, Thailand
e-mail: naweekug@gmail, nawee.kungwan@cmu.ac.th

Tautomerization taking place in organic molecules as a bifunctional group through the excited-state proton transfer (ESPT) between proton donor and proton acceptor (either ESIntraPT or ESInterPT with assistance of protic solvent) is one of the most studied and applicatively promising photoreactions. The most remarkable photophysical property of the ESPT molecules is the large Stokes shift of, compared to the normal chromophores. Their applications are found in many fields from fluorescent molecular probes (chemosensors and bioimaging) to luminescent materials (optoelectronic devices). Up to now, extensive spectroscopic and theoretical research studies on the photophysical process of ESPT molecules have been carried out, however their molecular structure-property relationship has not been well understood, particularly the role played by solvent assistance and absorption and fluorescent spectra controlled by chemical modification of well-known ESPT molecules. In this present contribution, we would like to investigate these mentioned properties with the help of quantum-mechanical tools both static calculations and dynamic simulations of some interesting systems.

Keywords: Tautomerization, Excited-state proton transfer, TD-DFT

References

1. Daengngern, R.; Kungwan, N., *J. Lumin.* 2015, **167**, 132-139.
2. Daengngern, R.; Prommin, C.; Rungrotmongkol, T.; Promarak, V.; Wolschann, P.; Kungwan, N., *Chem. Phys. Lett.* 2016, **657**, 113-118.
3. Kerdpol, K.; Daengngern, R.; Meeprasert, J.; Namuangruk, S.; Kungwan, N., *Theor. Chem. Acc.* 2016, **135** (8), 1-9.
4. Chansen, W.; Salaeh, R.; Prommin, C.; Kerdpol, K.; Daengngern, R.; Kungwan, N., *Comput. Theor. Chem.* 2017, **113**, 42-51.
5. Manojai, N.; Daengngern, R.; Kerdpol, K.; Ngaojampa, C.; Kungwan, N., *J. Lumin.* 2017, **188**, 275-282.
6. Prommin, C.; Kanlayakan, N.; Chansen, W.; Salaeh, R.; Kerdpol, K.; Daengngern, R.; Kungwan, N., *J. Phys. Chem. A* 2017, **121** (31), 5773-5784.

In Silico Model for Prediction of Silver Nanoparticle-mediated Cytochrome P450 Enzyme Inhibition

Nootcharin Wasukan^a, Mayuso Kuno^b, and Rawiwan Maniratanachote^{a,*}

^aNational Nanotechnology Center, National Science and Technology Development Agency (NSTDA), Pathum Thani, Thailand

^bDepartment of Chemistry, Faculty of Science, Srinakharinwirot University, Bangkok, Thailand

*e-mail: rawiwan@nanotec.or.th

Cytochrome P450 (CYP) is a major group of phase I drug metabolizing enzymes in the liver. Among CYP families, CYP1, CYP2 and CYP3 are responsible for oxidative metabolism of a large number of drugs, chemicals and endogenous substances in human. Some of them can be substrates and/or inhibitors, or inducers of specific CYP enzymes. Inhibition of CYP enzymes is considered clinical significance in term of safety aspect. Silver nanoparticles (AgNPs) are widely used in consumer products, which leading to intentional and unintentional exposures, as well as safety concern on human health and the environment. The aim of this study was to investigate potential inhibition of CYP enzymes by AgNPs using computational simulation. Molecular structure of AgNPs was optimized to Ag₃ cluster using a Hartree-Fock with the 3-21G basis set. Further, interactions of Ag₃ cluster with six important CYP enzyme isoforms including CYP1A2, CYP2C9, CYP2C19, CYP2D6, CYP2E1 and CYP3A4 were investigated using molecular docking. The results demonstrated interactions of Ag₃ on key amino acid residues of CYP2C9, CYP2C19 and CYP2D6. Interestingly, these results are consistent with *ex vivo* data we reported previously that AgNPs inhibited CYP2C and CYP2D in rat liver microsomes. In conclusion, *in silico* model is a promising tool to predict CYP inhibition and can be applied for other nanoparticles.

Keywords: Silver nanoparticles, Cytochrome P450, Inhibition, Molecular docking

References

1. U. M. Zanger, M. Schwab. *Pharmacol Ther.* **2013**, *138* (1), 103-141.
2. K. Kulthong, R. Maniratanachote, Y. Kobayashi, T. Fukami, T. Yokoi. *Xenobiotica.* 2012, *42* (9), 854-862.

The Esterification Reaction of Propanoic Acid with Bioethanol on H-Beta zeolite: An ONIOM study

Nattida Maeboonruan^a, Bundet Boekfa^{a*}, Thana Maihom^a, Piti Treesukol^a

Supawadee Namuangruk^b, Kanokwan Kongpatpanich^c, Jumras Limtrakul^c

^a Department of Chemistry, Faculty of Liberal Arts and Science, Kasetsart University, KamphaengSaen Campus, NakhonPathom 73140, Thailand.

^b National Nanotechnology Center (NANOTEC) National Science and Technology Development Agency (NSTDA) Pathum Thani 12120, Thailand

^c Department of Materials Science and Engineering, Vidyasirimedhi Institute of Science and Technology, Rayong 21210, Thailand.

*e-mail: bundet.b@ku.ac.th

Bioethanol, a product from agricultural wastes, is an important chemical feedstock for producing high value added chemicals. In this work, the esterification reaction of bioethanol with propanoic acid to ethyl propanoate and water has been studied on H-Beta zeolite. The computational ONIOM(MP2:M06-2X) calculation has been applied on 5T:34T model (T means tetrahedral of Si or Al atoms) of H-Beta zeolite. The basis set was 6-31G(d,p) level of theory. The calculated adsorption energies were -22.5 and -29.6 kcal/mol for ethanol and propanoic acid on H-Beta zeolite. The esterification reaction of ethanol and propanoic acid was found to take place in a single concerted step. The relative energies for the coadsorption, transition state and product were -44.4, -18.8 and -37.6 kcal/mol, respectively. We found that the framework of zeolite increases the adsorption energy for 10.1 kcal/mol and stabilizes the transition state by lowering the activation energy for 6.7 kcal/mol. The result of this study is important not only for a detailed understanding of the structure and reaction mechanisms of zeolite catalysts, but also for improving the capability of ethanol conversion to more valuable products.

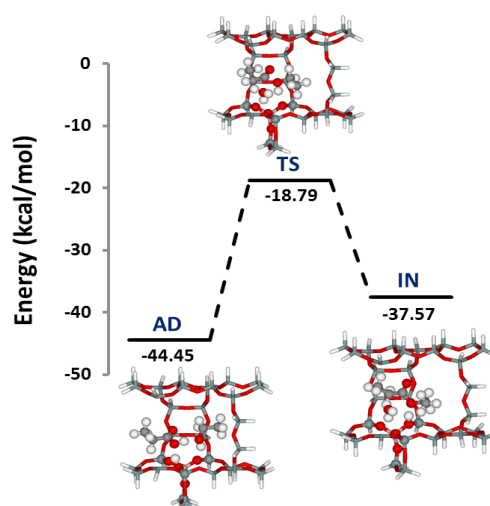


Figure 1: the energy profile for the esterification reaction of propanoic acid with bioethanol on H-Beta zeolite model 5T:34T optimized with ONIOM(MP2:M06-2X).

Keywords: Bioethanol, esterification, H-Beta zeolite, ONIOM

References

1. Q. zhang, Y. Xu, Y. Li, T. Wang, Q. Zhang, L. Ma, M. He, K. Li, *Applied Energy*. **2015**, *160*, 633-640.
2. P. Prinsen, R. Luque, C. González-Arellano, *Microporous and Mesoporous Materials*. **2018**, *262*, 133-139.

The Glycerol Dehydration on UiO-66-SO₃H Catalysts: A DFT Study

**Pattaporn Srirattanasakunsuk^a, Bundet Boekfa^{a*}, Thana Maihom^a,
Piti Treesukol^a, Kanokwan Kongpatpanich^b, Jumras Limtrakul^b**

^a Department of Chemistry, Faculty of Liberal Arts and Science, Kasetsart University, KamphaengSaen Campus, NakhonPathom 73140, Thailand.

^b Department of Materials Science and Engineering, Vidyasirimedhi Institute of Science and Technology, Rayong 21210, Thailand.

*e-mail: bundet.b@ku.ac.th

The glycerol dehydration over UiO-66-SO₃H metal-organic-framework catalysts has been studied using the density functional theory. The C₁₆₂H₁₂₂O₆₇SZr₁₂ cluster of the UiO-66-SO₃H model was optimized with M06-L functional. The 6-31G(d,p) basis set was chosen to describe C, H, O, S and N atoms while LANL2DZ was applied for the Zr atom. The glycerol adsorbed at the Brønsted acid site inside the UiO-66-SO₃H framework via strong hydrogen bonding. The adsorption energy was -26.1 kcal/mol. The first dehydration reaction step of glycerol, which is the rate-determining step, was predicted with activation energy of 40.5 kcal/mol. This energy is lower than the reaction on H-ZSM-5 zeolite (42.5 kcal/mol). Our study demonstrated that UiO-66-SO₃H can be used as a solid catalyst for the glycerol dehydration reaction.

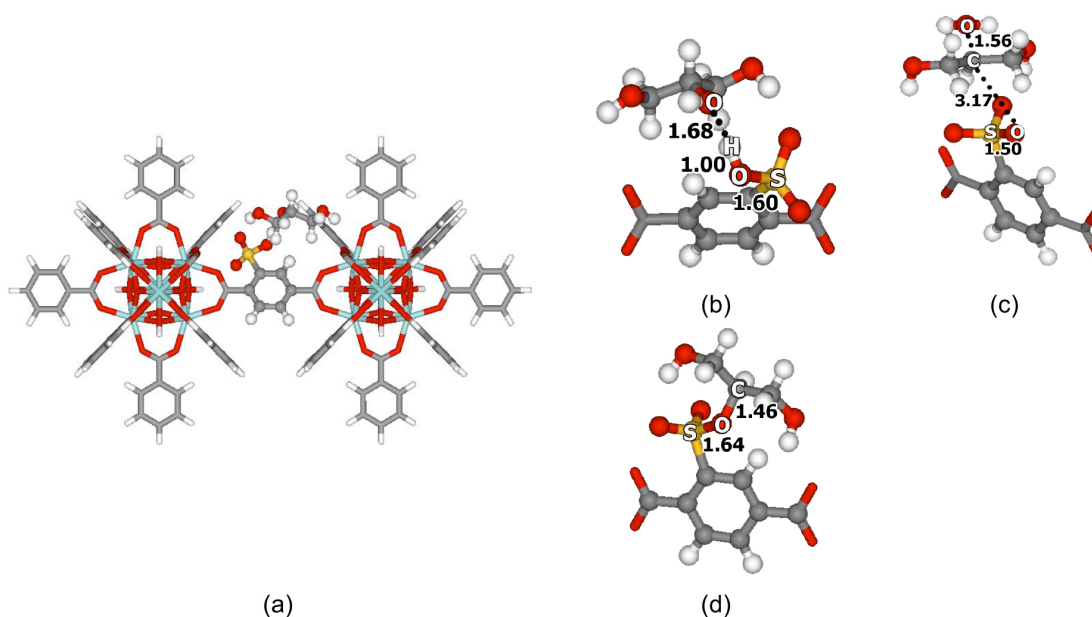


Figure 1: The glycerol dehydration over UiO-66-SO₃H metal-organic-framework catalysts optimized with M06L functional. (a) UiO-66-SO₃H, (b) adsorption, (c) transition state and (d) product. Distances are in Å.

Keywords: Glycerol, dehydration reaction, UiO-66-SO₃H, DFT

References

1. K. Kongpatpanich, T. Nanok, B. Boekfa, M. Probst, J. Limtrakul, *Phys. Chem. Chem. Phys.* **2011**, 13, 6462-6470.
2. S Phikulthai, Y Injongkol, T Maihom, P Treesukol, P Maitarad, V Tangsermvit, K Kongpatpanich, B Boekfa, *Key Eng. Mater.* **2018**, 757, 98-102.

THE-P-17

Structural and Electronic Properties of Co_{13} and Ni_{13} clusters on $\gamma\text{-Al}_2\text{O}_3$ support: A Density Functional Theory Study

Rusrina Salaeh^a, Supawadee Namuangruk^b, Naweek Kungwan^{a*}, and Pussana Hirunsit^{b**}

^a Department of Chemistry, Faculty of Science, Chiang Mai University, Chiang Mai 50200, Thailand

^b National Nanotechnology Center (NANOTEC), National Science and Technology Development Agency (NSTDA), Pathum Thani, 12120, Thailand

*e-mail: pussana@nanotec.or.th and naweekung@gmail.com

The atomic geometries of Co and Ni (3d transition-metal clusters) with 13 atoms were investigated by density functional theory calculations to explore the possible structural configurations on $\gamma\text{-Al}_2\text{O}_3$ surface. Understanding the structure-reactivity relationship of Co and Ni clusters requires the rationalization of the role of the metal-support interaction on the morphologies and electronic properties of nanometer size metallic particles. Therefore, the interaction energies and the structures of Co_{13} and Ni_{13} clusters were studied. The structures of Co_{13} and Ni_{13} clusters of four selected high-symmetry and three selected low-symmetry are calculated to reveal the most stable structure. From the calculations, it can be seen that Co_{13} cluster prefers low-symmetry; triangular biplanar (TBP) whereas Ni_{13} cluster favors high-symmetry; icosahedral (ICO) with lower energy than other structures. Furthermore, the metal clusters were deposited on two position of $\gamma\text{-Al}_2\text{O}_3$ to find the active site. The knowledge accumulated through this work provides structural and electronic properties for understanding of reactivity of investigated metal catalysts on $\gamma\text{-Al}_2\text{O}_3$ surface.

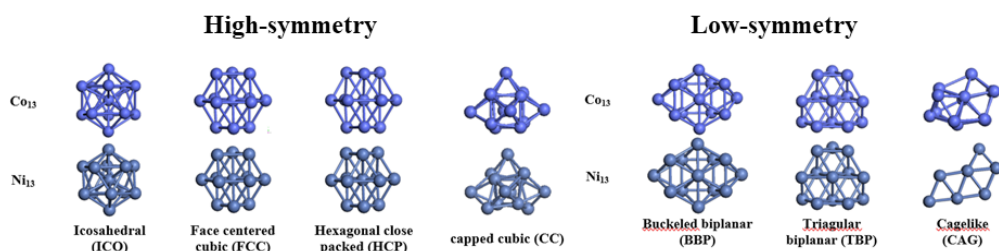


Figure 1. Possible structures of Co_{13} and Ni_{13} clusters.

Keywords: Supported catalyst, Cobalt, Nickel, gamma-alumina, Density functional theory

References

1. A. Srifa, K. Faungnawakij, V. Itthibenchapong and S. Assabumrungrat, *Chemical Engineering Journal* **2015**, 278, 249-258.
2. C. H. Hu, C. Chizallet, C. Mager-Maury, M. Corral-Valero, P. Sautet, H. Toulhoat and P. Raybaud, *Journal of Catalysis* **2010**, 274, 99-110.
3. C. M. Chang and M. Y. Chou, *Physical review letters* **2004**, 93, 133401.

Theoretical Insight into Methane Oxidation to Methanol on Single Fe-Embedded Nitrogen-Doped Graphene

Thantip Roongcharoen^a, Naweek Kungwan^{a,*}, Supawadee Namuangruk^{b*}

^aDepartment of Chemistry, Faculty of Science, Chiang Mai University, Chiang Mai, Thailand

^bNational Nanotechnology Center (NANOTEC), 111 Thailand Science Park, Patumthani 12120, Thailand

*e-mail: naweekung@gmail.com, supawadee@nanotec.or.th

Methane, a major component in natural gas and biogas, is an important chemical feedstock for synthesis of methanol as more valuable compound. Methanol is renewable source in many industries. To convert methane to methanol, there are several technologies such as supercritical water process, plasma technology, biological process, photo-catalysts, and catalytic process. Among them, catalytic process is a popular approach because the methane can be converted to methanol by oxidation processes under mild condition with high yield. Different types of catalysts methane oxidation such as metal-exchanged zeolites, metal catalyst, and carbon-based catalyst have been widely investigated. Modified graphene as one of carbon-based materials has become the attractive catalyst due to its the advantages of high specific surface volume ratio, low energy consumption, low cost, and non-toxic materials. Among the modified graphene materials, Fe embedded on nitrogen-doped graphene ($\text{Fe-N}_x\text{G}$; $x=1,2,3$) is one of the most interesting catalysts because it has specific active sites and can modulate the Fermi-level leading to enhancement of catalytic activity. These materials ($\text{Fe-N}_x\text{G}$; $x=1,2,3$) exhibit high chemical activity in various fields for example, $\text{Fe-N}_3\text{G}$, and $\text{Fe-N}_4\text{G}$ for oxygen reduction reaction (ORR), $\text{Fe-N}_3\text{G}$ for converting dinitrogen to ammonia, and $\text{Fe-N}_4\text{G}$ for NO reduction. However, the reactivity of $\text{Fe-N}_x\text{G}$ catalysts in methane oxidation are not well understood. Therefore, in this work, the methane oxidation mechanism using $\text{Fe-N}_x\text{G}$ catalysts will be systematically investigated. Finally, the reactivity of $\text{Fe-N}_x\text{G}$ will be compared with other catalysts.

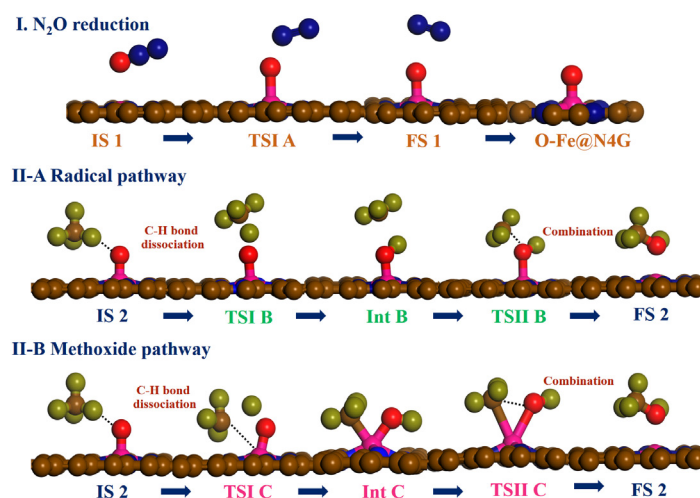


Fig.1 Proposed mechanism of methane oxidation present of N_2O reduction on Fe-embedded on functionalized graphene ($\text{Fe-N}_x\text{G}$).

Keywords: Methane oxidation, Fe-embedded on nitrogen-doped graphene, Non-precious metal catalyst.

References

1. Z. Zakaria, S.K. Kamarudin, Renewable and Sustainable Energy Reviews, 65 (2015) 250-261.
2. L. Yung-Chang, Nano Lett. 15 (2015), 7408–7413.
3. Q. Thalia, C. Pabitra, Molecular Catalysis 431 (2017) 9-14.

General Information

Congress Venue

The Thailand Science Park Convention Center (TSP-CC), Pathum Thani, Thailand

Date

December 12th-14th, 2018

Congress Secretariat

Website: <http://www.nano-thailand.com>

E-mail: nanothailand2018@gmail.com

Official Language

The official language of the Congress will be English.

Official Bank

The Siam Commercial Bank Public Company Limited has been appointed as the official bank of the Congress.

Traveller's Cheques and Credit Cards

Major credit cards, such as VISA and Master Card are widely accepted in hotels and shops. Traveller's cheques can be conveniently cashed at all commercial banks and authorized money exchanges.

Currency

The Thai currency is Baht, which is divided into 100 Satang. Coins are 25 and 50 Satang, 1, 5 and 10 Baht. Foreign currency may be exchanged at authorized exchange banks, hotels and shops.

(1 USD is approximately 36 Baht).

Electricity

Voltage in Thailand is 220 V AC. However, electric razor outlets, generally with multi-voltage fittings, are available in most hotels.

What to Wear/Dress & Weather

Definitely cool cottons rather than synthetics and comfortable footwear. To be ‘casual’ is quite acceptable, but Thais consider it impolite to wear shorts and skimpy tops on city streets. Only the top restaurants demand a jacket and tie.

Being in the Southeast Asia region, Thailand has a subtropical climate. During November the temperature averages 30°C in daytime and 25°C to 27°C at night.

Liability

The Congress will not assume any responsibility for accidents, losses, damages, delays, or any modifications in the program caused by unforeseen circumstances.

Time Difference

Thailand time is GMT plus 7 hours.

Registration Information

Pre-registered delegates are required to produce their confirmation of registration at the registration counters to obtain their registration badges and congress kits. On-site registration will also be accepted at the registration counters and can be made in cash (Baht and USD) or credit card by VISA and Master card.

Registration Hours

Date	Registration Hours
Wednesday 12 November 2018	8.00-17.00 hr.

Badges

All delegates are kindly requested to wear name badges when attending any meeting or social gathering. Only delegates who are wearing name badges can be admitted to the lecture halls. Please note: accompanying persons cannot be admitted to the scientific session.

iMScope Trio

Imaging Mass Microscope

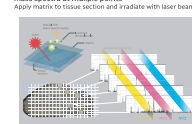


Imaging Mass Microscope

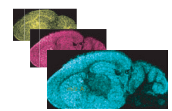
Optical microscope
Capture an optical microscope image



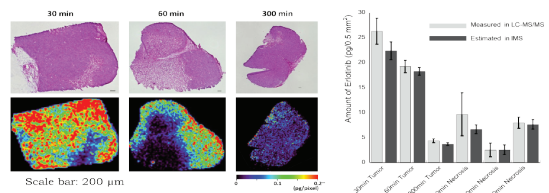
Mass Spectrometer
Mass spectra at multiple points



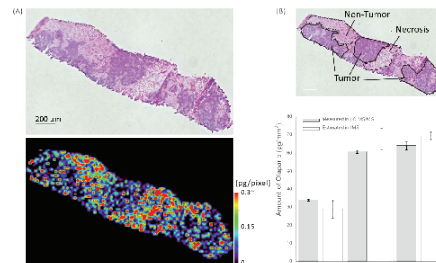
Multiplexed imaging
Generate molecular distribution images (multiplexed imaging) based on its signal intensity



Quantitative pharmacokinetic-IMS



World 1st Imaging Mass Microscope
World Best Spatial Resolution : 5 μ m
World Best Structure Analysis : MSn (IT-TOF MS)
Ionization : Atmospheric pressure MALDI
Mass range : m/z 50-3000



Olaparib was accumulated outside tumor regions

Optical Microscope
Magnification is variable from 1.25 to 40 times.

High-Speed and High Precision Sample Stage



High-Speed Laser Unit with Variable Beam Diameter
The laser beam diameter can be set from 5 μ m to 200 μ m.

Versatile and Reliable Quadrupole-Ion-Trap / TOF (MSn)



BARA SCIENTIFIC
Solution of Success

Bara Scientific Co., Ltd.
968 U Chu Liang Building Floor7
Rama 4 Road Silom Bangrak Bangkok 10500 Thailand
Tel : 02-6324300 (auto 20 lines) Fax : 02-6375496-7
www.barascientific.com





NANO
THAILAND 2018